Manufacture, characterisation, modelling and application of a novel ion-exchanger for protein separation

Ming, Fang

Award date:
1991

Awarding institution:
University of Bath

MANUFACTURE, CHARACTERISATION, MODELLING AND APPLICATION OF A NOVEL ION-EXCHANGER FOR PROTEIN SEPARATION

A thesis submitted in partial fulfilment for the degree of

Doctor of Philosophy

in the School of Chemical Engineering

of the University of Bath

by

Fang Ming (M.Sc.)

1991

ProQuest LLC
789 East Eisenhower Parkway
P.O. Box 1346
Ann Arbor, MI 48106-1346

DECLARATION

This thesis is based on the work carried out in the School of Chemical Engineering at University of Bath, During the period September, 1987 to April, 1988 and April, 1989 to January, 1991. It is the original and independent work of the Author, except where specific reference to other investigations are made.

No part of this thesis has been, or is currently being submitted to any other University as a requirement for any degree.

Candidate: (Fang Ming)

(FANG MING)

Supervisor:

(Prof. John A. Howell)

Date: 2 October 1991

ACKNOWLEDGMENTS

My profound gratitude goes to Prof. J. A. Howell, not only for his brilliant scientific supervision, but also for his criticism, friendship and the confidence which he showed in me throughout my research project.

I would like to thank Dr J. Hubble for his discussion and help, and Drs Petra Heinemann, Carman Rmero, Martin Addo, Pierre Aimar, Chrstin Taddei, Mark Pritchand and Omar Legrini who shared the office with me, for their help and friendship. Thanks are extended to Dr. D. Wu and Mr. Y. Wang.

I would also like to thank all the staff and the postgraduate students of the School of Chemical Engineering, for their friendship and warm attitude.

The financial support from SERC and Bio-Isolates Ltd. is grateful acknowledged.

Finally I am deeply grateful to my family for their inexhaustible source of support and encouragement.

DEDICATED TO MY PARENTS

CONTENT

		PAGE NO.
ABSTRACT		
CHAPTER 1		
INTRODUCTION		1
CHAPTER 2		
PRINCIPLES OF ION-EXCHANGE CHROMATOGRAPHY		
FOR PROTEIN - A REVIEW		6
2.1	Comparison of Ion-Exchange Chromatography With Other Liquid Chromatographic Techniques	6
2.2	Properties of Protein	8
2.3	Ion-Exchange Functional Group and Selection	9
2.4	Mechanism of Ion-Exchange Adsorption and Desorption of Protein	11
2.5	Elution Curve	12
2.6	Stationary Phase and Mobile Phase	12
2.7	Operation of Ion-Exchange Chromatography	13
2.8	Ion-Exchange Chromatography Processes	14
2.9	Adsorption Isotherm	15
2.10	Kinetics	15
2.11	Ion-Exchange Capacity	16
2.12	Column Regeneration	17
2.13	Swelling and Shrinking	17
2.14	Scale Up	18
CHAPTER 3		
REVIEW OF THE DEVELOPMENT OF THE ION-EXCHANGE		
PROCESS FOR PROTEIN SEPARATION		19
3.1	Ion Exchangers	19
3.1.1	Cellulose Ion-Exchanger	20
3.1.2	Other Ion-Exchangers	23
3.2	Brief Review the Development of Ion-Exchange Theory	24
3.3	The Considerations for Further development	34
CHAPTER 4		
MANUFACTURE OF SPONGE ION-EXCHANGERS		36
4.1	Introduction	36
4.2	Cellulose Sponge	37

4.3	Consideration	38
4.4	Cross Linking	38
4.5	Derivative Reaction	40
4.6	The Development of Cellulosic Sponge Ion-Exchanger	42
4.7	Materials	45
4.8	Experimental Methods	46
4.9	Results and Discussion	47
4.9.1	Stability of Cellulose Sponge in Aqueous Sodium Hydroxide	47
4.9.2	Degree of Cross-Linking of Sponge Ion-Exchange	48
4.9.3	Derivative Reaction for Making CM Sponge	51
4.10	Manufacture of SP and DEAE Sponge	56
4.10.1	Introduction	56
4.10.2	Recipes for DEAE Sponge	57
4.10.3	Recipes for Sp Sponge	58
4.11	Conclusion	60
CHAPTER 5		
CHARACTERISATION OF CM SPONGE ION-EXCHANGER		**71**
5.1	Introduction	71
5.2	Materials and Methods	72
5.3	Isotherm Adsorption of CM Sponge	79
5.3.1	Results and Discussion	84
5.4	Physical Stability	86
5.4.1	Results and Discussion	88
5.5	Flow-Rate of CM Sponge	89
5.5.1	Results and Discussion	91
5.6	Kinetics Behaviour of Adsorption and Desorption of CM Sponge Operated at High Flow-Rates	93
5.6.1	Results and Discussion	95
5.6.2	Establishment of Kinetic Parameters and Effect of Flow-Rate on Lumped K_1 and K_2	101
5.7	Chemical Stability	108
5.7.1	Results and Discussion	109
5.7.2	Swelling and Shrinking Properties	110
5.8	Stability and Reproducibility of CM Sponge	110
5.8.1	Results and Discussion	111

5.9 pH Titration of CM Sponge Ion-Exchanger 112
5.10 Conclusion 114
CHAPTER 6
MATHEMATICAL MODELLING AND PARAMETER ESTIMATION OF ION-EXCHANGE CHROMATOGRAPHY PROCESSES 127
6.1 Introduction 127
6.2 Hydrodynamic Parameters of Column Packed 129
6.2.1 Axial Dispersion Coefficient and Peclet Number 129
6.2.2 Pore Diffusion Coefficient 131
6.3 Moment Analysis 133
6.4 The Plate Theories and The Rate Theories 136
6.4.1 Column Material Balance 136
6.4.2 Material Balance Equation for the Adsorption Particle 138
6.5 Modelling For Stirred Batch Reactor and Differential Recirculation Batch Reactor 141
6.6 Experimental Methods and Material 142
6.7 Computational Method 143
6.8 Establishment of Transport Parameters of Column Packed 146
6.9 Modelling Simulation 154
6.9.1 Lumped Film Mass Transfer Control Model For Differential Recirculation Batch Reactor and Stirred Batch Reactor 155
6.9.2 Results and Discussion 157
6.9.3 An Heterogeneous Model Including External Film Diffusion Control and Intrapartical Diffusion Control 160
6.9.4 Results and Discussion 168
6.9.5 Modelling For A 250 x 10 mm I.D. CM Sponge Column 172
6.9.6 Results and Discussion 177
6.10 Conclusion 182
CHAPTER 7
APPLICATION OF CM-HVFM ION-EXCHANGE COLUMN IN THE SEPARATION OF FRESH HEN EGG WHITE PROTEINS 193
7.1 Introduction 193
7.2 Material and Methods 195
7.3 Results and Discussion 197

7.3.1 Effect of Feed Loading on the Resolution and Productivity 198
7.3.2 Effect of High Flow-Rate on the Kinetic Performance and Productivity 202
7.4 Conclusion 205
CHAPTER 8
SUMMARY OF CONCLUSIONS AND RECOMMENDATIONS 209
8.1 Summary of Conclusions 209
8.2 Recommendations of Further Work 212
REFERENCES 214
NOMENCLATURE 226
APPENDIX 229

ABSTRACT

A low concentration two-steps technique for making cellulosic sponge ion-exchanger has been developed (Europe Patent application No. 9011378.8). This new CM sponge ion-exchanger showed that; (1) a monolithic structure with a large pore, but interconnected surface of conventional media; (2) it can be formed into flexible blocks or sheets, making it possible to construct columns and other novel contacting devices giving good separation at high flow rates and low pressures; (3) lysozyme capacity ranged over 800 mg/g at conductivity 16.3 mS/cm to over 2000 mg/g for 0.7 mS/cm; (4) in comparison with two commercial CM cellulosic ion-exchangers, Indion HC (Phoenix) and CM-52 (Whatman), the CM sponge ion-exchanger was able to sustain a superficial velocity of up to 8.78 m/h in a 147 mm I.D. column. In a 26 mm I.D. column, an only slightly faster velocity of 10 m/h was obtained. This contrasted with a limiting flow of less than 1.5 m/h with the other two parking in a 26 mm I.D. column; (5) its swollen volume was not affected by NaOH and NaCl concentration up to 1 N concentration; (6) highly stability and reusability were confirmed by the results of 340 cycles operation in which the performance of CM sponge column was not degraded neither being fouled nor channelled.

An intrinsic adsorption rate and desorption rate were obtained by using a simple lumped surface reaction model applied to differential bed recirculation column. The adsorption process mainly depended on the flow-rate, while the desorption process was mainly affected by the ionic concentration and only slightly affected by the flow-rate

Several models have been developed. Both the simple lumped model and more sophisticated model can well fit the experimental data. The lumped model might be suitable as rough guide for scale-up and process control due to its simple calculation process. The sophisticated model, a heterogeneous model, gave more fundamental understanding. Solved by orthogonal collocation method, the heterogeneous model can rapidly predict the adsorption performance in both the recirculation batch reactor

and stirred batch reactor under different protein loading, stirrer speeds and superficial velocities. The heterogeneous model also demonstrated that the initial stage of adsorption was controlled by external mass transfer, whilst after the initial stage the adsorption process was governed by intraparticle diffusion. Moreover the heterogeneous model gave a picture of the protein concentration variation with time in the two phases. The external mass transfer coefficient estimated by the heterogeneous model was more accurate than that by a correlation.

A column model indicated that, for a column 250 x 10 mm I.D. packed with the novel coherent sponge ion-exchanger, the axial dispersion could be negligible if the Peclet number was larger than 10.

Applying a 250 x 10 mm I.D. CM sponge column to separate the fresh egg white protein showed that; (1) at a column loading of up to 450 kg/m^3(column volume) egg white and superficial velocity 6 m/h, the resolution can still maintain at 0.8; (2) despite high flow-rate, high column loading and without CDR pretreatment the egg white solution, the column's kinetic performance was not degraded, nor was the column blocked and channelled; (3) lysozyme was preferentially adsorbed in comparison with conalbumin; (4) with all three fraction desired, ovalbumin, conalbumin and lysozyme, it was better to load at 13.64 g/l egg white protein up to 150 kg/m^3. When only lysozyme was of real interest loading of 20.31 g/l egg white protein at 450 kg/m^3 was optimal; (5) protein recovery of 97% and productivity of 87.63 kg/m^3/h which was 12 folds higher in comparison with Whatman CM ion-exchanger (Levison *el at* 1990a and 1990b) can be obtained.

CHAPTER 1

INTRODUCTION

CHAPTER 1

INTRODUCTION

Ion exchange chromatography, which separates molecules according to charge differences, is the most commonly practised chromatographic method of biomolecules purification. Ion exchange chromatography, by adjusting the pH, the solute, molecules of interest carry a charge that is opposite to that of the insoluble ion-exchanger. As a result, the molecules bind as they are loaded onto the reactor. Conditions are altered by changing pH or ionic concentration so that then the bound substances elute. They are each then collected separately, in a purified and concentrated form.

With the great increase of demand for various biomolecular products, such as proteins, amino acids and enzymes, in the modern world, ion-exchange chromatography plays an important role in separation processes. In 1986 Bonnerjea et al. studied the published purification protocols and found that the ion exchange technique was used in 75% of all purifications. This widespread use of ion exchangers is due to their versatility, relative cheapness and their acceptance by the regulatory authorities in the production of pharmaceutical proteins. This is in contrast to affinity adsorbents which, although they result in good resolution, are limited to one protein or group of proteins, are

expensive and their use is currently questioned by regulatory bodies (Skidmore, Horstmann *et al.* 1990).

More than forty years have passed since Cohn (1949) successfully applied the ion-exchange technique to the separation of biomolecules. An ideal ion-exchanger process has been sought. Although numerous efforts have been devoted to the development or improvement of ion-exchangers, results remain far below expectation. Especially the development of ion-exchanger with high flow-rate, high protein capacity and fast kinetics for large scale separation is very slow.

Traditional ion-exchangers which are based on polystyrene, can not be applied to recover protein due to their highly hydrophobic character and low protein capacity. Porous silica ion-exchangers can tolerate high pressure. They are somewhat hydrophobic but this disadvantage can be reduced by coating the surface of the pore of the exchanger with a hydrophillic material (Tayot *et al.*, 1976). They are however susceptible to the effects of alkali cleaning which is preferred in a bioproduct environment. Cellulosic or cross-linked polysaccharides have suitably porous and hydrophillic properties but they are difficult to use in large-scale production because of their poor hydraulic properties (Skidmore and Chase, 1988) and slow kinetics. The regenerated cellulose ion-exchanger in the form of bead or microgranules are highly porous and hydrophillic, but they either have high flow-rate with slow kinetics, or have fast kinetics with low flow-rate (Fang Ming and Howell, 1991a). In

addition they deform under pressure and swell or shrink due to the ionic strength and pH being changed, which does not favour improving the productivity nor reliable scale up.

Janson and Hedman (1982) showed an example of industrial ion-exchange chromatography to produce egg white lysozyme using CM-Sephadex C-25. This ion-exchanger adsorbed the lysozyme which was then eluted by 1 M NaCl. The cycle time depended on whether the ionic strength was adjusted by dilution or by desalting on Sephadex G-25. In the former case, the cycle time was 42 hours and in the second case 15 hours. Both cases indicated that one of the main reasons which caused such long cycle time was the low flow-rate.

Levison *et al.* (1990a) achieved a flow rate of up to 25 ml/min.(superficial velocity of 0.9 m/h) using the Whatman microgranular cellulose QA52, or DE52 in a 100 ml axial flow column of 66 x 44 mm I.D., beyond which higher flow was impossible due to the compressibility of the resin. Levison *et al.* (1990b) also reported that they used a 160 x 450 mm I.D. column packed with DE52 at a volumetric flow rate of about 800 ml/min, superficial velocity of 0.3 m/h to separate egg white proteins. The productivity in both cases was less than 7 $kg/m^3/h$.

An ion-exchanger with the characteristics of fast kinetics, high flow-rate, high protein capacity and robustness has been sought for several years. Particulate and granular cellulosic media have the disadvantages of slow flow rate, plugging of the

bed, and mal-distribution of flow and also the need for considerable skill in filling a column to avoid channelling. Raw cellulose sponge was considered that not only was the cheapest ion exchange matrix but also could allow the high flow-rate. This sponge material, a monolithic structure with a high porosity, but interconnected surface area for adsorption does not have the deadended porous structure of conventional media. It can be formed into flexible blocks or sheets, making it possible to construct columns and other novel contacting devices giving good separation at high flow rates and low pressures. In 1982, Gosling (1985) started to investigate the possibility of cellulose ion-exchange with high flow-rate and fast kinetics using cellulosic sponge. Addo (1988) then continued this project from 1985. Although both of them had some encouraging results, there was no significant breakthrough, as the problems of low flow rate, low protein capacity and short product life had not been solved. During the work reported here, Fang Ming and Howell (1987a and 1990a) invented a low concentration-two steps recipe for producing a high protein capacity and fast flow-rate, fast kinetics and robustness cellulose sponge ion-exchanger. This technique was then transferred to BPS Ltd. (BPs Separation Ltd., Mountjoy Research Centre, Durham University, U.K.). Applying the CM sponge ion-exchanger in a practical separation process, separation of fresh egg white protein, showed that productivity was more than 12 times (86 $kg/m^3/h$) higher than that of Whatman cellulose ion-exchangers used by Levison *et al* (1990a, 1990b).

This thesis first deals with the general literature and theory of ion-exchange processes to give the basic concepts and terminology relative to ion-exchange chromatography. There is also a short literature survey and detailed background specific to each particular chapter. The techniques for making cellulose sponge ion-exchangers are described in Chapter 4. Characteristics of the novel CM sponge ion-exchanger are discussed in Chapter 5. Demonstration of the effects of the external mass transfer and intraparticle diffusion on the adsorption process, parameters estimation, and prediction of breakthrough curve using a 250 x 10 I.D. mm CM sponge column are presented in Chapter 6. Finally, the 250 x 10 mm I.D. CM-HVFM ion-exchange columns were used to separate the fresh egg-white protein. Effects of high loading and flow-rate on productivities, resolution and kinetics are also discussed.

CHAPTER 2

PRINCIPLES OF ION-EXCHANGE CHROMATOGRAPHY FOR PROTEIN - A REVIEW

CHAPTER 2

PRINCIPLES OF ION-EXCHANGE CHROMATOGRAPHY FOR PROTEIN - A REVIEW

2.1 Comparison of Ion-Exchange Chromatography With Other Liquid Chromatographic Techniques

There are five main types of liquid chromatography for protein separations and analysis. Affinity chromatography, as Dunnill *et al.* (1978) and Eketorp *et al.* (1982) pointed out, is the most selective separating tool because the ligand is normally specific to a single protein. Its disadvantages are that the ligand media can be expensive, have low adsorptive capacities, and often tend to be unstable, producing a contaminated product due to leaking of the ligand. Atkinson (1973) considered that for purification of high value proteins such as enzymes, these disadvantages may be outweighed by the many advantages conferred by the specificity of the ligand.

Gel filtration or size exclusion chromatography separates proteins according to their molecular size. If the proteins have the same size with different charge, gel filtration could not separate them. Moreover, Janson and Hedman (1982) considered that the main disadvantage for scale-up was poor throughput compared with ion-exchange chromatography, due to the relatively poor mechanical properties of the column packing.

Hydrophobic interaction chromatography (HIC) is based on hydrophobic interaction between the sample and hydrophobic groups in the stationary phase. In other words, proteins are adsorbed on to hydrophobic supports at a high ionic concentration and subsequently eluted using a falling salt gradient when the ionic concentration is lower, *i.e.* when the hydrophobic interaction become weaker. The procedure is employed for feeds containing high levels of salt and as a routine means of separating water-soluble proteins. It can also be used to remove strongly hydrophobic constituents from protein solutions. The disadvantages of HIC are; (1) the effectiveness of HIC is generally reduced by the presence of hydrophobic contaminants in the feed; (2) strong conditions are frequently required to elute proteins from hydrophobic matrices. This may involve the use of non-ionic detergents or ethylene glycol which can increase the likelihood of protein denaturation (Roe, 1989).

Reverse-phase chromatography (RPC) techniques have traditionally been applied to the analysis of low molecular weight compounds using HPLC, It is characterized by the use of silica derivatized with alkyl functionalities (typically C_2-C_{18} alkyl chains) and an aqueous mobile phase containing on organic solvent such as methanol, propanol, acetonitrile and ethanol. The drawbacks of RPC are in the frequent use of toxic solvents such as acetonitrile and in its limited application to protein purification where denaturation is unacceptable. Moreover, the silica based metrix used in RPC will dissolve above pH 7.5 (Roe 1989).

Ion-exchange chromatography separates proteins according to their charge regardless of the molecular size. Selectivity of ion-exchange chromatography is considered to be medium degree compared with that of affinity chromatography. Throughput or productivity of ion-exchange is the highest of these five types of chromatography because high loading and high flow-rate could be applied to it. The likelihood of protein denaturation is less than the HIC and RPC due to the mild conditions of adsorption and desorption. In addition, low cost is another main advantage of ion-exchange chromatography.

2.2 Properties of Protein

The basic units of proteins are amino acids. These are linearly polymerised by peptide bonds to form high molecular weight compounds, which may be globular in shape. They posses therefore a large number of residual amino-acid-groups which are dissociable. These residual amino-acid-groups that can be divided into positive and negative charged groups distributed on the surface of protein. The positive charges are contributed by histidine, lysine, arginine and, to a lesser extent, N-terminal amines. The negative groups are due to aspartic, and glutamic acids, C-terminal carboxyl groups and, to a lesser extent, cysteine. Dissociation constants, pK, of residual amino-acid-groups differ even within the same kind of group, depending on the micromolecular environment. When the sum charge of all the residual amino-acid-groups in the protein is equal to zero, this is termed the isoelectric point, pI, of the protein. The number of net negative charge increases, however, with pH above the pI.

In comparison, the net positive charge of the protein increases with a decrease in pH below the pI. In these cases the protein acts as a amphoteric compound.

Proteins are sensitive to environmental fluctuations, such as pH and temperature. Normally the optimum pH range for protein is from 4 to 9 and the optimum temperature is not more than 25 °C, If the protein environment becomes harsh, protein loses its activity, which is termed denaturation. This may be reversible or irreversible.

2.3 Ion-Exchange Functional Group And Selection

An ion-exchanger is a solid material with fixed ionisable functional anionic groups, such as carboxymethyl (CM) and sulphopropyl (SP), or cationic groups, for instance diethylaminoethyl (DEAE) and Quaternary aminoethyl (QAE). When the ion-exchange reaction occurs, the ion-exchanger with a fixed an anionic group exchanges the associated cations therefore this kind of ion-exchanger is called cation ion-exchanger. In contrast, the ion-exchanger with a fixed cationic group is called an anion ion-exchanger, since it exchanges an anion during the ion exchange. Table 2.1 gives a list of cation and anion exchangers. Both cation exchangers and anion exchangers can be further divided into strong and weak groups. Strong ionogenic groups, such as QAE and SP remain ionized over the whole operating pH normally used in protein purification while weak groups, such as CM and DEAE, have a narrow effective pH range and are largely only partly ionized.

Table 2.1 Cation and anion exchangers and effective pH range

Cation exchangers	Functional groups	Effective pH range
Sulphopropyl (SP)	$-(CH_2)_3SO_3^-$	2-12
Carboxymethyl (CM)	$-CH_2COO^-$	3-10
Phosho (PH)	$-PO_4H_2^-$	2-9
Anion exchangers	**Functional groups**	**Effective pH range**
Diethylaminoethyl (DEAE)	$-C_2H_4N^+(C_2H_5)_2$	2-9
Quaternary aminoethyl (QAE)	$-C_2H_4N^+(C_2H_5)_3C_3H_6OH$	2-11

Roe (1989) stated that the most commonly used functionalities are the weak ionogenic groups. The diethylaminoethyl (DEAE) group is usually in anion exchange to purify negatively-charged proteins while the carboxymethyl (CM) group is frequently used in cation exchange for the recovery of positively-charged groups.

Selecting the most suitable functional group for a purification the pH stability of the desired protein should be considered. Protein are amphoteric; as mentioned before, they may carry a net positive or negative charge depending on whether the buffer pH is below or above the isoelectric point, respectively. The choice must therefore be made between using an anion or cation exchanger. In practice the decision is sometimes restricted by the pH stability of the protein. If a protein is more stable above its pI then an anion exchanger should be chosen. Conversely if the protein is more stable below its pI

then a cation exchanger should be chosen.

2.4 Mechanism of Ion-Exchange Adsorption and Desorption of protein

At a given pH value, a protein is either positively charged or negatively charged and a chosen ion-exchanger is therefore ionized. The substitution reaction could involve a charged protein such as following;

$$R\text{-}CH_2COO^-Na^+ + Protein^+ \rightleftharpoons R\text{-}CH_2COO^-Protein^+ + Na^+$$

$$R\text{-}C_2H_4N^+OH^-(CH_2CH_5)_2 + Protein^- \rightleftharpoons R\text{-}C_2H_4N^+Protein^-(CH_2CH_5)_2 + OH^-$$

if the protein concentration is high enough to promote the reaction from left to right. This is known as an adsorption process and is strongly affected by ionic concentration and pH. Peterson (1970) explained that polyelectrolytes, such as proteins and amino acids, are bound to ion-exchangers through the formation of electrostatic bonds, between opposite charges on the adsorbed biomolecule; the more bonds formed, the greater the affinity. These individual electrostatic linkages are constantly dissociating and reforming as other ions, for example salt ions, compete for the binding sites. If sufficient charges of appropriate polarity are offered by the polyelectrolyte and by the adsorbent, the number of bonds formed becomes large enough to allow simultaneous dissociation which is a rare occurrence. The higher the ionic strength, the greater the number of competitive ions. These ions either compete with protein for the

sites on the ion-exchanger or weaken the electrostatic attraction between the protein and the ion-exchanger. If pH is changed which may be regarded as an increase in ionic strength with respect to hydrogen or hrdyoxyl ions, the net charge on the protein will be increased or decreased. This will also result in weakening the electrostatic attraction and reducing the degree of dissociation of the ion-exchanger.

To desorb the adsorbed protein, either salt or pH gradient or stepwise elution is usually used. Using salt elution for each particular protein of interest, the conditions should be chosen so that there is sufficient competition from the eluent ions to release it from its bound sites on the ion-exchanger, but without releasing other proteins. A pH elution changes the charge on the proteins causing them to release from the exchanger as their individual pIs are reached.

2.5 Elution Curve.

The concentration of the sample at the outlet of the column is plotted against the time or the volume from the start of the elution. This is referred to as the elution curve or elution profile.

2.6 Stationary Phase And Mobile Phase.

The mobile phase is the fluid passing through the column and its volume is the space (intraparticle space) occupied by the fluid and is usually termed the void volume, V_o. Packing material inside the column tube is called the stationary phase. Yamamoto

et al. (1988) suggested that the stationary phase could be considered to be homogeneous since it is difficult to distinguish the phase inside ion-exchangers. The total column volume, V_t minuses void volume is the volume of stationary phase, V_s.

$$V_t - V_o = V_s \qquad (2.1)$$

2.7 Operation of Ion-Exchange Chromatography

Ion-exchange chromatography can usually either be carried out in a stirred vessel or in a packed bed column. In the stirred vessel mode, a fixed volume of protein solution at a specific concentration is contacted with the ion exchanger and then agitated until equilibrium is achieved. After this the solution is drained off and the ion-exchanger is washed before the protein adsorbed is eluted by adding a suitable eluent. In the packed column bed mode. ion-exchanger is first packed into a column tube. The column is equilibrated to a buffer pH. Feed in the mobile phase flows down or up the column; the objective protein is adsorbed by the ion-exchanger, while the unbound substances can be washed out from the column bed using the starting buffer. During the elution process, the effluent from the outlet of the column is monitored either continuously or discontinuously, while solvent (eluant) is fed to the inlet of the column. The adsorbed proteins can be desorbed sequentially , since different proteins have different affinities for the ion-exchanger. These affinities are controlled by varying conditions, such as ionic strength and pH. A regeneration step might be initiated if the adsorption

capacity of the ion-exchange column has been considered to be degraded.

2.8 Ion-Exchange Chromatography Processes.

A column packed by ion-exchanger with counterion, I, (Fig. 2.1-(1) A) can be exchanged for a charged protein, Pro, once the column feed has entered the column (Fig. 2.1-(1) B). After a short time, the exchanger in the upper section of the column is completely loaded with protein ions, Pro, as counterions. Additional protein ions flow unhindered through this part of the column bed and reach the exchange zone further down, where the I counterions exchange sites quantitatively with the protein ions. The liberated I ions are eluted at the lower end of the column. As one can see, in these two stages, that there is not any protein appearance in the elution profile (Fig. 2.1-(2)). Continuing this process, the exchange zone in the column continues to migrate until it reaches the lower end and the overall process has come to the point where I and protein ions are simultaneously eluted from the column. Breakthrough takes place (Fig. 2.1-(2)) at which point the concentration of protein ions in the flow begins to increase prominently until it finally reaches the same concentration as in the feed which was initially used to charge the column (Fig. 2.1-(1) C). If the protein ions are charged once more (Fig. 2.1-(1) D), no further ion exchange can take place. The protein ions flow through the column without hindrance, as the entire exchanger already has the protein ion form. During flow through the column, the ions to be exchanged move continuously in the desired direction. In comparison to a

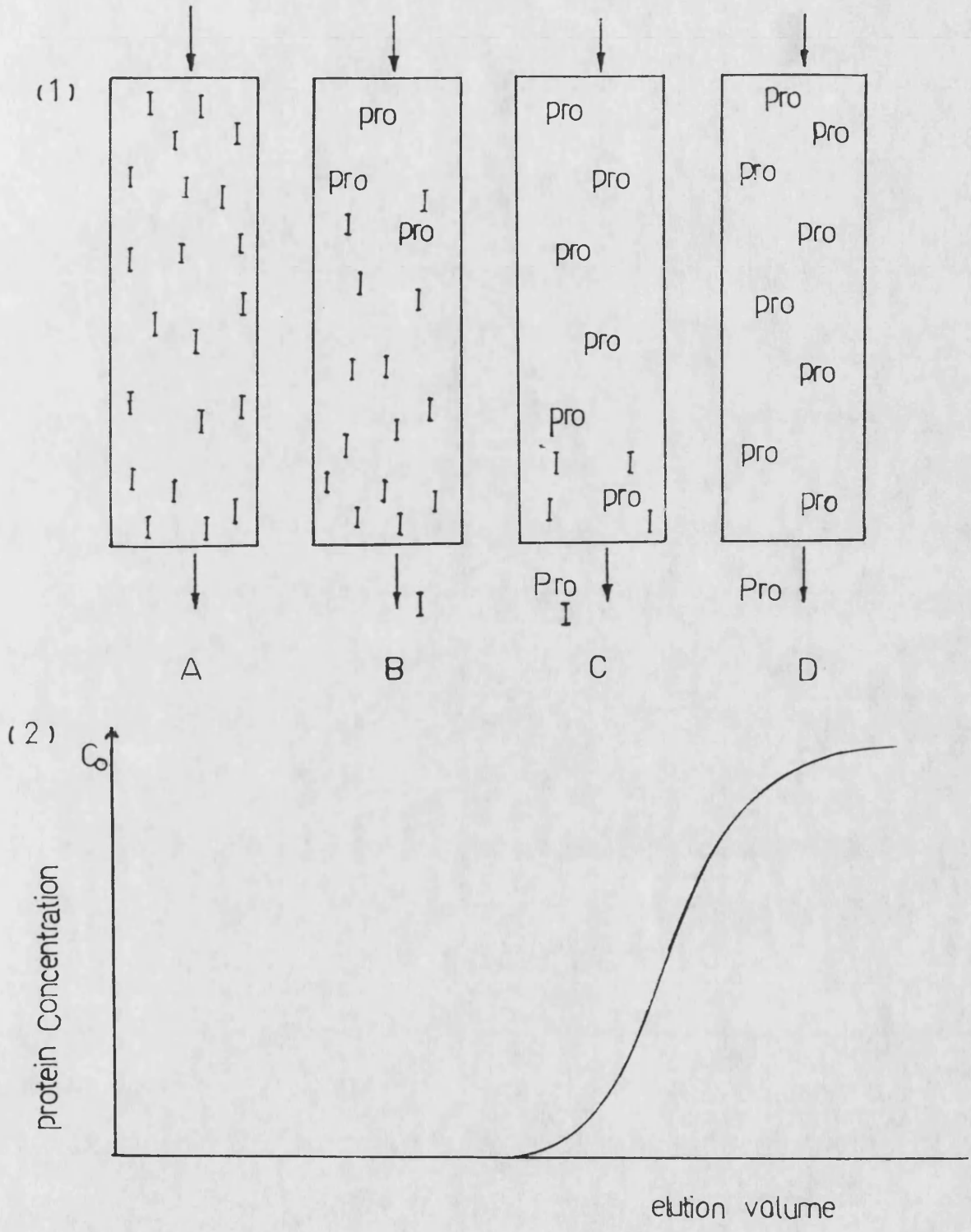

Fig. 2.1 Protein ions (Pro) and counter ions (I) exchange chromatography in a packed column.

batch techniques, ion-exchange column chromatography here becomes a complete and simple process.

2.9 Adsorption Isotherm

At a constant temperature, the protein concentration in bulk liquid and in the ion-exchanger eventually reaches a thermodynamic equilibrium. An adsorption isotherm can therefore describe the distribution of a solute between the solid phase and the liquid phase at equilibrium. The amount of protein bound by an ion-exchanger is highly dependent on the protein concentration, pH and ionic strength. A plot of the solid concentration against the residual liquid concentration, under constant temperature conditions, forms the isotherm plot.

2.10 Kinetics

In order for the protein molecules to interact with the ion exchanger they must overcome resistances present in several diffusion steps, before reaching ion-exchanger sites. These steps include: (1) transfer of protein from bulk liquid to the liquid film surrounding the particle, (2) diffusion through the liquid film, and (3) diffusion within the pores of the particle to the reaction site. Steps 1 and 2 are strongly affected by column fluid flow. All these steps are affected by temperature, viscosity, and molecular size. Ion-exchange particle size also affects the protein diffusion inside the particle. For large diameter particles, the protein needs more time to diffuse. Small ion-exchanger particles can provide more surface area per unit volume than large particle, and the protein can only be adsorbed

on the surface without necessary to penetrate the particle. The disadvantage associated with small particles is the creation of large pressure drops due to reduction in column voidage unless the particles are monodisperse spheres in which case they can be very expensive.

2.11 Ion-Exchange Capacity

The small ion exchange capacity (IEC) of ion-exchangers is the number of ion exchange sites per unit weight or volume of ion-exchanger. This is usually expressed either as the number of milliequivalents, per gram of oven dried ion-exchanger or per millilitre of hydrated ion-exchanger, or millilitre of hydrated ion-exchanger (in a packed column). For the larger protein molecules under any given conditions, there are two kinds of capacity, i.e. total protein capacity and available or dynamic capacity. Total protein capacity is the mass of protein per unit of exchangers which is measured under ideal conditions, while dynamic capacity is measured under the providing environmental condition. Protein capacity depends on a series of factors, including: porosity of ion-exchange matrix, ionic strength, concentration and the nature of the protein. Accessibility of the functional groups, pH and temperature of the eluent are also important, especially for weakly acidic and weakly basic ion-exchangers. Dorfner (1972) summarized the influence of the pH on the ion-exchanger. Since the ionic groups represent strong or weak acids and strong or weak base, they are naturally pH-dependent. Weakly acidic groups such as carboxyl groups therefore remain partially or completely associated at low pH

values, so that the exchange capacity of exchangers with such groups for protein is lower in acid and neutral solution is lower than in alkaline solution. Anion exchangers with primary, secondary, and tertiary amino groups exchange acid anions from alkaline and neutral solutions to a lesser degree than from acidic solutions. Ion exchangers with strong acid or strong basic groups (in the latter case, quaternary ammonium groups), however, are capacity-independent over a broad pH range.

2.12 Column Regeneration

Following desorption of the desired protein, some non-target proteins or non-protein material are still adsorbed on the ion-exchanger. These should be removed from the ion-exchanger to prevent a slow built-up of contamination which would result in column fouling, loss of adsorption capacity and blockage. For an ion-exchanger, usually a high salt concentration (e.g. 1 M NaCl) is used to removed the bound protein. High concentrations of NaOH (ranging from 0.2 to 1 M) is also used, to remove the very strongly bound material, to sterilize the column packing and to remove any lipids and pyrogens.

2.13 Swelling And Shrinking

Dorfner (1972) believed that the volume of an ion exchanger depends on several factors; (1)the surrounding medium (air, water, organic solvents); (2) the nature of the resin skeleton (type of matrix and cross-linking); (3) the charge of density (nature and concentration of ionic groups); and (4) the type of counterions from one medium into another and which is influenced

by the other factors is known as shrinking and swelling.

Shrinking often occurs for the column packed with non-rigid polysaccharide based medium when the flow rate is increased. Excessive shrinking during desorption conditions can also reduce recoverable protein capacity (Knight, 1967).

2.14 Scale Up

Scale up of ion-exchange chromatography is divided into two main parts; (1) the chromatographic equipment which includes the reactor material (column or stirred tank), tubing or pipes, valves, pumps, tank, monitors, sensors, fraction collector and control system; (2) the separation process which includes the flow-rate, feed load and adsorbent volume. The column bed height, linear flow rate or superficial velocity, feed concentration and ionic strength and ratio of feed to adsorbent should be optimized on a laboratory scale and then kept the same. The feed load, volumetric flow-rate and reactor diameter should be scaled up (Soffr and Nystrom,1989). In order to improve the scale-up process and obtain the information necessary for the optimal design and operation of separation, theoretical predictions as well as experimental data on the performance of the system are needed. Theoretical predictions using appropriate models developed from bench experiment and describing the performance of an ion exchange chromatography system will give an indication of the effects of important parameters. Simulation of these effects will give important guidelines for the optimal design and operation of the scaled-up process.

CHAPTER 3

REVIEW OF THE DEVELOPMENT OF THE ION-EXCHANGE PROCESS FOR PROTEIN SEPARATION

CHAPTER 3

REVIEW OF THE DEVELOPMENT OF THE ION-EXCHANGE PROCESS FOR PROTEIN SEPARATION

3.1 Ion Exchangers

Before introducing the types of ion exchanger, it is necessary to understand the physicochemical properties of some ion-exchange media, which might affect the hydrodynamics and kinetics of ion-exchange chromatography. Roe (1989) summarized the important criteria in the choice of a matrix: (1) high mechanical stability in order to have the optimum hydraulic properties, (2) chemical stability which can maintain the bed structure and allow sterilization and minimize contamination of protein mixture, (3) the matrix or at least the surface of the matrix should be inert so that the non-specific adsorption can be minimized, (4) in porous matrices, pore size must be sufficiently large to allow access of proteins to the internal surface.

In 1850, Thomspon and Way reported on the observation that cultivated soil can exchange various ions, such as ammonium ions, for calcium or magnesium ions. Adams and Holmes (1935) synthesized the phenol-formaldehyde resin, a hydrophobic ion-exchanger, which was one of the most important events in the history of ion exchangers. Ion-exchange technique however still

had not been considered for use in protein separation. Cohn (1949) might be the first person who used the ion-exchange technique for the separation of biochemical low-molecular-weight substances. Two years later this technique was applied to a automatic amino acid analyzer by Moore and Stein (1951). Hirs *et al* (1951), separated ribonuclease using an Amberlite IRC-50 ion-exchanger.

3.1.1 Cellulose Ion-Exchanger

Cellulose was used as an ion-exchange matrix by Hoffpauir and Guthrie in 1950. Cellulose is a linear polysaccharide of ß1-4 linked glucose monomers. Each glucose residue has three hydroxyl groups which makes the matrix very hydrophillic and easily derived.

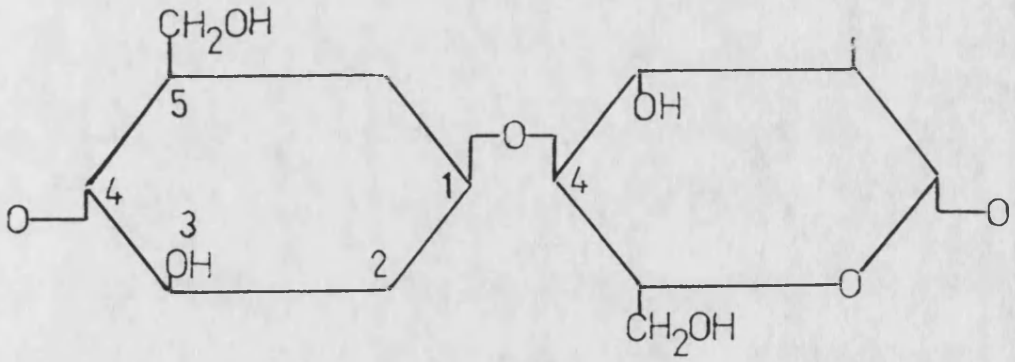

ß 1—4

Cellulose itself is relatively inert towards proteins and unstable towards mineral acids, alkalis and oxidants. Cross-linked cellulose however is stable in high concentration of HCl, H_2SO_4 and NaOH as has been demonstrated by Motozato and Hirayama (1984), Gosling (1985), Addo (1988), and Fang Ming and Howell (1990a). The pores in cellulose are formed at regions of the polymer structure where hydrogen bonding between chains is

reduced.

In 1956 Peterson and Sober published the technique of making a cellulose ion-exchanger, a hydrophilic ion-exchanger. Although the hydraulic characteristics of hydrophilic ion-exchangers were much poorer than those of hydrophobic ion-exchangers, the latter were replaced eventually by the former because of the following advantages: (1) a large pore size inside the resin to allow a protein molecule to diffuse easily in or out, and (2) the hydrophillic character ensures that the adsorbed protein is not denaturated.

Using the standard viscose-rayon process, the regenerated cellulose powders had a low porosity. This precluded their use as a separating medium for gel chromatography and limited their utility for the synthesis of ion-exchange derivatives. Ayers and Peters el at .(1984) reported that a series of insoluble cross-linked hydroxypropylated cellulose (HP-Regcell) were prepared by reacting regenerated cellulose powder with epichlorohydrin and propylene oxide in the presence of strong aqueous sodium hydroxide at a temperature of 40 °C or higher. The products had gel-like properties with pore size up to about 110 Å which can allow protein to penetrate. These porous cellulose ion-exchange powders therefore had a protein capacity as high as the high-porosity cellulose beads.

Motozato and Hirayama (1984) described the preparation of cellulose spherical particles and their ion exchangers. A

solution of cellulose tractate in a mixed solvent consisting of dichloromethane and a diluent was suspended in an aqueous medium to form droplets, then the dichloromethane in the droplets was removed by evaporation at about 38 °C to obtain cellulose triacetate beads containing the diluent. The beads thus obtained were saponified and diluent was subsequently removed to give porous cellulose beads. The cross-linking reaction was carried out by reacting the porous cellulose beads with epichlorohydrin in 4 M NaOH solution. Cross-linked DEAE-cellulose exchangers were prepared from alkali-containing cross-linked spherical particles by treatment with ß-diethylaminoethyl chloride.

Leaver (1984) and Leaver, Conder and Howell (1989) used a cellulose Vistec-DEAE exchanger to separate bovine serum albumin (BSA) from both bovine serum and plasma. The BSA separated chromatographically was superior in electrophoretic purity to that produced by the commercial Cohn precipitation method. Although they had established the optimization of the most operation parameters for scale-up, the industrial scale-up of this project was taken to a 1 meter diameter bed where good product was obtained but there was a problem of crack development in the large column bed.

Gosling (1985) investigated the cellulose sponge quaternary amine (QAE) ion-exchanger, the ion-exchange capacity of this sponge QAE ion-exchange had some similarities to both standard DEAE and QAE particulate cellulosic ion-exchangers.

Addo (1988) developed that the methods for preparation of diethylaminoethyl (DEAE), carboxymethyl (CM) and sulphopropyl (SP) derivatives of cellulose sponge. The adsorbent was characterised by measuring ion exchange capacity, protein capacity, stability and flow-rate properties.

More detailed discussion of the work of Gosling (1985) and of Addo (1988) on the sponge ion-exchanger appear in Chapter 4.

There are few publications referring to the use of high flow-rates with cellulose ion-exchanger and usually a superficial velocity of around 0.3-0.4 $m.h^{-1}$ was chosen. Levison *et al.* (1990a) using the Whatman microgranular QA52, or DE52 in a 100 ml axial flow column(66 mm x 44 mm I.D.) achieved a flow rate of up to 25 ml min^{-1}, 0.99 $m.h^{-1}$ superficial velocity, beyond which higher flow was impossible due to the compressibility of the resin. Levison *et al.* (1990b) also reported that they used a 160 x 450 mm I.D. column packed with DE 52, a microgranular cellulose anion-exchanger, at a volumetric flow rate of approximately 800 ml min^{-1} i.e., a superficial velocity of only 0.3 m h^{-1} to separate egg white proteins. As mentioned in Chapter 1, the low flow rate resulted in a low productivity.

3.1.2 Other Ion-Exchangers

Cross-linked dextran gel was developed in 1959 by Porath and Flodin. This material was not used in ion-exchange chromatography until 1971 (Porath *et al.*). Produced by the bacterium *Leuconostoc*

msenteroides, dextran (Morris and Morris, 1976) is also a polysaccharide which consists of glucose residues linked α1-6 bonds.

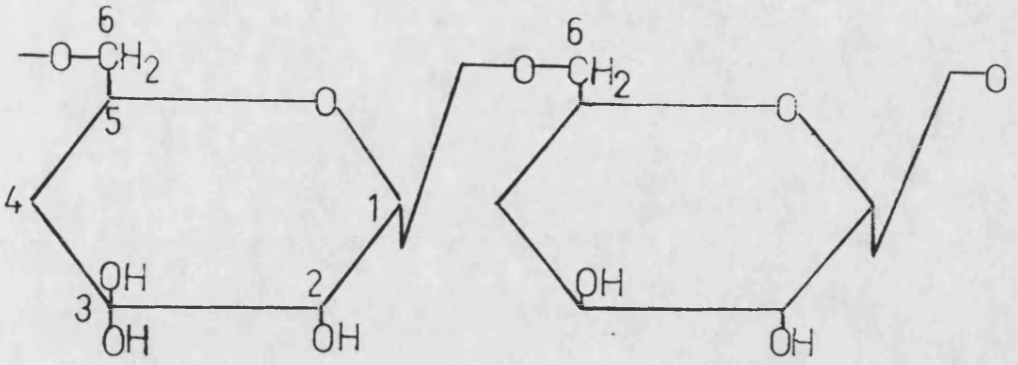

α1—6

Each residue has six hydroxyl groups providing a very hydrophillic matrix which is relatively chemically inert and easily derivatized. Dextran gels are rather soft, easily compressed and swell considerably in aqueous solutions. Cross-linked dextrans are autoclavable but biodegradable. In addition, dextran matrices are less stable than cellulose to acid hydrolysis but can withstand 0.1 HCl for up to 2 hours (Roe, 1989).

Fornsted and Porath (1989) published a simple method, which was developed about 15 years ago, for preparing cation exchangers by sulphation of cross-linked agarose. Epichlorohydrin cross-linked Sepharose (ECD-Sepharose 6B) was first washed by distilled water, ethanol and Pyridine. The suction-dried ECD-Sepharose 6B was reacted with sulphur trioxide-pyridine complex at room temperature overnight. In comparison with the capacity commercially available cation exchangers SE-Sephadex C-25 and SP-Sephadex C-50 (Pharmacia Lit. Uppsala, Sweden), they believed

that this method was still useful.

Sephadex (dextran based) ion-exchanger (Pharmacia Ltd.) is a resin with soft, gellike structures, which can be severely compressed during the column operation and its volume is very sensitive to the changes of ionic concentration. For example, Sephadex A50 can be shrunk to 72% its original volume by an increase of salt concentration from 0 to 1%. These disadvantages would make regeneration or recovery of protein bound on Sephadex A 50 very difficult in column operation (Tsou and Grham 1985).

In 1962 Hjerten reported the successive synthesis of polyacrylamide gel and agarose gel which were used as ion-exchangers. Polyacrylamide gels do not seem to be suitable for protein recovery due to the fact that the toxic acrylamides may slowly leach.

Agarose is a polysaccharide which is composed of polymeric chains of the disaccharide agarobiose (D-galactose and 3,6-anhydro-1-galactose). Agarose structure will be irreversibly changed if the structured water of agarose is lost. Drying should be avoided.

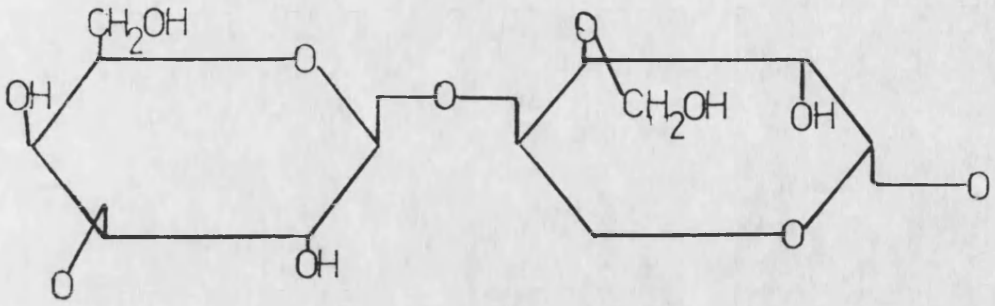

Porath and Fornstedt (1970) described a method for preparation of arginine-and sulphanilic acid-agarose. A Sepharose 6B (obtained from Pharmacia Fine Chemicals, Uppsala, Sweden) was first cross-linked by epichlorhydrin in 1 N NaOH at 60 °C for two hours. The cross-linked Sepharose 6B was then reacted either with arginine in 0.01 N NaOH at 60 °C for two 2 hours, or with sulphanilic acid in 2 N potassium carbonate buffer for 6 days.

Bite *et al.*(1987) described" Macrosorb Kieselguhr-Agarose Composite Adsorbents" as new tools for downstream process design and scale-up. This adsorbent which is mainly intended for HPLC system was made by filling the macropore volume of rigid Kieselguhr beads (45% of total particle volume) with a cross-linked agarose gel containing ion-exchange groups.

Silica matrices (Bernardi, 1971) are formed by the acidification of sodium silicate to form a sol of orthosilicic acid which is subject to polycondensation during ageing to yield silica particles.

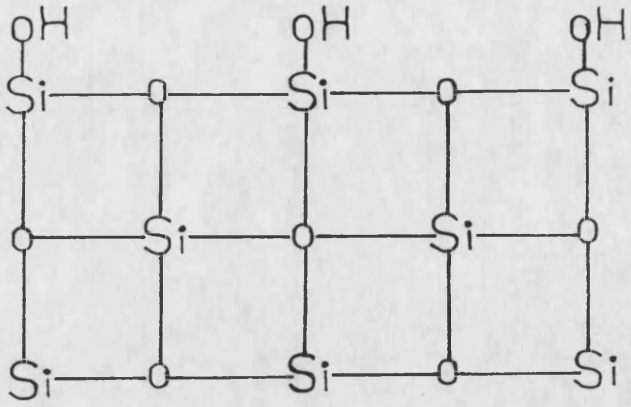

Silica matrices are incompressible, unaffected by organic solvents and mechanically stable but gradually dissolve above pH 8. Small particle ion-exchangers, about 10 μm in diameter, for example silica gel and hydrophilic porous vinyl polymer gel were reported respectively by Chang *et al.* (1976) and Kato and Komiga (1982).

Alpert and Regnier (1979) developed a hydrophilic anion-exchange material. Polyethyleneimime and simpler amines were adsorbed to porous, microparticulate silica so strongly that the adsorbed coating might be cross linked into a stable layer by a wide variety of reagents in organic solution. They claimed that this porous microparticulate ion-exchanger was quite reproducible and of high ion-exchange capacity.

Spherosil$^{(R)}$ ion-exchange (Rhone Poulenc) was also made by coating silica with a co-polymer of styrene divinyl triethoxysilane to which the functional groups were attached (Thomson, 1984).

Conventional and medium-performance anion exchangers (Pharmacia's DEAE-Sephacel, DEAE-Sepharose CL-6B, DEAE-Sephadex A-25 and A50; Whatman's DEAE-Cellulose DE52 and DE-23; Toyo Soda's DEAE-Toyopearl 650s and 650M; LKB's DEAE-Trisacry M and BIo-Rad Labs' DEAE-Bio-Gel A) were compared for proteins separation with respect to titration curve, protein adsorption capacity, pore size, mechanical stability, swelling property and resolution in column chromatography by Kato and Nakamura *et al.*(1982). Under the conditions used, although each anion exchanger had different characteristics, the properties of DEAE-Toyopearl 650s seemed to be advantageous over other anion exchangers.

Artificial polymer-based ion-exchange adsorbents such as Trisacryl$^{(R)}$ (LKB-produker AB, 1984) and MonoBeads^{TMO} (Pharmacia AB, 1985) were developed respectively in 1984 and 1985.

Bio-Rad Laboratories (1990) published a bulletin to introduce new Macro-Prep^{TM} 50 ion exchanger which is based on pressure stable polymeric supports.

3.2 Brief Review The Development of Ion-Exchange Theory

In 1959 Helfferich summarized the theoretical aspects of equilibrium isotherm and adsorption/desorption kinetics of the ion-exchanger. Peterson (1970) summarized the characteristics of cellulosic ion-exchanger, the method of column preparation and the effect of various factors on the separation of proteins.

Applying equilibrium data and a simple two-film theory, Graham *et al.* (1982) described the rate data which showed that during the initial period of adsorption the rate was controlled by film diffusion, after which it was controlled by intraparticle diffusion. The desorption was largely intraparticle diffusion controlled except for a very short surface desorption step.

Yamamoto *et al.* (1983a,b) investigated, theoretically and experimentally, gradient elution in ion exchange chromatography of protein. By applying a continuous-flow plate theory, they described the effect of linear and stepwise increases of ionic strength on elution characteristics (peak position and width). While their results for the retention time (first moment) were identical to those of the Kang and McCoy (1988), the approach to band-broadening, based on a plate theory, required some simplifying assumptions. Despite the approximations in Yamamoto *et al*'s work, they convincingly demonstrated how a simple analysis of small scale experiments can guide the design and operation of large-scale separation of protein by ion exchange chromatography. Kang and McCoy (1988) continuously investigated the model for gradient elution in that extended for the first time the moment theory to gradient elution in ion-exchange chromatography; (2) considered linear, exponential, and step gradients; and (3) related retention time (first moment) and band spreading (second moment) to separation efficiency for gradient elution processes.

Tsou and Graham (1985) investigated the equilibrium and

kinetic adsorption and desorption of bovine serum albumin (BSA) on Sephadex A50 (dextran-based ion-exchanger, Pharmacia Ltd.). They found that; (1) DEAE Sephadex A50 was very sensitive to ionic strength. An increase in salt concentration from 0 to 1% caused the swollen exchanger to shrink by as much as 72% of its original volume; (2) the kinetics of desorption of BSA in a batch system showed a very fast initial rate due to the rapid shrinkage of the ion-exchanger with changed in salt concentration. They developed a model included a protein exclusion term caused by shrinkage in kinetics for desorption. The shrinkage of resin could enhance the desorption rate, as they stated, the flow rate of the column was not stable due to shrinkage of resin. In order to achieve a designed flow rate, the column needed to be stabilised by passing the buffer at a flow-rate which was higher than the design flow rate for 1-2 hours. This indicated that although the shrinkage could enhance the desorption rate, but that the flow-rate was difficult to control.

Gosling (1985) used bovine serum albumin as a model protein and anionic type quaternary amine cellulose ion-exchanger to investigate the effect of ionic strength of small ions on the adsorption isotherm. It was found from experiment that each mole of BSA protein exchanged with 10-15 moles of chloride ions.

Addo (1988) developed a two shells model based on Graham *et al.* (1982)'s two-phase resistance model. In the two shells model, it is assumed that a sponge fibre consists of a macroporous shell and a solid core. Adsorption occurs first in the macroporous

shell at a rate governed by external mass transfer. Intraparticle diffusion only occurs within the solid core, following saturation of the outer shell.

Maa and Antia *et al.* (1988) investigated protein retention using a high-performance liquid chromatography columns packed with mixtures of different types of cation and anion exchangers. Separation of a mixture of lysozyme, ovalbumin, conalbumin and chymotrypsinogen A were carried out on the mixed bed column by using gradient elution. This process was modelled mathematically. Retention factors at both low and high salt concentration in the eluent and their dependence on the bed composition was found to be linear in some cases, but non-linear in others. The retention times predicted by computer calculations correspond closely to the experimental findings. They suggested therefore that the mixed-adsorbent columns would find extensive use in the large-scale purification of biological compounds and in routine analysis.

Yamamoto *et al* (1988) described comprehensively ion exchange chromatography of proteins and enzymes. He treated the Chromatographic theory on two levels so that both the chemical engineering scientist and the nonengineer are served. The mixing-cell transport-rate models applied by the authors to attain expressions for temporal moments of concentration responses, leading to equations for separation resolution and number of theoretical plates are demonstrated. How each variable affects the separation, based on the theoretical principles and

experimental evidence are also discussed. As McCoy (1989) commented, aside from a few sentences that could have been edited into more conventional modern English, Yamamoto *el at*'s book is clearly and carefully written.

Smith and Gillespie (1989) used potentiometric acid-base titration to investigate the ionization of DEAE-cellulose dependence of pK on ionic strength. They found that two ionizable groups were identified. The pK of the major group was exponentially related to ionic strength, while the minor group was very much less sensitive to changes in ionic strength.

Whitley and Brown *et al.* (1989) applied an impulse technique to determine the Langmuir isotherm parameters of amino acids and proteins. The ion-exchange column was approximated as many stages in series. Within each stage, the mass transfer rate of a given solute between mobile and stationary phase was finite. Response to pulse and step changes were calculated using a fast and stable algorithm. The equilibrium parameters were estimated by comparing the responses with the experimental data. The accuracy of estimation of the equilibrium parameters depends strongly on the pulse volume and pulse concentration. The stage model represented pulse data as closely as a more detailed rate equation model while requiring two orders of magnitude less computation time. This technique also offered a fast alternative to the conventional batch equilibrium and frontal analysis methods for determining equilibrium isotherms.

Gosling *et al.* (1989) described the role of adsorption isotherms in the design of chromatographic separations for downstream processing. He accounted for the error associated with the experimental measurements by expressing the isotherm parameters as a range rather than a single value. The largest errors were associated with measuring the difference between two high solution concentrations in the adsorption stage and in the presence of high concentrations of eluant. When measuring isotherms to determine competition effects, the use of different masses of adsorbent and different volumes of solution unnecessarily complicates data interpretation. It is easier to vary the initial solution concentration and maintain a constant volume of solution and constant mass of adsorbent.

Skidmore and Horstmann *et al.* (1990), using the strong cation exchanger S Sepharose FF, compared the rate of protein adsorption in two different models. The first model was based on a single lumped kinetic parameter, whilst the second model considered the individual transport processes occurring prior to the adsorption reaction. They took into account diffusion across the liquid film surrounding individual particles and also the diffusion within the ion-exchanger particle itself. They found that the adsorption of lysozyme to S Sepharose FF, in both batch, agitated tanks and in packed bed was consistent with both models. In the case of BSA, however, the agitated tank adsorption profile was consistent only with the pore diffusion model and neither model correctly predicted the latter part of the breakthrough profile observed in packed-bed experiments.

3.3 The Considerations For Further Development

As Ayers *et al.*(1984) claimed that, in comparison with the above mentioned ion-exchanger matrices for protein separation, cellulose being robust and abundant is an obvious choice for preparing an inexpensive ion-exchanger matrix for industrial chromatography. Although the cellulose ion-exchangers of bead and microgranular types have been commercially available, the problems of low flow-rate and slow kinetics have not been solved. Making the cellulose sponge ion-exchanger by taking into account the high flow-rate of the raw cellulose sponge, Gosling (1985) achieved the superficial velocity to be 1.83 m/h in a 20 x 20 mm I.D. column, but the protein capacity was rather low (200 mg BSA/g for QAE). Addo (1988) improved the protein capacity of cellulose sponge to be 610-1000 mg lysozyme/g for CM sponge and the superficial velocity to be 2 m/h in a 31 x 43 mm I.D. column. Apart from the superficial velocity and protein capacity are still lower than that are expected, the problem of short life of product is also not solved. A new technology and recipe for making the ideal cellulose sponge ion-exchanger obviously needs to be developed.

In addition, there are two aspects in the modelling and parameter estimation might need to be further considered. Firstly, by taking into account the time for on-line parameter estimation, a fast calculation method is needed to replace the finite difference method to solve the second order partial differential equation. Secondly, the models developed for protein separation so far were either treated the ion-exchanger as a

homogeneous model, such as either only the pore diffusion or only the solid diffusion was considered, or as two distinguished parts which was a solid core surrounded by a macropore shell. In fact, cellulose, dextran and agarose are the porous matrices. Pores are randomised within the matrix. When the matrices are saturated with the liquid, the pores are filled with the liquid which is regarded as a liquid phase. The matrix is therefore heterogenous which consists of liquid phase and solid phase so that the diffusion is simultaneously occurred within these two phases. A heterogeneous model therefore might need to be developed.

CHAPTER 4

MANUFACTURE OF SPONGE ION-EXCHANGERS

CHAPTER 4

MANUFACTURE OF SPONGE ION-EXCHANGERS

4.1 Introduction

It is not novel to make sponge ion exchangers. The prior methods which will be discussed in following section lead to products which have serious disadvantages such as poor mechanical properties, low protein capacity and short life. Hence these sponge ion exchangers have not previously appeared on the market. The main aim of the experiments described here was to discover a method or a recipe which can produce a cellulose sponge ion-exchanger with high protein capacity, high flow-rate and robustness.

Firstly, the research strategy needed to be established. Secondly it was focused on the CM type of ion-exchanger to optimize the conditions which might later be applied to develop other types of ion-exchangers. Owing to considerations of cost, environmental aspect and recovery problems in large scale manufacture, water was chosen as a reaction medium rather than organic solvent. As there is little information about the stochiometrical calculation of cross-linking reaction and derivative reaction in making cellulose ion-exchangers, nor quantitative criterion for the physical and chemical properties of the cellulose ion-exchanger, the successful recipes were therefore determined empirically through methodical experiment.

As the experiments were carried out stage by stage, in order to decide on conditions for the next stage, some characteristics of the semifinished product and finished product needed to be established. These characteristics are therefore discussed in this chapter rather than in chapter 5 where the remaining characteristics are discussed.

4.2 Cellulose Sponge

Addo (1988) summarized the process of making cellulose sponge. An aqueous cellulose xanthate solution known as viscose, is produced by adding carbon disulphide to solve the natural cellulose, which is then regenerated back into an insoluble cellulose by the addition of acids, or by heat treatment (Peska *et al.*, 1976). In order to make a porous structural cellulose sponge, hydrated sodium sulphate in small crystals is added to the cellulose xanthate solution during the regeneration stage. Cotton or hemp fibres are added and the cellulose xanthate-crystal paste is decomposed by heat coagulation to cellulose. After regeneration, the sodium sulphate crystal is washed out to leave a porous sponge structure containing both macropores and micropores. In comparison with the native or microcrystalline cellulose, the degree of polymerisation of the cellulose molecules is lower, the amorphous structure is higher and the stability of cellulose sponge for swelling in alkali thus is lower.

Fig. 4.1 (end of this chapter) shows the cellulose sponge which was produced by Spontex Ltd.. A nylon net is laid inside

the cellulose sponge for reinforcement. Fig 4.2 and 4.3 (end of this chapter) are respectively the cross section and longitudinal section of cellulose sponge. Fig.4.4 (end of this chapter) is the surface of the cellulose sponge which has less voidage than that of the interior cross section. Through Fig. 4.1 to 4.4, it can be seen that cellulose sponge is constructed of amorphous filaments, flakes, hemps and fibres with a very open structure. These "fibres" have dimensions of length and width, ranging from 5 to 80 μm. Moreover, it is evident that the density of sponge is lower than that of particle ion-exchanger because of the high voidage of the sponge (0.95 voidage measured by Gosling 1985).

4.3 Considerations

As cellulose sponge has a very open structure and a high voidage it can allow a high flow-rate. Several points should be borne in mind. The structure of sponge must be maintained after conversion into an ion-exchanger and it must be stable during normal operation and regeneration procedures. As the density of sponge is low, a high protein capacity is therefore essential to ensure that the volumetric capacity of sponge should be higher than or approximately equal to that of the particle, otherwise this kind of novel ion-exchanger would not be adopted by the market.

4.4 Cross Linking

As was mentioned in section 4.3, cellulose sponge is unstable in alkali and acids. It is necessary therefore to cross link between the polysaccharide chains to enhance the robustness

of the cellulose sponge. Table 4.1 gives a list of cross-linking reagents, of which dichlorohydrin and epichlorohydrin were used in this study due to the less toxic and readily obtainable. In the cross-linking reaction, halogen or epoxy groups of dichlorohydrin and epichlorohydrin react with the hydroxyl group on the polysaccharide in aqueous sodium hydroxide.

Table 4.1 cross-linking reagents

Chemical	Formula
1,3-dichloro-2-propanol (Dichlorohydrin)	$Cl-CH_2-\underset{OH}{CH}-CH_2-Cl$
1,3-Dibromopropanol	$Br-CH_2-\underset{OH}{CH}-CH_2-Br$
1-chloro-2,3-epoxypropane (Epichlorohydrin)	$\underset{\diagdown O \diagup}{CH_2}-CH-CH_2-Cl$
1,2:3,4-Diepoxybutane	$\underset{\diagdown O \diagup}{CH_2}-CH-\underset{\diagdown O \diagup}{CH}-CH_2$

The functions of sodium hydroxide are to swell the cellulosic sponge and to convert the cellulose, polysaccharide, into the sodium cellulose, that is:

$$Cel\text{-}OH + NaOH \text{ -----> } Cel\text{-}ONa + H_2O$$

where Cel-OH represents a hydroxyl group of a glucopyranose unit of the polysaccharide. The sodium cellulose is then substituted either by cross-linking reagents such as dichlorohydrin or epichlorohydrin,

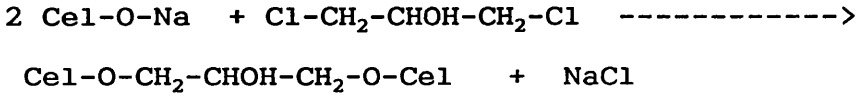

The cellulosate, sodium cellulose, reacts with the chloride terminus of the epichlorohydrin molecule by a nucleophilic displacement mechanism to form cellulose ethers, while the epoxy ring opening is catalysed by the base and then couples with the cellulosate ion (Morrison and Boyd 1973).

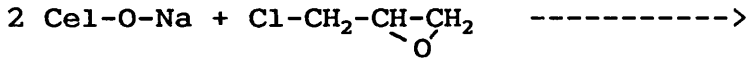

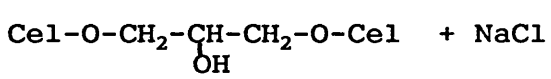

The stabilities and mechanical properties of cross-linked cellulose sponge are directly proportional to the degree of cross-linking. In direct contrast, the higher the degree of cross-linking , the lower the protein capacity. Selectivity also depends on the degree of cross-linking. Knight et al. (1966) and Grant (1971) proposed that the degree of cross-linking of cellulose ranged from 1 to 20% in terms of the volume of cross-linking reagent to the dry weight of cellulose.

4.5 Derivative Reaction

The most commonly used derivative reagents are the aliphate range of compounds with either a halogen group or an epoxy group (Table 4.2). These two functional groups react with the hydroxyl groups on the glucopyranose units of the cellulose which have been activated by sodium hydroxide. The remaining terminal of the derivative reagents is responsible for imparting the ion exchange

Table 4.2 Derivative reagents

Chemical	Formula
Sodium chloroacetate	$Cl-CH_2-COONa$
1,3-Propanesultone	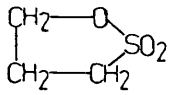
Sodium 2-chlor(alkyl)-sulphonate	$Cl-(CH_2)_n-SO_3Na$ (n=1 or 3)
Chloromethylphosphonic acid	$Cl-CH_2-PO_3H_2$
Diethylaminoethyl-chloride hydrochloride	$Cl-CH_2-CH_2-N(C_2H_5)_2$ HCl

properties. The reaction steps are as following

(1) $Cel-OH + NaOH \longrightarrow Cel-ONa + H_2O$

(2) for sodium chloroacetate

$$Cel-O-Na + Cl-CH_2-COONa \longrightarrow Cel-O-CH_2-COONa + NaCl$$

for the diethylaminoethyl chloride

$$Cel-O-Na + Cl-CH_2-CH_2-N(CH_2CH_3)_2 \longrightarrow Cel-O-CH_2-CH_2-N(CH_2CH_3)_2 + NaCl$$

and for 1, 3-propanesultone

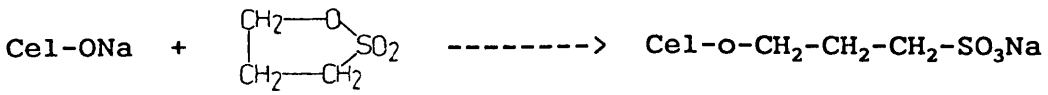

Usually water is used as the reaction medium in both cross-linking and derivative reactions. Organic solvents such as isopropanol or benzene could be used in order to produce a more uniform product. Grant (1971) and Knight (1966) suggested that isopropanol could be used to make the strongly acidic sulphonate cellulose because the isopropanol might control the greater swelling tendency of the cellulose derivative during the reaction. The temperature to be considered could range from 20 to 120 °C.

4.6 The Development of Cellulosic Sponge Ion-exchanger

The cellulose ion-exchanger, as Dorfner (1972) described, is hydrophillic in contrast to the hydrophobic polystyrene ion-exchanger. As a result of the fibrous properties of cellulose, *i.e.* its loose network cross-linked by hydrogen bridges, the majority of active exchange groups located at distances of about 50 Å along the chain can become activated for the exchange of large molecules. Within the cellulose structure, the cellulose molecule has hydroxyl groups at the carbon atoms 2, 3, and 6, to which the active exchange groups are bound, of which 2 and 6 are the most reactive. Because of the heterogeneous nature of the cross-linking or the ligand attachment reaction, it should be kept in mind that unmodified cellulose molecules are also present in the exchangers, while others are mono-, di-, or trisubstituted.

Most of the work on cellulose ion-exchangers is described in patents, there are very few other publications on the manufacture of cellulosic ion-exchangers. Hoffpauir and Guthrie (1950), described the characteristics of chemically modified cotton fabrics which could be used as an ion-exchanger. In 1956, Peterson and Sober showed a method of making carboxymethyl cellulosic powder without using any cross linking reagent. In 1963, Jones *et al.* declared the invention of a cellulosic sponge ion exchanger. They described the manufacture using 6.6%w/w sodium chloroacetate and 12%(w/w) sodium hydroxide with a piece of dried sponge cloth at temperature 30 °C for 16.5 hours. Three years later, Knight *et al.* (1966), claimed that the known methods to make ion-exchange cellulose had several disadvantages, for example, being difficult to pack as a uniform column . They then described their own method to prepare a cellulosic ion-exchanger using the following steps:

A. treating a cellulosic material with acid to remove the amorphous regions of the cellulose,

B. mercerising the resulting acid-degraded product using 17%w/w to 46%w/w alkali solution,

C. reacting the cross-linked mercerised product with a reagent to form the desired cellulosic ion-exchange material.

This might be the basic method of the Whatman range of microgranular ion-exchangers. Determann and Pharmacia (1970, 1976) published patents which covered the manufacture of regenerated cellulose in bead form and its ion-exchange derivatives. Three patents from Grant (1971) and Ayers (1980)

which described the preparation of granular and cross-linked hydroxypropylated regenerated cellulose might be the basis for manufacturing the Indion range of industrial ion-exchanger. This following recipe was used by Grant (1971):

10 g	cellulose powder or sponge cloth
3.3 g	diethylaminoethyl (chloride hydrochlorride, DEAE)
6.5 ml	30 %w/v NaOH
0.1 ml	epichlorohydrin.

Gosling (1985) made a QAE sponge ion-exchanger with an available protein capacity of around 100 mg (BSA)/g using the following recipe:

2 g	sponge
5 ml	epichlorohydrin
15 ml	triethylamine
50 ml	water
0.2 g	NaOH

and heated to 120 °C for 30 minutes. Protein capacity could not be raised above 200 mg (BSA)/g, otherwise the product disintegrated. Gosling stated that: (1) it might not necessarily be an advantage to increase the ion-exchange capacity because this affected the swelling, (2) good stability and a low degree of swelling were just as important as a high ion-exchange capacity, and (3) although the derivative procedure was successful it was rather wasteful of reactants, being 5% efficient.

The protein capacities of sponge ion-exchangers made by Addo (1988) were higher than of these made by Gosling. The flow-rate properties of these ion-exchangers, as Addo (1988) claimed, were however moderate in comparison with the Phoenix regenerated cellulose granules and Pharmacia Fast Flow Sepharose. For example, in a short column bed dimension of 31 x 43 mm I.D., the maximum superficial velocity only reached 2 m/h at a back pressure of 2 bar. Addo's standard recipe for making CM cellulose sponge was as follows:

5 g	cellulose sponge cloth
5 ml	25% NaoH
1.25 g	reagents (might be dichlorohydrin and sodium chlorohydrin)
3 ml	water

The protein capacity of CM sponge was 610-1000 mg (lysozyme)/g.

4.7 Materials

Cellulose sponges were purchased from Sainsbury supermarket. The cellulose sponges included white strip sponge (Spontex Drip Strip) which was produced by Spontex Ltd. Maritime Quarter, Swansea, U.K.. Epichlorohydrin, dichlorohydrin, and sodium chloroacetate were purchased from BDH Ltd., Pool, Dorset. Diethylaminoethylchloride hydrochloride, 1,3-propane sultone were purchased from Sigma Chemicals, Pool, Dorset.

Lysozyme (from chicken egg white, grade 1) and Bovine serium albumin (BSA) fraction V powder (96-99% albumin) were purchased from Sigma Chemicals, Poole, Dorset. All other reagents were of

the highest quality commercially available.

4.8 Experimental Methods

Method for determining the stability of cellulose sponge in aqueous sodium hydroxide. A 20 x 20 mm piece of cellulose sponge was immersed in a series of beakers with different concentrations of sodium hydroxide for a designed time. The cellulose sponge was then taken out and carefully washed with water to remove the NaOH. The appearance (occurence of gel) and the ability of the modeified sponge to regain its original store after compression were observed in comparison with the original sponge.

Method for cross-linking. Cross-linking reagent was dissolved in the NaOH solution and then liquid was applied to a air dried sponge. The sponge was gently squeezed several times to expel entrapped air and then the sponge was placed in a covered tray in 100°C oven for a designated period of time. The cross-linking sponge was washed with water.

Method for derivative reaction. Air dried cross-linked sponge was allowed to soak up sodium hydroxide solution containing sodium chloroacetate. The sponge was slightly squeezed several times to expel the air in the sponge. Excess liquid was removed from the sponge by gently squeezing. The moist sponge was placed in a covered tray with and reacted at 100°C oven for the required time. After cooling down the ion-exchange sponge was washed with distilled water until the pH value was neutral.

Method of protein capacity. (1) Lysozyme capacity; Sponge

ion-exchanger was cut into approximately 3 x 3 x 3 mm piece and was equilibrated with 0.4 M sodium acetate duffer, pH 5 for 4 hours. The sponge was washed with 0.01 M sodium acetate buffer, pH 5 until the conductivity of the sponge was the same as the 0.01 M sodium acetate buffer, and then the imbibed water in the sponge was removed by suction on a Bucher funnel followed by blotting with tissue paper until the sponge was damp dry. In order to calculate the water content of the damp dry sponge, a piece was weighed and then left in an oven at 110 °C overnight. The water content was obtained by comparing the weight of oven dry sponge with that of the damp dry sponge. The weighed damp dry sponge was placed into a beaker containing 10 mg/ml lysozyme solution, in 0.01 M sodium acetate buffer, pH 5. The beaker was placed in shaker at a constant 15 °c overnight. The residual lysozyme concentration was determined by a ultraviolet spectrophotometer at 280 nm.

(2) BSA capacity; The protein capacity of anion exchanger was evaluated using 5 mg/ml BSA in 0.01 M Tris-HCl buffer, pH 8. The process was the same as the method of determining lysozyme capacity, except that the buffer was changed to Tris-HCl buffer, pH 8.

4.9 Results and Discussion

4.9.1 Stability of Cellulose Sponge in Aqueous Sodium Hydroxide.

The results are shown in Table 4.3, The cellulosic sponge can withstand 6.5% sodium hydroxide solution for 10 minutes at

18°C without being visibly damaged, while 7.5 % NaOH can damage the sponge in even 30 seconds. A critical NaOH concentration point could be considered to lie between 6.5 and 7.5% at 18 °C.

Table 4.3

reaction time(min)	concentration of sodium hydroxide (w/v)			
	6.5	7.5	10	15
0.5	+	++	+++	++++
3	+	++	++++	++++
10	+	+++	++++	++++

\+ sponge structure was maintained with good springiness
++ sponge structure was maintained but with poor springiness
+++ slight gel-like material was on the surface of sponge
++++ part of the sponge was disintegrated and gel-like material was formed.

4.9.2 Degree of cross-linking of Sponge Ion-Exchanger

Based on the results of Table 4.3 , another experiment was designed to optimize the concentration of sodium hydroxide between 0.1 M and 2 M using a fixed concentration of cross-linking reagent, 4%(v/v) dichlorohydrin. The reaction temperature was also fixed at 100 °C in the oven. A 30 x30 mm piece of air dried sponge was added and fully saturated in a series of beakers containing 4%(v/v) dichlorohydrin in different concentrations of sodium hydroxide (Table 4.4). The saturated sponge was then removed to a 100 °C oven to be cross-linked at a different time. Thereafter the cross-linked sponge was immersed in 30 %(w/v) sodium hydroxide solution for 40 minutes and then was washed by water. The mechanical properties of these cross-linked sponge were examine whether the product being visibly damaged.

As showed in Table 4.4, the cellulosic sponge which was cross-linked by 4%(v/v) dichlorohydrin in 1 M NaoH solution at 100 °C oven was stable in 30%(w/v) NaOH solution at ambient temperature. The results of using low concentration NaOH, equal to or below 0.5 M, the mechanical properties were rather poor which indicated that the cross-linking reaction in the sponge might not be sufficient for stability. Increasing the reaction time might improve the degree of cross-linking in the sponge, but the manufacturing cost would increase. Using 2 M NaOH solution probably gives sufficient cross-linking for stability, but some part of sponge was damaged before the cross-linking reaction took place . This explanation is confirmed in 4.9.1.

Table 4.4

NaOH solution (M)	reaction time (min)	comments
0.1	30	+++++
	60	+++++
0.3	30	++++
	60	++++
	10	+++
0.5	30	+++
	60	+++
	10	+
1	30	+
	60	+
	10	++
.2	30	++
	60	++

\+ sponge structure was maintained with good springiness
++ sponge structure was maintained but with poor springiness
+++ slight gel-like material was on the surface of sponge
++++ part of sponge was disintegrated and gel-like material was formed
+++++ sponge was disintegrated.

The experiment reported in Table 4.5 was to determine the optimum amount of dichlorohydrin in the 1 M NaOH solution, and used the same procedures as those in Table 4.4, except that the series of beakers were treated with different concentrations of dichlorohydrin in 100 ml of 1 M NaOH solution . From Table 4.5 it appears that the concentration of dichlorohydrin should be more than 2%(v/v). Below 2%(v/v), the degree of cross-linking in sponge was too low.

Table 4.5

Dichlorohydrin concentration in 1 M NaOH % (v/v)	comments
1	between +++ and ++++
2	++
3	+
4	+

An optimum cross-linking procedure was adopted from the results of Table 4.3, 4.4 and 4.5, which requires

50 g	cellulosic sponge (air dried)
8-18 ml	dichlorohydrin
200-450 ml	1 M NaOH solution

The dichlorohydrin was dissolved in the 1 M sodium hydroxide

solution, then it was applied to the air dried sponge. The sponge was slightly squeezed to expel the air in the sponge, excess liquid was removed from the sponge by gently squeezing . The moist sponge was placed in a tray with a cover and reacted at 100 °C in an oven. The reaction time could range from 10 to 60 minutes to allow the temperature to reach 100 °C depending on the amount of sponge.

4.9.3 Derivative Reaction for Making CM Sponge

In order to allow more ion-exchange groups, such as carboxymethyl, to be introduced, a high concentration of NaOH solution is needed to swell and activate the remaining hydroxyl group in the cross-linking sponge. At this stage, it might not be necessary need to consider that the excess degree of derivative would cause excess swelling because the sponge has been cross-linked.

It can be seen from Table 4.6 that the lysozyme capacity of CM sponge was not dramatically raised by increasing the concentration of NaOH solution to 30%(w/v). Increasing the concentration of sodium chloroacetate in the NaoH solution results in a decrease in the protein capacity, and also it was difficult to dissolve in the NaOH solution.

Table 4.6 Effect of NaOH and sodium chloroacetate concentration on the protein capacity

cross-linked sponge weight (g)	NaoH concentr. (w/v)	$ClCH_3COONa$ in NaoH solution (%w/v)	liquid volume (ml)	lysozyme capacity (mg/g)
1.67	20	20	14.2	1350
1.67	20	30 *	14.2	1332
1.67	20	40 *	14.2	1008
1.67	30	20	14.2	1492
1.67	30	30	14.2	1292

* difficult to dissolve in NaOH solution
reaction at 100 °C oven for 1 hour

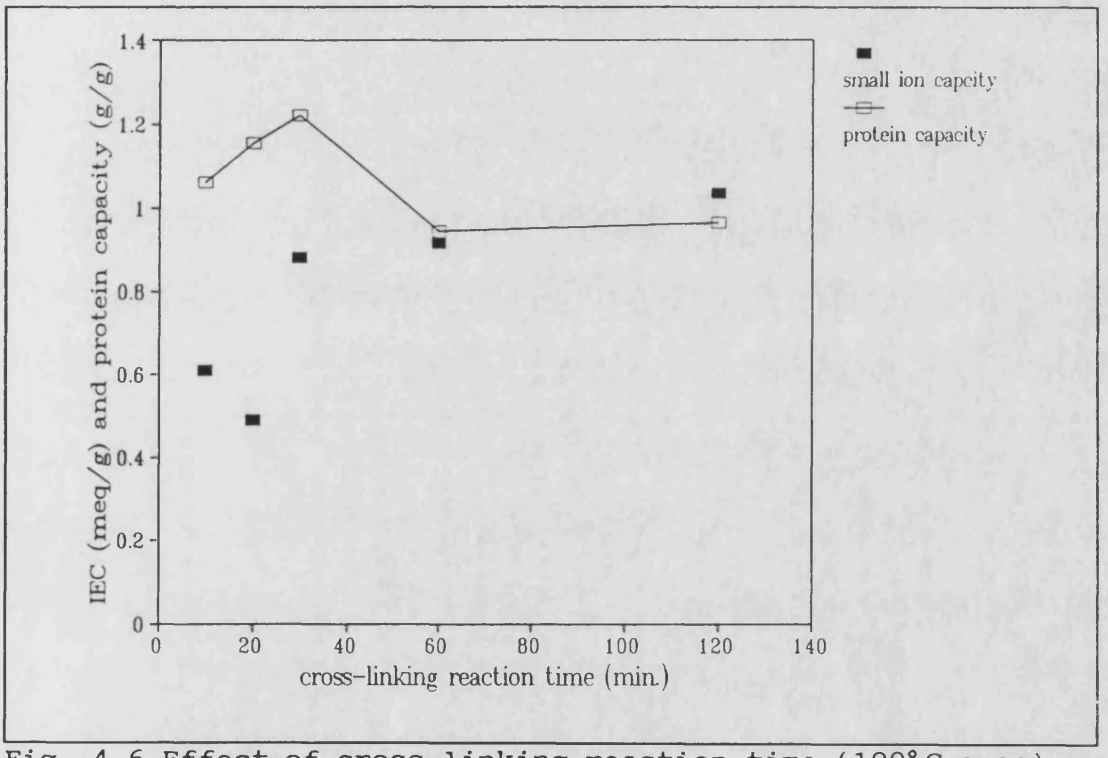

Fig. 4.6 Effect of cross-linking reaction time (100°C oven) on CM sponge protein capacity and total equilibrium weight capacity (IEC).

The lysozyme capacity of CM sponge increased with the reaction time from 10 to 30 minutes, and then slightly reduced by further increasing the reaction time from 60 to 120 minutes, The total equilibrium weight capacity (IEC) however, increased

with the reaction time. The lysozyme capacity seemed to be proportional to the IEC (Fig.4.6).

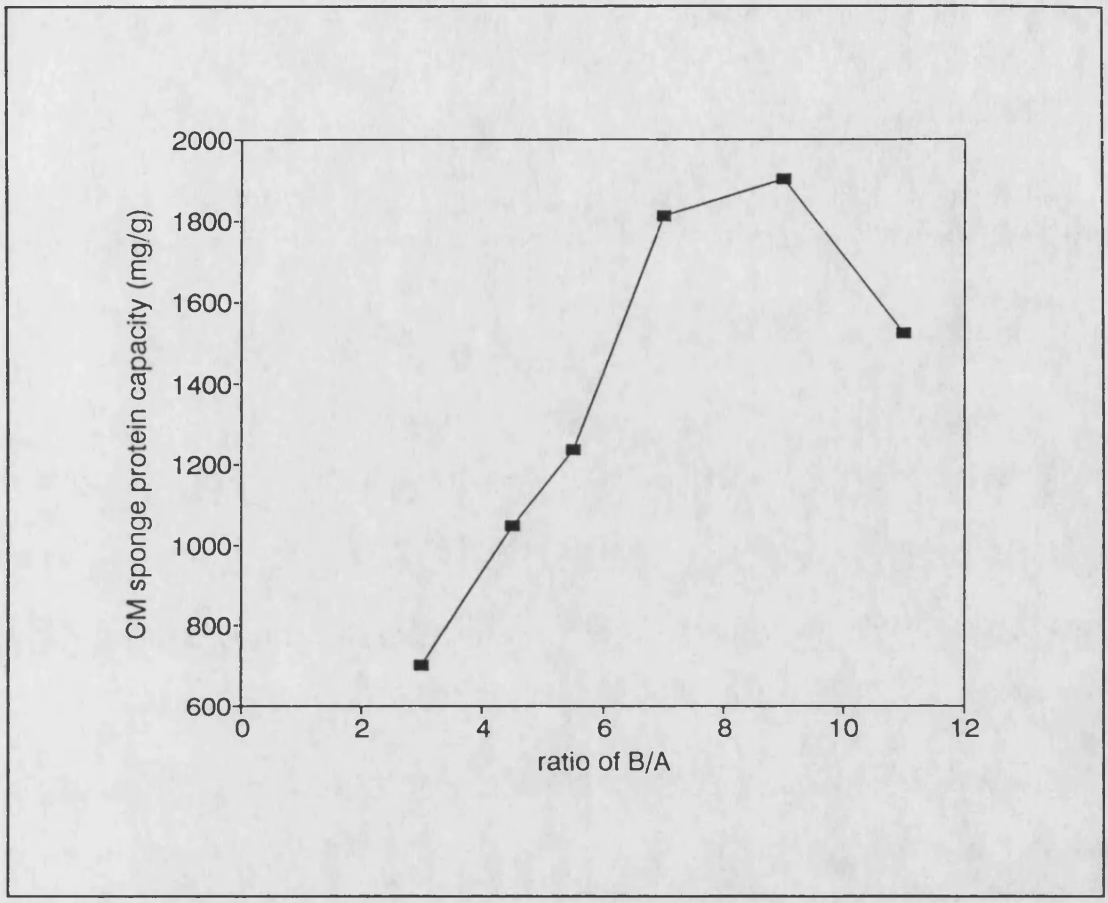

Fig. 4.7 Effect of ratio B/A on the protein capacity of CM sponge.
B = the volume of 20%(w/v) of sodium chloroacetate
A = the weight of cross-linked sponge.

The conditions for Fig.4.6 were following;

1. The volume of cross-linking solution and the volume of derivative solution were 5 times that of the weight of air dried sponge.

2. The derivative solution was 20%(w/v) of sodium chloroacetate in 20%(w/v) of NaOH solution.

3. The derivative reaction took place at 100 °C oven for 1 hour.

Fig.4.7 shows that the lysozyme capacity of CM sponge increased with the volume of derivative solution, *i.e.* the amount of sodium chloroacetate and sodium hydroxide, and then tended to decrease after having reached a maximum. It appears that excess derivative solution resulted in low protein capacity. This was confirmed by the following experiment. When the cross-linked sponge was boiled in excess derivative solution, the lysozyme capacity of CM sponge, as shown in Table 4.7, was around 25% lower than that made by the standard derivative recipe.

Table 4.7

derivative process	sample number	protein capacity (mg/g)
boiled in excess derivative solution for 1 hour	1	1200
	2	1040
using standard derivative recipe at 100 °C oven	3	1850
	4	1802

The derivative reaction time at an oven temperature of 100 °C seems to slightly affect the protein capacity, which is showed in Fig 4.8. The reaction time can be range from 20 to 120 minutes. The product produced using 120 minutes reaction time, however had a gel-like material on some parts of the sponge surface. Moreover, longer reaction time is not recommended in the large scale manufacture.

Increasing the dichlorohydrin during the cross-linking, it resulted in decreasing the protein capacity, which can be seen from Fig.4.9. The higher the degree of cross-linking was, the lower the protein capacity.

Four points can be concluded from the above and are as follows:

1. 20%(w/v) of sodium chloroacetate in 20%(w/v) of NaOH solution is recommended to be applied in the derivative reaction of the CM group.

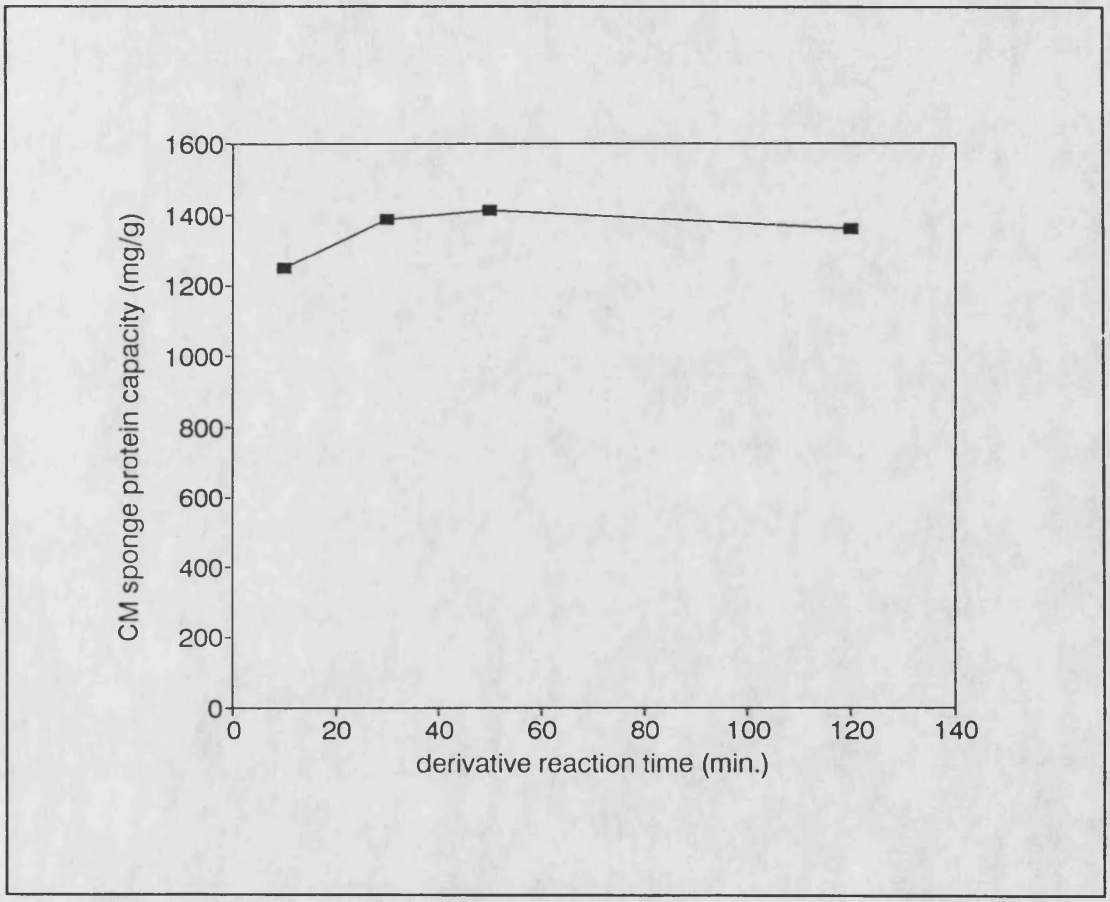

Fig. 4.8 Effect of derivative reaction time on the protein capacity of CM sponge.

2. The time for cross-linking is a between 10 and 60 minutes. If a large amount of sample is required, it would need 60 minutes due to slow heat transfer in the oven.

3. The ratio of B , the volume of 20%(w/v) of sodium chloroacetate in 20%(w/v) of NaOH solution, to A, the weight of cross-linked sponge, should be from 6 to 10.

4. The derivative reaction should be at 100 °C for 20 to 60 minutes.

The derivative recipe therefore can be written as follows;

50 g	cross-linked sponge (air dried)
60-90 g	sodium chloroacetate
300-450 ml	20%(w/v) of sodium hydroxide

at 100 °C oven from 20 to 60 minutes.

Using the optimized two steps method, a batch of CM sponge with 2100 mg/g of lysozyme capacity was produced (Table 4.8).

Table 4.8

Batch	Sample	lysozyme capacity (mg/g)
27/5/89	2	1802
	5	1820
5/3/88	H4	2100
	H5	1900

4.10 Manufacture of SP and DEAE Sponge

4.10.1 Introduction

The method of cross-linking using a low concentration of

NaOH solution can also applied to the reaction of cross-linking of SP (sulphopropyl) sponge and DEAE (diethylaminoethyl) sponge. The recipe for cross-linking of CM sponge was directly applied to the cross-linking of SP sponge. For cross-linking DEAE sponge, epichlorohydrin was used as the cross-linking reagent instead of dichlorohydrin.

4.10.2 Recipes for DEAE Sponge

The recipes for making DEAE cellulosic sponge are as following:

1. Cross-linking recipe

6 g	air dried sponge
30-60 ml	1 M NaOH solution
0.48-0.96 ml	epichlorohydrin

Epichlorhydrin was added to the 1 M NaOH solution and vigorously stirred , the liquid was then applied to the sponge. The sponge was slightly squeezed several times to expel entrapped air in the sponge. Then the sponge was placed in a covered tray with in a 100 °C oven for 1 hour. The cross-linked sponge was washed with distilled water until the pH value was neutral.

2. Recipe for coupling the diethylaminoethyl function group

6 g	cross-linked sponge (air dried)
1.98-2.96 g	diethylaminoethyl chloride

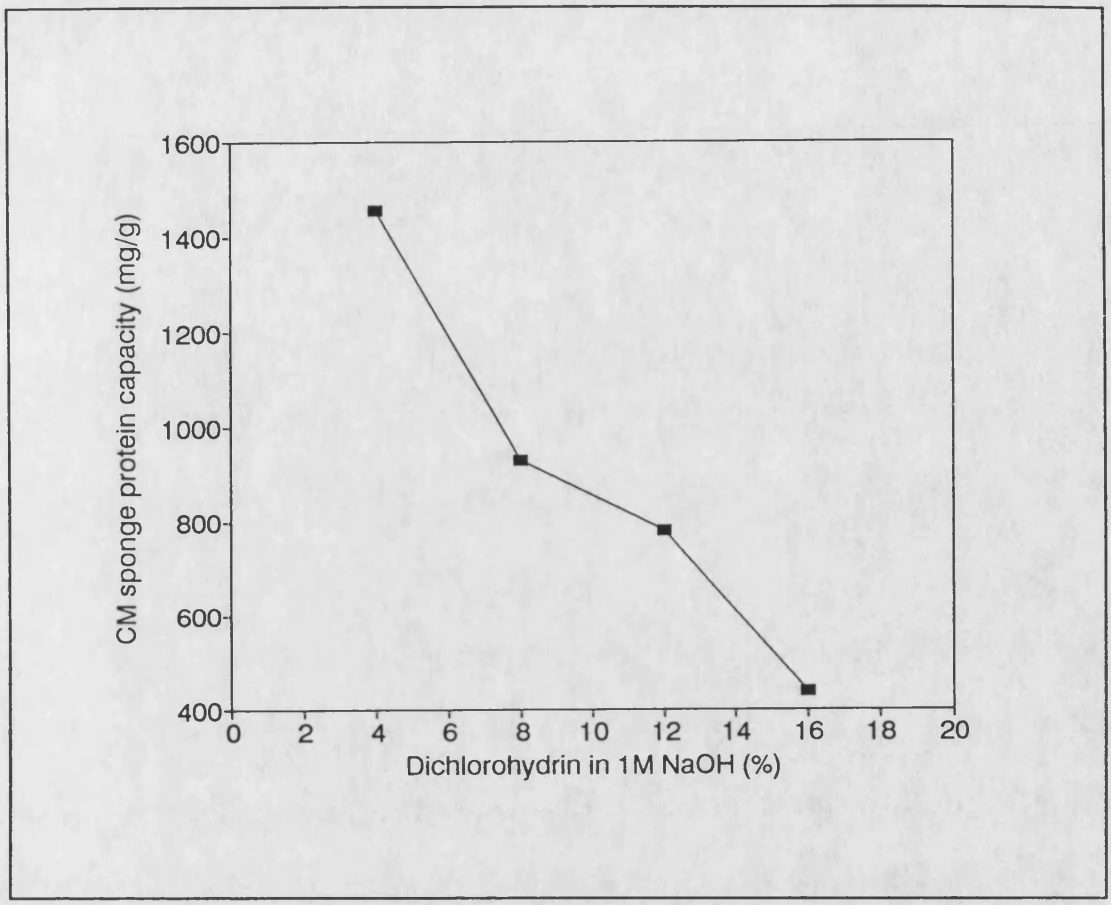

Fig.4.9 Effect of a amount of dichlorohydrin on CM sponge protein capacity.

30-60 ml 20%(w/v) NaOH solution

Diethylaminoethyl chloride was added to the NaOH solution and strongly stirred to form an emulsion, and was then applied to the cross-linked sponge. The sponge was quickly and gently squeezed several times to expel entrapped air in the sponge. Then the sponge was placed in a covered tray in a 100 ^{0}C oven for 1 hour. The DEAE sponge was washed with distilled water.

4.10.3 Recipes for SP Sponge

The recipes for making SP sponge are as follows:

1. Cross-linking recipe

50 g	cellulosic sponge (air dried)
8-18 ml	dichlorohydrin
200-450 ml	1 M NaOH solution

Dichlorohydrin was dissolved in the 1 M NaOH solution and then the liquid was applied to the sponge. The sponge was gently squeezed several times to expel entrapped air in the sponge and then, the sponge was placed in a covered tray in 100 ^{0}C oven from 10 to 60 minutes. The cross-linked sponge was washed with distilled water.

2. Recipe for derivative of 1,3-propane sultone function group

11 g	cross-linked sponge (air dried)
6-10 g	1,3-propane sultone
66-100 ml	20-30%(w/v) NaOH solution

1,3-propane sultone was dissolved in the NaOH solution. The cross-linked sponge was applied to the liquid and gently squeezed several times to expel the air in the sponge. Then the sponge was placed in a covered tray in 100 °C oven for 1 hour. The SP sponge was washed with distilled water.

Using the cross-linking method optimized from the manufacture of CM sponge, as shown in Table 4.9, DEAE and SP sponges had as good mechanical properties as CM sponge. The protein capacity of DEAE and SP sponge however had not been optimized. This could be considered as further work for the next

project.

Table 4.9

functional group	protein capacity (mg/g)	comments on mechanical property of ion-exchange sponge
CM	2100 (lysozyme)	sponge structure was maintained with good springiness
SP	780 (lysozyme)	sponge structure was maintained and the spring property as the original sponge
DEAE	467 (BSA)	sponge structure was maintained

4.11 Conclusion

Experimental results showed that the sponge structure was visibly damaged by more than 7.5% NaOH solution in a contact time of 30 seconds at temperature 18°C, while the cross-linking reaction needed more than 30 seconds to complete at room temperature. This indicates that if a more than 7% NaOH concentration was applied at the cross-linking stage, the sponge structure would be damaged before the cross-linking reaction was complete. However cross-linking using 4%(v/v) dichlorohydrin in 1 M NaOH was successful.

Sponge structure damage caused by NaOH was observed as a visible loss of spring ability and excessively swelling. When excessive water is adsorbed to form a gelatinous material which has extremely high resistance to liquid flow and eventually leads

the sponge to be disintegrated. This problem was solved by the new two-steps low concentration NaOH recipe. Earlier work had attempted simultaneous cross-linking and derivation. It was found in this study that these should be carried out sequentially.

In addition, it was also found that; (1) sodium substituted sponge could become soluble if the cellulosic sponge was not first cross-linked; (2) the hydraulic and mechanical properties of ion-exchange sponge were directly proportional to the degree of cross-linking, while the protein capacity and IEC of the ion-exchange sponge was inversely proportional to the cross-linking; (3) although the function of sodium hydroxide was to swell the cellulose thereby ' activating ' it for reaction with the cross-linking reagent or the deriving reagent, excessive activation could lead the cellulosic sponge to be soluble or to form a gelatinous materials; (4) the time for cross-linking was a between 10 and 60 minutes. If a large amount of sponge is required, it could be need 60 minutes due to slow heat transfer in the oven; (5) 20%(w/v) of sodium chloroacetate concentration in 20%(w/v) of NaOH solution was recommended, which ensured the highest protein capacity; (6) the ratio of B (the volume of 20%(w/v) of sodium chloroacetate in 20%(w/v) of NaOH solution) to A (the weight of cross-linked sponge) was range from 6 to 10; (7) protein capacity slight affected by the derivative reaction time which ranged from 20 to 120 minutes, but the longer reaction times could result in the gel-like material on the surface of sponge ion-exchanger.

In comparison experimental results obtained in this study with history of making cellulose ion-exchangers, it appeared in the earlier work that either a high concentration sodium hydroxide solution, from 12% to 45%, or too low concentration sodium hydroxide, less than 0.5% , with cross-linking reagent, was used to cross-link the cellulosic material or attach the functional group. The sponge ion-exchangers did not retain good hydraulic properties. This could have been due to any of several factors including an inadequate degree of cross-linking or too low a sodium hydroxide concentration, or alkali damage before the cross-linking took place.

In summary, in order to overcome the poor hydraulic and mechanical properties of ion-exchange sponges, the cross-linking reaction and deriving reaction was separated into two steps each using a the different in concentration of sodium hydroxide applied, which is reviewed as the following;

1. cross-linking step;

50 g	cellulosic sponge (air dried)
8-18 ml	dichlorohydrin
200-450 ml	1 M NaOH solution

The dichlorohydrin was dissolved in the 1 M sodium hydroxide solution, then it was applied to the air dried sponge. The sponge was slightly squeezed to expel the air in the sponge, excess liquid was removed from the sponge by gently squeezing . The moist sponge was placed in a tray with a cover and reacted at 100

°C in an oven. The reaction time could range from 10 to 60 minutes to allow the temperature to reach 100 °C depending on the amount of sponge.

2. derivative recipe;

50 g	cross-linked sponge (air dried)
60-90 g	sodium chloroacetate
300-450 ml	20%(w/v) of sodium hydroxide

at 100 °C oven from 20 to 60 minutes.

A CM sponge with high protein capacity and highly stable mechanical property was produced using the optimum two steps method. The cross-linking method can also be applied to make DEAE and SP sponge with good mechanical properties. Fig. 4.10 shows that the physical structure of Cm sponge (cross section) is maintained as that of original one in comparison with Figs 4.2,4.3 and 4.4. The apparent of CM sponge (Fig. 4.5) is also maintained by comparing with the original sponge (Fig. 4.11).

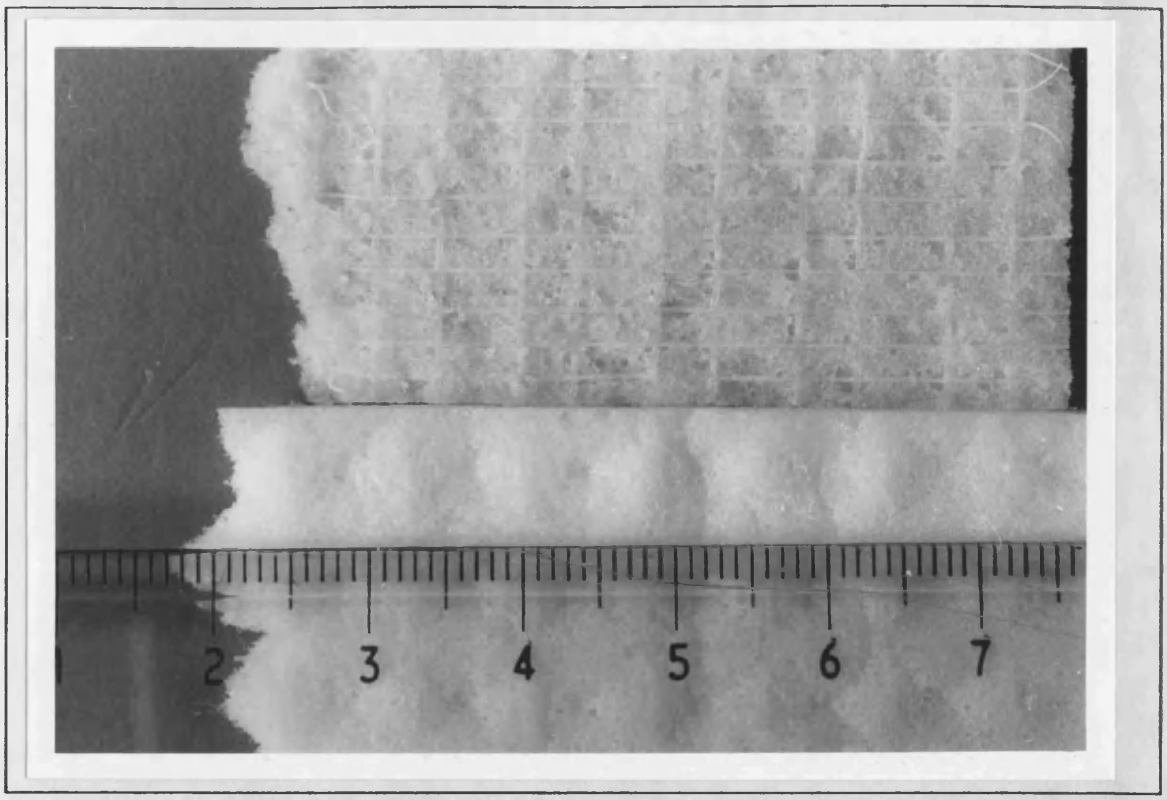

Fig. 4.1 Cellulose sponge (wet). The sponge on the top showing the nylon net reinforcement. Scale (cm)

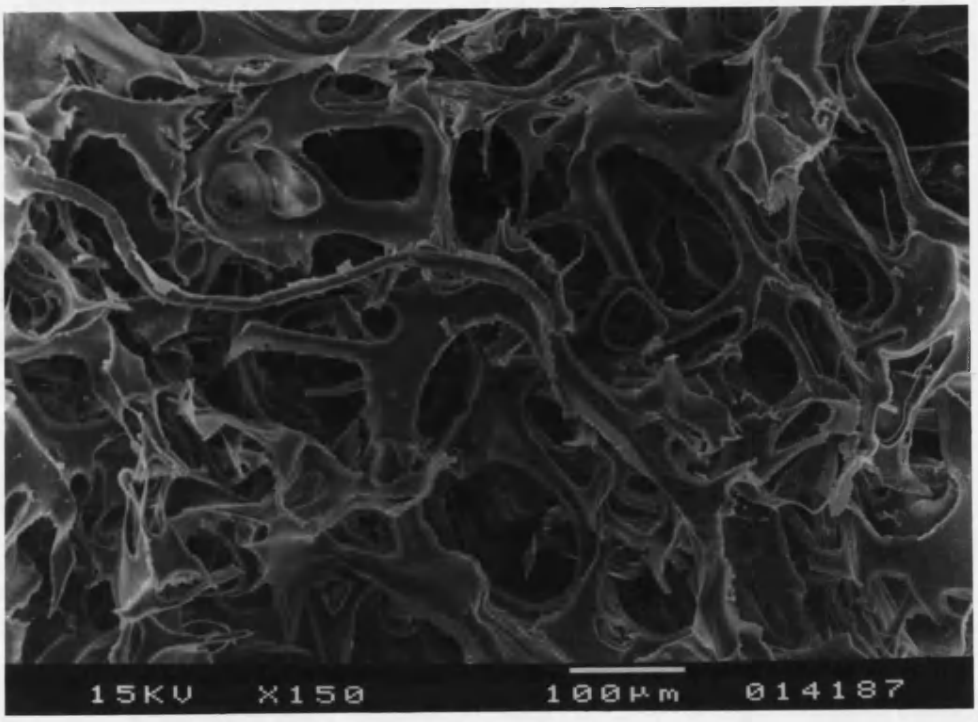

Fig. 4.2 Cross section of cellulose sponge (dry)

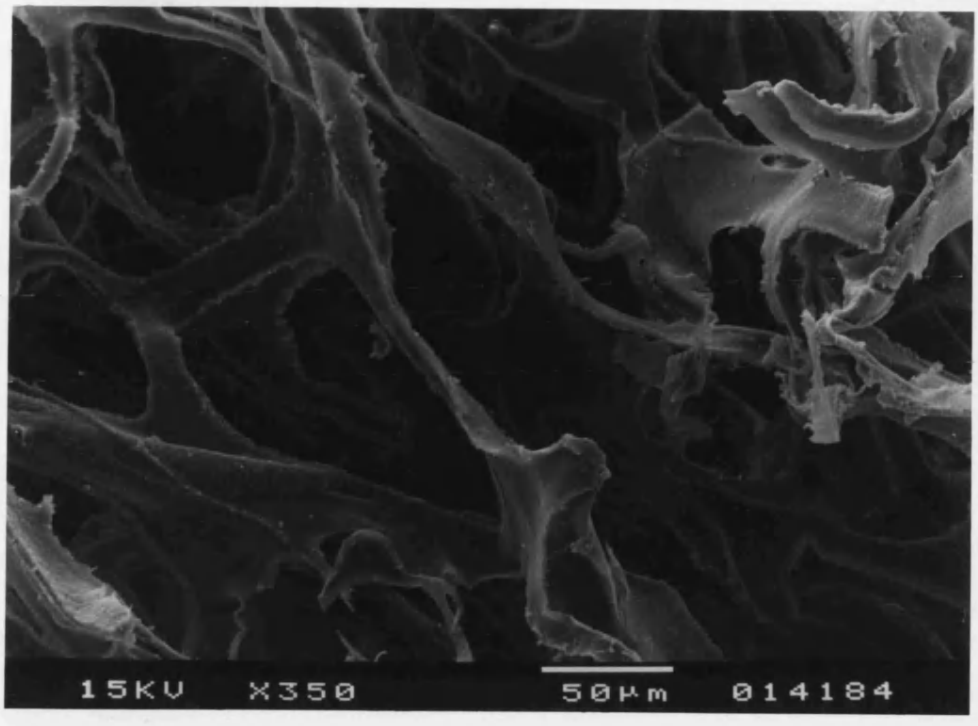

Fig. 4.3 Longitudinal section of cellulose sponge (dry)

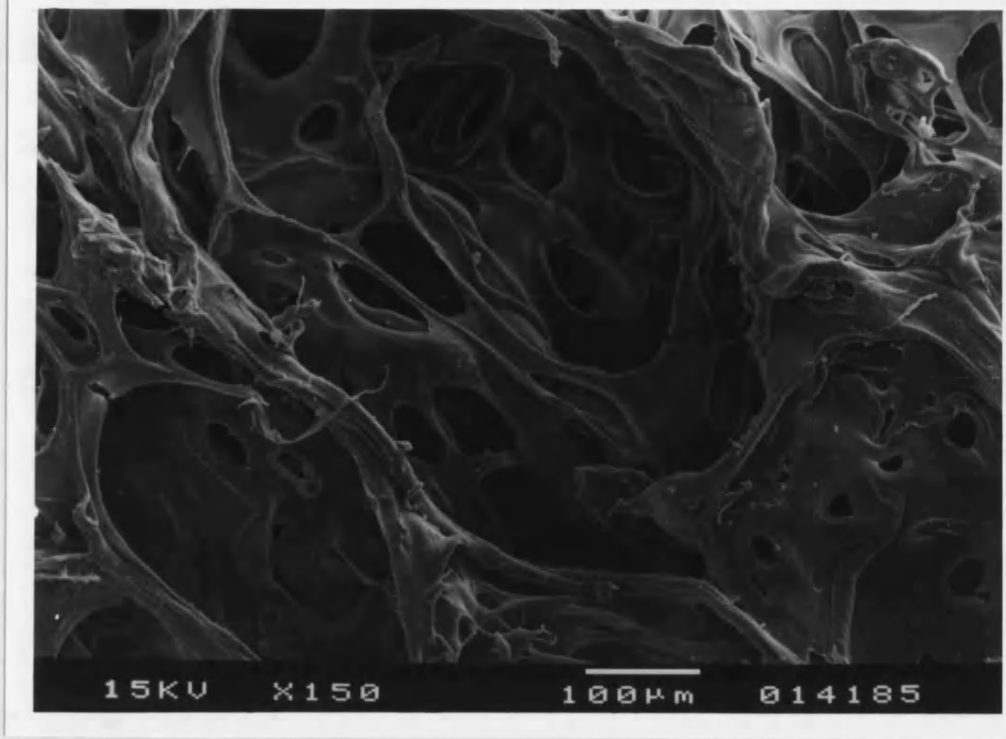

Fig. 4.4 Top surface of the cellulose sponge (dry)

Fig. 4.5 Cellulose sponge (wet). Scale (cm)

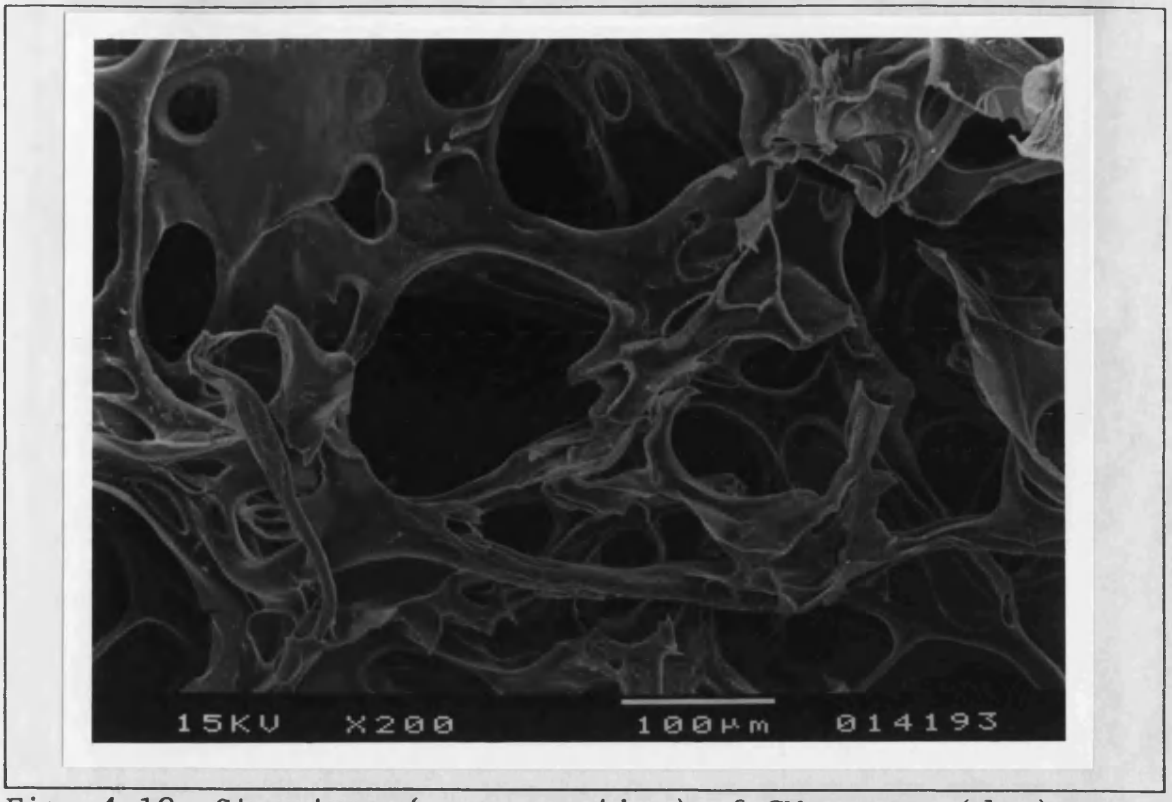

Fig. 4.10 Structure (cross section) of CM sponge (dry)

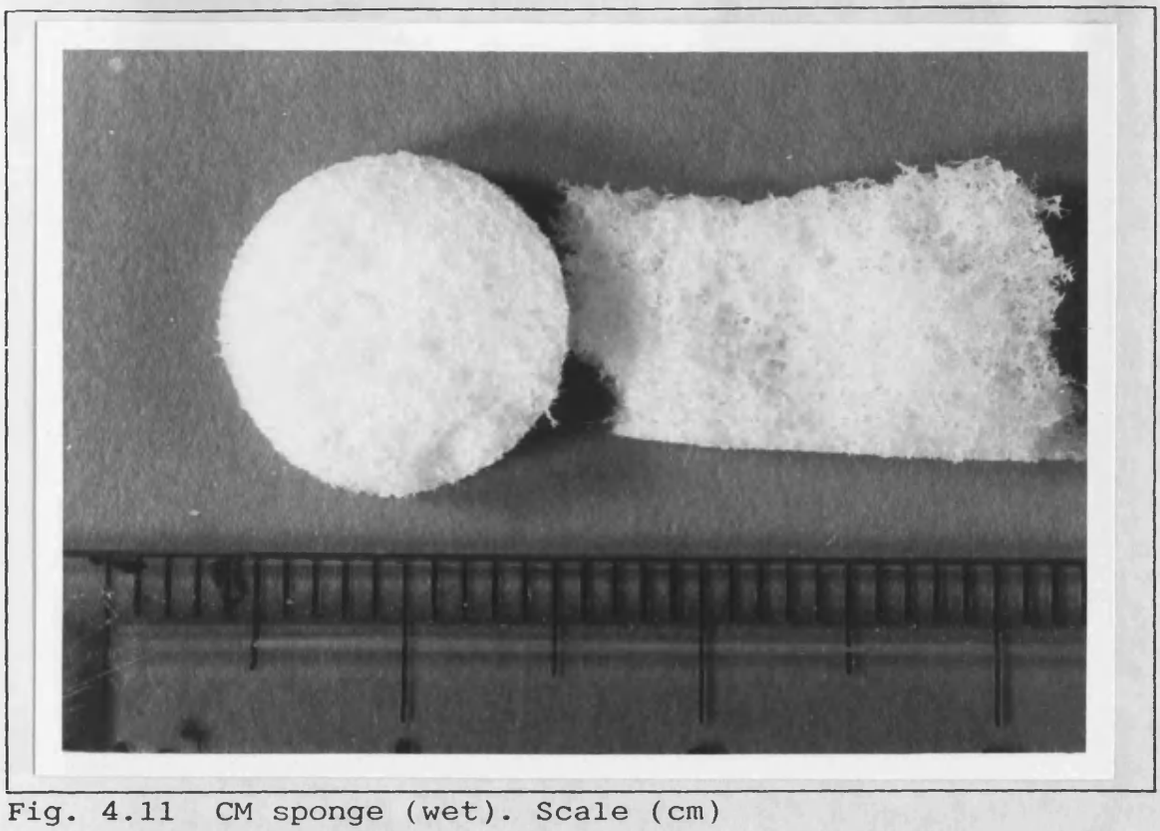

Fig. 4.11 CM sponge (wet). Scale (cm)

CHAPTER 5

CHARACTERISATION OF CM SPONGE ION-EXCHANGER

CHAPTER 5

CHARACTERISATION OF CM SPONGE ION-EXCHANGER

5.1 Introduction

Ion-exchangers are usually characterised by a number of properties such as ion exchange capacity, chemical stability, physical stability, hydraulic properties and kinetics. All these characteristics were measured and the results discussed below for a CM sponge ion-exchanger. The chemical stability of cross-linked sponge, the effect of derivative reaction on the structure of cross-linked sponge which have been discussed previously in chapter 4, are therefore not repeated here.

Ion-exchange capacity is a very important property of an ion-exchanger since it permits a quantitative determination of the amount of adsorbate which can be taken up by an exchanger. Protein capacity is used to quantify the exchange capacity of the CM sponge ion-exchanger because the most likely application is for protein separation. As a result of the molecular size and the affinity between the protein and ion-exchanger, ion-exchangers can show different capacities for different proteins. Both protein capacity and total equilibrium weight capacity (IEC), *i.e.* small ion capacity, are highly affected by pH and concentration of competitive ions. Temperature also affects these capacities.

In laboratory experiments as well as in industrial applications of ion exchangers, the stability of the ion exchangers during the process cycle and also during regeneration and sterilization is important. It influences the life time and thus the total costs of a process. Chemical stability, physical stability and stability of reproducibility are discussed later in this chapter.

Flow-rate is mainly dependent on the physical rigidity and is affected by compressibility, swelling and shrinking. Flow-rate influences mass transfer and thus overall process times. High flow rates are achievable with CM sponge and to make best use of the material so the adsorption and desorption kinetics should be fast. Kinetic studies have been conducted on the effect of flow-rate and ionic strength on the processes of adsorption and desorption.

Whatman CM 52 and Indion HC were chosen for comparison because not only are they cross-linked cellulose ion-exchangers, but also they are in the different physical forms, *i.e.* microgranular particles (diameter of 60-150 μm) for Whatman CM 52 and spherical particles (diameter of 350-450 μm) for Indion HC, respectively.

5.2 Materials and Methods

Kinetics Experiment. Lysozyme (Sigma Chemical Co., Dorset, U.K.) was dissolved in 0.01 M acetic acid-sodium acetate buffer, pH 5.0.

A CM cellulosic ion exchanger (Batch H1 and W1) which was later named CM-HVFM, carboxymethyl high velocity fine matrix, were used. CM 52, a microgranular CM ion exchanger, was purchased from Whatman BioSystems Ltd., Kent, U.K. and Indion HC (CM resin, size between 350-400 μm) Batch 1246 was obtained from Phoenix Chemical Ltd., C/- Waitaki NZ Refrigerating Ltd., Nelson, New Zealand.

A Sartorius GmbH D-3400 filter holder with distributor (Sartorius Inst. Ltd., Surrey, U.K.) was packed with either 2.7 g (0.3 g dry weight) CM sponge or 5 g of 1:1 slurry of CM 52 or 4.3 g of 1:0.8 slurry of HC. This produced a short 5.8 ml column 4 mm deep x 43 mm I.D.

A 160 mm x 10 mm I.D. adjustable glass column(Amicon Ltd., Stonehouse, U.K.) packed with 0.5 g (dry weight) CM-HVFM was used for a 110 mm x 10 mm I.D. column of 8.64 ml packed volume.

A gear micropump (Micropump Co.,Concord, CA, USA) was used to feed a 4 x 43 mm I.D. column otherwise a Millipore peristaltic pump (Millipore Co., Bedford, MA, USA) or Autoclude peristaltic pump (F.T. Sci. Ins. Ltd., Tewkesbury, Glos, U.K.) were used.

A LKB Uvicord II monitor (LKB-Produkter AB, Bromma, Sweden) was used at 280 nm on-line to detect the lysozyme concentration.

The experiment was carried out using the systems shown in Fig. 5.1 The sample to be loaded was placed in a stirred beaker

from which it was pumped upwards through the column. In the case of the short column (Fig.5.1), a separate stream loop (less than 25 cm) was pumped from the beaker to the UV monitor and back to the beaker at a superficial velocity of 30 m /min whilst for the longer columns (Fig. 5.1b) the stream passed from the top of the column through the UV detector. The short column was operated at a fast recycle rate and acted as a differential bed, in order to study the kinetics of the adsorption and desorption on the ion-exchangers. Before each adsorption run, the ion-exchanger bed was equilibrated with 0.01 M sodium acetate/acetic buffer, pH 5. The whole system (Fig. 5.1a) was then drained before starting the run. Following adsorption, the column was washed with 0.01 M sodium acetate/acetic buffer, pH 5, and then eluted using 0.7 M NaCl solution. The CM sponge column was regenerated by 2 M NaCl or 0.7 M NaOH solution.

A batch experiment was carried out in a 160 x 90 mm I.D. vessel equipped with a motor stirrer (Seta, Stanhope-seta, Ltd., Surrey, England). A fine nylon mesh was fitted at the bottom of the vessel. An Autoclude peristaltic pump was used to pump the solution through the UV detector and back to the vessel at 26 m/min superficial velocity. In this case the liquid recirculation loop through the peristaltic pump and UV detector was 23 cm. CM sponge was ground by a cell grinder (Waring commercial blender, Waring products Division, New Hartford, Conn. U.S.A.) into microgranular fibre. The CM microgranular fibre was equilibrated by 0.5 M sodium acetate/acetic buffer, pH 5 for 4 hour, and then washed with 0.01 M sodium acetate/acetic buffer,

pH 5. The CM microgranular fibre was added into the vessel containing a designed value of 0.5 mg/ml lysozyme in 0.01 M sodium acetate/acetic buffer, pH5. The speed of motor stirrer was controlled and measured by a Digital-Handtachometer (Jaquetag, Thannerstrasse15,CH-4009 Basel, Swiss). A pH meter was used on line to measure the pH value of the solution. It was, however, found that the pH value was stable at 5 through all these adsorption and desorption processes. After adsorption the CM microgranular fibre was washed with 0.01 M sodium acetate/acetic buffer, pH 5 until the elution curve reached the base line in the UV trace. A designed volume and NaCl concentration in 0.01 M sodium acetate/acetic buffer as an eluent, pH 5 was then added into the vessel to start the desorption process.

Physical stability and flow-rate experiment. The ion-exchanger was packed into a column and then equilibrated with distilled water. A pressure gauge was placed between the pump outlet and column inlet. The ion-exchanger compression was then examined by gradually increasing the flow-rate of distilled water to the designed back pressure. Flow-rate was measure using a stop watch and a volumetric cylinder.

Two other larger diameter columns were used to measure the relationship between flow-rate and pressure drop through the columns. These were both about 100 mm deep with 26 mm or 147 mm I.D. respectively. Pressure was increased by increasing the flow rate.

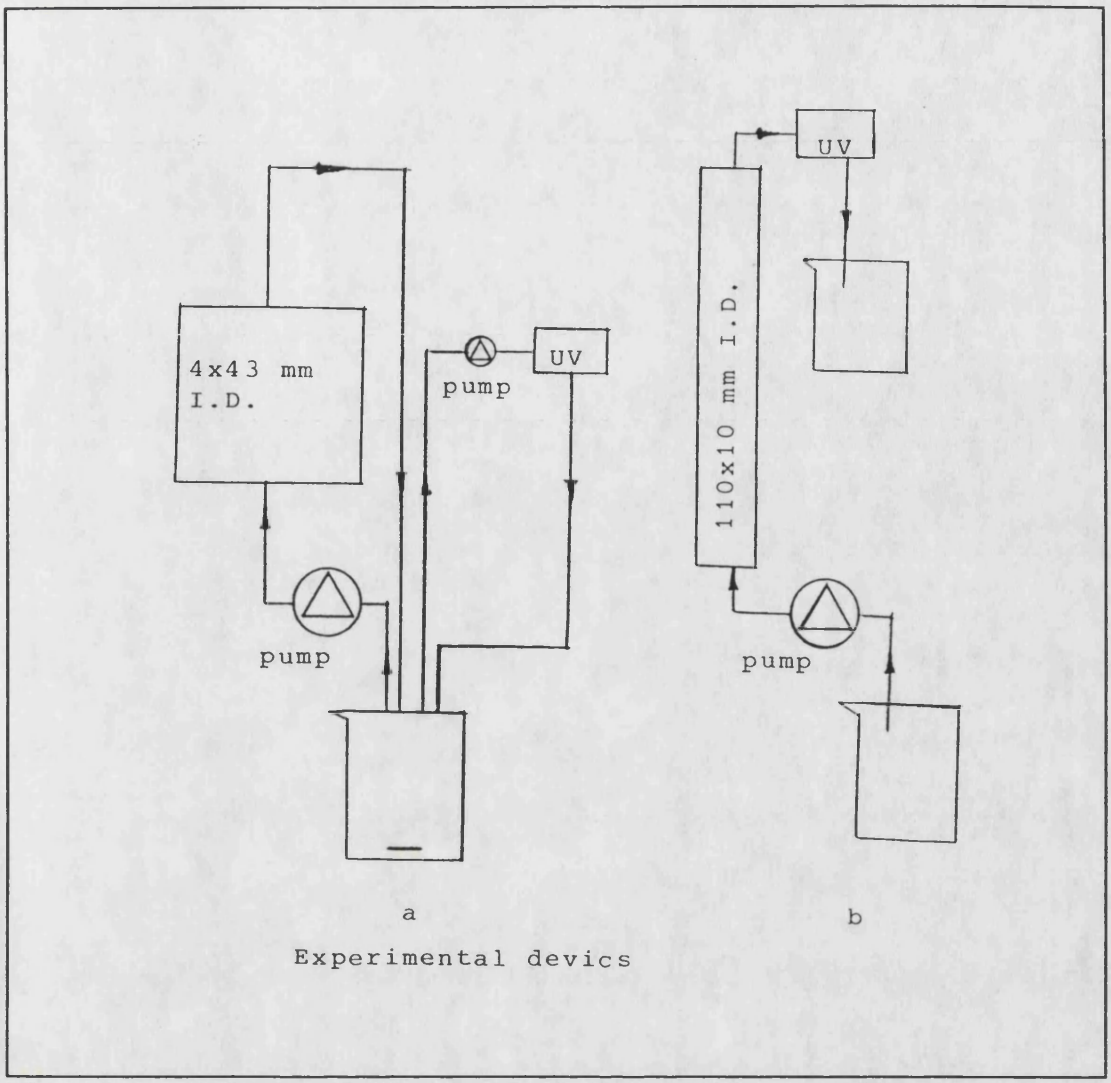

Fig. 5.1 Column adsorption and desorption experiment

Chemical stability experiment. CM sponge was added to a series beakers containing different concentrations of acids and alkali. After a designted time at a designted temperature, CM sponge was taken out and washed carefully with water. The stability, which meant that the sponge structure was maintained after having been treated, was then visually examined in comparison with the original sponge to determine its stability.

Protein capacity and isotherm adsorption experiment. Sponge ion-exchanger was cut into around a 3 x 3 mm (approx.) cube piece and was equilibrated with 0.4 M sodium acetate buffer at pH 5 for 4 hours. The sponge was washed with 0.01 M sodium acetate buffer, pH 5 until the conductivity of the liquid in the vessel was the same as the 0.01 M sodium acetate buffer. Then the imbibed water in sponge was removed by suction on a Buncher funnel, followed by blotting with tissue paper until the sponge was damp dry. In order to calculate the water content of the damp dry sponge, a part was weighed and then oven dried at 110 °C overnight. The water content was obtained by the difference. Weighed pieces of damp dry sponge were added to a series of beakers containing lysozyme solution, the concentration of which ranged from 0.25 to 10 mg/ml, in 0.01 M sodium acetate buffer, pH 5. The volume of solution was controlled so that the amount of residual lysozyme was not less than 70% of the original. These beakers were placed in a shaker at a constant 15 °c overnight. The residual lysozyme concentration was determined by an ultraviolet spectrophotometer at 280 nm.

Swelling and shrinking experiments. The swelling and shrinking properties were evaluated by measuring the bed volume in 0.1 M acetate buffer at various pH, various NaOH and NaCl concentrations. CM sponge was packed into a 100 x 10 mm I.D. column. The exact bed height in a above sample solution was determined after elution of the sample solution had been continued for 2 hours at a flow-rate 2 ml/min. This was repeated for all above sample solutions with the same column.

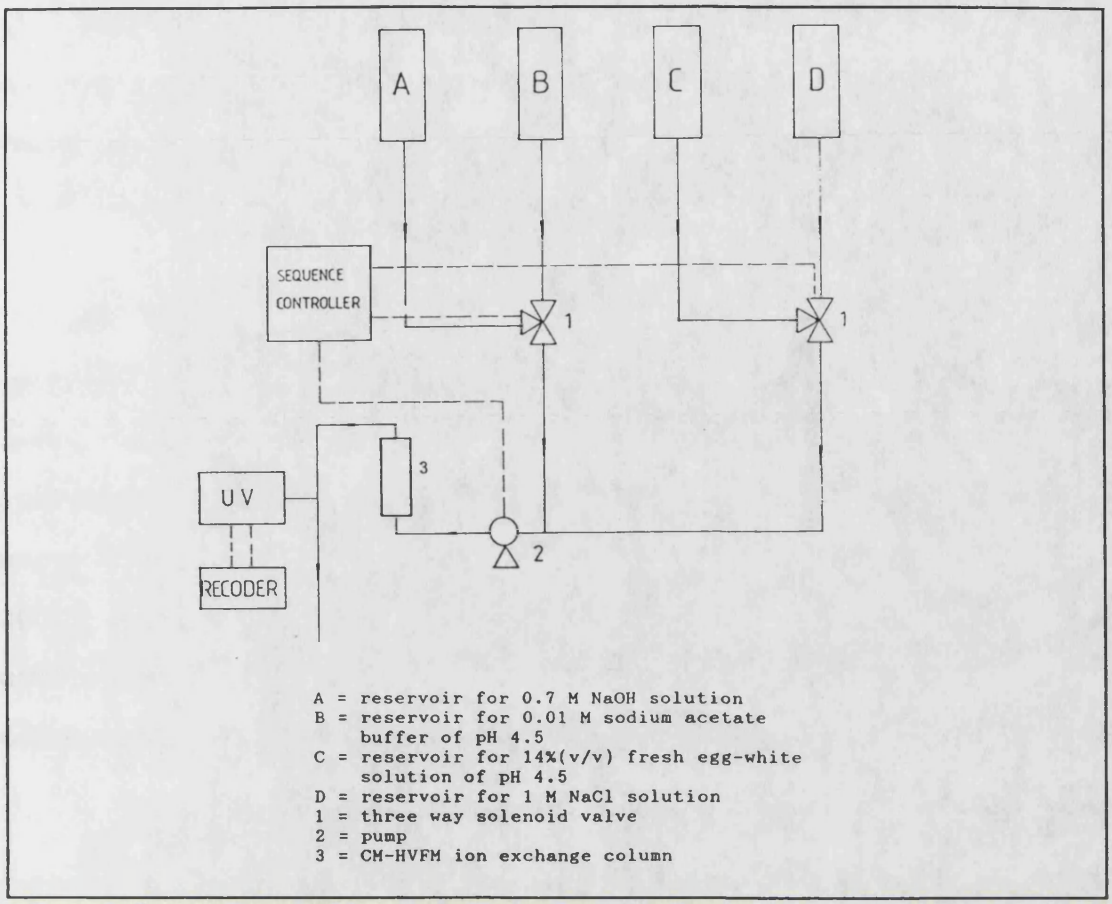

Fig. 5.2 Programme controller

Reproducibility experiment. A plc, Sequence Controller (Omron Tateisi Electronics, Co.,Osaka 541,Japan), was the control device for the repetitive loading of fresh egg white solution which is described in Chapter 7 onto the column. A 68 mm x 17 mm I.D. column was packed with 0.5 g (dry weight) of CM sponge, and used to process 340 cycles of loading and elution at the superficial velocity of 503 ml cm^{-2} h^{-1} (Fig. 5.2). Each cycle consisted of the following steps: (1) 1.3 times bed volume of 14%(v/v) fresh egg white solution at pH 4.5 was applied to the column, (2) the column was washed with 0.01 M sodium acetate buffer at pH 4.5, to the UV trace base line, (3) absorbed egg-

white proteins were eluted by 1 M NaCl, (4) the column was washed and equilibrated using 0.01 M sodium acetate buffer, pH 4.5. Every tenth cycle was followed by a caustic regeneration using 0.7 M NaOH solution .

pH titration experiment. A micro 2 pH/Ion meter and combination type pH electrode were purchased from Courtcloud Ltd. Dover, England AN EDTR Research Group Company. Prior to an experiment, the pH meter and electrode were calibrated using BDH colour-key buffer solutions at pH 4.00±0.02 (20°C), pH 7.00±0.02 (20°C) and pH 10.00±0.02 (20°C). A standard solution of 0.1 M sodium hydroxide (carbonate free) was supplied by BDH Ltd., Poole, Dorset.

The CM sponge was cut into approx 3 mm^3 cubes. Around 10 g of wet cubes were placed in a beaker containing 50 ml 1 M HCl and stirred for one hour. The CM sponge was then washed with distilled water to remove the HCl. Around 6 g (wet weight) of acid treated CM sponge cubes were placed in a beaker containing 50 ml 1 M NaCl and titrated with 0.1 M NaOH. Thereafter CM sponge cubes were removed from the titration beaker, dried at 110°C oven overnight and weighed

5.3 Isotherm Adsorption of CM Sponge

At a constant temperature, the protein concentration is eventually equilibrated between the solid phase (ion exchanger) and liquid phase. The relationship between them is termed the adsorption isotherm. There are three commonly recognised isotherm

types (Yamamoto *et al.*, 1988) as shown in (Fig. 5.3): (1) the isotherm is concave upward (curve A in Fig. 5.3) which is termed an unfavourable isotherm, (2) the isotherm is convex upward (curve C in Fig. 5.3) which is termed a favourable isotherm, (3) the isotherm is linear, curve B in Fig.5.3, where C/q is constant. Yamamoto *et al.* (1988) believed that the isotherms in ion-exchange chromatography are usually favourable, and can be modelled by the Langmuir equation or the Freundlich equation.

In deriving the Langmuir isotherm process for gas adsorption Langmuir(1918) assumed an energetically homogeneous adsorbent surface with equivalent sites is assumed, *i.e.* the energy of adsorption is constant for all sites. This results in a monolayer adsorption on the adsorbent surface and the formation of a constant adsorbent capacity.

For simplicity, an ion-exchanger is generally considered as an homogeneous adsorbent (Yamamoto *et al.*, 1988). The Langmuir isotherm equation, can be derived as follows. During the adsorption process, protein, P, is adsorbed by the ion-exchanger, AI, simultaneously protein is desorbed from the ion-exchanger, *i.e.*

$$P + AI \underset{K_2}{\overset{K_1}{\rightleftharpoons}} PAI \qquad (5.1)$$

where K_1 is the adsorption constant and K_2 is the desorption

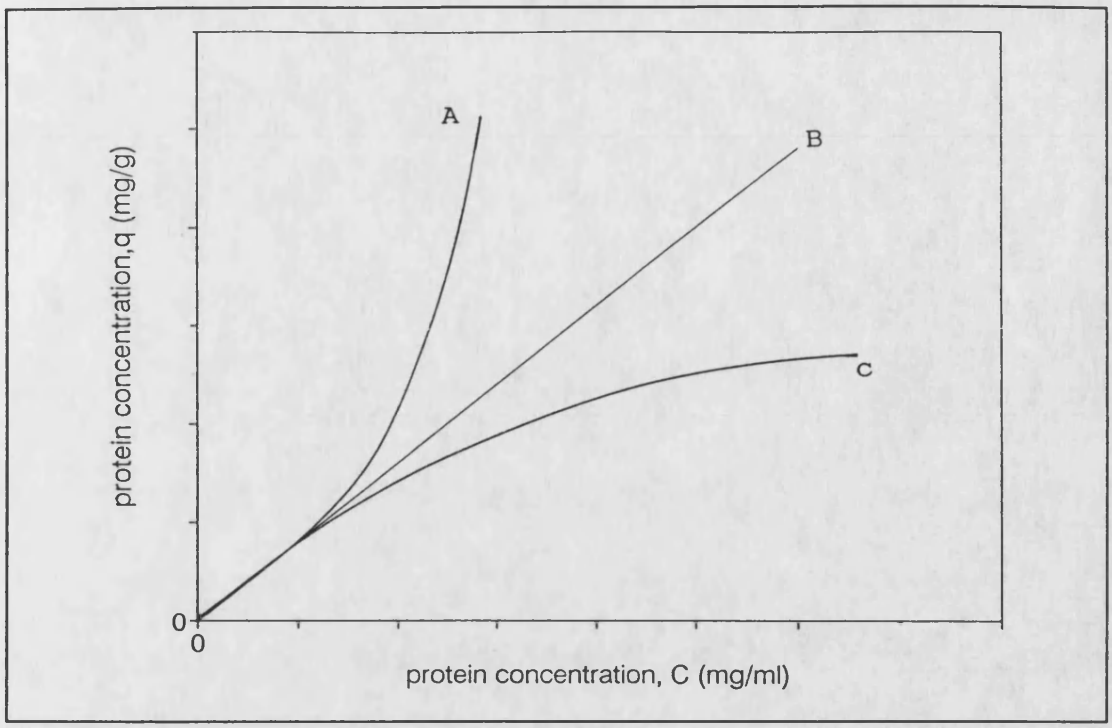

Fig.5.3 Shapes of adsorption isotherm

constant. From simple mass conservation, the above processes can be described as

rate of accumulation of adsorbate on ion exchanger = rate of adsorbate adsorption - rate of adsorbate desorption

that is,

$$\frac{dq}{dt} = K_1 C(q_m - q) - K_2 q \qquad (5.2)$$

where q_m, q and C are the maximum protein capacity, protein concentration in the ion-exchanger and liquid phase respectively.

The equation 5.2 was also used by Skidmore and Chase (1988), and Skidmore *et al* (1990) to describe the processes of ion-exchange adsorption for protein.

When the above process reaches an equilibrium state, dq/dt = 0, then

$$K_1 C_e (q_m - q_e) - K_2 q_e = 0 \tag{5.3}$$

$$q_e = \frac{K_1 C_e q_m}{K_1 C_e + K_2} \tag{5.4}$$

or

$$q_e = \frac{C_e q_m}{C_e + (\frac{K_2}{K_1})} = \frac{C_e q_m}{K_d + C_e} \tag{5.5}$$

where $K_d = K_2/K_1$, q_m, maximum protein capacity (the subscript e represents the equilibrium concentration). The ratio $K_d = K_2/K_1$ can be determined from an adsorption isotherm experiment by using the linear regression method or non-linear regression (simplex method). If the linear regression method is applied, the equation 5.5 can be rewritten as

$$\frac{C_e}{q_e} = \frac{K_d}{q_m} + \frac{C_e}{q_m} \qquad (5.6)$$

Using this equation to estimate K_d and q_m might however result in inaccurate values of K_d and q_m due to the distortion of the error distribution introduced by the reciprocols.

The Freundlich isotherm (Freundlich, 1926) describes the equilibrium at heterogeneous surfaces, where the assumption of a single adsorbed molecule per site is no longer valid.

$$q_e = A_f C_e^b \qquad (5.7)$$

where A_f and b are Freundlich constants, of which b is the heterogeneity factor that characterizes this isotherm. These constant can be obtained by linearization of the Freundlich equation:

$$\log q_e = \log A_f + b \log C_e \qquad (5.8)$$

where b is the slope, log A_f is the intercept.

Al-Duri and Mckay (1990) mentioned that their experimental data is most accurately described by a general isotherm equation proposed by Fritz and Schlunder (1974), which is the following, where A_1, B_1 and d_1 are the constants. d_1 (< 1) is termed the

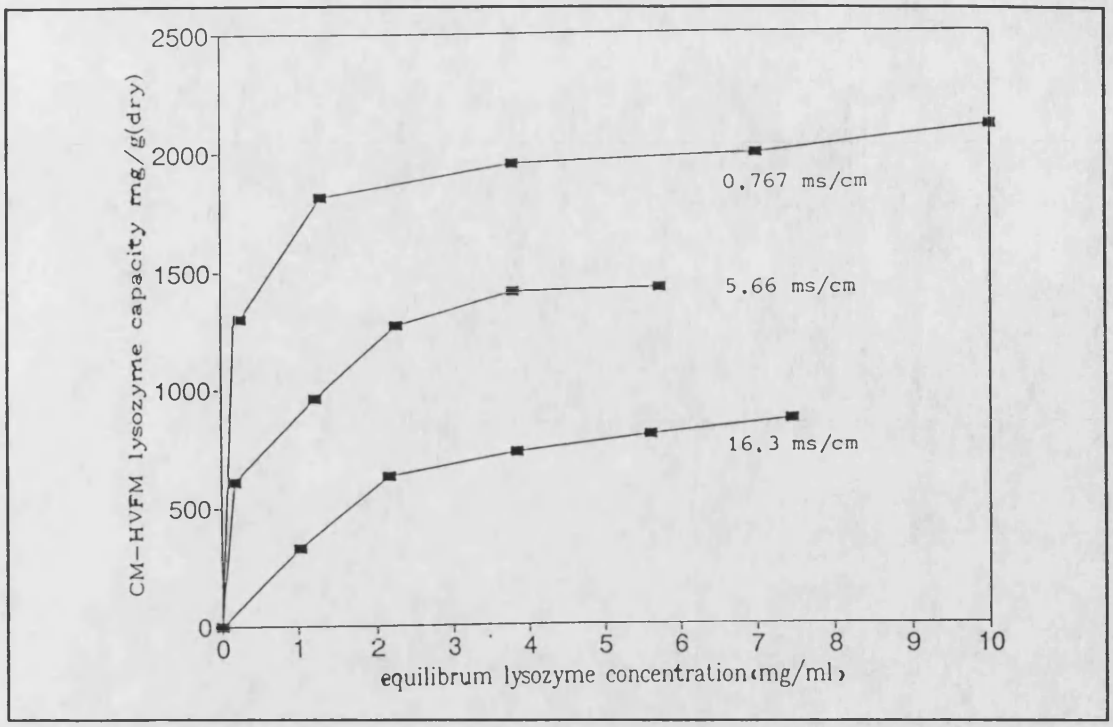

Fig. 5.4a Effect of ionic concentration on CM sponge adsorption isotherm.

$$q_e = \frac{q_m C_e}{A_1 + B_1 C_e^{d1}} \qquad (5.8a)$$

heterogeneity factor. Equation 5.8a is applicable to both heterogeneous and homogeneous surfaces.

5.3.1 Results and Discussion

The CM sponge adsorption isotherms curves were obtained for adsorption of lysozyme at pH 5, at a temperature of 15 °C. In order to examine how the protein capacity of CM sponge was affected by ionic concentration, the lysozyme solution was adjusted to different ionic strengths using sodium chloride (Fig.5.4a). All these curves were fitted by a Langmuir isotherm A K_d of 0.08 mg/ml and a q_m, maximum protein capacity, of 2100 mg/g were obtained with the 0.767 ms/cm ionic concentration,

which was calculated from the slope and intercept of the linear regression plot on Fig.5.4b. The K_d, q_m values were slightly different when the non-linear regression (Simplex method) was applied to estimate these isotherm parameters (Table 5.1 and Fig.5.4b). The low K_d meant that at a very low lysozyme concentration, the CM sponge showed a high equilibrium protein capacity, *i.e.* 1300 mg/g in equilibrium with 0.2 mg/ml of lysozyme solution. When the ionic concentration was increased

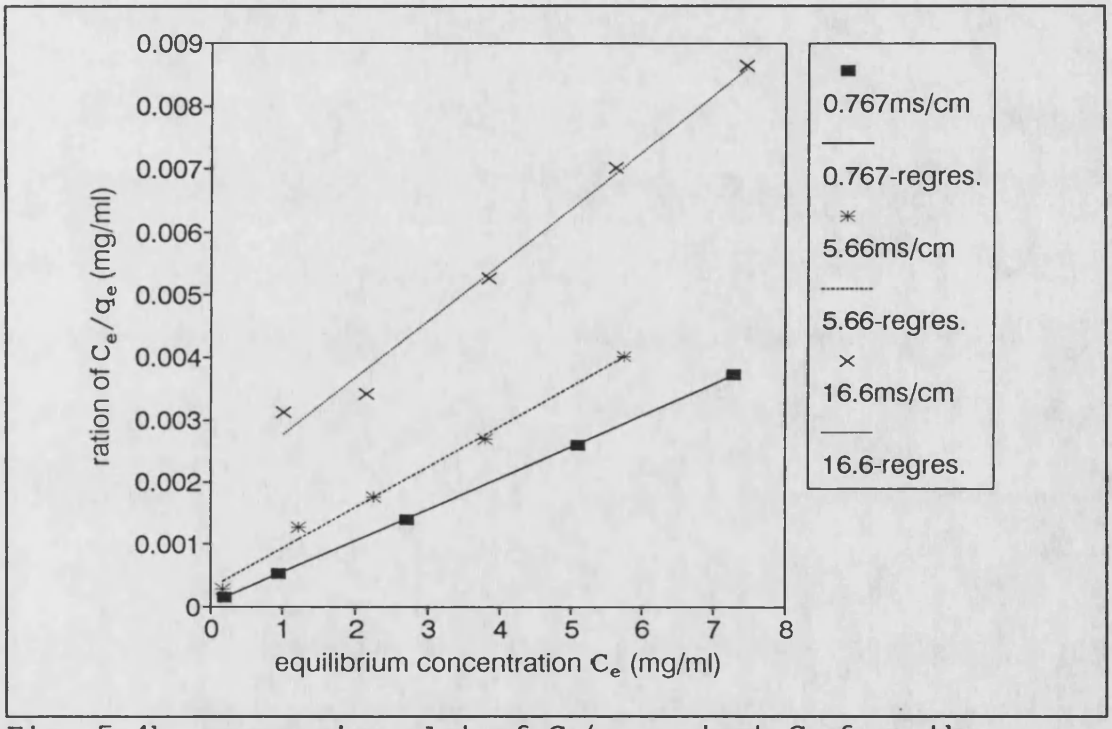

Fig. 5.4b. regression plot of C_e/q_e against C_e from the isotherm adsorption.

21 times to 16.3 mS/cm , the lysozyme capacity of CM sponge only dropped to 1100 mg/g. Fig. 5.4a therefore suggests that CM sponge could be used to recover protein from relatively low concentration streams at moderate ionic concentrations of between 0.7-8 mS/cm. The affinity between the lysozyme and CM sponge,

which is represented by $1/K_d$, and the maximum protein capacity of CM sponge, decreased with increasing of ionic strength. This can be seen from Fig.5.4d, in which the values of q_m and K_d are plotted against the ionic strength showing that the higher the ionic concentration, the higher K_d, and the lower the protein capacity. The slopes and intercepts of the C_e/q_e against C_e line were determined by linear regression analysis with regression coefficients of 0.99.

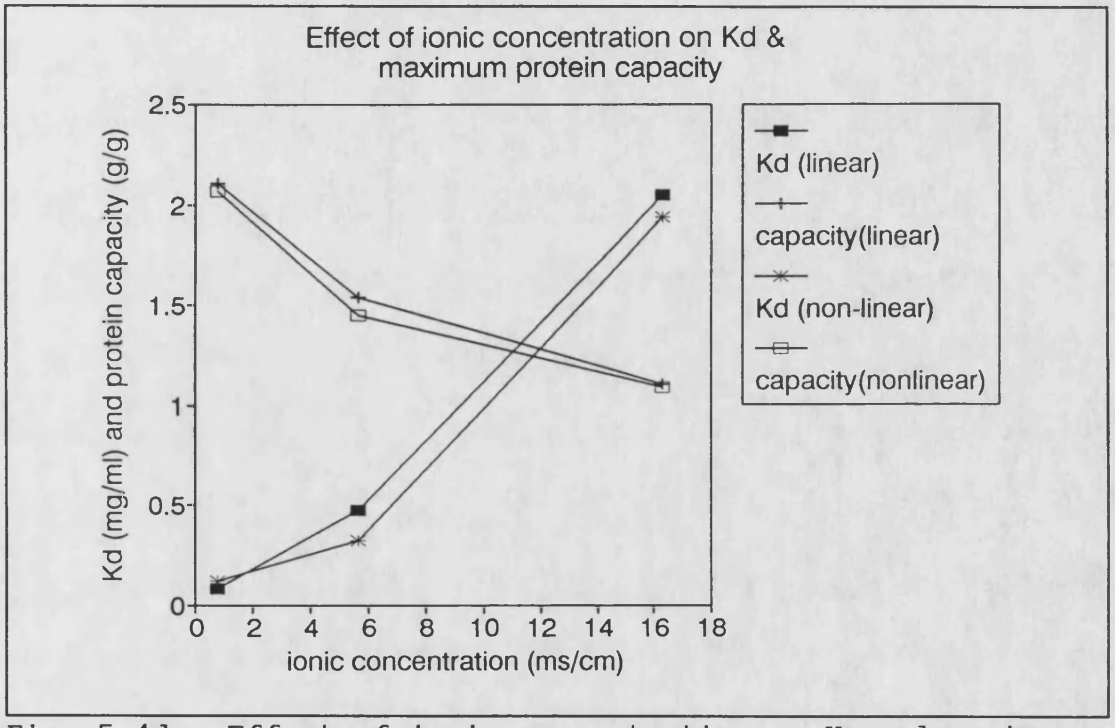

Fig. 5.4d Effect of ionic concentration on K_d and maximum protein capacity.

5.4 Physical Stability

The physical stability of an ion-exchanger primarily resides

Table 5.1 isotherm parameters estimated by linear and nonlinear regression

Method	K_d mg/ml	q_m mg/g	Ionic Strength ms/cm
	0.08	2108	0.767
linear	0.475	1542	5.66
regression	2.047	1105	16.3
	0.1216	2071	0.767
non-linear	0.321	1454	5.66
regression	1.942	1094	16.3

in its strength. Good ion-exchangers are characterized as being resistant to mechanical compression, having a sufficient bursting and disintegration resistance under given loading and regeneration conditions. The thermal stability of ion-exchanger is also considered to be one of the physical stabilities. Since the derivative reaction of CM sponge was in 20% NaOH solution at 100 °C for 1 hour, the thermal stability of CM sponge was considered to be satisfactory. This section is focused on the compression of CM sponge. Other features physical stability are in the section of reproducility

Cellulose ion-exchangers are not rigid materials and would therefore not be expected to operate at pressures of more than 1.5 bar. Peterson (1970) found that at a flow rate of 130 $ml/cm^2/h$, which he considered to be a very high flow-rate, a column packed with coarse DEAE-cellulose particles (diameter

range from 400-600 μm) shrank markedly in height after half the effluent had emerged. The resistance to flow increased rapidly to the point where the weakest connection in the system yielded to the mounting pressure.

One measure of physical stability is the degree of support compression which results when the support is subjected to large hydrostatic pressure heads (Matson and Siebert 1988). This is usually measured relative to the resultant back pressure, as the superficial velocity is increased across the ion-exchanger held within a column. Unger and Janzen (1986) suggested that as according to Darcy's Law, a linear relationship held between the fluid velocity and the column pressure drop, any significant deviation from linearity can be regarded as an indication of chromatographic support compression.

5.4.1 Results and Discussion

As demonstrated in Fig. 5.5, CM sponge showed good linearity between fluid velocity and pressure up to a velocity of more than 950 cm/h when the pressure was still below 0.04 bar/cm. Whatman CM 52 microgrannular material could not perform at a superficial velocity of more than 100 cm/h. The Indion CM spherical material showed two results: (1) A significant deviation from linearity was found at a superficial velocity less than 120 cm/h for the Indion HC (batch 1246), (2) the second Indion CM bead material (diameter 75-150 μm), which has been recently developed, had greatly improved resistance to the compression, but still only gave linearity up to approximately 400 cm/h superficial

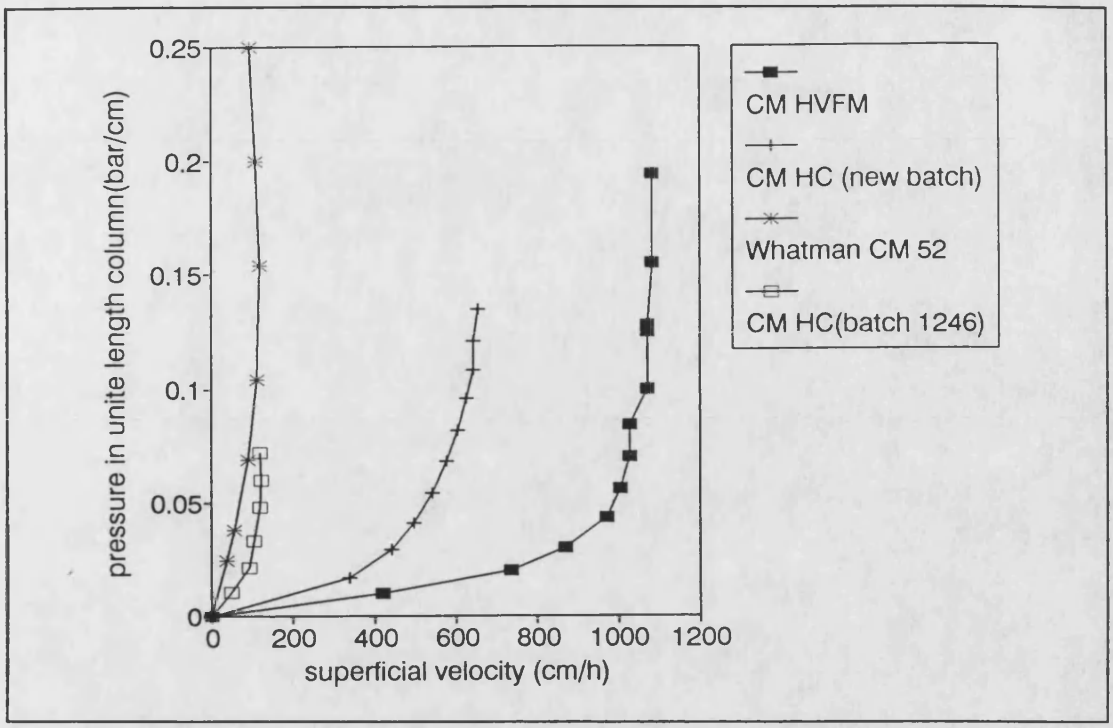

Fig. 5.5 Compressibility of cellulose ion-exchangers under water flow.

velocity. It should be noted that the small column used in these studies might, in fact, stabilize the bed (the so-called "wall effect") to some degree. Thus, the extrapolation of the pressure against flow characteristics to larger column dimensions is unwarranted (Matson and Siebert, 1988), especially in columns packed with small particle ion-exchangers. As CM sponge is a coherent block material with very open structure, it therefore can retain some wall support even in the middle of relatively large column. CM sponge was less sensitive to compression under pressure than these other two commercial cellulose ion-exchangers, under the conditions of the experiment.

5.5 Flow-Rate of CM Sponge

Flow-rate through ion-exchangers is usually limited by the

compressibility of the matrix. A large particle size can allow fast flows but it creates internal transfer resistances which slow the overall kinetics of the process. Productivity of these exchange columns, is thus limited by either the diffusion within the particles or the flow through the bed.

A higher flow-rate will reduce the resistance of film diffusion and hence increase productivity by decreasing processing time. High resolution in ion-exchange chromatography requires the column to have a certain length, whilst the flow-rate is inversely proportional to column length. Even stirred tank operations have to consider flow-rate because the thickness of the resin bed affects the flow-rates during drainage. For the problem of recovering a biological molecule present in very low concentration in a large volume of feedstream, flow-rate is the major factor which has to be optimised. Coarse cellulose resin allows a high flow-rate to pass, but it has to be operated at a low flow-rate in order to match the slow kinetic processes inherent in having large particles and long diffusion pathways. Fibre and fine resin have fast adsorption kinetics, but the flow-rate can be poor due to the compression of the column bed.

In the physical stability section, the CM sponge has been identified as being less sensitive to compression than other commercial cellulose ion-exchangers. This section examines the effect of various diameters and lengths of column on the column flow-rate.

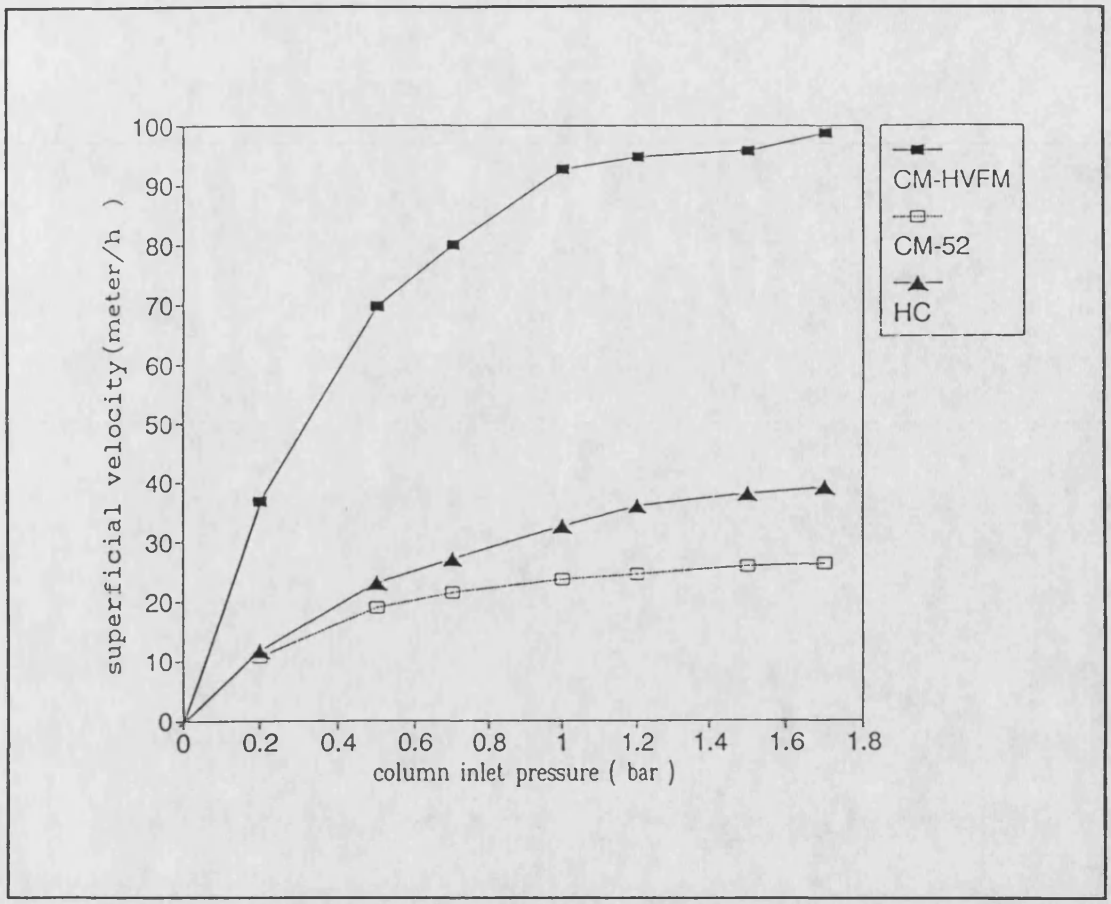

Fig. 5.6 The effect of pressure on superficial velocity for CM sponge, CM 52 and HC (batch 1246) in a 4 x 43 mm I.D. column.

5.5.1 Results and Discussion

Fig.5.6 indicates that the superficial velocity through the CM sponge or CM 52, or HC (batch 1246) in the short column(4 x 43 mm I.D. column) could reach 92.76 $m.h^{-1}$ for CM sponge, 32.00 $m.h^{-1}$ for Indion HC (batch 1246) and only 23.64 $m.h^{-1}$ for Whatman CM 52 at an inlet pressure of 1 bar. All three kinds of ion exchangers tended to plateau, even when the inlet pressure was increased to 1.7 bar.

Although very high flow-rates are obtainable for very short beds, this is not possible for long beds, with conventional materials. When the CM sponge or 60 g of a 1:1 slurry of CM 52 or the HC (batch 1246), was packed in a polycarbonate column of dimension 106 x 26 mm I.D. (Fig.5.7), it could be seen that, at an inlet pressure of 0.4 bar, the superficial velocity through CM sponge could still be increased to 9.50 $m.h^{-1}$ in the upflow mode. The CM 52 and HC could not however maintain their previous performance. The maximum superficial velocity of both of the latter was only around 1.00 $m.h^{-1}$ and the CM 52 inside the column was compressed to around 18% of its original length at the inlet pressure of 0.7 bar, due to pressure forces within the system. This accords with the findings of Levison *et al.*(1990a). The superficial velocity through the HC was slightly higher than that through CM 52 because the particle size of HC was 3-4 times larger than that of CM 52. Therefore scale up of the CM 52 and HC was not considered further.

Scaling the column diameter up 5.7-fold to 147 mm I.D. would be expected to create a serious flow problem as the effect of the wall support is lost. Data from Levison *et al.* (1990a,b) showed that with DEAE 52 the most practicable flow for a column with diameters above 100 mm was 0.3 $m.h^{-1}$. With CM sponge (Fig.5.7) the increase in diameter caused only a further loss of flow of about 15%, depending slightly on whether the flow was up or down through the column.

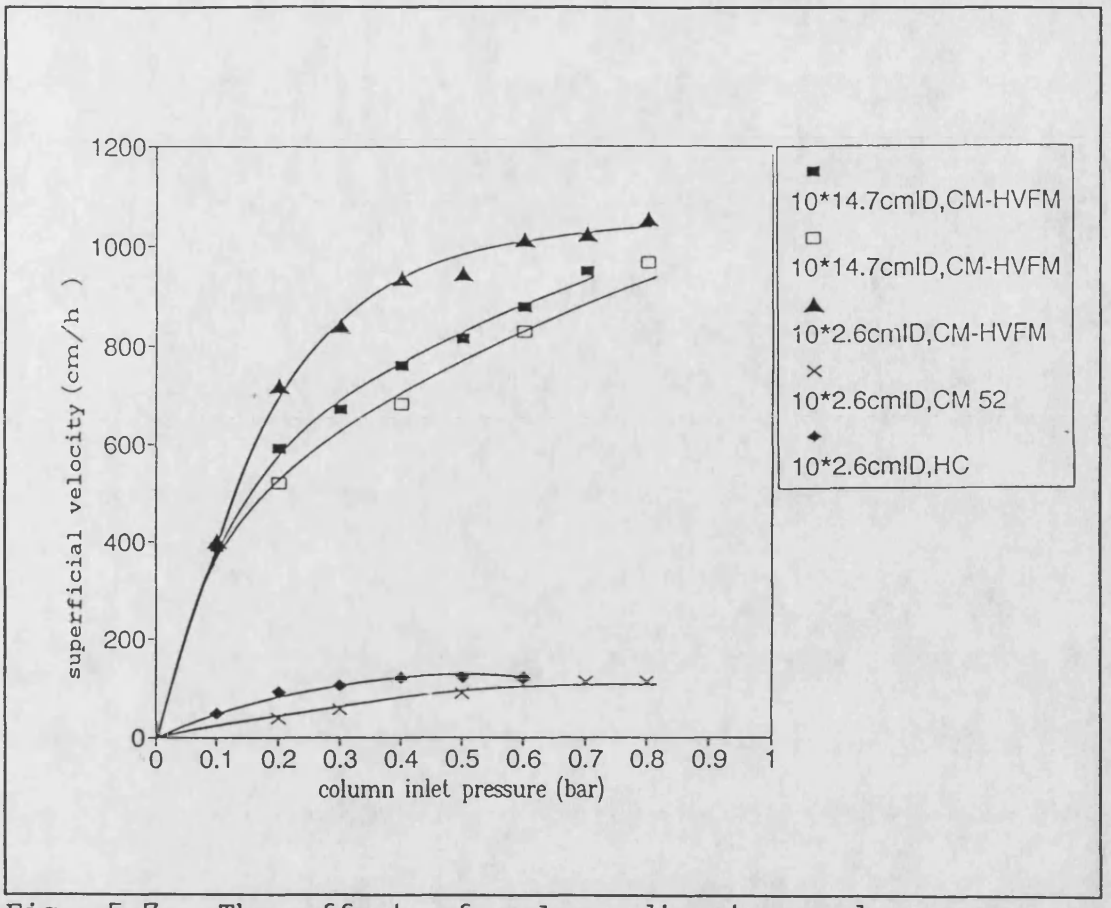

Fig. 5.7 The effect of column diameter and pressure on superficial velocity of CM sponge and comparison with 26 mm diameter column packed with CM52 and HC(batch 1246).
(■ ▲ × ◆ upflow mode, □ downflow mode)

The superficial velocity was not reduced at 0.1 bar compared to the small column, and at 0.4 bar reached 7 $m.h^{-1}$. This suggested that a superficial velocity of 5 - 7 $m.h^{-1}$ might be applied on the process scale.

5.6 Kinetic Behaviour of Adsorption and Desorption of CM Sponge Operated at High Flow-Rates

The ion-exchange process is diffusion limited. The adsorption reaction at the adsorbent surface is usually assumed

to be fast whilst the limiting processes for adsorption and elution are considered to be the film diffusion resistance around the matrix and the pore diffusion resistance within it. In this section the surface reaction model was used to determine apparent kinetic constants. Hubble (1989) stated that the surface reaction model (equation 5.2) was extremely simple and a useful aid to experimental design, although more rigorous models would be needed for process design purposes. More detailed models in which the film diffusion and pore diffusion resistance are included are discussed in the next chapter.

In practice the adsorption and desorption constants as fitted by the surface reaction model represent the rates of adsorption and desorption of the adsorbate onto the functional site on the surface of adsorbent lumped together with the mass transfer rates. Kinetics are usually studied using batch adsorption experiments. At a sufficiently high stirring speed, the effect of diffusion in the liquid film surrounding the adsorbent particle could be reduced to a minimum. The surface reaction is controlling and the intrinsic K_1 can be determined using the surface reaction model (equation 5.2), based on the adsorption data, and K_2 can be obtained from the product of K_d and K_1, where K_d has been determined from the isotherm. These kinetic parameters in a surface reaction model, as Chase (1984a) and Skidmorn and Chase (1988) stated, combined all mass transfer resistances because: (1) the liquid film can not be completely eliminated in practice, and (2) the diffusion resistances inside the particle and pore diffusion resistances are still in

existence. These K_1 and K_2 are thus lumped parameters.

As CM sponge can sustain high flow-rates, this section demonstrates the effect of flow-rate on the lumped kinetic parameters. In order to simulate the kinetic behaviour in the column operation, and as it is also impossible to convert the stirred speed into a superficial velocity of a column, the kinetic experiments were carried out in a differential recirculation bed column , 4 x 43 mm I.D.. For the mathematic model the lumped parameter surface reaction equation was used. In the differential bed column experiment, the column wall effect, axial dispersion and uneven distribution could be neglected due to the recycle mode of the differential bed. Moreover, the kinetic behaviour also showed the effects of back pressure deformation which could not be simulated in a stirred beaker. For general comparison kinetic experiments were also carried out on CM sponge while had been finely chopped in a laboratory blender and then suspended in a stirred vessel 160 x 90 mm I.D..

5.6.1 Results and Discussion

Figs. 5.8 and 5.9 show the relationship between the kinetic rates of adsorption and desorption of 5.8 ml of CM-HVFM in the 4 mm x 43 mm I.D. column. The column was first fed with 180 ml of 0.5 mg/ml lysozyme in 0.01 M sodium acetate/acetic buffer, pH 5.0 to adsorb the lysozyme and then eluted the adsorbed lysozyme using 180 ml of 0.7 M NaCl at various superficial velocities.

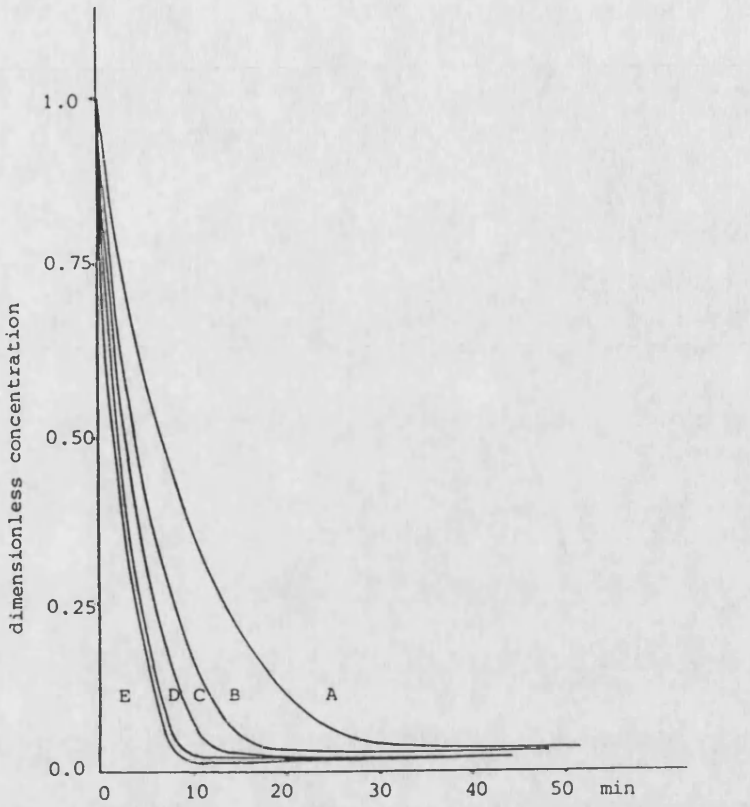

The adsorption of 180 ml of 0.5 mg/ml lysozyme in o.o1 M NaAc buffer pH 5 in a 4 mm deep by 43 mm I.D. column at various superficial velocity.
A = 297 cm/h, B = 644 cm/h, C = 1388 cm/h
D = 4443 cm/h, E = 9276 cm/h.

Fig. 5.8 The adsorption of 180 ml of 0.5 mg/ml lysozyme in 0.01 M NaAc buffer, pH5 in a 4 x 43 mm I.D. column at various superficial velocity.

The same volume was used for both elution and adsorption so that an indication of the overall mass balance and the percentage adsorption could be gauged readily from the UV chart trace.

From Fig.5.8 curves A to E and Fig.5.9 curves A to E illustrate that with the superficial velocity varying from 2.97 $m.h^{-1}$. to 92.76 $m.h^{-1}$., the rate of adsorption and desorption

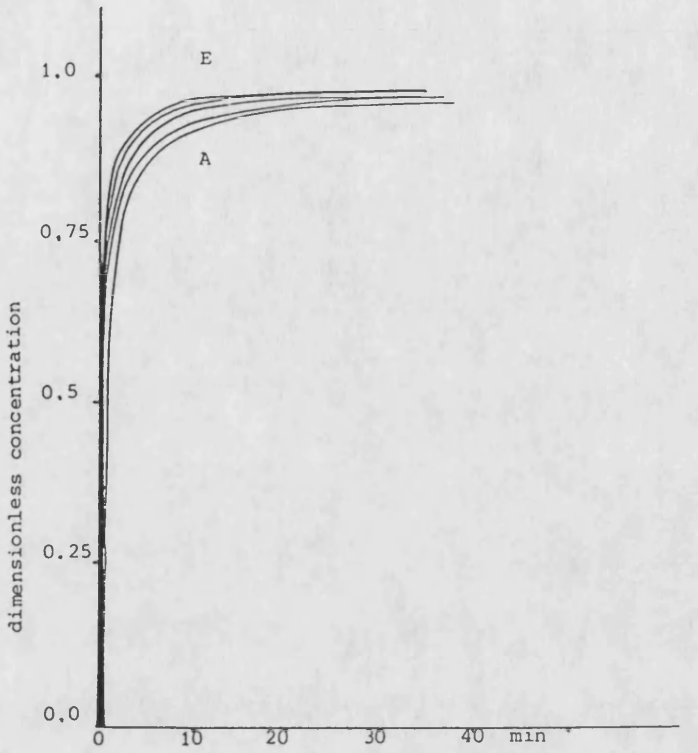

The desorption of the adsorbed lysozyme with 180 ml of 0.7 M NaCl in a 4 mm deep by 43 mm I.D. column at various superficial velocity.
A = 297 cm/h, B = 644 cm/h, C = 1388 cm/h,
D = 4443 cm/h, E = 9276 cm/h.

Fig. 5.9 The desorption of the adsorbed lysozyme using 180 ml of 0.7 M NaCl in a 4 x 43 mm I.D. column at various superficial velocity.

increased with increasing superficial velocity. 80% of the total lysozyme was adsorbed in 14 min and 90% of adsorbed lysozyme was eluted in 10 min at the superficial velocity 2.97 $m.h^{-1}$. (Fig. 5.8-A and 5.9-A). At a superficial velocity of 13.88 $m.h^{-1}$., 90% of lysozyme was adsorbed in 8 min and 90% of adsorbed lysozyme was eluted in 6 min (Fig. 5.8-C and 5.9-C). Further increasing the superficial velocity to 44.43 $m.h^{-1}$. at the inlet pressure

0.21 bar required only 3.5 min for 90% of lysozyme to be adsorbed and only 5 min for 90% of the adsorbed lysozyme to be desorbed (Fig.5.8-D and 5.9-D). These times of adsorption and desorption were only slightly improved when the flow velocity was increased to 92.76 $m.h^{-1}$. at an inlet pressure of 1 bar (Fig.5.8-E and 5.9-E). It appeared that the flow rate was no longer the main limiting factor above about 50 $m.h^{-1}$. This also meant that the liquid film mass transfer was no longer controlling. Conversely, at slower flow-rates the fastest kinetics were not attainable due to decreased mass transfer in the fluid phase. The adsorption time for 90% lysozyme adsorption and desorption of 90% adsorbed lysozyme was reduced by factors of 5.7 and 2 respectively by increasing the superficial velocity 15 fold, from 2.97 $m.h^{-1}$. to 44.43 $m.h^{-1}$.

It is interesting to note that the desorption of CM-HVFM is less influenced by external mass transfer in comparison with the adsorption processes (Fig. 5.9). Graham and Fook (1982) used DEAE cellulose to adsorb bovine serum albumin (BSA) at pH 6.5 and then desorb BSA at pH 10 with 3% NaCl, and found that the desorption was largely intraparticle diffusion controlled.

Since the flow-rate of CM 52 and HC are restrained(Fig.5.7), the kinetic behaviour of adsorption and desorption of CM 52 and HC (batch 1246) had to be described at superficial velocity less than 1 m/h, *i.e.* 0.99 $m.h^{-1}$ and 0.51 $m.h^{-1}$ respectively. Otherwise, the loading and process conditions for the kinetics study of both CM 52 and HC were exactly the same as

for CM-HVFM.

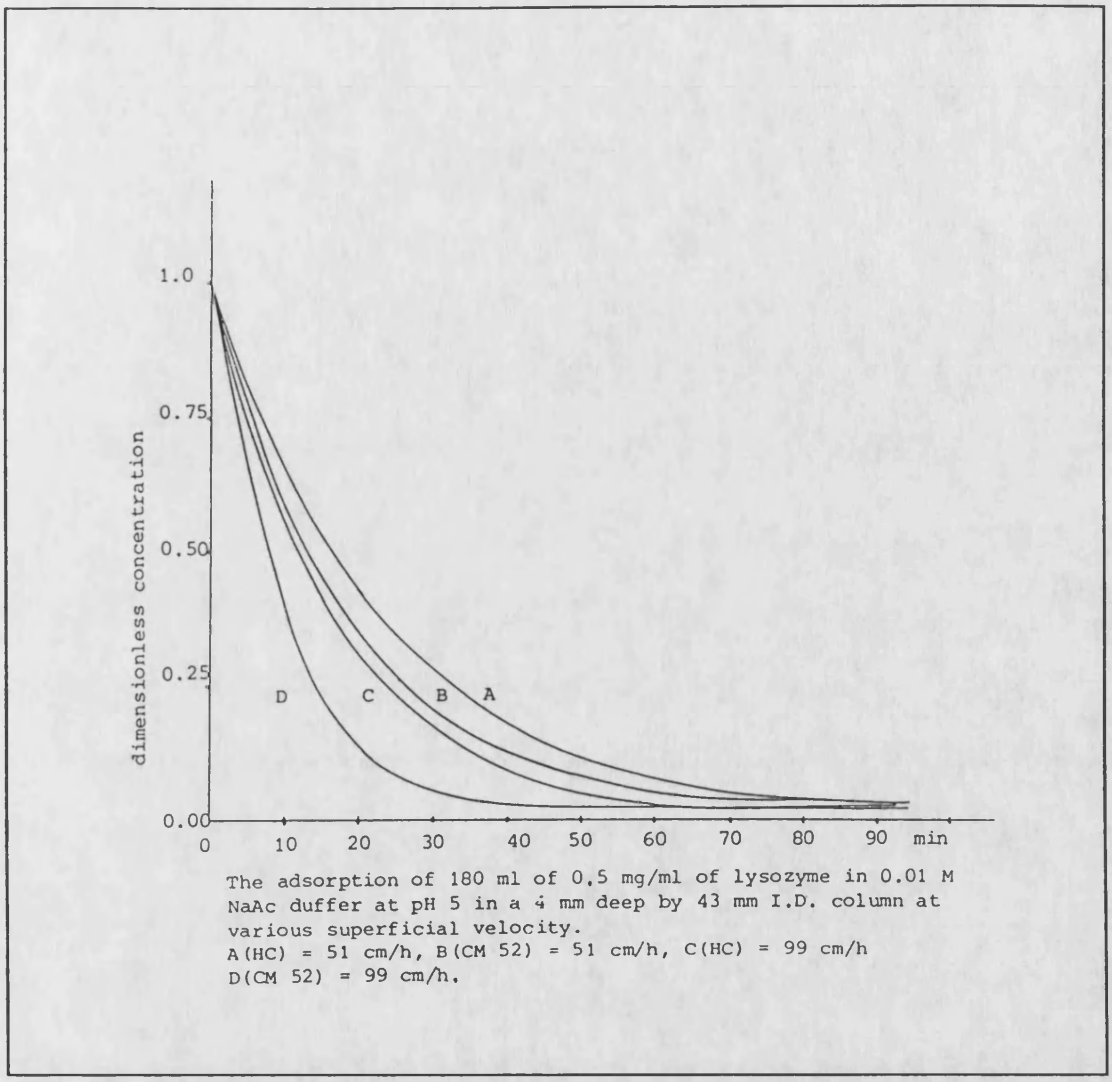

Fig. 5.10 The adsorption of 180 ml of 0.5 mg/ml lysozyme in 0.01 M NaAc buffer, pH 5 in a 4 x 43 mm I.D. column at various superficial velocity.

Fig. 5.10 and Fig. 5.11 illustrate that the kinetic processes of CM 52 are faster than those of HC in both cases due to the large surface area to volume ratio of microgranular material.

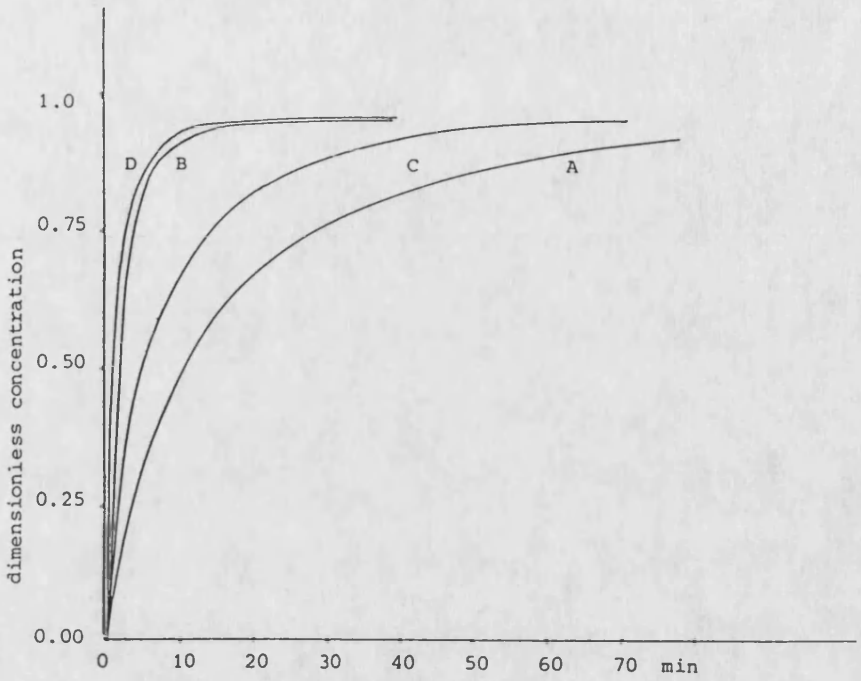

The desorption of adsorbed lysozyme with 180 ml of 0.7 M NaCl in a 4 mm deep by 43 mm I.D. column at various superficial velocity.
A(HC) = 51 cm/h, B(CM 52) = 51 cm/h, C(HC) = 99 cm/h
D(CM 52) = 99 cm/h.

Fig. 5.11 The desorption of adsorbed lysozyme using 180 ml of 0.7 M NaCl in a 4 x 43 mm I.D. column at various superficial velocity.

With the same loading conditions as for the CM-HVFM, it needed 17 min and 31 minutes respectively to adsorb 80% of loaded lysozyme for CM 52 at the superficial velocity 0.99 $m.h^{-1}$ and 0.51 $m.h^{-1}$. For HC, however it needed 27 min and 37 min under the same conditions (Fig. 5.10). Although the CM 52 exhibited faster desorption than HC, it still needed 10 min and 14 min to elute 90% of the adsorbed lysozyme at 0.99 m h^{-1} and 0.51 $m.h^{-1}$

respectively. The HC needed more than 40 min to elute the same amount of protein. Experiment (Fig. 5.7) indicated that it was difficult to operate the 100 x 26 mm I.D. column packed with CM 52 at a superficial velocity of more than 0.90 $m.h^{-1}$ because the microgranular material was becoming more and more compressible. This required in higher and higher pressures at the same flow rates. It was apparent from the above data that this would result in significant mass transfer limitation in the external film. It was thus not possible to use the microgranular CM-52 or HC2 at their optimum kinetic rate owing to the flow restrictions.

The higher flow velocities attainable through the new matrix, CM sponge, allowed much faster kinetics to be exhibited. Even this material had reduced flows in the larger scale columns and whilst 40 m/h would be kinetically optimal only 7 m/h could be sustained on the 100 mm x 147 mm I.D. column. This was about 20 times faster than that attainable on the Whatman and Indion materials in the same size column.

5.6.2 Establishment of Kinetic Parameters and Effect of Flow-Rate on Lumped K_1 and K_2

q_m and the ratio of $K_d = K_2 / K_1$ can be determined by fitting a Langmuir isotherm to equilibrium data, *i.e.* using equation 5.6 the K_d and q_m can be determined from the slope and intercept of linear regression or the non-linear regression. This is shown in

Fig.5.4b. For a non-steady-state system, equations 5.9, 5.10 and 5.11, 5.12 can be used to determine the K_1 and K_2. During the adsorption process, protein concentration in the liquid phase is given as following

$$C=C_o-\frac{qM}{V} \tag{5.9}$$

where M and V are the mass of adsorbent and feed volume respectively, and C_o is the initial protein concentration. The K_2 is replaced with K_d and K_1 in equation 5.10. The initial conditions are when t=0, $C=C_o$, q=0. The K_2 obtained from the adsorption process, however, does not represent an absolute desorption, or equilibrium, constant for the process as it will depend on the conditions used *i.e wether a adsorption or desorptionis being carried out.*

$$\frac{dq}{dt}=K_1\left(C_o-\frac{qM}{V}\right)(q_m-q)-K_dK_1q \tag{5.10}$$

For the desorption process, equation 5.10 is rewritten as equation 5.11 and the initial conditions are when t=0, $q=q_o$, C=0.

$$dq/dt=\frac{K_2}{K_d}C(q_m-q)-K_2q \tag{5.11}$$

where

$$C=(q_o-q)\frac{M}{V} \qquad (5.12)$$

q_o is the initial protein concentration of adsorbent.

Equations 5.9, 5.10 and 5.11, 5.12 were solved and simulated by the ISIM programm using the 5th order variable step Runge-Kutta method (Fang-ads and Fang-des in Appendix 1). The theoretical curves generated by equations 5.9 to 5.12 were compared with the experimental values that were taken from the recorder trace of the UV monitor. All these curve fittings are shown in end of this chapter. The values of K_1 and K_2 at a variety of conditions were thus determined as that which gave the best fit of the theoretical curve, calculated from equations 5.10 (for adsorption) and 5.11 (for desorption), to the experimental data points. The values of K_d and q_m determined from the isotherm were used without alteration and only the adsorption constant K_1 needed to be adjusted in the adsorption processes unless otherwise stated. Through Figs. A1.1 to A1.4 (in Appendix 1), it can be seen that the theoretical curves, or model curves, agree well with the experimental data. In order to fit the adsorption curves obtained from the stirred vessel experiments (Figs. A1.5 to A1.7 in end of this chapter) the initial part of the adsorption curve was dependent on adjusting the K_1, whilst either K_d or qm required adjustment in order to fit the curve tail. The long tail is probably due to the effects of the internal diffusion processes of the adsorbent which were not considered in the model used. K_d or q_m thus had to be readjusted. For the differential bed column, the applied lysozyme loading capacity

was only 14% of the column's maximum lysozyme capacity. At this low loading, all the adsorbate could be adsorbed onto the outside surface of adsorbent. In this case the internal diffusion was unimportant and the surface reaction model fits the experimental data well.

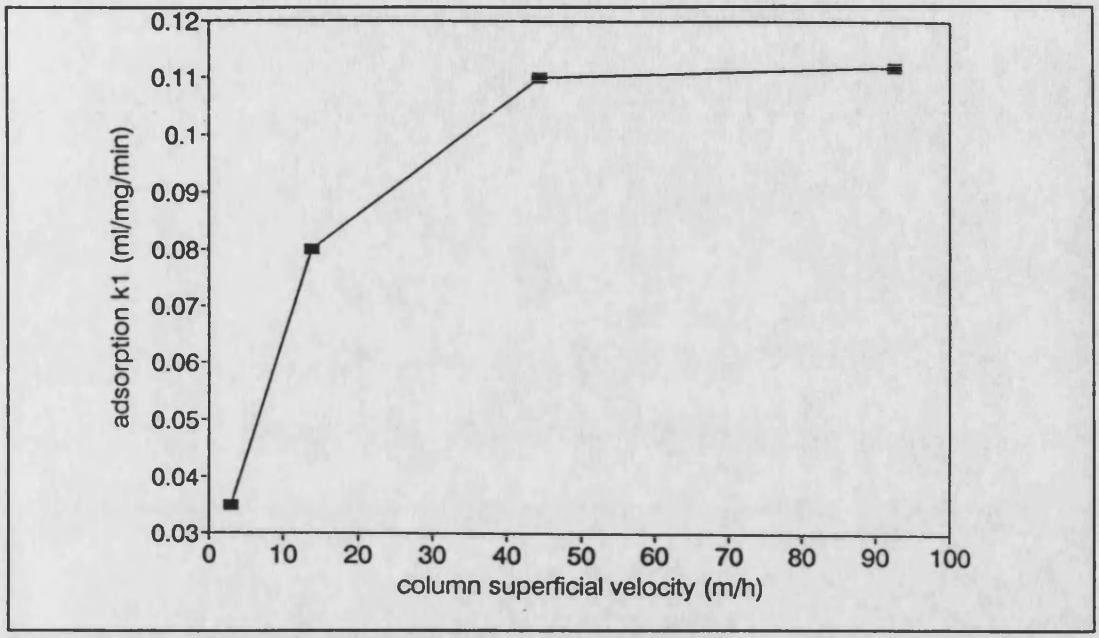

Fig. 5.17 Effect of superficial velocity on the adsorption constant K_1

In the stirred vessel experiments, the lysozyme loading was overloaded in excess so that the adsorbent was not wholly adsorbed onto the surface but also diffused into the particle. This resulted in a long tail on the adsorption curve. Graham and Fook (1982) applied cellulose DEAE adsorbent to adsorb BSA. They concluded that during the initial period of adsorption the adsorption rate was controlled by film diffusion, after which it was controlled by intraparticle diffusion. Addo (1988) found similar results.

Fig.5.12 gives the results of K_1 at various superficial velocities. At a superficial velocity below 45 m/h, the lumped K_1 dramatically increased with increasing flow-rate. This means that the lumped K_1 was highly dependent on the flow-rate. Beyond a superficial velocity of 45 m/h, flow-rate no longer affected the lumped K_1. On the other hand, from the flow independent region it was found that the intrinsic adsorption constant K_1 was in the range from 0.105 to 0.12 ml/mg/min. This was an identical conclusion from the stirred tank experiment in Fig.5.13, in which found the adsorption constant K_1, in the range 0.1 to 0.11, where it was slightly influenced by the motor stirrer speed.

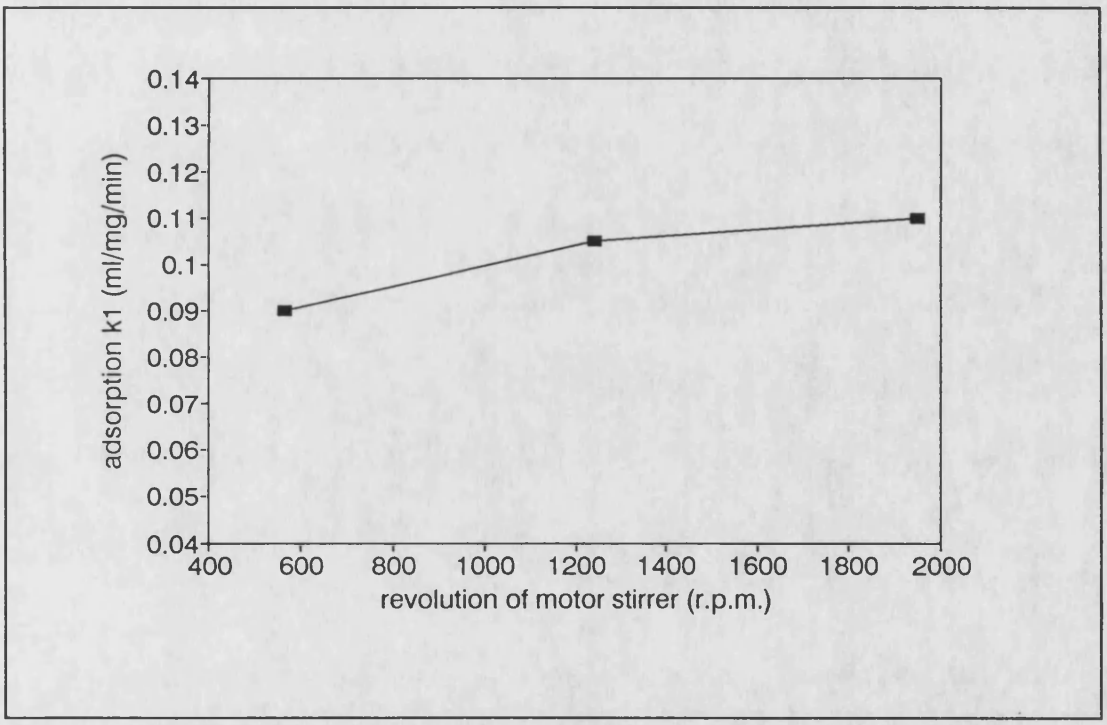

Fig. 5.13. Effect of rotation speed of motor stirrer on adsorption constant K_1

The curve fitting of the desorption process is shown in Fig.A1.8 to Fig.A1.19 (end of this chapter). The effect of the

ionic strength of eluent on the desorption constant K_2 was also investigated, Figs.A1.16 to A1.19 (end of this chapter). The simulation result from the differential recirculation column showed that ; (1) the sharpness of the desorption curve was dependent on the K_2, the larger K_2, the sharper the curve; (2) the desorption percentage which increased with K_d and the decrease of q_m was fully governed by K_d and q_m. It is noted from Fig.5.4d that the values of K_d and maximum protein capacity q_m are 2 mg/ml and 1100 mg/g respectively in the high ionic strength 16.6 ms/cm (0.17 M NaCl). During the desorption one would expect the K_d be larger than, or equal to, 2 mg/ml and q_m smaller than, or equal to, 1100 mg/g respectively since the NaCl concentrations of eluent during desorption experiment were greater than 0.17 M. As with desorption in the stirred vessel, the initial part of desorption curve depended on K_2, whilst the tail of the desorption curve was mainly affected by K_d and q_m. In contrast to the adsorption process, the K_2, obtained from both the differential bed column and the stirred vessel, were slightly reduced at low the superficial velocity and stirred speed of the motor stirrer (Fig.5.14 and Fig.5.15). The intrinsic K_2 value, which was independent of superficial velocity and stirred speed, was larger than 0.9/min.(Fig.5.14 and Fig.5.15)

The desorption constant K_2 greatly depended on the ionic strength of the eluent, as seen in Fig.5.16. At NaCl concentration below 0.5 M, the K_2 increased with NaCl concentration in the eluent, whilst greater than 0.5 M the K_2 seemed to be independent of the NaCl concentration. This leads

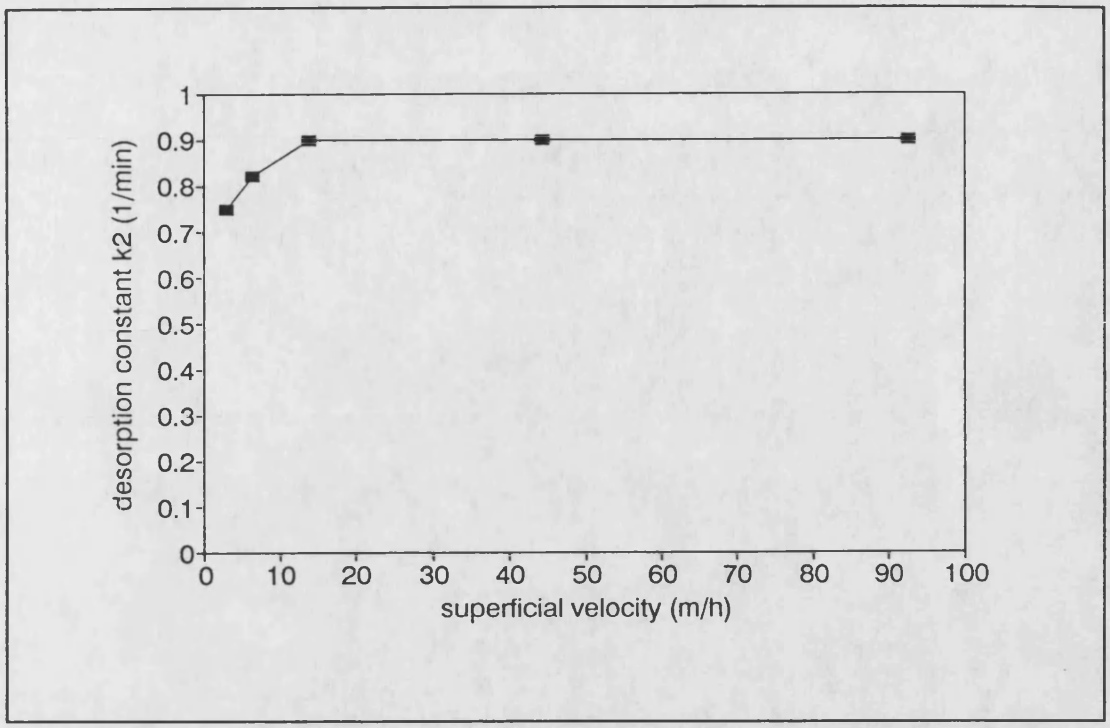

Fig. 5.14. effect of superficial velocity on desorption constant K_2

to a conclusion that the NaCl concentration in the eluent should be larger than, or equal to 0.5 M for maximum desorption rate.

The surface reaction model can describe the desorption process reasonably although the simulation results seem to leave a deviate systematically from the experimental data (Fig.A1.8 to Fig.A1.19 in end of this chapter), which was not the case with adsorption. This also suggests that diffusion processes play a more important role throughout the desorption process. Again this is not considered in the surface reaction model.

The K_1 and K_2 have little in common with rate constants of true chemical reactions, and instead are empirical lumped mass

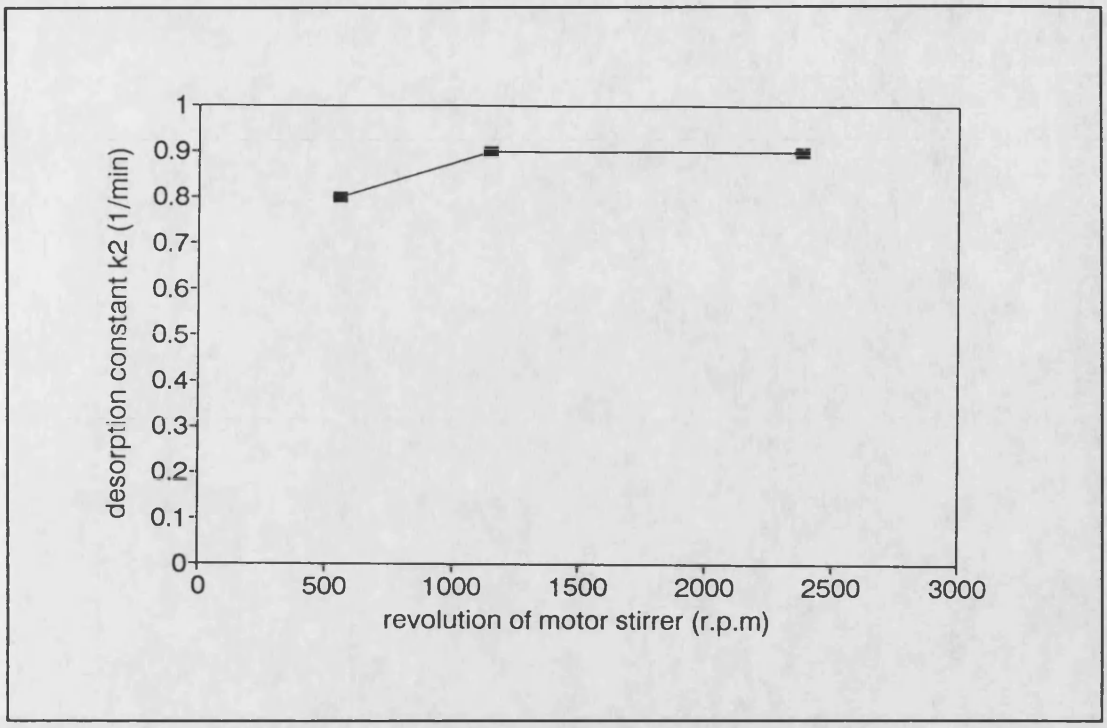

Fig.5.15. Effect of rotation speed of motor stirrer on desorption constant K_2

transfer parameters which will be functions of the system's operation variable. K_2 is hardly affected by mass transfer, whilst the intrinsic K_1 (unaffected by mass transfer) can be obtained at high stirred speed or flow rate. But in practice even with CM sponge flow rates are slower and K_1 is a lumped parameter strongly influenced by mass transfer.

5.7 Chemical Stability

Ion exchange functional groups are well known to be stable in strong acids and bases. This is the reason why they can be regenerated by strong acids and bases as long as the matrix can withstand such severe conditions. On repeated use, cellulose ion exchangers do not deteriorate in quality. They can be stored for months in aqueous solution of 0.5 M NaH_2PO_4 to 1 M NaOH and

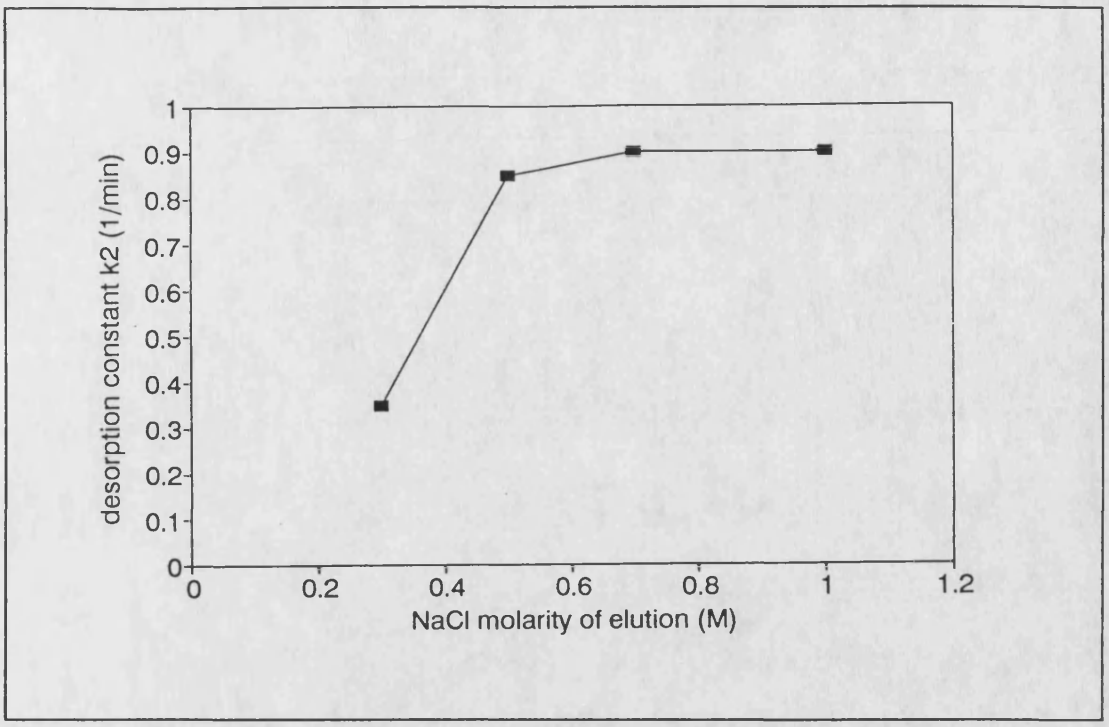

Fig. 5.16 effect of ionic strength of eluent on the desorption constant K_2

there is no degradation effect by a brief contact with 1 M HCl (Dorfner 1972). The study of chemical stability of CM sponge reported here, is focused on the chemical resistance of the cellulose itself, which was cross-linked using the author's standard recipe by visible examination.

5.7.1 Results and Discussion

Results in Table 5.2 indicate that CM sponge was highly resistant to high concentrations of alkali, high concentrations of acid (HCl and H_2SO_4) and high concentration of oxidation regent H_2O_2. This means that either the high alkali and acid could be used for pyrogen removal and microorganism destruction if the CM sponge were contaminated. This also means that the CM

sponge has a high reusability and robustness.

Table 5.2 Stabilities of CM Sponge

test solution	temperature (^{0}C)	time (hour)	comments (visible examination)
40%(w/v) NaOH	20	1	*stable
20%(w/v) NaOH	100	1	stable
2.75 M H_2SO_4	40	1	stable
6.5 M HCl	20	2	stable
15% H_2O_2	20	48	stable

* In comparison with the original sponge which was damaged under above conditions

5.7.2 Swelling And Shrinking Properties

Fig. 5.17, 5.18 and 5.19 show the dependence of the swollen or shrank volume of CM sponge at the various pH, salt and NaOH concentrations. No volume change was observed in the pH range 2-10 using the 0.1 M acetate buffer. Only slightly swollen or shrank volume occurred in the high NaOH or NaCl concentration (Fig. 5.18 and 5.19). These indicate that the CM sponge column can repeat separation, re-equilibrium and regeneration without repacking.

5.8 Stability and Reproducibility of CM Sponge

The ion exchanger could lose its ability to carry out ion exchange over time by losing functional groups during the operation. This might be due to: (1) the chemical breakdown of the ion exchange groups, (2) irreversible protein adsorption, (3) fouling, and (4) channelling, for example in the column operation. Ideally the ion exchanger should have a long life for

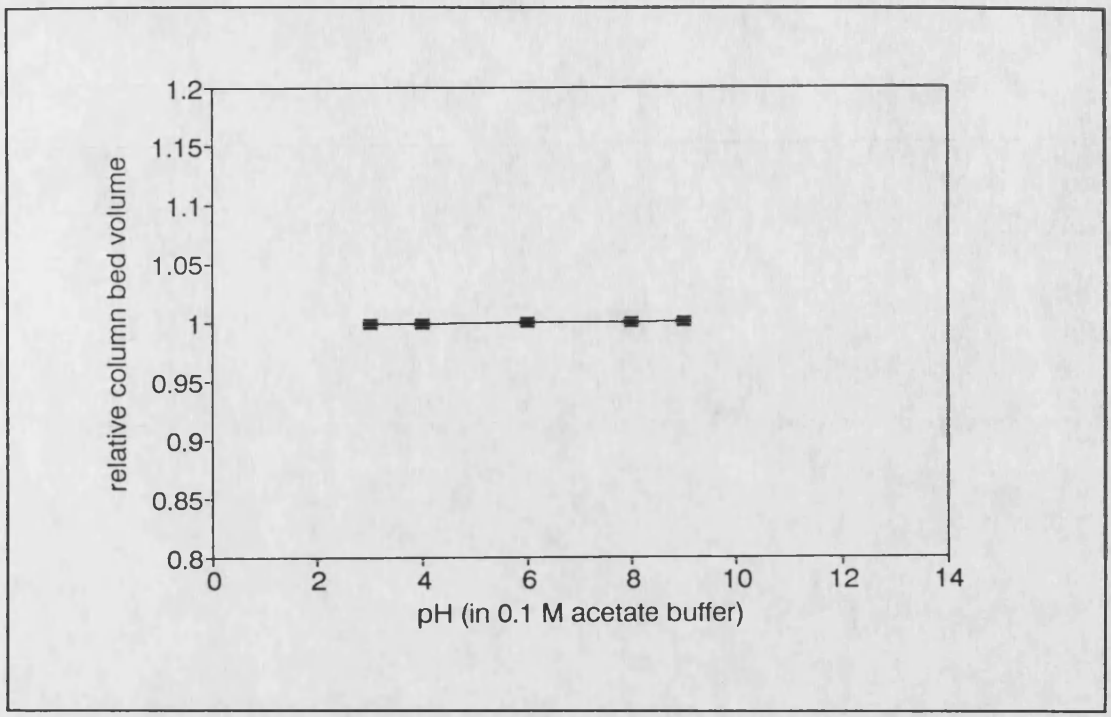

Fig. 5.17 Effect of pH on the volume of CM sponge column using 0.1 M acetate buffer

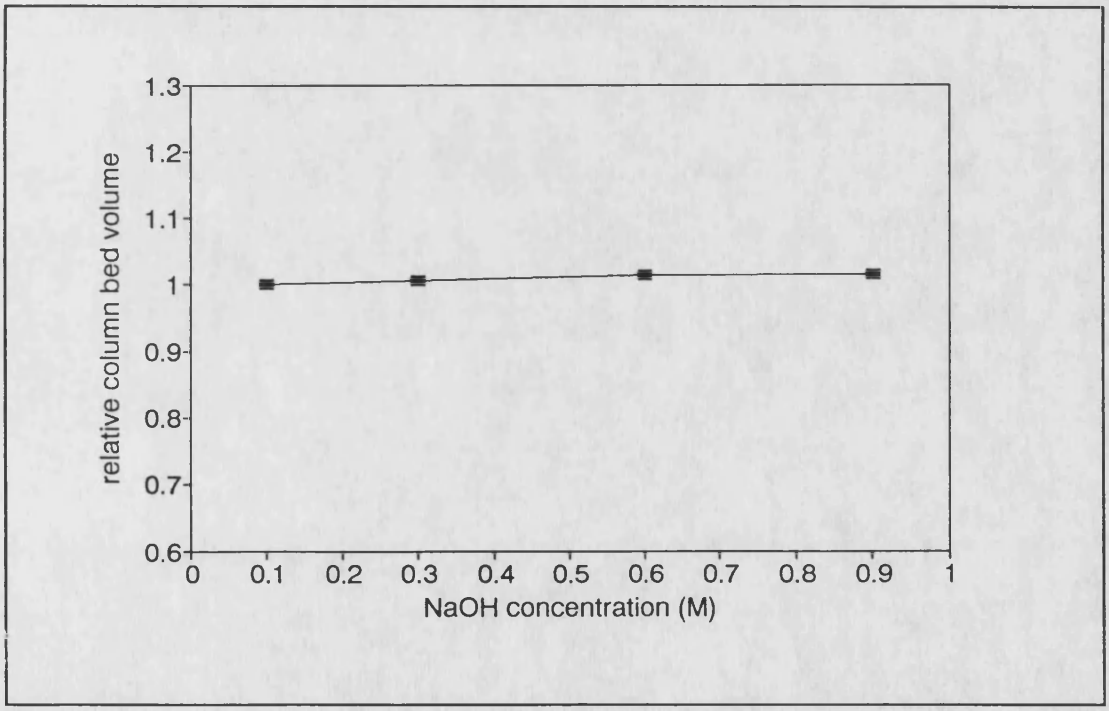

Fig. 5.18 Effect of NaOH concentration on the volume of CM sponge column

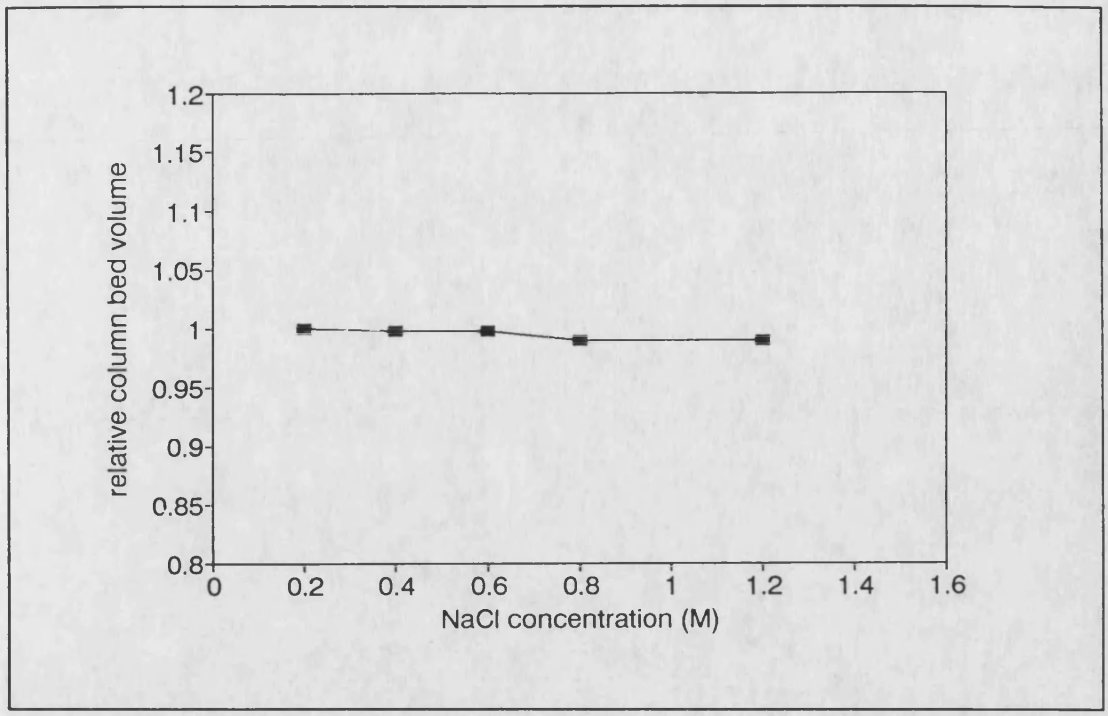

Fig. 5.19 Effect of NaCl concentration on the volume of CM sponge column

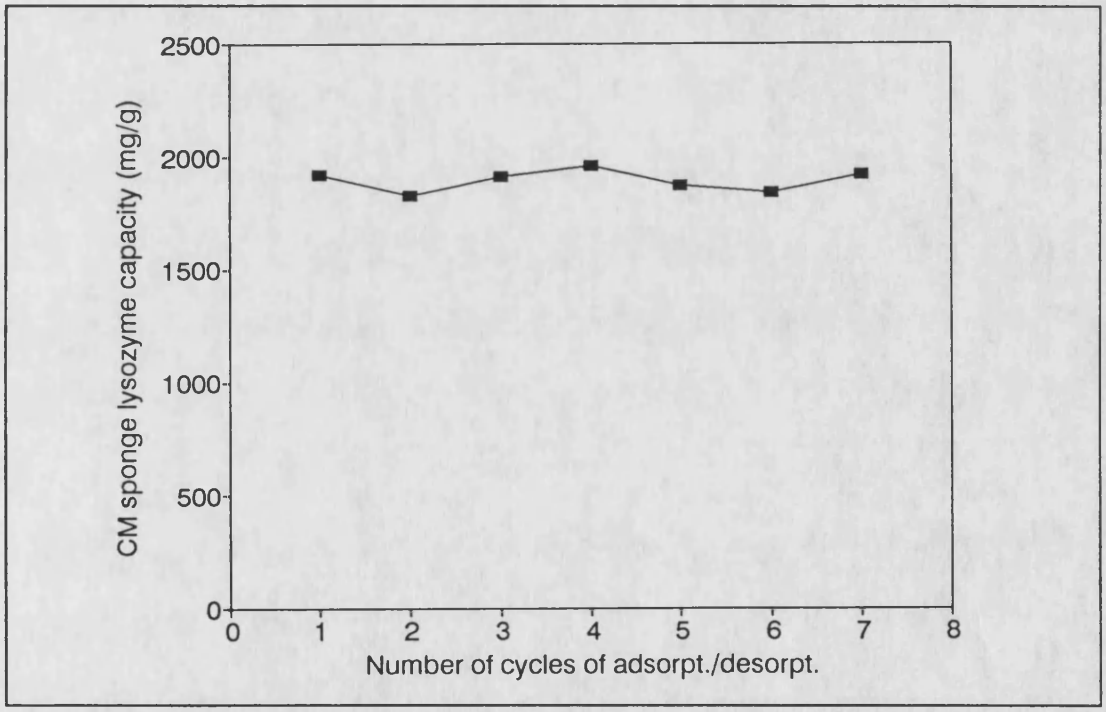

Fig.5.20 Effect of repeated adsorption-desorption cycles on CM sponge lysozyme capacity

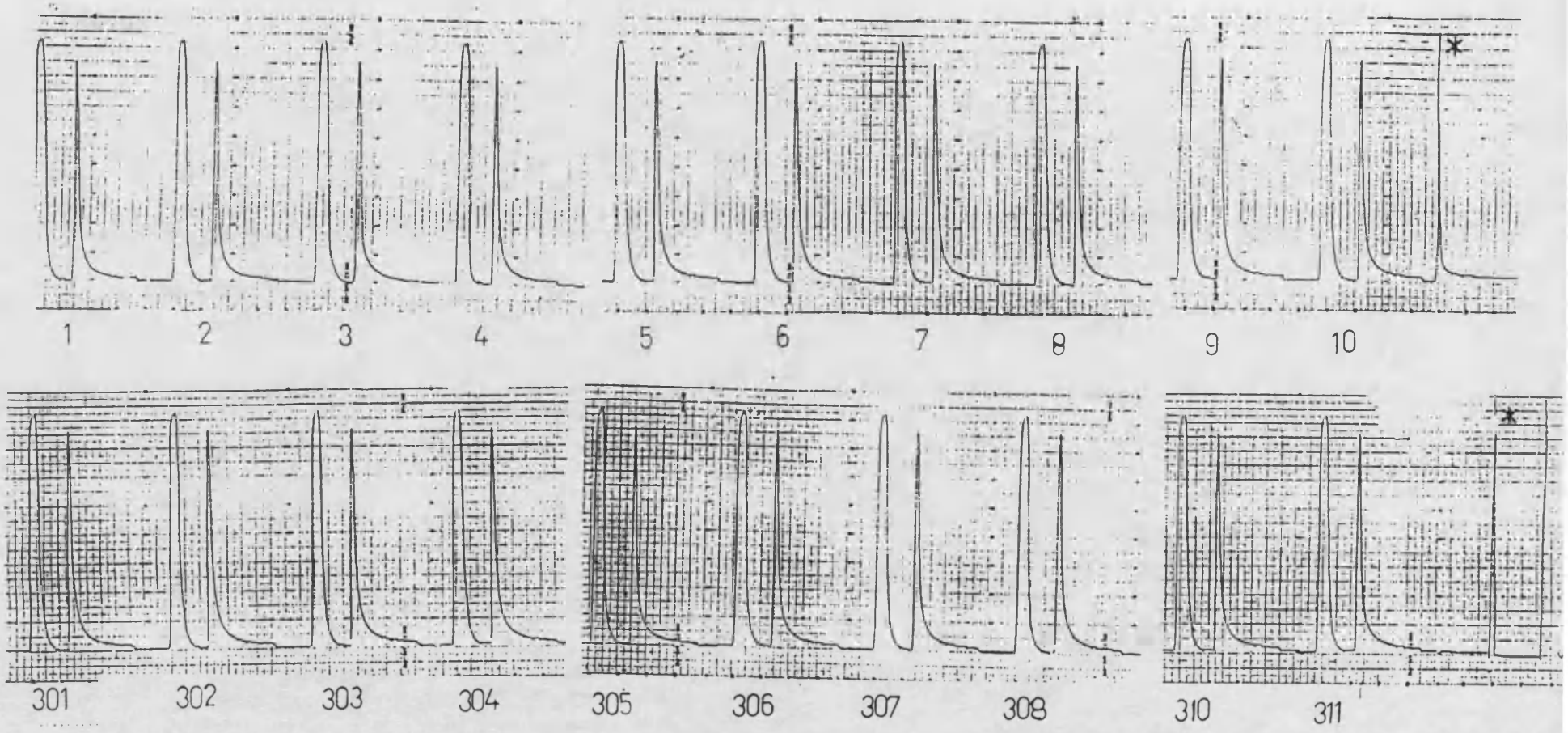

Each loading cycle consisted of a large peak and small peak
The large park was the effluent of egg-white, ovalbumin fraction, then was followed by the elution peak, conalbumin and lysozyme fraction.
Every tenth cycle was followed by a regeneration stage using 0.7 M NaOH solution which was represented by *.

Fig.5.21 The repetitive loading on egg-white of CM-HVFM column. The first row was the first ten cycles, the second was the thirtieth.

practical use. Two experiments were designed to examine the reproducibility and stability of CM sponge during many cycles of adsorption/desorption. The first one was designed to mainly examine whether the carboxymethyl group was still maintained after several cycles of adsorption/desorption . This could be showed by measuring the protein capacity changes over time. The second was concerned with not only the protein capacity but also the fouling and channelling of CM sponge column bed at high flow rate. In addition, the reproducibility of CM sponge performance in a practical separation was also examined. In order to do this, a considerable number of cycles of adsorption/desorption had to be carried out. An automatic control process was designed using a programmable logic controller to carry out 340 cycles of adsorption/ desorption. 1.3 times bed volume of 14%(v/v) fresh egg white solution at pH 4.5 was applied to a 68 x 17 mm I.D. CM sponge column at superficial velocity 503 ml/cm^2/h.

5.8.1 Results and Discussion

There are seven cycles in Fig. 5.20. The first three cycles involved adsorption followed by simultaneous desorption and regeneration by 2 M NaCl, in which the protein capacity was relatively constant. The last four cycles were first adsorption followed by desorption by 1 M NaCl and thereafter regeneration by 0.7 M NaOH. The protein capacity still remained relatively constant. The above results demonstrated that there was no significant leakage of ionogenic groups and the carboxymethyl group maintained its active state without deterioration regardless of the high salt and the high alkali concentration.

In a realistic production process, raw feed solution contains various impurities such as proteins, amino acids, sugar and starch which might be in high concentrations, while the protein of interest might be in low concentrations. This could not only cause the problem of column fouling, but also some irreversible protein adsorption would occur, which could gradually reduce the ion-exchange column capacity. The results of 340 cycles of egg white adsorption elution are given in Fig. 5.21. The eluent and elution peaks in the first cycle were identical with that in the last one. This indicated that the column performance, which included the adsorption and desorption kinetics, was not degraded. The column in fact withstood the loading of 20 mg/ml fresh egg-white, for 340 times, 1 M NaCl desorption for 340 times and 0.7 M NaOH regeneration for 34 times without being fouled or channelled. This robust character indicated a good potential for industrial application of CM sponge ion-exchanger. The experiment was concluded without observing any change in performance.

5.9 pH Titration of CM Sponge Ion-Exchanger (Helfferich, 1962 and peterson, 1970)

The total equilibrium weight capacity (IEC) can be expressed in milliequivalents of the H^+ form (cation exchanger) or Cl^+ form (anion exchanger) per dry gram of adsorbent. This then indicates the number of exchangeable counter ions in the adsorbent. For example, CM sponge ion-exchanger in the H^+ form can be considered as insoluble acids and thus can be titrated with standard bases. A pH titration curve can be recorded when the CM sponge is

titrated which is then analyzed to give the number of exchange groups present in it.

Ion-exchangers are often titrated in the presence of sodium chloride. This salt has little effect on the titration curves of dissolved acids and bases, but it changes the titration curves of ion exchangers. This is because

$$Cel\text{-}CH^2\text{-}COOH + Na^+ \rightleftharpoons Cel\text{-}CH^2\text{-}COONa + H^+$$

$$H^+ + OH^- \text{-------}> H_2O$$

When NaOH is added, the H^+ and OH^- is progressively neutralized and the ion exchange is driven to completion. The titration curve thus shows a gradual rise in the early stages of the titration and a sharp rise at the end of neutralization stage. The early part of the titration curve is lower and slightly more sloping due to the presence of NaCl.

The total equilibrium weight capacity (IEC) can be calculated from Fig. 5.22, *i.e.*

$$IEC\ (meq/g) = (N_{NaOH} \times V_{NaOH}) / (W)$$

where N_{NaOH} = normality of NaOH (M)

V_{NaOH} = consuming alkali volume (ml)

W = CM sponge dry weight (g)

For the CM sponge this gives

$$IEC = \frac{22.75ml x 0.1M}{1.863g} = 1.22 \pm 0.3meq/g$$

5.10 Conclusion

The CM sponge ion-exchanger has several advantages over the microgranular and spherical cellulosic ion-exchanger and some additional characteristics: (1) the irregular network structure provides a large surface area to volume ratio that allows a high protein capacity of over 2 g lysozyme/ g matrix, (2) The bed of CM-HVFM matrix can maintain an open structure ever under moderate pressure which caused beds of microgranular and spherical particle matrices to become blocked, (3) The physical stability of CM sponge ion-exchanger was highly superior to that of the Whatman CM 52 and Phoenix CM resin. This resulted in the CM sponge ion-exchanger being able to sustain superficial velocities of over 7 m h-1 in a 100 x 147 mm diameter column, (4) Due to the coherent block sponge structure, the CM sponge was less deflected under the same conditions of fluid flow in comparison with the scattered spherical particles. In addition, considering the very open structure of CM sponge might explain the compressibility and high flow-rate of CM sponge. (5) The K_d and lysozyme capacity of CM sponge were mainly affected by ionic concentration. 2100 mg/g capacity and 0.08 mg/ml K_d were obtained at the lowest ionic concentration. High protein capacity, for example 1460 mg/g, was still maintained even though the ionic concentration rose to 5.6 ms/cm. (6) The fine structure of the new matrix is such that

there are short diffusion pathways within the cellulose and a very high percentage of the surface is accessible to direct convective flow, which leads to rapid kinetics. The later was also commensurate with the flow rate allowing very fast large scale separations. (7) At a superficial velocity of below 40 m/h, the lumped adsorption rate, K_1, was mainly controlled by external mass transfer resistances, while beyond that superficial velocity, the external mass transfer resistances were no longer the limiting factor. In this case, K_1 might be only controlled by intraparticle and pore diffusion. The value of K_1 ranged from 0.105 to 0.12 ml/mg/min was thus considered to be a intrinsic adsorption rate, regardless of external mass transfer resistances. (8) The desorption constant K_2 mainly depended on the NaCl concentration of the eluent at which below 0.5 M, whilst above 0.5 M NaCl concentration K_2 seemed to be independent of the NaCl concentration. The NaCl concentration of the eluent should therefore be equate to, or larger than, 0.5 M in order to obtain the maximum desorption rate. With 0.7 M NaCl as eluent, the desorption process was not strongly affected by the flow rate but a slightly reduction of K_2 was observed at lower flow rate. These were the same conclusions drawn by Graham and Fook (1982). (9) The kinetic constants K_1 and K_2, which obtained from the differential bed column experiment, were identical with those from the stirred vessel at the highest flow rates and stirred speeds. This indicates that the differential bed column method is reliable and convenient for measuring K_1 and K_2. It only requires 14% of maximum protein capacity of adsorbent, and directly gives the relationship between the superficial velocity

and kinetic constants. This relationship is impossible to determine from the stirred tank method. (10) almost no volume change was observed in the CM sponge column at various pH, high NaCl and NaOH concentrations, which indicated CM sponge column not being swollen or shrauk. (11) The high chemical stability and the reusability means that the CM sponge ion-exchanger was very robust and withstood severe operation conditions. The column performance was not degraded neither being fouled nor channelled during 340 cycles operation. This shows the potential industrial application value of CM sponge ion-exchanger.

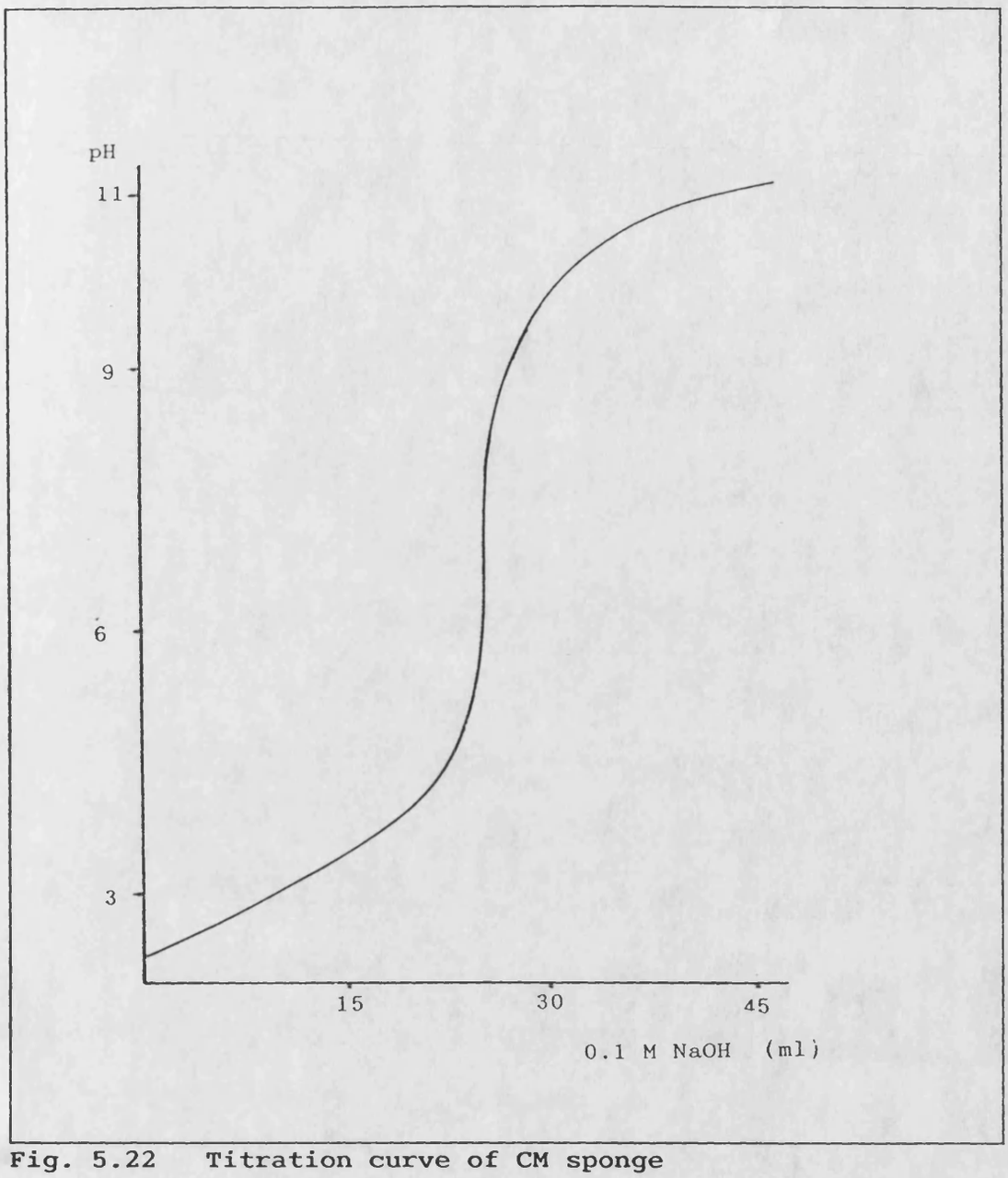

Fig. 5.22 Titration curve of CM sponge

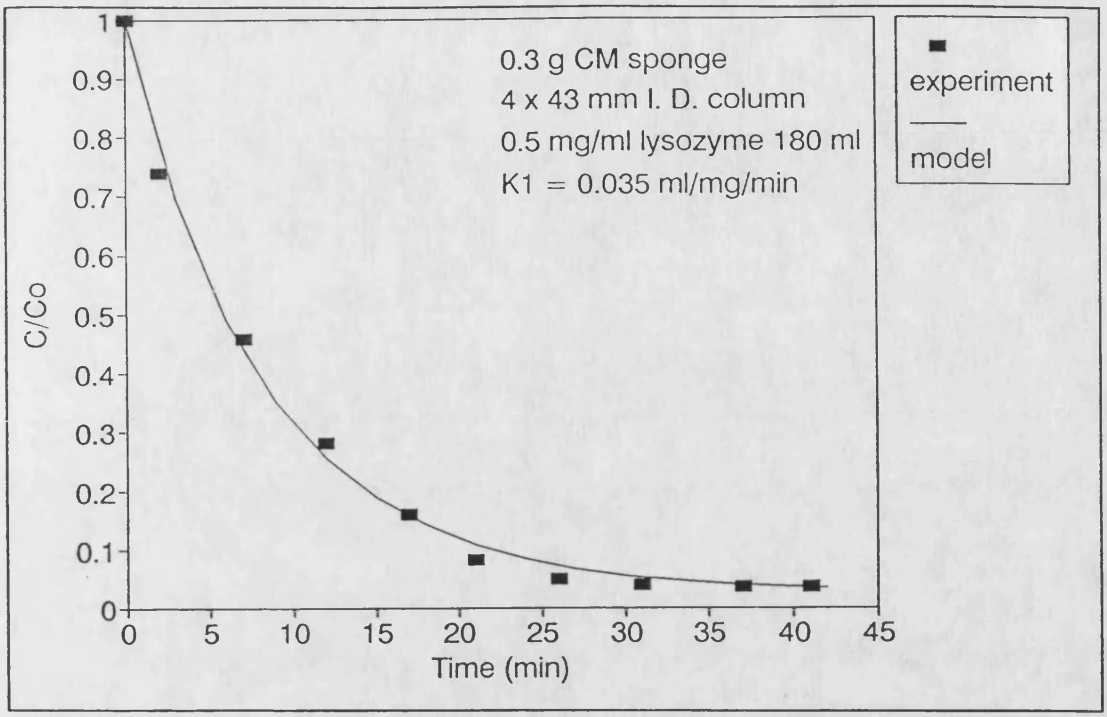

Fig. A1.1 Model simulation (K_1= 0.035 ml/mg/min) of adsorption at the flow-rate 72 ml/min or superficial velocity 2.97 m/h

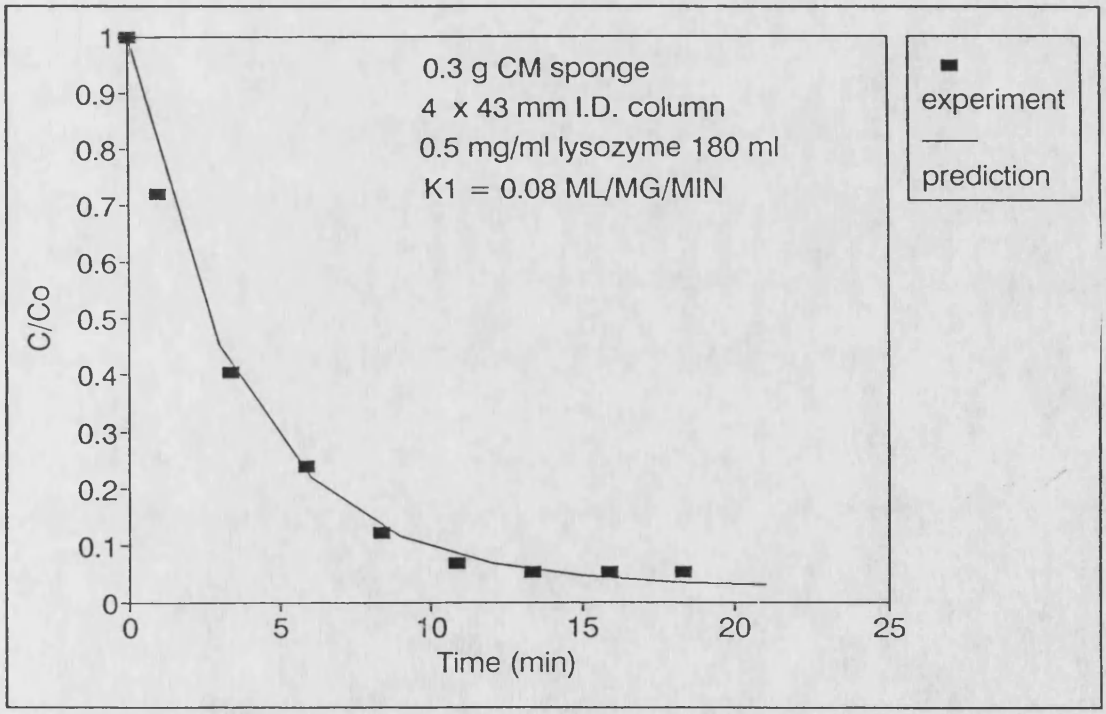

Fig. A1.2 Model simulation (K_1=0.08 ml/mg/min) of adsorption kinetics the flow-rate 336 ml/min or superficial velocity 13.88 m/h

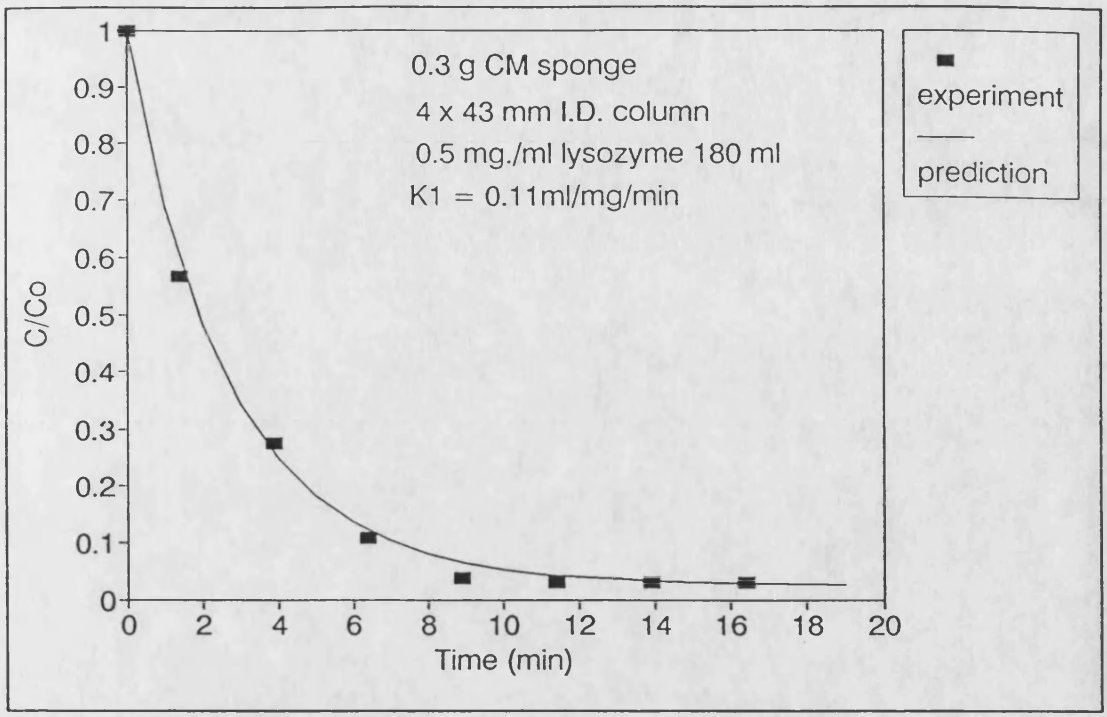

Fig. A1.3 Model simulation (K_1 = 0.11 ml/mg/min) of adsorption kinetics at the flow-rate 1075 ml/min or superficial velocity 44.3 m/h.

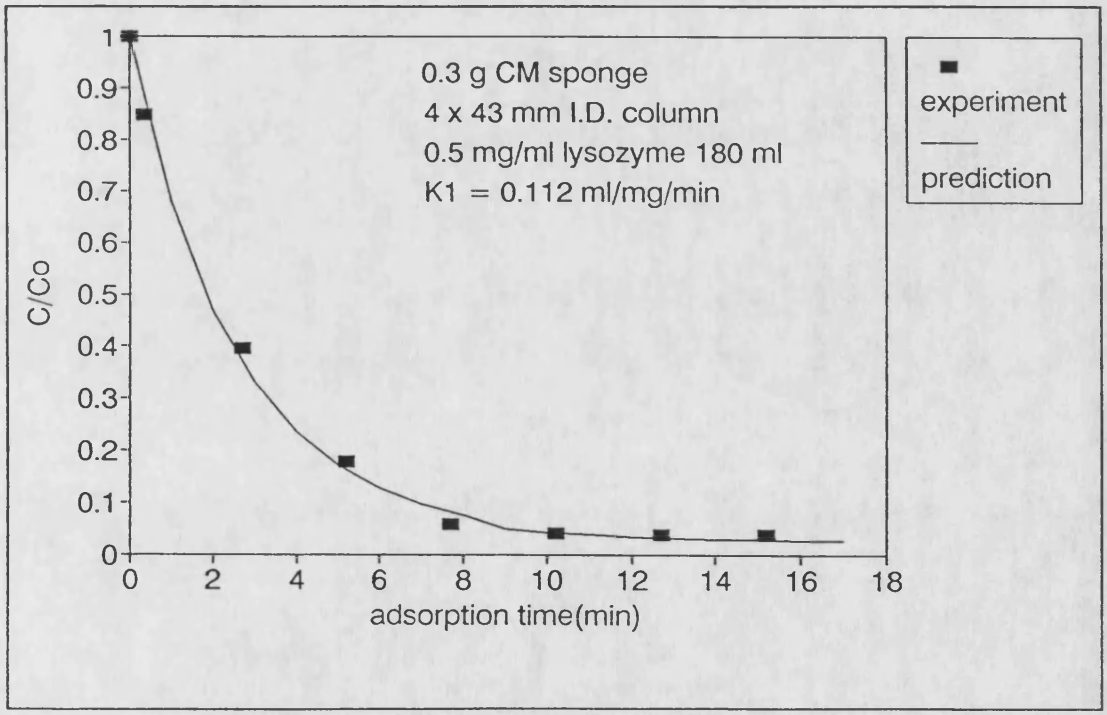

Fig. A1.4 Model simulation (K_1=0.12 mg/ml/min) of adsorption kinetics at the flow-rate 2244 ml/min or superficial velocity 92.7 m/h

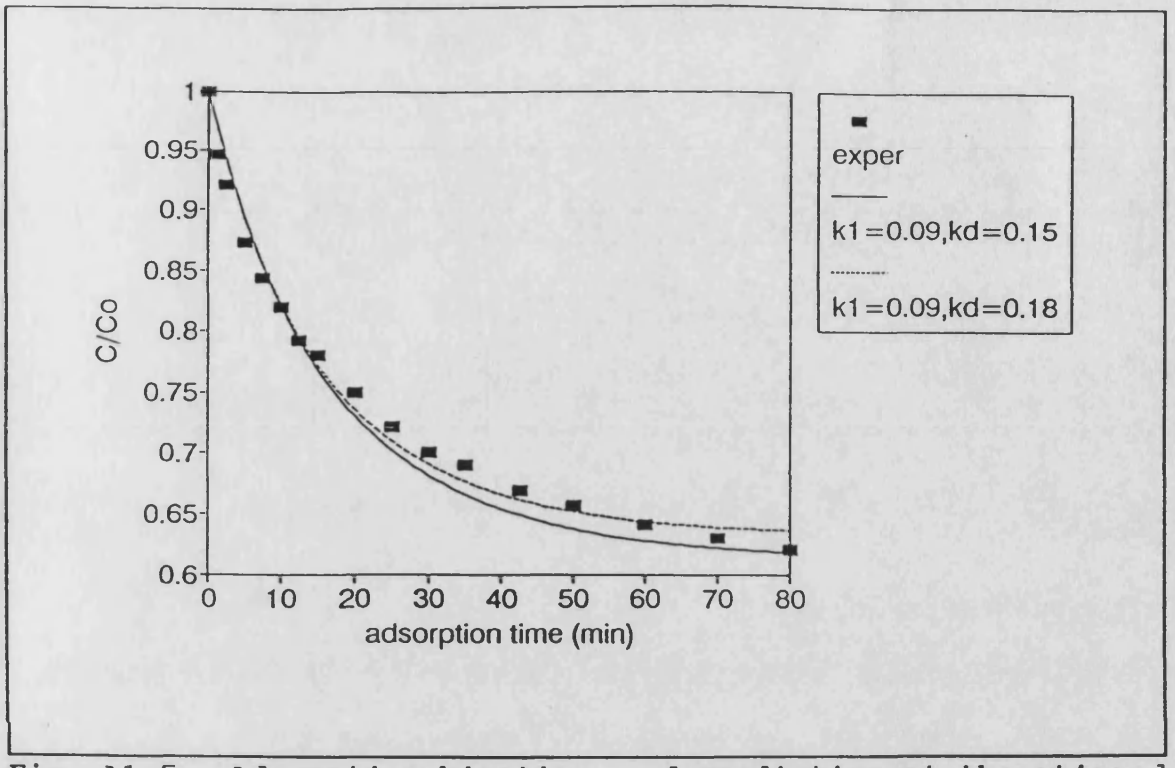

Fig. A1.5 Adsorption kinetics and prediction at the stirred speed 560 r.p.m.. (0.08235g CM sponge, 0.5mg/ml lys. 600ml)

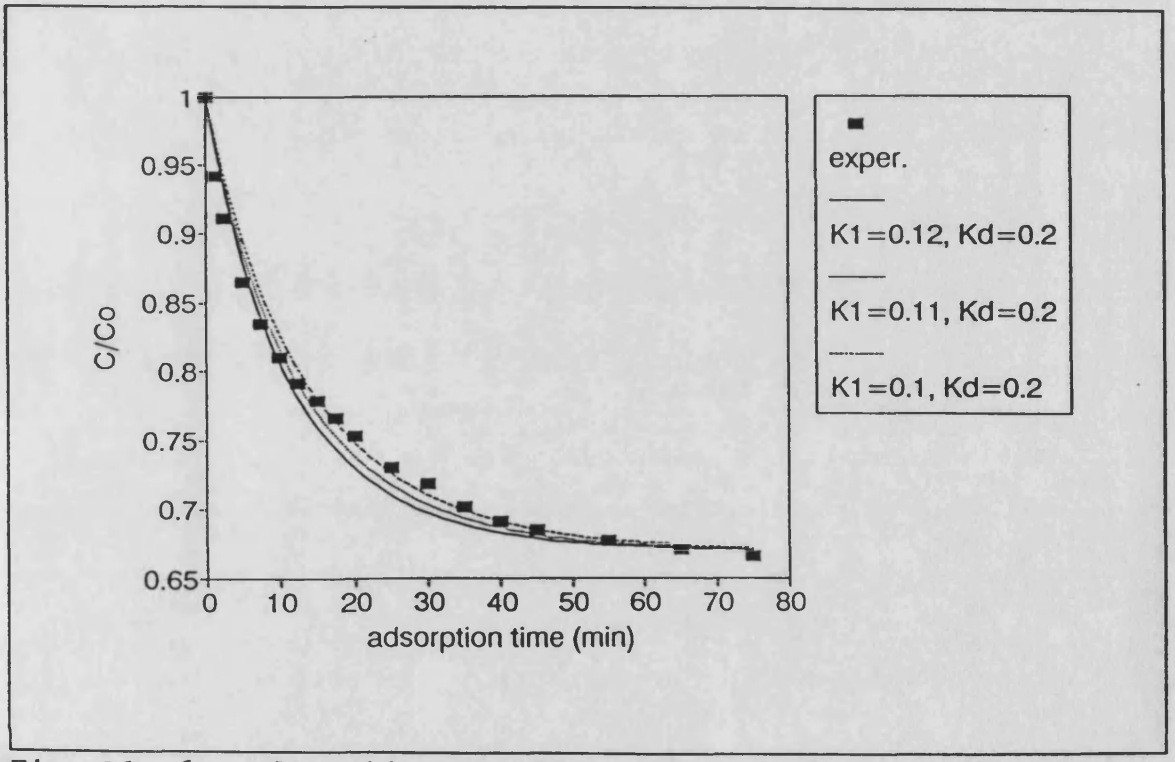

Fig. A1. 6 Adsorption kinetics and prediction at the stirred speed 1240 r.p.m..(0.0817g CM sponge, 0.5mg/ml lys. 650ml)

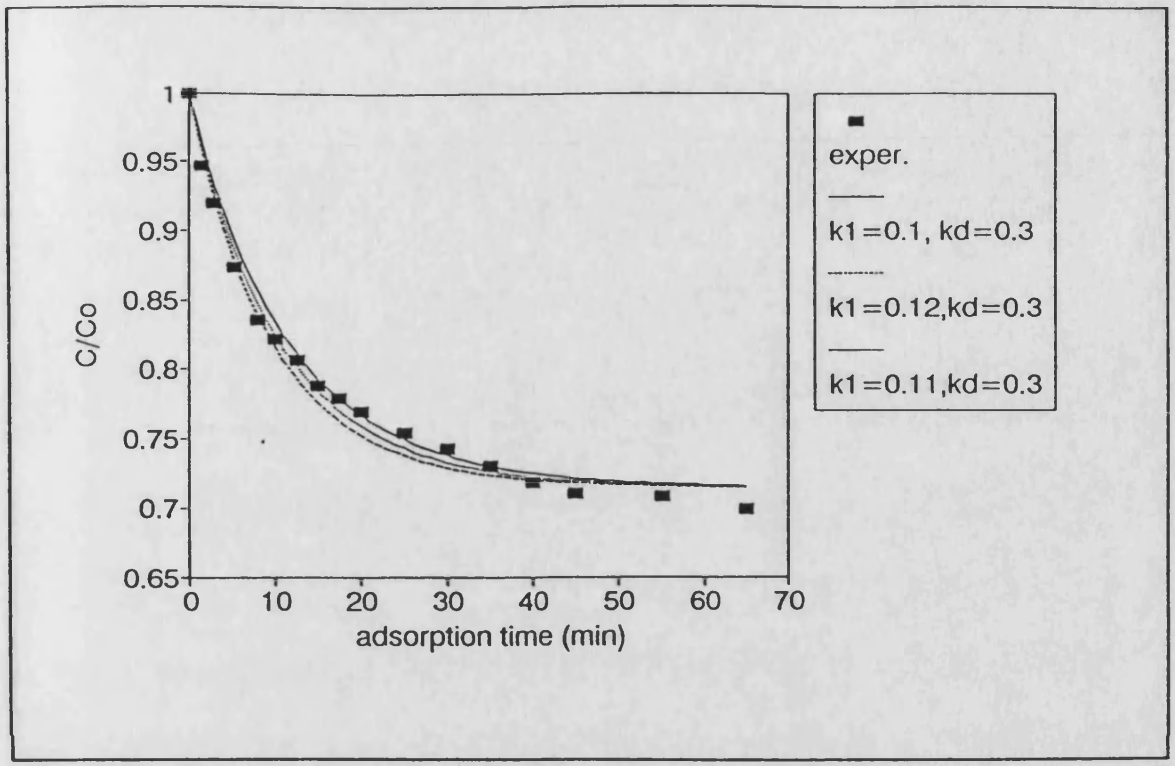

Fig. A1. 7 Adsorption kinetics and prediction at the stirred speed 1950 r.p.m..(0.0815g CM sponge, 0.5mg/ml lys. 650ml)

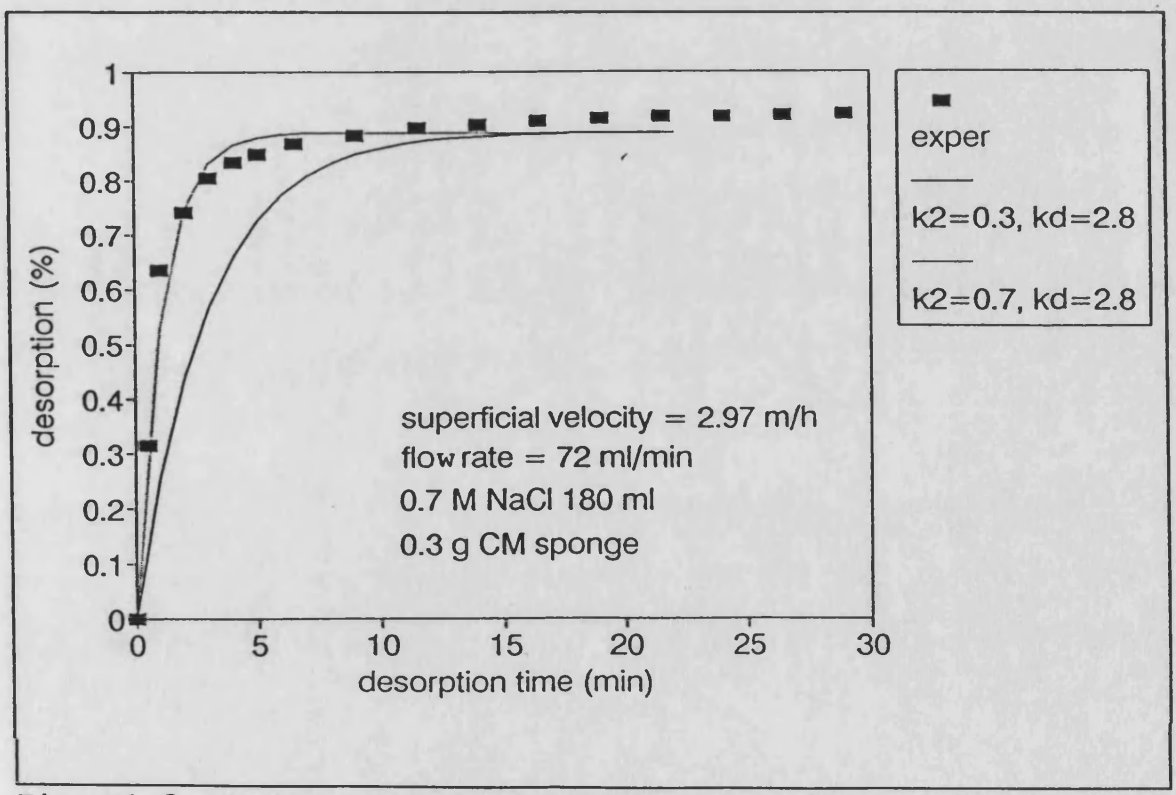

Fig. A1.8 Desorption kinetics at the superficial velocity 2.97 m/h.

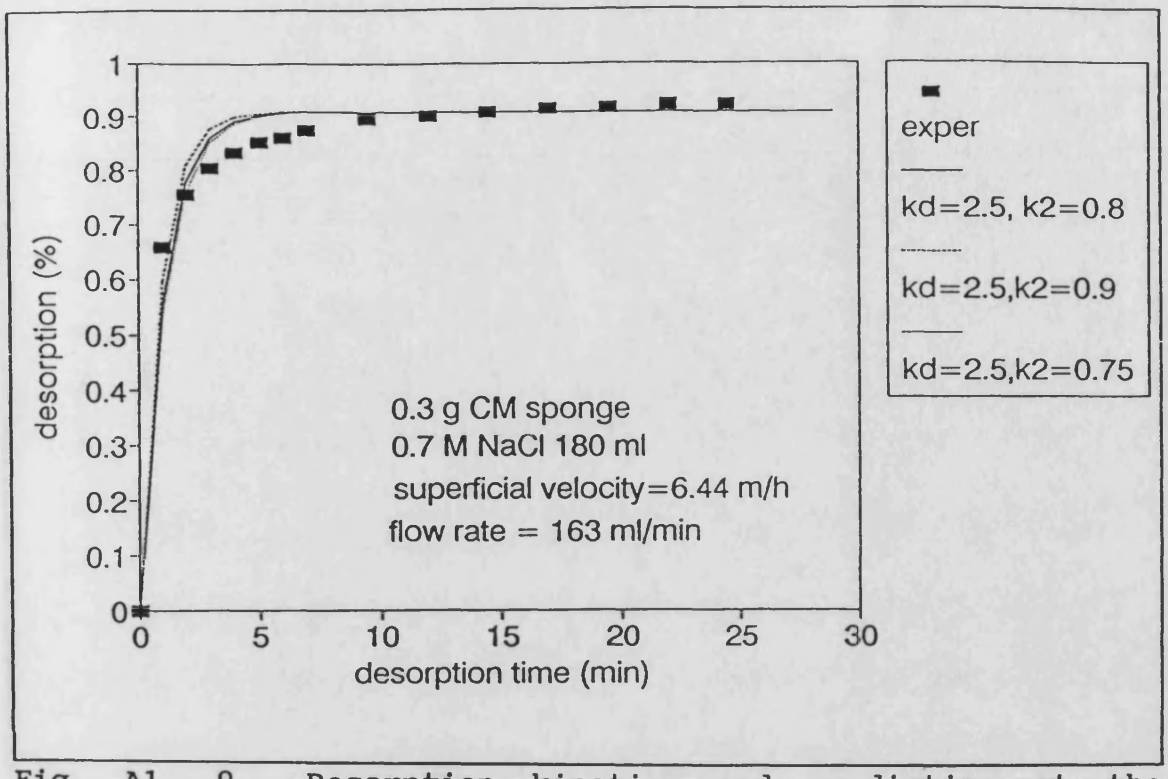

Fig. A1. 9 Desorption kinetics and prediction at the superficial velocity 6.44m/h

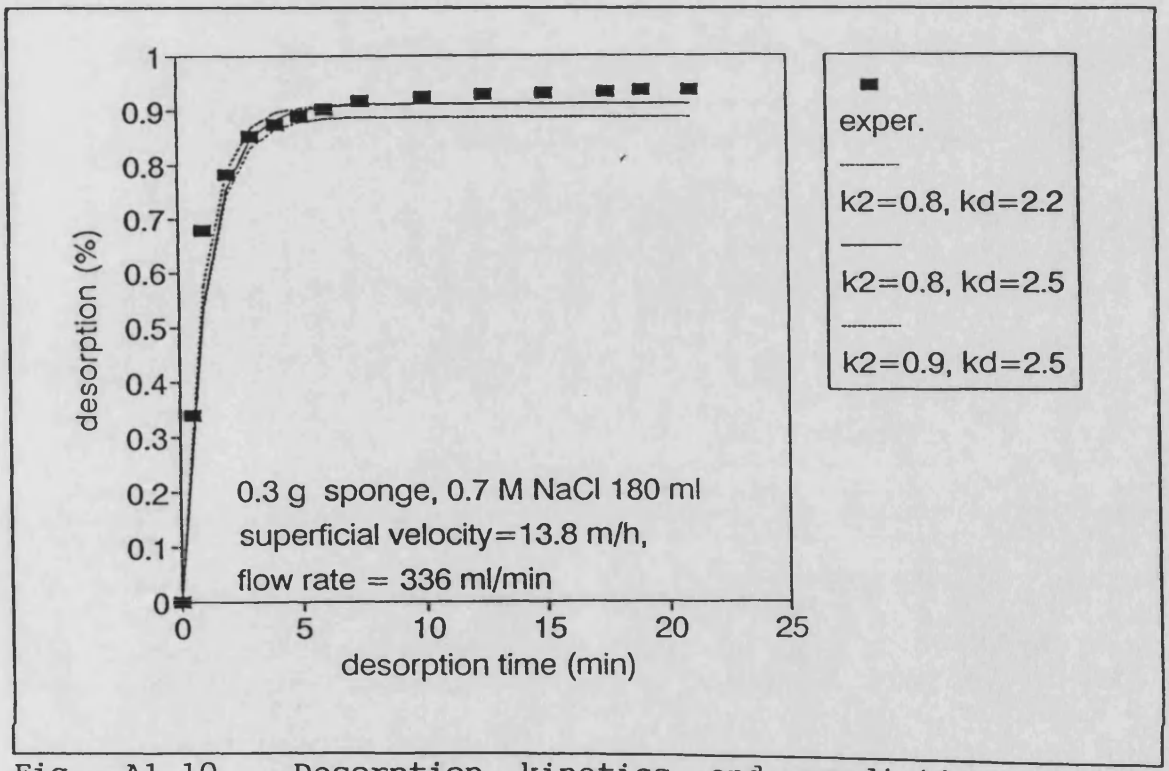

Fig. A1.10 Desorption kinetics and prediction at the superficial velocity 13.8 m/h

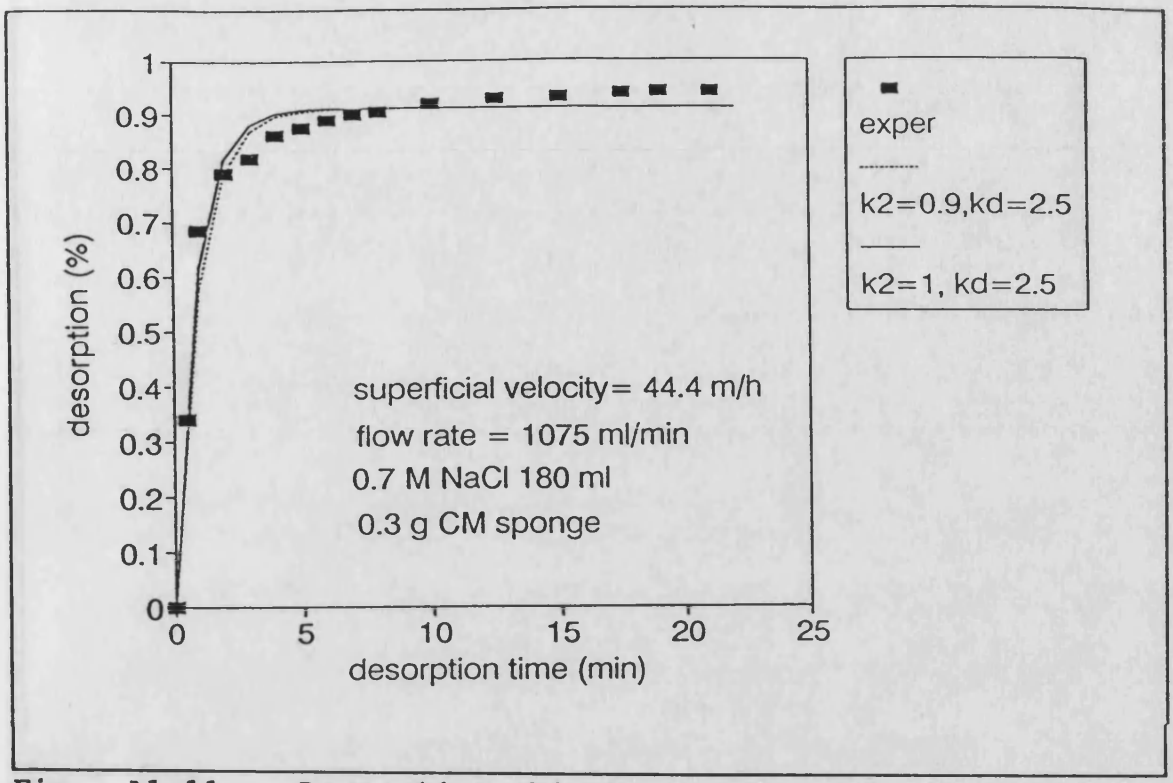

Fig. A1.11 Desorption kinetics and prediction at the superficial velocity 44.4m/h

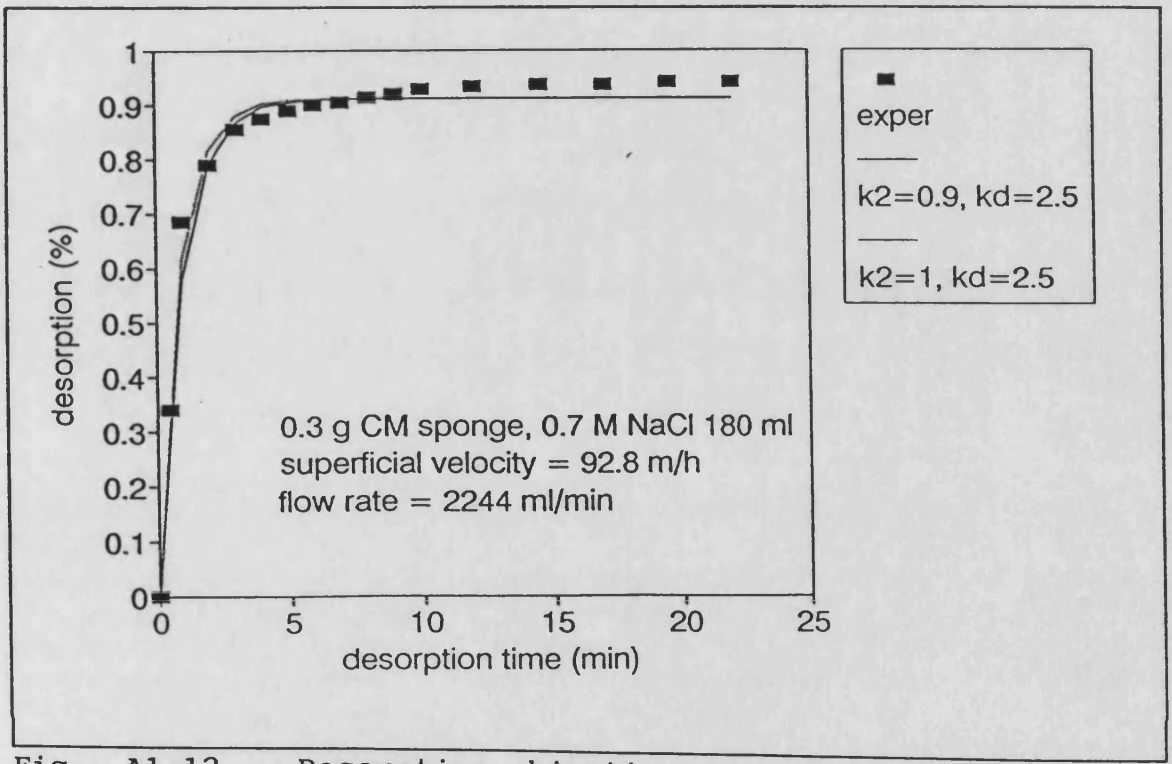

Fig. A1.12 Desorption kinetics and prediction at the superficial velocity 92.8 m/h

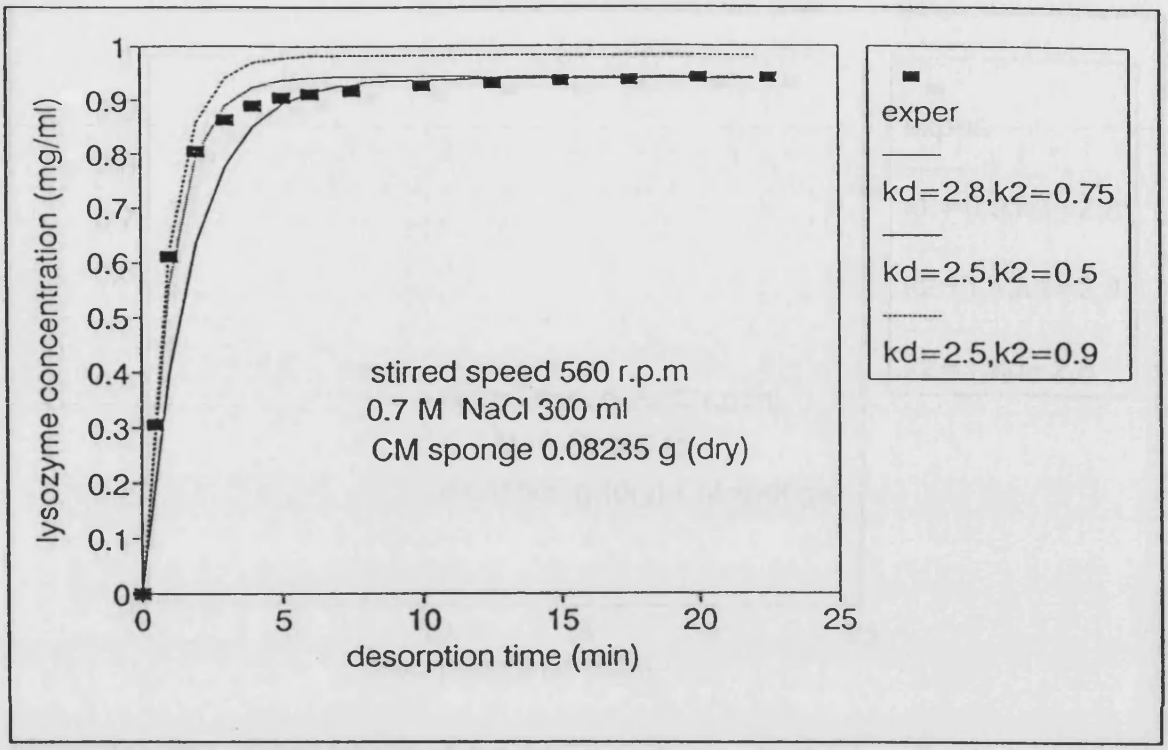

Fig. A1.13 Desorption kinetics and prediction at the stirred speed 560 r.p.m

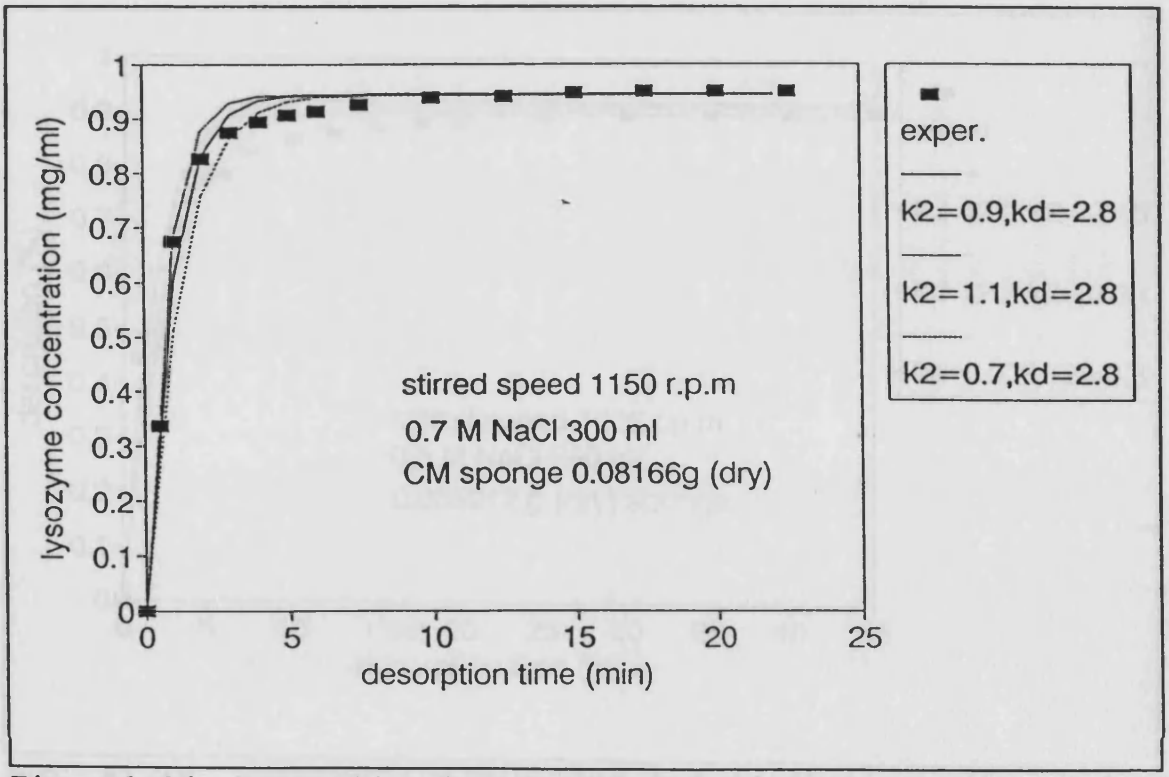

Fig. A1.14 Desorption kinetics and prediction at the stirred speed 1150 r.p.m.

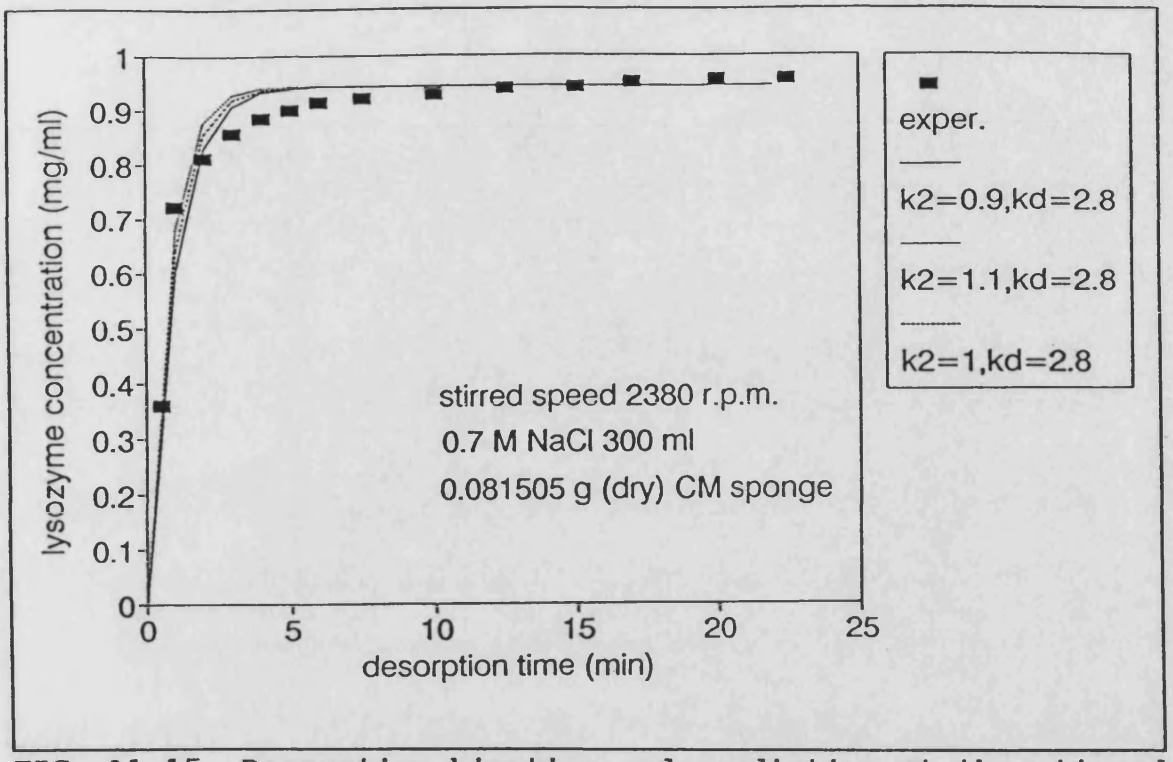

FIG. A1.15 Desorption kinetics and prediction at the stirred speed 2380 r.p.m.

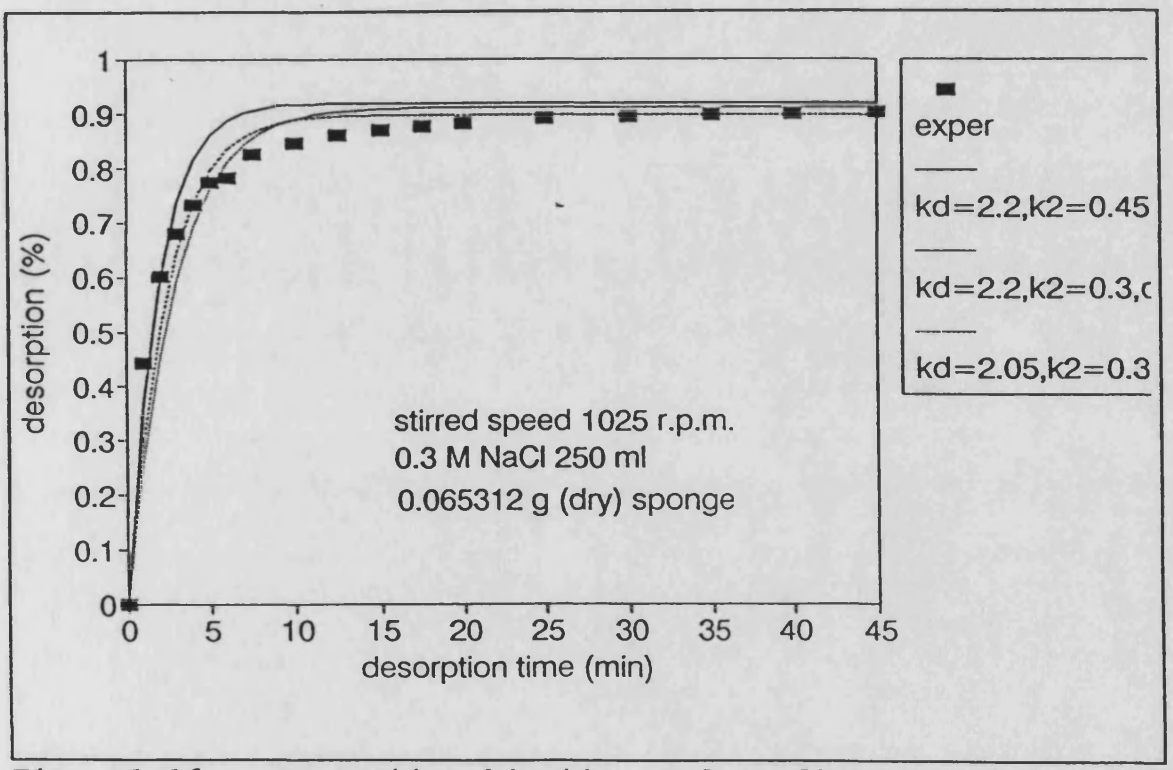

Fig. A1.16 Desorption kinetics and prediction using 0.3 M NaCl eluent

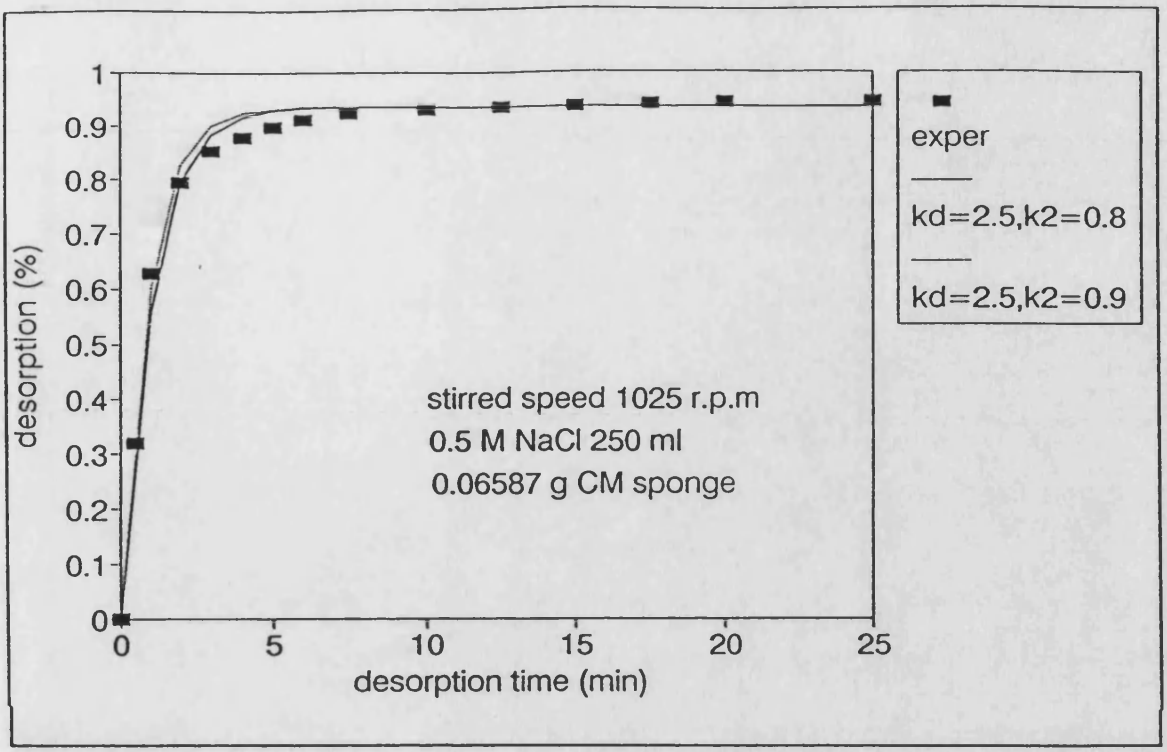

Fig. A1.17 Desorption kinetics and prediction using 0.5 M NaCl eluent

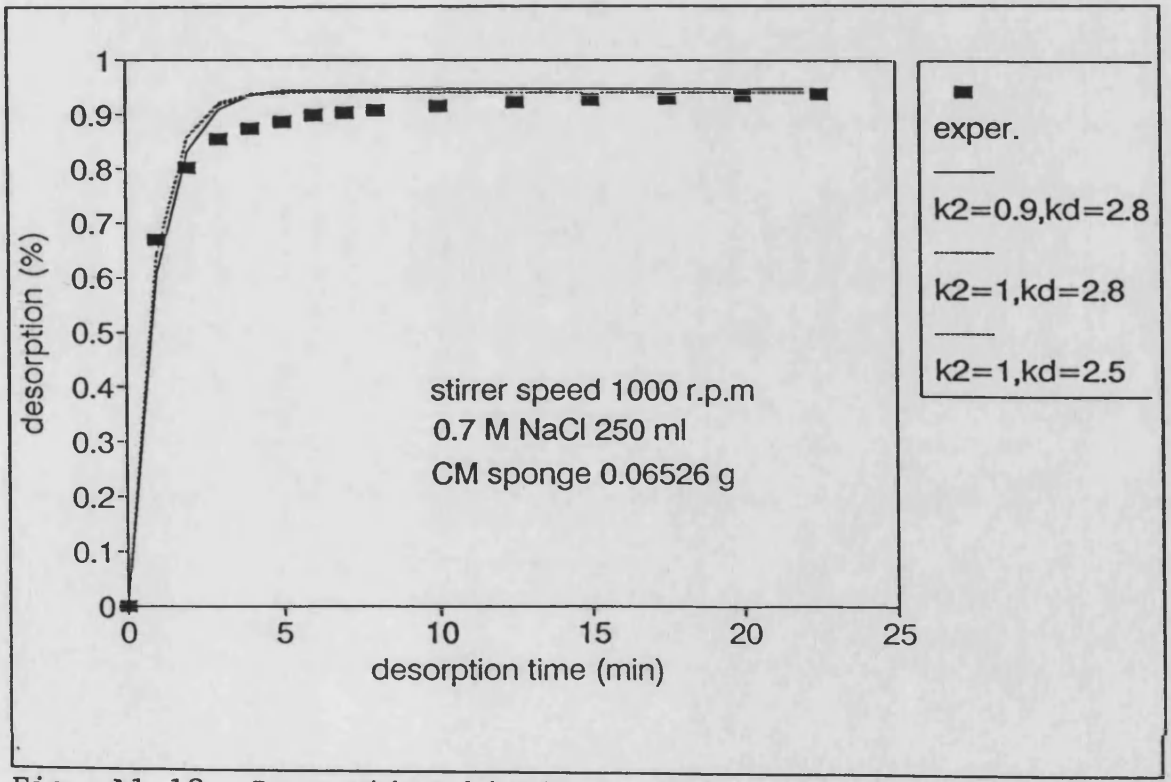

Fig. A1.18 Desorption kinetics and prediction using 0.7 M NaCl eluent

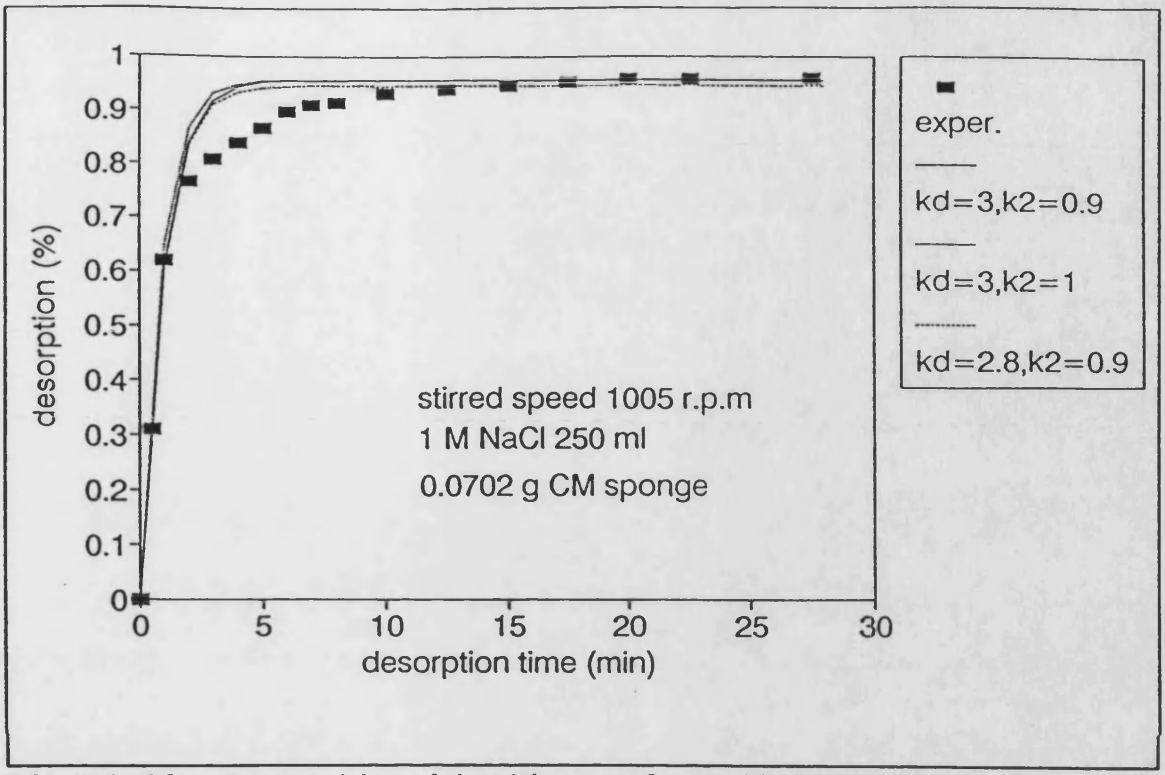

Fig A1.19 Desorption kinetics and prediction using 1 M NaCl eluent

CHAPTER 6

MATHEMATICAL MODELLING AND PARAMETER ESTIMATION OF ION-EXCHANGE CHROMATOGRAPHY PROCESSES

CHAPTER 6

MATHEMATICAL MODELLING AND PARAMETERS ESTIMATION OF ION-EXCHANGE CHROMATOGRAPHY PROCESSES

6.1 Introduction

Mathematical modelling is a powerful technique for process control, optimisation and scale-up. A mathematical model which describes chemical and physical phenomenons in a separation process represents quantitatively our current insight into the behaviour of an ion-exchange chromatography process. A model is nearly always a simplification and concerned with only a restricted number of aspects of reality. In any particular case, the mathematical model is made slightly more sophisticated or complicated than a previous version, in order to describe an additional process as completely as possible. A simple model can be used widely, for example, the equations 5.9 to 5.12, which do not distinguish the effects of external mass transfer , porous diffusion and reaction rate constant, are the lumped parameter model. A simplified or empirical model does not, however, increase the fundamental understanding of the adsorption process. Being simple, it is only suitable as a rough guide for scale-up and process control. In this chapter, an attempt was made to develop two models for the stirred vessel and recirculation column reactor. The first model is a lumped film mass transfer

control model. The second model is a heterogeneous model which included most of the fundamental characteristics, such as; (1) external mass transfer; (2) intraparticle diffusion in the solid phase and liquid phase; (3) surface reaction on the external surface of sponge fibre and the surface of pore wall inside the fibre, without involving too complicated a mathematic process in order to keep calculation time reasonable. The model should; (1) describe the adsorption behaviour appeared in the bulk liquid; (2) explain the effect of external mass transfer on the stirred speed or superficial velocity; (3) describe the protein concentration various with time inside the fibre; (4) explain the influence of effective diffusivity on the whole adsorption process. Moreover, fast calculation would means that the model could be used on line to estimate the parameters. The aim of this work described in this chapter was to built these two models compare their performances and consider the physical meaning of the parameters estimated.

A column model was then developed based on the above local kinetic model to be used for both scale-up and control. Transport parameters in the column were estimated by the method of moments (pulse response method).

The CM sponge ion-exchanger, CM-HVFM (Batch B10) used for this stage of the work was provided by BPS Separation Ltd. due to the fact that the manufacturing technique had been transferred to this Company. The hydraulic properties of this batch CM-HVFM were better than those of the one used in the previous chapter,

but the lysozyme capacity was only 1360 mg/g. It was assumed that the mass transfer results obtained from the differential bed experiment can be applied to the batch B10 CM-HVFM. The exchanger was packed in the 250 x 10 mm I.D. column.

6.2 Hydrodynamic Parameters of Column Packed.

Hydrodynamic parameters , or transport parameters, of a column packed bed include the column void volume, ϵ, Particle internal porosity, ϵ_i, Axial diffusion, D_L, effective pore diffusivity, D_e and tortuosity, τ. CM sponge ion-exchanger is a porous cellulose fibre material (Fig. 6.1), and when it is packed into a column the external void volume is constructed which is the free volume between the fibre particle in a bed. The internal void volume is the volume within the porous cellulose particle, form which only very large molecules such as dextran (M.W. 2 x 10^6), might be excluded.

6.2.1 Axial Dispersion Coefficient and Peclet Number

Axial dispersion, D_L, is the dispersion in the longitudinal direction, which is caused by two major factors: (1) non-uniformity of linear velocity in the mobile phase, over the cross section of a column, or eddy diffusion, and (2) molecular diffusion along the column length. The latter can be neglected if the flow-rate, F, is very low. Giddings (1965) listed the following five factors which cause the non-uniformity of linear velocity: (1) a short-range interchannel effect caused by a difference in the packing state on a relatively small scale, (2) a transcolumn effect caused by a velocity difference on a column

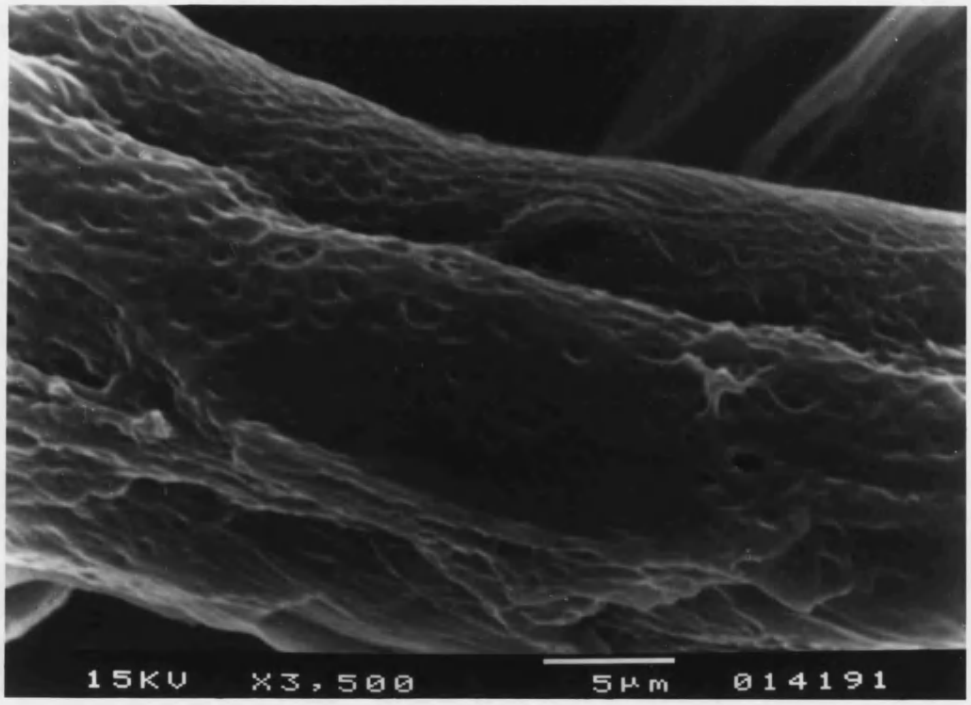

Fig. 6.1 A porous fibre of CM sponge ion-exchanger (dry)

wide scale, (3) a longrange interchannel effect, (4) a transparticle effect, due to the existence of the stagnant mobile phase, and (5) a transchannel effect owing to a velocity non-uniformity in each interstitial flow channel. The axial longitudinal dispersion coefficient, D_L, can be written as

$$D_L=\gamma D_m+\lambda u d_p \tag{6.1}$$

where d_p is the particle diameter, D_m is the molecular diffusion coefficient and u is the linear mobile phase velocity, given by:

$$u=\frac{F}{A\epsilon} \tag{6.2}$$

where F and A are the flow rate and the cross area of column respectively. Yamamoto *et al.* (1988) introduced γ, the labyrinth factor, which is a correction factor for the tortuous flow channels, and λ, a correction factor for eddy diffusion. Equation 6.2 can be rewritten as follows:

$$\frac{D_L}{ud_p}=D_m\frac{\gamma}{ud_p}+\lambda \tag{6.3}$$

or

$$\frac{1}{p'_e} = \frac{\gamma}{\nu} + \lambda$$

where $\nu = u\ d_p/D_m$ and $p'_e = u\ d_p/D_L$. ν is the nondimensional reduced velocity. An important parameter in the fixed bed column reactor is the Peclet number, $P_e = u\ l/D_L$ (where l is the length of column), which indicates the degree of axial dispersion in a column. The smaller the Peclet number, the higher the dispersion of a solute in a column. According to the discussion of Giddings (1965), Marrazzo and Merson (1975), Cluff and Hawkes (1976) and Yamamoto *el at.* (1988), the Peclet number is affected by more than ten factors: (1) flow rate, (2) matrix size, (3) shape of the ion-exchange matrix, (4) column diameter and length, (5) the ratio of matrix diameter to column diameter, (6) matrix size distribution, (7) external and internal void volume of column bed, (8) the packing method (by which the nonuniformity of a packing state changes, (9) properties of the elution buffer such as viscosity and density, and (10) the measuring method for the Peclet number.

6.2.2 Pore Diffusion Coefficient

Marrazzo and Merson (1975) believed that the effective pore diffusivity, D_e, is empirically related to the free solution diffusivity D_m by

$$D_e = D_m \frac{\epsilon_i}{\tau} \qquad (6.4)$$

where the tortuosity τ is a function of the size and shape of the pore and the diffusing molecule. Marrazzo and Merson (1975) described that the tortuosity could be determined from second moments in pulse response experiments if the data was accurate, and generally it had values between two and ten. Horstmann and Chase (1989), however, established the effective diffusivity by fitting the simulation curve to the experimental data

In order to investigate these hydrodynamic parameters in a ion-exchange column, a pulse response method is usually used. This technique was applied in a gas-phase packed bed column by Schneider and Smith (1968) , Cerro and Smith (1970), and Hashimoto and Simth (1973). Marrazzo and Merson (1975) then applied the pulse response method to an immobilized enzyme packed-bed. Yamamoto *et al.* (1983a), Goto (1983, 1990) also used this method in an ion-exchange packed-bed to establish transport parameters in the ion-exchange column. To determine the values of the column void fraction ϵ and particle internal porosity ϵ_i , the electrostatic interaction between the protein, or tracer and ion-exchanger should be suppressed. To do this one can either change the pH value or the ion strength , or even both the pH value and ion strength. Gosling (1985) chose an acidified solution with a BSA concentration of 30 mg/ml in an anion exchanger, while Yamamoto *et al.* (1983a) used Tris-HCl buffer at pH 7.9, containing 0.5 M NaCl to equilibrate the ion-exchanger column. Under these conditions, an ion-exchange column acts as a gel filtration or size exclusion column because the

electrostatic interaction between protein and ion-exchanger is negligible.

In a gel permeation chromatographic process (Pharmacia LKB Biotechnology), a solute passes down a gel bed and its movement depends on the bulk flow of the mobile phase and on the Brownian motion of the solute molecules which causes their diffusion both into and out of the stationary phase. The separation in the gel filtration depends on the different abilities of the various sample molecules to enter pores, which are inside the stationary phase. Smaller molecules, which can enter the gel pores, move more slowly through the column, while the larger molecules move through the chromatographic bed faster due to the factor that they can not enter the gel pores. Molecules are, therefore, eluted in order of decreasing molecular size because they spend a varying proportion of their time in the stationary phase.

6.3 Moment Analysis

Kubin (1965, 1975) applied the moment method to analyze the experimental data because of mathematical difficulties in solving the complete concentration profile of an elution curve described by the full set of rate equations such as equation 6.11 (Nakanishi *et al.*, 1977). The normalized nth statistical moment μ_n' of the concentration profile of an elution curve c(z,t) is defined by equation 6.5 where z, t are the space and time coordinate, respectively.

$$\mu'_n = \int_0^\infty t^n c(z,t)\,dt \Big/ \int_0^\infty c(z,t)\,dt \qquad (6.5)$$

The zeroth moment is simply the normalized area of the elution curve, *i.e.*, unity. The first moment gives the location of the mean of the peak in output concentration, or the mean retention time of a solute in a column. The shape of the curve is characterized by the nth normalized central moment as

$$\mu_n = \int_0^\infty (t-\mu_1)^n c(z,t)\,dt \Big/ \int_0^\infty c(z,t)\,dt \qquad (6.5a)$$

The second central moment represents the peak variance. In practice calculation, equations 6.5 and 6.6 become the following form:

$$\mu_1 = \int_{t_1}^{t_2} t c(z,t)\,dt \Big/ \int_{t_1}^{t_2} c(z,t)\,dt \qquad (6.6)$$

$$\mu_2 = \int_{t_1}^{t_2} (t-\mu_1)\, c(z,t)\,dt \Big/ \int_{t_1}^{t_2} c(z,t)\,dt \qquad (6.6a)$$

where t_1 is the time at the beginning of the elution peak, and t_2 is the time at the end of the elution peak.

The moments can also expressed by being solved from the

Laplace transform of the elution curve. For the case where no adsorption occurs and the injection time of sample is negligibly short, Furusawa (1976) and Sirott and Emery(1983) have given μ_1 and μ_2 in the following forms:

$$\mu_1=\frac{Z}{u_o}[\epsilon+(1-\epsilon)\epsilon_i] \tag{6.7}$$

$$\frac{\mu_2}{(2Z/u_o)}=\delta_D+\delta_f+\frac{D_L}{u^2_o}[\epsilon+(1-\epsilon)\epsilon_i]^2 \tag{6.8}$$

$$\delta_D=\frac{\epsilon_i^2R^2(1-\epsilon)}{15D_e} \tag{6.9}$$

$$\delta_f=\frac{\epsilon_i^2R(1-\epsilon)}{3k_f} \tag{6.10}$$

where u_o is the superficial velocity. These equations indicate that: (1) a plot of μ_1 vs Z/u_o (the superficial residence time) should be linear, with a slope of $\epsilon + (1 - \epsilon)\epsilon_i$, which is the total void fraction of the bed (Equation 6.7); (2) $\mu_2 /2Z/u_o$ should be plotted against $1/u_o$ to give a linear graph, the intersection of which with the ordinate would then yield the sum $\delta_D+\delta_f$. The axial dispersion coefficient D_L is a function of the superficial velocity, and can be obtained from the slope D_L/u_o in the Equation 6.8. The mass transfer coefficient, k_f, can be estimated from a correlation equation, the effective diffusivity

D_e is then obtained δ_D.

6.4 The Plate Theories and The Rate Theories

Theories of chromatography are mainly divided into the plate theories and the rate theories. They focus on predicting the shape of the breakthrough curve.

Martin and Synge (1941) first introduced the plate theory as an equilibrium-stage model. By assuming that equilibrium is always attained between the two phase contacting at each stage, the process is treated as a series of ideal mixed flow contactors. The material balance equations obtained can be solved analytically by assuming a linear equilibrium isotherm. This model was later modified by Mayer and Tompkins (1947) and Crig and Craig (1956). Van Deemter *et al.* (1956), however, considered that there were some disadvantages in the plate theory based model; (1) the discontinuous flow model was inadequate in representing the physical picture of the process and would lead to large errors, even in a column of 1000 theoretical stages, (2) the number of stages must be found by trial and error, and (3) the plate theories were only exact where a linear isotherm was assumed, because plate height was a function of the linear equilibrium constant.

6.4.1 Column Material Balance

Rate theories of chromatography consist of material balance equations together with appropriate boundary and initial conditions, which have been used mainly in application to fixed-

bed adsorption and ion-exchange operation (Yang and Tsao, 1982). The theory is based on the continuous flow of solute fluid through the column, a finite rate of mass transfer, and a certain sorption kinetics. There are no assumptions which relate to local equilibrium in individual stages. The general solute mass conservation of the elemental volume in the column can thus be written as :

Net accumulation rate = flux in - flux out + accumulation rate
in the fluid phase in the adsorbent

Assuming the axial diffusion coefficient D_L and linear velocity are constant, the diffusion flux per unit area is $-D_L \partial C/\partial x$. The one dimensional mass balance equation which stands for the accumulation in the column fluid phase, transport by axial dispersion, convective transport and volume-average accumulation in the adsorbent is therefore formulated as;

$$\frac{\partial C}{\partial t} = D_L \frac{\partial^2 C}{\partial x^2} - u\frac{\partial C}{\partial x} - \frac{1}{\epsilon} R_m \qquad (6.11)$$

The boundary conditions and initial conditions are:

$t = 0, \quad x > 0, \quad C = 0$

$t > 0 \quad x = 0, \quad C = C_o(t), \quad$ or $\quad D_L \partial C/\partial x = -u(C_{x=0} - C_{x=0+})$

where R_m = the rate of interface mass transfer

C = the adsorbate concentration

x and t = the space and time coordinates, respectively.

L = the length of the column

u = linear velocity

D_L = axial dispersion

ϵ = column vodiage

6.4.2 Material Balance Equation For The Adsorbent Particle

As the CM sponge material is in the form of fibre. A cylindrical particle geometry is considered. According to Fick's second law, a solute diffuses within a pore of cylinder particle in a manner described by an effective diffusivity D_e, which is assumed to be independent of the solute concentration but depends on the particular adsorbent matrix, which can be written as;

$$\frac{\partial c_i}{\partial t} = D_e \frac{1}{r} \frac{\partial}{\partial r} \left(r \frac{\partial c_i(r,t)}{\partial r} \right) \qquad (6.12)$$

If a concurrent adsorption with diffusion occurs, the rate of solute accumulation in the liquid should be equal to the difference of diffusion and uptake by adsorption reaction, *i.e.*;

$$\frac{\partial c_i}{\partial t} = D_e \frac{1}{r} \frac{\partial}{\partial r} \left(r \frac{\partial c_i(r,t)}{\partial r} \right) - \frac{1}{\epsilon_i} R_v \qquad (6.13)$$

In addition a boundary condition is needed to link the solute concentration in the bulk liquid and the particle. This boundary equation states mathematically that the mass entering or leaving the particles must equal the flow of mass transported across a stagnant fluid film at the external surface, namely;

at r = R

$$\frac{\partial c_i}{\partial r} = \frac{k_f(C-c_i)}{D_e \epsilon_i} \qquad (6.14)$$

at the centre of the cylinder, where r = 0

$$\frac{\partial c_i}{\partial r} = 0 \qquad (6.15)$$

A unknown function of time can also be used as the boundary condition which is a implicit boundary condition for the protein concentration of adsorbent *i.e.;*

at r = R, $q_i(R, t) = q_s(t)$; at r=0, $\partial q_i/\partial t = 0$

The relationship between q_s and c_s could then be assumed as a linear or nonlinear isotherm form.

where c_s , q_s = interfacial concentration of liquid and solid

r = space coordinate

R = cylinder radius

K_f = external mass transfer coefficient

c_i = solute concentration within the cylinder

D_e = effective diffusivity

ϵ_i = adsorbent porosity

q_i = protein concentration of the adsorbent

R_v = uptake rate by reaction

The rate equations, R_v, can be divided into kinetic rate expression and linear driving force. The kinetic expressions can be written in the form of : (1) linear isotherm type, *i.e.*

$$R_v = K_1C-K_2q_i \qquad (6.16)$$

which was used by Thomas (1948), or (2) Langmuir isotherm type, i.e.

$$R_v = K_1C(q_m-q_i)-K_2q_i \qquad (6.17)$$

where C = solute concentration in the liquid

q_i = solute concentration in the solid

which was applied by Thomas (1944). Cowan *et al.*(1986) also used the Langmuir adsorption kinetics to study aspartic acid adsorption on Duolite A162 ion exchange resin.

For the linear driving force equation, it is assumed that the rate is proportional to the rate of mass transfer to the particle, namely:

$$R_v = k_f a_v (C-c_s) \qquad (6.18)$$

where a_v is the interfacial area of solid phase per unit interstitial void volume, c_s is the adsorbed phase concentration at the interface, (at equilibrium with the bulk solution). Graham and Fook (1982) and Tsou and Graham (1985) applied the linear

driving force equation to model the adsorption /desorption of bovine serum albumin on DEAE cellulose and DEAE Sephadex A50 ion-exchangers.

6.5 Modelling For Stirred Batch Reactor And Differential Recirculation Batch Reactor

The differential bed column can be considered as a differential recirculation batch reactor. In a stirred batch reactor and a recirculation batch reactor, which can be considered as a well-mixed batch reactor, no material is supplied to or withdrawn from it during the adsorption/desorption processes so that the total volume of the reaction mixture remains constant. The protein, which is assumed to be uniformly distributed in the vessel, varies only as function of time. The concentration gradient only occurs between the bulk liquid and inside the ion exchanger. As a result of the difference of protein concentration that protein diffuses from the bulk liquid through the liquid film surrounding the surface of particle protein into the surface of the particle. This diffusion then continues from the surface of the particle into the centre of the particle. The mass balance for the movement of protein from the liquid phase into the surface of the particle is therefore described by the mass-transfer equation:

$$V\frac{dC}{dt}=-v_i a_v k_f(C-ci) \qquad (6.19)$$

where $v_i = W/\rho$,

v_i = volume of ion-exchange (ml)

W = weight of ion-exchanger (g)

ρ = density of ion-exchanger (g/ml)

V = protein feed volume (ml)

R = particle radius (mm)

a_v = particle surface volume ratio.

k_f = external mass transfer coefficient (mm/min)

c_s = interfacial concentration (mg/ml)

A material balance equation describes conservation of protein, *i.e.* any protein which is not in the fluid must be inside the ion-exchanger particle. Thus at any time t

$$V C = V C_o - qW \quad \text{or} \quad dC/dt = -(W/V)(dq/dt) \quad (6.20)$$

where C_o is the initial concentration of protein in the liquid phase, q is the average solute concentration of the particle.

6.6 Experimental Methods and Material

A pulse response experiment was carried out in a 250 x 10 mm I.D. column packed with 1.775 g (dry weight) CM sponge (Batch B10). The parameters of this Batch B10 are below;

IEC = 1.4 meq/g, K_d = 0.056 mg/ml

Lysozyme capacity = 1360 mg/g.

The column was operated in upflow mode based on Fig.5.1b.

Additionally, a micro three-way valve with syringe adaptator was fitted at the inlet of the column so that around 0.1 ml sample could be injected into the column. The three-way valve was off on the direction of the column inlet during the injection, but otherwise was open to the column. The injection pulse lasted for around 2 seconds. The column was equilibrated with 0.5 M NaCl, which was also used an elunt, for 30 minutes at the flow-rate of 6 ml/min. 0.5 mg/ml lysozyme, 0.5 mg/ml conalbumin and 0.4 mg/ml blue dextran (molecular weight 2 x 10^{-6}) in 0.5 M NaCl were chosen as tracers. A peristaltic pump (Watson-Marlow Ltd., Falmouth Cornwall, UK) was operated at a required flow-rate to pump the elunt through the column unless the sample being injected. The column elant was monitored by a UV (LKB Unicrod II, LKB-Produkter AB, Bromma,Sweden) detector at 280 nm and recorded on a chart.

A protein breakthrough curve experiment was carried out by continuously pumping protein solution through the column until the breakthrough curve was obtained.

The experiments for the stirred vessel and differential column bed is described in Chapter 5.

6.7 Computational Method

The orthogonal collocation method, which was developed largely by Villadsen (1970) and Finlayson (1972), was used to solve the partial differential equations. The particle diffusion equation and column rate theory equation can be recognized as

belonging to the case of second order coupled parabolic partial differential equations of the boundary value type. The orthogonal collocation method is particularly useful for the solution of these types of differential equations and, for a given accuracy of solution, has often been found to require less computer time than a standard finite difference method (Raghavan and Ruthven, 1982). Fang Ming and Howell (1987b,1989,1991b) applied this orthogonal collocation method to the dynamic study of an anaerobic fixed biofilm reactor. Onwuasoanya (1987) also applied this method to solve the model of an affinity packed column.

The orthogonal collocation method consists of expressing the concentration in terms of a polynomial function to the Nth order which contains N unknown coefficients. The trial function is substituted in the differential equation to form a residual which is set equal to zero at N collocation points. The N values of the concentration at these points are then evaluated rather than in terms of the coefficients of the polynomial. The details of the method are available in literature such as Fang Ming (1987b).

For a symmetrical particle, the concentration can be approximated by the trial function of the following form:

$$c(x) = c(1) + (1-x^2)\sum_{i=1}^{N} a_i P_{i-1}(x^2) \qquad (6.21)$$

where

a_i = arbitrary coefficients

$P_{i-1}(x^2)$ = orthogonal polynomial which may be of Jacobi, Legendre or Chebycheff type

x = space coordinate

The first derivative and the Laplacian can be expressed in terms of the concentrations at the collocation points;

$$\frac{\partial c(x_j)}{\partial x}) = \sum_{i=1}^{N+1} A_{j,i} c(x_i) \qquad (6.22)$$

$$\frac{\partial^2 c(x_j)}{\partial x^2} = \sum_{i=1}^{N+1} B_{ji} c(x_i) \qquad (6.23)$$

where A_{ji} and B_{ji} are the collocation matrices, which can be found in Fang Ming (1987b).

For a non-symmetric system, for example the whole packed column, the concentration profile for the bulk liquid can be similarly expanded in terms of the non-symmetric polynomial, of the order of M of the type:

$$C(z) = (1-z)\,C(0) + zC(1) \sum_{i=1}^{M} a_i p_{i-1}(z) \qquad (6.24)$$

where $p_{i-1}(z)$ are now the Shifted orthogonal polynomials, z is the space coordinate.

The first and second derivatives are written as

$$\frac{dC(z_j)}{dz} = \sum_{i=1}^{N+2} A'_{j,i} C(z_i) \qquad (6.25)$$

$$\frac{d^2C(z_j)}{dz^2} = \sum_{i=1}^{N+2} B'_{j,i} C(z_i) \qquad (6.26)$$

where A'_{ji} and B'_{ji} are the non-symmetric collocation matrices which can be found in Onwuasoanya (1987).

For the calculation of the moments, the experimental data was then digitised from the continuous chart recorder trace (Fig.6.2) and used to calculate the first moment and the second central moment. The Gauss-Kronrod quadrature method with a subprogramme (Fang-moment in Appendix), which allowed the input of arbitrary data points rather than even data points was used to integrate the equation 6.6 and 6.6a. This subprogramme was written by Yuyan Wang (School of Chemical Engineering, University of Bath, U.K.).

6.8 Establishment of Transport Parameters of Column Packed

The protein diffusivity in free aqueous solution was estimated using the correlation of Young *et al.*(1980), which is below

$$D_m = 8.34x10^{-15}\frac{T}{\mu M^{1/3}} \qquad (6.27)$$

where D_m = protein molecular diffusivity in free solution (m^2/s)

T = absolute temperature (K)

μ = solution viscosity (0.001 kg/ms)

M = protein molecular weight

Tyn and Gusek (1990) believed that the above correlation was in fact identical to the correlation which was proposed by Polson (1950). For lysozyme, conalbumin and ovalbumin solutions, it was assumed the viscosity of dilute protein solutions is the same as that of water, at the same temperature. Table 6.1 gives a list of the estimated free solution diffusion coefficients for the above proteins at 4 °c and 20 °c.

Table 6.1 protein diffusion coefficient in free solution

PROTEIN	MOLECULAR WEIGHT	VISCOSITY μ (kg/ms)	DIFFUSION COEFFICIENT D_m x $10^{-11}m^2/s$	TEMP (K)
lysozyme	14400		5.68	
conalbumin	78000	0.00167	3.238	277
ovalbumin	45000		3.889	
lysozyme	14400		10.138	
conalbumin	78000	0.001	5.719	293
ovalbumin	45000		6.87	

Wilson and Geankoplis (1966) proposed the following

correlation for the mass transfer coefficient from liquid stream to particle in a packed bed at Reynolds number of between 0.0016 and 55.

$$k_f = 1.09 \frac{D_m}{2R_h \epsilon} R_e^{1/3} S_c^{1/3} \qquad (6.28)$$

$$R_h = Rd \frac{\epsilon}{3d(1-\epsilon)+4R} \qquad (6.29)$$

$$R_e = 2\rho_f u \frac{R_h}{\mu} \qquad (6.30)$$

$$S_c = \frac{\mu}{\rho D_m} \qquad (6.31)$$

where R_h = hydraulic radius of the particle (m)

R_e = particle Reynolds number

S_c = Schmidt number

ρ_f = fluid density (kg/m^3)

μ = feed solution viscosity (kg/ms)

u = axial velocity (m/s)

k_f = film mass transfer coefficient (m/s)

d = column diameter (m)

R = radius of packed spherical particle (m)

The fluid density and feed viscosity are assumed to be 1000 kg/m^3 and 0.001 kg/ms respectively, which are the same as water at 20

Table 6.2 External film mass transfer coefficient value k_f at various flow velocity (Schmit number for lysozyme = 9864, for conalbumin = 17485)

k_f (m/s) lysozyme	conalbumin	flow rate (ml/min)	superficial velocity (m/s)	linear velocity (m/s)	Reynold number
5.76e-6	3.93e-6	2.2	4.67e-4	5.46e-5	4.26e-3
1.55e-5	1.06e-5	4.32	9.2e-4	1.07e-3	0.0836
1.86e-5	1.27e-5	7.46	1.58e-3	1.85e-3	0.144
2.14e-5	1.46e-5	11.5	2.4e-3	2.8e-3	0.2187
2.3e-5	1.57e-5	14.1	2.99e-3	3.5e-3	0.27

* in a 250 x 10 mm I.D. column

°C. The sponge particle has an irregular particle structure, unlike a spherical particle. The hydraulic radius, R_h, equation 6.29, which was defined by Marrazzo et al. (1975), was applied to correct the shape factor of the sponge particle. The diameter of the sponge particle fibre observed from the electron-micrograph is between 10-120 μm. The average diameter of the sponge was hence established as 40 μm which was the same result as Addo's (1988). Gosling (1985) measured that the diameter of sponge fibre was 50 μm. The R_h value was thus calculated to be 3.9049×10^{-5} m. The film mass transfer coefficient for lysozyme therefore was calculated and is shown in Table 6.2.

The elution curves of the pulse response experiment are shown in the Fig.6.2. Under the conditions used, the higher the flow-rate, the greater the symmetry of the elution. At the same flow-rate, the elution curves of conalbumin and dextran were more symmetric than that of lysozyme. Applied equations 6.6 and 6.6a to integrate these elution curves in Fig.6.2, the first moment and second central moment were obtained.

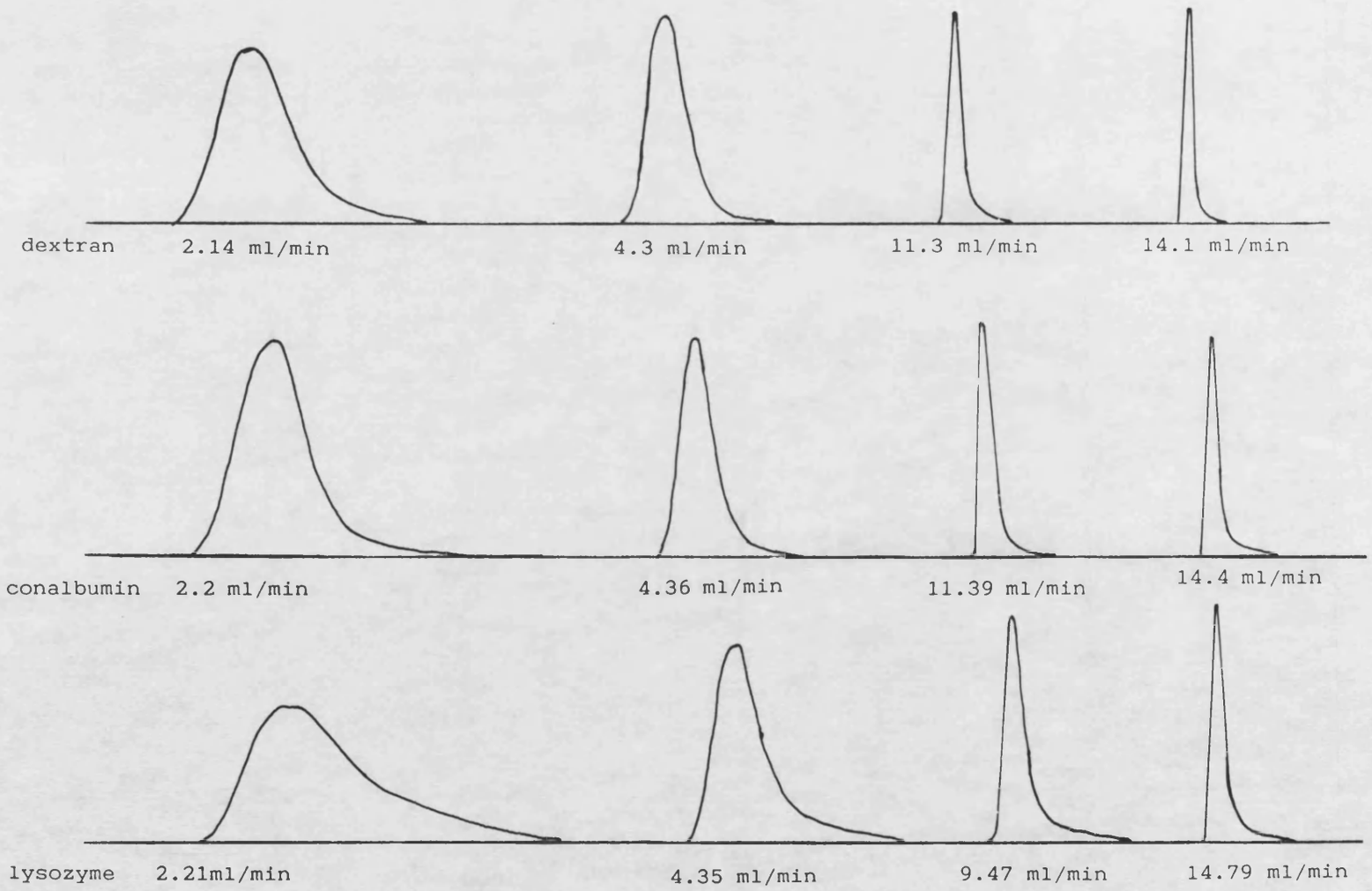

Fig. 6.2 Effect offlow-rate on the pulse respones of lysozyme, conalbumin and dextran

Table 6.3 250 x 10 mm I.D. CM sponge (1.775g) column bed voidage and sponge porosity at 0.5 M NaCl eluent

Adsorbate	slope (-) (linear regression)	ϵ (-)	ϵ_i (-)
dextran	0.8547	0.8547	0
lysozyme	0.9921	0.8547	0.95
conalbumin	0.8843	0.8547	0.2037

Fig. 6.3 shows the first moments of lysozyme, conalbumin and dextran at various flow-rates. The dextran molecule is excluded from the particle due to the huge molecule size. This means that the internal voidage, ϵ_i, = 0 for the dextran in the equation 6.7, so that the slope of dextran, 0.8547, (Fig.6.3 and equation 6.7) was regarded as the external voidage of the column bed. After the voidage of the column bed was established, the porosity, ϵ_i, of CM-sponge ion-exchanger for lysozyme and conalbumin were calculated and listed in Table 6.3

According to equation 6.8, the relationship of $\mu_2/2Z/u_o$ and $1/u_o$ should be linear. This was confirmed by the experimental results displayed in Fig.6.4. The axial dispersion coefficient, D_L, and Peclet number, Pe, were calculated from the slope, D_L/u, of the $\mu_2/2Z/u_o$ vs $1/u_o$ at various superficial and linear velocities, which is shown in Fig.6.4. The Peclet number of lysozyme was around over three times less than that of either conalbumin or dextran. The effect of Peclet number on the axial

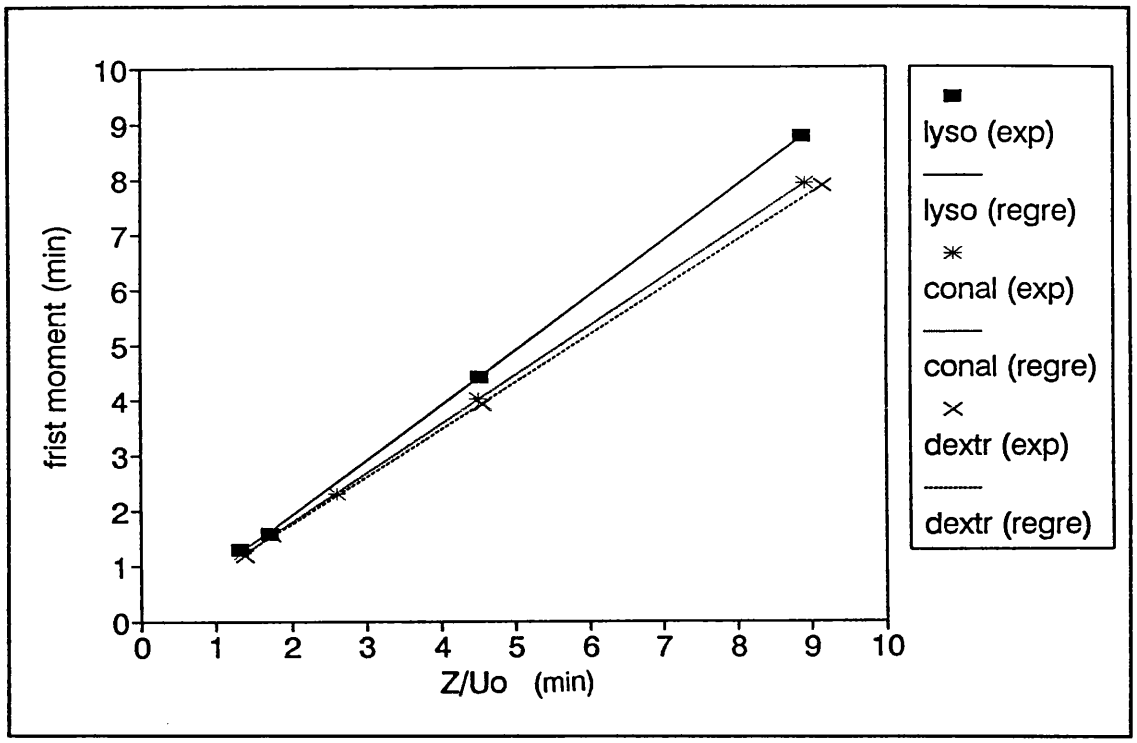

Fig.6.3 First moment of lysozyme, conalbumin and dextran vs Z/u_o

dispersion is discussed in section 6.9.5.

For the 250 x 10 mm I.D. CM sponge column, the relationship between the axial dispersion and linear velocity for lysozyme, conalbumin and dextran can be read from the slopes of $\mu_2/2Z/u_o$ vs $1/u_o$, namely:

for lysozyme	D_L/u = 0.38997 cm,	Peclet number = 64.1
for conalbumin	D_L/u = 0.1008 cm,	Peclet number = 247.9
for dextran	D_L/u = 0.0883 cm,	Peclet number = 281.5

The δ_f and δ_D were calculated by substituting the R_h for R, namely:

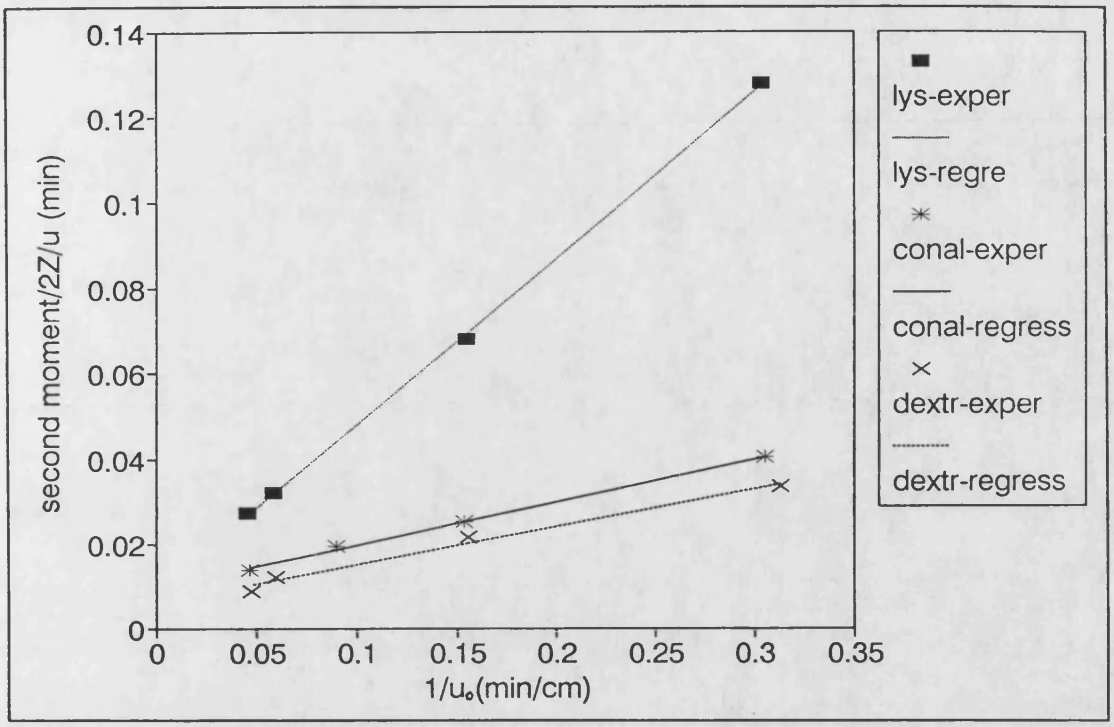

Fig.6.4 Second central moment of lysozyme, conalbumin and dextran/$2Z/u_o$ vs $1/u_o$

$$\delta_D = [\ \epsilon_i^2\ R_h^2\ (1 - \epsilon)\ ]/(15\ D_e) \qquad \text{and}$$

$$\delta_f = [\ \epsilon_i^2\ R_h\ (1- \epsilon)]/(3\ k_f) \qquad (6.32)$$

where the intraparticle voidage for lysozyme is $\epsilon_i = 0.95$, and for conalbumin is $\epsilon_i = 0.2037$

$$R_h = 3.9049 \times 10^{-5}\ m,\ \epsilon = 0.8547$$

the results in the Table 6.4

The tortuosity of the sponge column for lysozyme and conalbumin were thus calculated by equation 6.4 :

for lysozyme $\tau = 3.19$,

Table 6.4 Estimated effective diffusivity D_e and D_L/u

material	slope D_L/u (m)	intercept $\delta_D+\delta_f$ (sec)	average k_f (m/s)	δ_f (sec)	D_e m^2/s
lysozyme	0.003899	0.5443	1.68e-5	0.102	3.01e-11
conalbumin	0.001008	0.5831	1.15e-5	6.88e-3	1.07e-12
dextran	8.88e-4	0.38079			

for conalbumin τ = 10.9

Table 6.5 Effects of fluid velocity on 1st and 2nd moment of 250 x 10 mm I.D. CM sponge (1.775g) column (t_1 = column bed residence time)

feed	μ_1 (min)	μ_2 $(min)^2$	u_o (cm/min)	$1/u_o$ (min/cm)	$2nd/2Z/u_o$ (min)	Z/u_o (min)	t_1 (min)
dextran	7.869	0.524	2.73	0.3663	0.0286	9.158	7.64
	3.927	0.169	5.48	0.1825	0.01852	4.566	3.89
	1.56	0.0368	14.39	0.0695	0.01059	1.737	1.50
	1.199	0.0213	17.96	0.0557	0.00765	1.392	1.14
lysozyme	8.76	1.94	2.815	0.3552	0.10922	8.88	8.75
	4.41	0.525	5.529	0.1809	0.05805	4.52	3.99
	1.6	0.0939	14.65	0.0683	0.02751	1.707	1.49
	1.3	0.0624	18.84	0.0531	0.0235	1.327	1.21
conalb-umin	7.91	6.157	2.802	0.366	0.04037	8.922	7.77
	4.022	0.1936	5.551	0.1802	0.02149	4.504	3.91
	2.317	0.0869	9.554	0.1046	0.0166	2.617	2.24
	1.233	0.0321	18.4	0.05434	0.01183	1.359	1.18

As mention before, in the pulse experiment, the ion-exchange column acted as a gel filtration column due to the electrostatic interaction between the adsorbent and solute being suppressed. The intraparticle voidage, ϵ_i, actually depends on the molecule size, because a big molecule can not enter the

micropores. Similarly, different proteins should show different tortuosity which is not only a function of the pore shape and size but also protein molecule size. As a conalbumin molecule is five times larger than lysozyme molecule, the intraparticle voidage for conalbumin is certainly less than that for lysozyme, and τ for conalbumin is certainly larger than that for lysozyme.

As a summary, Table 6.5 and 6.6 give the data for the first and second moment at various flow-rates, and a list of transport parameters estimated for the 250 x 10 mm I.D. CM sponge ion-exchange column. The t_1 in Table 6.5 was measured from an experimental curve, which was from the start of the curve to the peak maximum point because the injected sample was so small that could be neglected.

Table 6.6 List of transport parameters estimated for 250 x 10 mm I.D. CM sponge column

column transport parameters	proteins lysozyme	conalbumin
D_L/u (m)	0.0038997	0.001008
D_e (m^2/s)	3.01×10^{-11}	1.07×10^{-12}
τ	3.1997	10.9
average k_f (m/s)	1.68×10^{-5}	1.15×10^{-5}
ϵ_i	0.95	0.2037
ϵ	0.8547	0.8547
R (m)	2×10^{-5}	2×10^{-5}
R_h (m)	3.905×10^{-5}	3.905×10^{-5}
D_m (m^2/s)	10.14×10^{-11}	5.72×10^{-11}
Peclet number (Zu/D_L)	64.1	247.9

6.9 Modelling Simulation

6.9.1 Lumped Film Mass Transfer Control Model For Differential Recirculation Batch Reactor And Stirred Batch Reactor

This lumped film mass transfer model considered the following factors: (1) transport of protein from the bulk liquid to the solution/adsorbent interface across the boundary layer (film diffusion); (2) adsorption onto external surface sites is developed from the lumped model (equation 5.10). Diffusion inside the adsorbent is not considered in this model. It is assumed that : (1) mass transfer to the surface of sponge ion-exchanger is governed by a lumped mass transfer coefficient K_{ff}; (2) there is no concentration gradient caused by solid or pore diffusion inside the sponge fibre; (3) the adsorption sites are identical and evenly distributed on the surface; (4) all the adsorption occurs at the reaction rate K_1 = 0.12 ml/mg/min which has been established as the intrinsic adsorption rate (Chapter 5); (5) the protein concentration on the adsorbent surface represents the average protein concentration of the adsorbent; (6) the rate of total removal protein from the bulk liquid is equal to the rate of accumulation of total protein in the adsorbent, in which case the c_s, the interfacial concentration, can be expressed as the function of lumped mass transfer K_{ff} , protein concentration of the adsorbent, and the protein concentration of the bulk liquid; (7) the film diffusion alone is rate controlling, so that the lumped film diffusion coefficient is first varied to give a fit to the experimental data, and not determined by other means. If poor fitting is obtained by only adjusting the K_{ff}, the K_d then is adjusted to give the best fitting, In this case K_d should be considered as a

lumped K_d. The mass-transfer equation which describes the movement of protein from bulk liquid to the cylindrical fibre adsorbent is therefore given as follows:

$$\frac{dC}{dt} = -\frac{2Wk_{ff}}{RV\rho}(C-c_s) \qquad (6.34)$$

The kinetic expression is

$$\frac{dq}{dt} = K_1 c_s (q_m - q) - K_1 K_d q \qquad (6.35)$$

The fibre surface area and volume are $2\pi RL_f$ and $\pi R2L_f$ respectively, where L_f is the length of fibre. The surface area volume ratio is therefore equal to 2/R.

The c_s expressed as the function of K_{ff}, C and q can be derived as below;

$$V C_o - V C = W q \qquad (6.36)$$

$$V\frac{dc}{dt} = -W\frac{dq}{dt}$$

$$-2WK_{ff}\frac{(C-C_s)}{(R\rho)} = -W[K_1 c_s (q_m - q) - K_1 K_d q] \qquad (6.37)$$

The c_s can be thus rewritten as

$$c_s = (K_1 K_d q + \frac{2}{R\rho} k_{ff} C) / [K_1 (q_m - q) + \frac{2}{R\rho} k_{ff}] \qquad (6.38)$$

The initial conditions are t = 0, C = C_o and q = 0.

where c_s = interfacial concentration (mg/ml)

W = weight of CM sponge (g)

K_1 = adsorption rate constant (ml/mg/min)

K_d = dissociation constant (mg/ml)

q = average protein concentration in the solid (mg/g)

V = protein solution volume (ml)

C_0 = initial protein concentration (mg/ml)

C = protein concentration in bulk liquid (mg/ml)

q_m = maximum protein capacity of CM sponge (mg/g)

K_{ff} = lumped mass transfer coefficient (mm/min)

R = radius of CM sponge fibre (mm)

ρ = density of CM sponge (g/ml)

The above equations were solved and simulated by ISIM package using fixed step Runge-Kutta method (Film-ad7 in Appendix).

6.9.2 Results and Discussion

Most of the parameters involved were fixed during the curve fitting (Fig.6.6 to 6.12 in end of this chapter) as follows (except where otherwise indicated within the individual figure.

For the differential recirculation column;

q_m = 2100 mg/g R = 0.02 mm ρ = 0.1144 g/ml

W = 0.3 g V = 180 ml C_0=0.5 mg/ml lysozyme

K_1 = 0.12 ml/mg/min K_d = 0.08 mg/ml

For the stirred vessel;

ρ = 0.303 g/ml C_0 = 0.5 mg/ml lysozyme q_m = 2100 mg/g

R = 0.02 mm K_1 = 0.12 ml/mg/min

By only adjusting the lumped mass transfer coefficient K_{ff}, curves Fig. 6.6 to Fig.6.9 were easily fitted. These results shows that the simulation curves agree well with the experimental points. As a summary of Fig.6.6 to 6.9, Fig. 6.10 gives the effects of K_{ff} on the simulated adsorption curves. At K_{ff} less than 0.7 mm/min, the simulation curves are highly sensitive to the lumped mass transfer parameter (Fig. 6.6, 6.7 and 6.10), but when the K_{ff} is more than 0.7 mm/min, the simulated adsorption curves are hardly affected by K_{ff}. One can seen that changing the K_{ff} by a factor of more than 950, from 0.8 to 800 mm/min (Fig. 6.9 and 6.10), only changed the simulation adsorption curve slightly deeper.

In the case of a stirred vessel, in order to fit the experimental data, K_{ff} is estimated as being between 1.4 and 3 mm/min (Fig.6.11 and 6.12), which is rather larger than that from the differential recirculation batch reactor at the maximum superficial velocity. It may be that internal diffusion, which

is not the main controlling factor in the underloaded differential recirculation batch experiment but plays a more important role in the overloaded stirred vessel experiment. Its effect would be included in the lumped mass transfer coefficient, K_{ff}.

The K_d value, 0.1 ± 0.02 mg/ml obtained from the isotherm experiment (Chapter 5) which depended on the estimation method either by linear regression or non-linear regression, was used unchanged when fitting the differential bed column data (Fig.6.6 to 6.9). In the case of stirred tank, K_d, however, had to be adjusted to a larger value in order to simulate correctly the tail of adsorption curve (Fig. 6.11 , 6.12 and Table 6.7). On can see in Fig. 6.11 that when K_d = 0.1 mg/ml is chosen, the tail of the simulation curve is far away from that of experiment. It could be that the internal diffusion is significant in the case of stirred tank due to; (1) long adsorption time; (2) protein overload. In the case of differential column, however, the protein was underload (only 15% of total protein capacity of packed CM sponge) and the adsorption time was short so that the effect of internal diffusion on the tail of adsorption curve was not significant.

The evidences given by the lumped film mass transfer control model confirms that; (1) at the superficial velocity more than 44 m/h, the lumped K_{ff} does not increase with the superficial velocity. This would indicate that the liquid film mass transfer is no longer the main limiting factor for the adsorption process;

(2) using K_1 = 0.115-0.12 ml/mg/min as a intrinsic adsorption rate constant is reliable; (3) in the case of overloading such as stirred tank, the tail of the adsorption curve is only fitted by changing K_d. This might indicate that the effect of internal diffusion is included in the K_d, so that K_d in this model should be regarded as a lumped parameter. The K_{ff} estimated from both the differential recirculation reactor and the stirred vessel experiments might also include the effect of internal diffusion as the values are higher than would be expected for film mass transfer (Table 6.7).

6.9.3 An Heterogeneous Model Including External Film Diffusion Control And Intraparticle Diffusion Control

As the porosity of sponge ion-exchanger for lysozyme is 0.95, this indicates that whole adsorbent fibre particle consists of two phases, *i.e.* liquid phase which exists in the pore or in the channel, and solid phase. The effect of intraparticle diffusion therefore needs to be considered. This also has been suggested by the simulation results using a lumped film mass transfer model.

Protein, which is transferred to the external surface of the ion-exchange particle, diffuses inside the pore to the reaction site on the surface of the pore wall and reacts at reaction sites apart from being adsorbed on the particle external surface. Thus, there would be an "interpore" gradient for the transport of protein to the reaction sites on the surface of channel or pore wall. There is also a concentration gradient in the solid phase.

Protein adsorbed on the surface immigrates along the solid phase forward the centre of the particle where the concentration is the lowest. When the whole system reaches an equilibrium state, protein concentration at any point inside the fibre cylinder should be equilibrium across the phase boundary. This means that protein concentration of bulk liquid is equal to that of liquid phase in the fibre cylinder, and the average protein concentration of adsorbent is equal to protein concentration at any point in the solid phase within the fibre cylinder.

It is assumed that; (1) the adsorption only occurs on the external surface of the fibre cylinder or the surface of pore wall; (2) protein diffuses within the liquid phase and as surface diffusion along the pore wall; (3) protein adsorbed from the liquid to the solid along the length of the pores; (4) for simplicity, the pore diffusion coefficient and solid diffusion coefficient are assumed to be identical which are considered as an effective diffusivity, D_e.

External mass transfer resistance in a well mixed reactor is principally in the hydrodynamic film surrounding the sponge fibre cylinder. The total rate of mass transfer from the bulk liquid to the fibre surface is equal to the rate of change of the protein mass in the bulk liquid

$$\frac{dc}{dt} = -\frac{2Wk_f}{RV\rho}(C-C_s) \qquad (6.39)$$

The total accumulation of protein within the solid phase by means of surface diffusion and adsorption from the liquid is given below

$$\frac{\partial q_i}{\partial t} = \frac{D_e}{r}\frac{\partial}{\partial r}\left[r\frac{\partial q_i(r,t)}{\partial r}\right] + \left[K_1 c_i (q_m - q_i) - K_1 K_d q_i\right] \tag{6.40}$$

The rate of change of protein concentration inside the pore by means of diffusion and adsorption to the pore wall is described by

$$\frac{\partial c_i}{\partial t} = \frac{D_e}{r}\frac{\partial}{\partial r}\left[r\frac{\partial c_i(r,t)}{\partial r}\right] - \rho\frac{(1-\epsilon_i)}{\epsilon_i}\left[K_1 c_i (q_m - q_i) - K_1 K_d q_i\right] \tag{6.41}$$

The interfacial concentration C_s is related to q_s by means of adsorption isotherm, in this model it is assumed that the isotherm has the form:

$$C_s = \frac{k_d q_s}{q_m - q_s} \tag{6.42}$$

Equation 6.42 is the form of a rearrangement of Langmuir isotherm and also the general isotherm equation 5.2a (Chapter 5) in which the heterogeneity factor is assumed $d_1 = 1$.

The average concentration of protein in the cylindrical

$$q=\frac{2}{R^2}\int_0^R q_i(r,t)\,r\,dr \qquad (6.43)$$

fibre adsorbent, q, is obtained by integrating the pointwise concentration over the volume of the fibre cylinder.

q also can be written as the following form, this means that any protein which is not in the fluid must be inside the adsorbent particle.

$$q=(Co-C)\frac{V}{W} \qquad (6.44)$$

The boundary conditions, for the fibre cylinder are specified as implicit function of time and the derivative of concentration at the centre of the fibre cylinder is zero. This means that the external surface concentration in the solid phase is an unknown function of time and the protein flux at the centre of the fibre is zero at all times, *i.e.*;

$$\begin{array}{lll} r = R & q(R,t) = q_s\ (t) & \\ r=0 & \partial q_i\ (0,t)\ /\partial r = 0 & (6.45) \end{array}$$

The initial conditions are

$$t = 0, \quad C = C_0, \quad q = 0$$

The advantage of the implicit boundary function is that it can be used for different boundary condition without necessarily

knowing the explicit boundary function. This also means that the model can be used for different cases. This implicit boundary function was also applied by Mathews and Weber(1977,1983), McKey *et al.* (1984), and Addo (1988).

Trapezoidal rule can be used to integrate the average protein concentration in the fibre cylinder, the external surface protein concentration of solid phase q_s is therefore calculated from the integration of average protein concentration.

$$q=\frac{2}{R^2}\sum_{i=0}^{N+1}\left(\frac{q_i r_i+q_{i+1}r_{i+1}}{2}\right)(r_{i+1}-r_i)$$

(6.46)

$$q=\frac{2}{R^2}\sum_{i=0}^{N-1}\left(\frac{q_i r_i+q_{i+1}r_{i+1}}{2}\right)(r_{i+1}-r_i)+\frac{(q_N r_N+q_{N+1}r_{N+1})}{2}(r_{N+1}-r_N)$$

$$q_s=\left\{\frac{2}{(r_{N+1}-r_N)}\left[\frac{qR^2}{2}-\sum_{i=0}^{N-1}\left(\frac{q_i r_i+q_{i+1}r_{i+1}}{2}\right)(r_{i+1}-r_i)\right]-q_N r_N\right\}\frac{1}{r_{N+1}}$$

(6.47)

where $q_s = q_{N+1}$, $r_{N+1} = R$.

As mentioned before, when the system reaches the equilibrium, the average protein concentration of adsorbent is equal to the protein concentration at any space point in the solid phase. This indicates that the integration equation 6.43 should be rewritten as below because the q_i is a constant and equal to q, in this case equation 6.49 is thus equal to 0.5.

$$\frac{q}{q_i} = \frac{2}{R^2}\int_0^R r dr \qquad (6.48)$$

$$\frac{1}{2} = \frac{1}{R^2}\int_0^R r dr \qquad (6.49)$$

As q_i is a pointwise value in the fibre rather than a continuous function the integration equation 6.43 can not be solved analytically so that a numerical quadrature must be employed. The truncation error of numerical quadrature mainly depends on the number of space points, N, in the interval of integration, when N tends to infinity, the truncation error of integration tends to zero. In practice computation, N can only be a finite number, which means that the concentration, q_i, at infinity time will not tend to be exactly equal to q. In this case an "equilibrium correcting factor, c_f is therefore introduced to ensure the qi = q. The exact value of c_f is dependent on which numerical quadrature being chosen, but c_f always tends to one when the space points, N, tends to infinity. For the trapezoidal rule used in the equation 6.46, the c_f is expressed as following;

$$c_f \frac{2}{R^2}\sum_{i=1}^{N+1} \left(\frac{r_i + r_{i+1}}{2}\right)(r_{i+1} - r_i) = 1$$

$$c_f = \frac{0.5R^2}{\sum_{i=0}^{N+1} \left(\frac{r_i + r_{i+1}}{2}\right)(r_{i+1} - r_i)}$$

(6.50)

Orthogonal collocation method was applied to solve the second order partial differential diffusion equations 6.40 and 6.41, these equations were then reduced to a set of N first order ordinary differential equations. According to Constantinides (1987) the orthogonal collocation method is more accurate than either the finite difference method or the collocation method. The choice of collocation points at the roots of the orthogonal polynomials reduces the error considerably. In addition, orthogonal collocation is faster than finite differences. Ramachandran (1975) applied orthogonal collocation to an immobilized enzyme system with rate dependent on position in the spherical pellet. He stated that it was worth mentioning that for many problems, an approximation using a value of N = 1 was sufficiently accurate.

The above system equations 6.39 to 6.45 are then rewritten as the following from:

$$\frac{dC}{dt} = -2w\frac{K_f}{RV\rho}(C - c_s) \qquad (6.51)$$

$$\frac{dc_j}{dt} = D_e\sum_{i=1}^{N+1} B_{ji}c_i - \rho\frac{(1-\epsilon_i)}{\epsilon_i}[K_1c_j(q_m - q_j) - K_1K_dq_j] \qquad (6.52)$$

$$\frac{dq_j}{dt} = D_e\sum_{i=1}^{N+1} B_{ji}q_i + [K_1c_j(q_m - q_j) - K_1K_dq_j]$$

(6.53)

$$q_s=\left\{\frac{2}{(x_{N+1}-x_N)}\left[\frac{q}{2c_f}-\sum_{i=0}^{N-1}\left(\frac{q_ix_i+q_{i+1}x_{i+1}}{2}\right)(x_{i+1}-x_i)\right]-q_Nx_N\right\}\frac{1}{x_{N+1}}$$

(6.54)

$$q=(C_o-C)\frac{V}{W} \qquad (6.55)$$

$$c_s=\frac{K_dq_s}{(q_m-q_s)} \qquad (6.56)$$

where $r_i = R\ x_i$, $x_{N+1} = 1$, $x_0 = 0$, x_i is the collocation spaced point

$c_s = c_{N+1}$, $q_s = q_{N+1}$ the interfacial protein concentration for liquid phase and solid phase, (mg/ml, mg/g) respectively

j, N = number of collocation points

C = protein concentration in bulk liquid (mg/ml)

c_i, c_j, q_i, q_j, = protein concentration in liquid phase and solid phase, (mg/ml, mg/g), at the collocation point respectively

q = average protein concentration in the particle (mg/g)

Co = initial protein concentration (mg/ml)

R = the radius of cylindrical fibre (mm)

D_e = effective diffusivity (mm^2 / min)

K_f = external mass transfer coefficient (mm/min)

W = weight of sponge (g)

ρ = the density of sponge (q/ml)

V = protein feed volume (ml)

ϵ_i = CM sponge fibre porosity

The orthogonal collocation used three points, the values of x_i and B_{ji} were obtained from Villadsen and Stewart (1976). The above equations were solved and simulated by fixed step Runge-Kutta method in ISIM package (Fang-c2 in Appendix). The calculation time was around 30 seconds in PC386SX personal computer (Opus Technology).

6.9.4 Results And Discussion

The principal parameters required for use of the two phase model are the external mass transfer coefficient, K_f, effective diffusivity, D_e, isotherm constants and adsorption rate constant. The external mass transfer coefficient was estimated by correlation procedures by Geankopolis (1983) as below;

$$K_f = \frac{2D_m}{d} + 0.31\left(\frac{\mu}{\rho D_m}\right)^{-\frac{2}{3}}\left(\frac{\Delta\rho\mu g}{\rho^2}\right)^{\frac{1}{3}} \qquad (6.57)$$

where D_m = 1.013×10^{-10} m^2 s^{-1} (lysozyme diffusion coefficient in free solution)

ρ = 1000 kg m^{-3} (liquid density, which assumed is equal to water density at 20 °C)

μ = 0.001 kg $(ms)^{-1}$ (liquid viscosity, which assumed is equal to water viscosity at 20 °C)

g_o = 9.80665 m s^{-2} (gravity)

$d = 4 \times 10^{-5}$ m (mean particle diameter)

$\Delta\rho = 92$ kg m^{-3} (density difference between adsorbent and liquid. wet sponge density = 1092 kg m^{-3} (swollen volume)

K_f was therefore calculated to be 0.694 mm min^{-1} for lysozyme. The only unknown parameter is effective diffusivity which can be obtained by giving the best curve fitting at the experimental points. The effective diffusivity, D_e is independent of reactor geometry, but the K_f depends on the reactor geometry and stirrer speed.

The parameters used in the stirred vessel are the following but otherwise indicated within the individual Figure;

$\rho = 0.303$ g/ml $K_1 = 0.12$ ml/mg/min

$R = 0.02$ mm $q_m = 2030$ mg/g $K_d = 0.1$ mg/ml

$C_0 = 0.5$ mg/ml lysozyme

K_f (mm/min) and D_e (mm^2/min) indicated in the Figures.

Fig 6.13 (Fig. 6.13 to Fig. 6.20 in the end of this chapter) shows that the predicted adsorption curve is in excellent agreement with the experimental points by choosing $D_e = 0.0039$ mm^2 min^{-1}. This D_e value is close to the one (0.00183 mm^2 min^{-1}) obtained by pulse method. The effect of D_e on the adsorption rate profile is also displayed by Fig.6.13. The initial stage of adsorption is not controlled by the effective diffusivity although the latter stages are fully controlled by D_e. When the effective diffusivity tends to a minimum (D_e =0.00001 mm^2 min^{-1}), the protein hardly penetrates into the adsorbent, and the

adsorption only occurs on the adsorbent surface. It is apparent that the assumption of negligible intraparticle diffusion resistance is a valid assumption, in the initial period, for protein that exhibit a large solid to liquid phase equilibrium protein distribution. When D_e (0.02 mm^2 min^{-1}) is much larger than the D_m (0.007 mm^2 min^{-1}), protein diffusion coefficient in free solution, the intraparticle diffusion resistance is no longer controlling and external film transfer resistance is assumed to control the adsorption processes. It is however apparent from the poor fit in Fig.6.13 that the single resistance, K_f, is inadequate for predicting the adsorption profile beyond the initial stage.

Fig. 6.14 and 6.15 show how the protein concentrations vary with time in the solid phase and liquid phase inside the fibre cylinder. When the adsorption processes tend to be equilibrium, the protein concentration in liquid phase of the fibre tend to be equal to that in the bulk liquid (Fig.6.14). The protein concentration in the solid phase also tend to be equal (Fig. 6.15).

Once the effective intraparticle diffusivity is established (D_e = 0.0039 mm^2 min^{-1}), it can be applied to the other cases with different stirrer speeds and different flow-rates in the stirred vessel and differential column reactor. But the external mass transfer coefficient estimated from the Geankopolis (1983) correlation might need to be adjusted. Mathews and Weber (1983) concluded that the correlation equations do not provide

sufficiently accurate vales for the external mass transfer coefficient, and the use of single or multicomponent rate model could result in poor predictions for the adsorption rate profiles. The adsorption profile are sufficiently sensitive to variations in the transport coefficient to preclude the use of such correlation for accurate predictions. At 1240 r.p.m. stirrer speed and by fixing D_e = 0.0039 mm^2 min^{-1}, Fig 6.16 suggests the external mass transfer coefficient K_f = 0.8 mm min^{-1} due to the higher stirred speed than in Fig. 6.13. The simulated curve is in a reasonable agreement with the experimental data.

The heterogeneous model is then applied to predict the protein adsorption in the differential bed column by fixing all the parameters used in the lumped K_{ff} model except the K_f . The D_e is fixed as 0.0039 mm^2/min. The only unknown parameter in the simulation of the differential bed experiment is K_f which can be obtained by a best fit. Table 6.7 and Fig. 6.10 give the relationship between the superficial velocity and K_f. Using these K_f values, a fairly good agreement between the predicted curves and experimental points are obtained , which can be seen in Fig.6.17 to 6.20. Although the K_f is different from the K_{ff} at the superficial velocity less than 44 m/h, the behaviour of K_f as a function of superficial velocity is the same as that of K_{ff} (Fig. 6.10). At the high superficial velocity (more than 44 m/h), Both K_f and K_{ff} are equal (Fig.6.10 and Table 6.7).

where K_d = 0.1±0.02 mg/ml estimated from isotherm experiment

K_{ff} and K_d^c = lumped external mass transfer coefficient and

Table 6.7 Values of K_{ff}, K_f and K_d estimated from the differential recirculation batch reactor, stirred batch reactor and correlation.

superfic. velocity m/h	K_{ff} mm/min	K_f^a mm/min	K_f^b mm/min	K_d^c mg/ml	K_d^a mg/ml	stirrer speed r.p.m.
2.97	0.2	0.23		0.08	0.08	
13.88	0.43	0.6		0.08	0.08	
44.43	0.8	0.8		0.08	0.08	
92.7	0.8	0.8		0.08	0.08	
	1.4	0.7	0.694	0.18	0.1	560
	3	0.8	0.694	0.2	0.1	1240

lumped disassociation constant in the lumped K_{ff} model

K_f^a and K_d^a = external mass transfer coefficient and disassociation constant in the heterogeneous model

K_f^b = external mass transfer coefficient calculated from the correlation (Geankopolis 1983)

6.9.5 Modelling For A 250 x 10 mm I.D. CM Sponge Column

The effects of external mass transfer and diffusion inside the adsorbent fibre on the adsorption processes have been discussed and described in the previous sections. A simple lumped model can be satisfactorily fitted to the adsorption curve, although the effects of the external mass transfer, reaction rate constant and diffusion inside the particle were not distinguished. As a guide to scale-up and control and due to the consideration of calculation time, a simple column model with a reasonable physical meaning, which can well describe and predict the position and the initial shape of the breakthrough curve

should be acceptable.

There are four important points in the breakthrough curve, i.e. the initial breakthrough point, and the points at the 10% (0.1 C/C_0), 50% (0.5 C/C_0) and 90% (0.9 C/C_0) of breakthrough curve respectively. These points usually are the "control signal" to terminate the loading of the column when the level of adsorbate in the outflow from the column reaches to these levels. If loading of the column continues beyond this point, a considerable amount of adsorbate may pass through the column without being adsorbed. This not only wastes the adsorbate but also prolong the processing time. To choose the point of loading termination depend critically on the shape of the breakthrough curve and cost of the feed. For a shallow breakthrough curve or expensive feed, the loading could be stopped at or less than the 10% breakthrough curve, whilst for the sharper curve the loading could be terminated at the 50% breakthrough curve. In practice, Chase (1984a)believed that, it is unlikely that the column will be loaded to its maximum capacity, *i.e.* not more than 90% of the breakthrough due to the fact that the productivity then is considerably reduced. This can be seen in following sections in Figures from 6.21 to 6.25, after the breakthrough curve reaches 0.9 C/C_0, the further development of curve becomes very slow. It usually needs almost two or four folds as much time to complete is due to the slow intraparticle diffusion.

As mentioned before, Hubble (1988) used a very simple model, i.e. $dq/dt = K_1 C (q_m - q) - K_2 q$, without the consideration of

axial diffusion and convection within the column to simulate the breakthrough curve. Chase (1984) considered the effect of convection within the column together with lumped parameter, K_1, he did not, however, considered the external mass transfer and axial diffusion within the column even a column length was less than 15 mm. Onwuasoanya (1987), in order to simplify the affinity sponge packed column model, assumed that the sponge fibre to be a non-porous particle and did not consider external mass transfer. The main aims of simplifying the column model is to reduce calculation time.

The column model developed in this chapter includes the porosity of the fibre, flow convection and axial dispersion within the column. Although the pulse repone experiment in this work gave the Peclet number = 64, the axial dispersion was still considered important for this model so that the Peclet number could be determined for the novel matrix, which might be important in a short column. As the surface reaction model (equation 5.10) can fit well the adsorption curve , it was used to describe the adsorption kinetic precess. The external mass transfer item is not expressed in the column model but is included in the lumped parameters.

Including the factors of axial diffusion and convection, the equation 6.11 is written as follows, which is the column model for CM sponge packed in a 250 x 10 mm I.D. column.

$$\epsilon\frac{\partial C}{\partial t}=\epsilon D_L\frac{\partial^2 C}{\partial x^2}-\epsilon u\frac{\partial C}{\partial x}-\rho\frac{\partial q}{\partial t} \qquad (6.58)$$

$$\frac{\partial q}{\partial t}=K_1 C(q_m-q)-K_1 K_d q \qquad (6.59)$$

the Dunckwerts boundary conditions are at the start of the column, x = 0;

$$D_L\frac{dC}{dz}=u(C_o^{+}-C_o^{-}) \qquad (6.60)$$

at the end of the column x = 1;

$$dC/dz = 0$$

The initial conditions are t = 0, C = 0, q = 0, $C^{-}_o = C_o$.

Let the dimensionless variables and constants be

$y = C/C_o$, $g = q/q_m$, $s = x/l$, $T = ut/l$, $Pe = ul/D_L$ (Peclet number), $K_a = C_o l K_1/u$, $K_b = K_1 K_d l/u$, $K_p = \rho q_m/\epsilon C_o$

where l = the length of column. The dimensionless equations are thus written as:

$$\frac{\partial y}{\partial T} = \frac{1}{P_e}\frac{\partial^2 y}{\partial s^2} - \frac{\partial y}{\partial s} - K_p\frac{\partial q}{\partial T} \qquad (6.61)$$

$$\frac{\partial g}{\partial T} = K_a y(1-g) - K_b g \qquad (6.62)$$

with the boundary conditions:

at s = 0, dy/ds = Pe(y-1), at s = 1, dy/ds =0

The number of parameters in the dimensionless equations are then reduced to 4.

By applying the orthogonal collocation method to equations 6.60 and 6.62, these differential equations can now be expressed at the collocation point s_j as follows:

$$\frac{dy_j}{dT} = \frac{1}{P_e}\sum_{i=1}^{N+2} B'_{ji}y_i - \sum_{i=1}^{N+2} A'_{ji}y_i - K_p\frac{dg_j}{dT} \qquad (6.63)$$

$$\frac{dg_j}{dT} = K_a y_j(1-g_j) - K_b g_j \qquad (6.64)$$

where y_j is the concentration of the protein in the bulk liquid at the point s_j. Here the point s_1 corresponds to the inlet of the column, (s = 0); the point s_{N+2} refers to the outlet of the column (s = 1).

The boundary conditions permit the elimination of y_1 and y_{N+2}, namely:

at $s = s_{N+2}$, i.e. $s = 1$,

$$\sum_{i=1}^{N+2} A'_{N+2,i} y_i = 0 \qquad (6.65)$$

at $s = s_1$, i.e. $s = 0$,

$$\sum_{i=1}^{N+2} A'_{1,i} y_i = P_e (y_1 - 1) \qquad (6.66)$$

The set of simultaneous first order ordinary differential equations was solved and simulated by the fixed step Runge-Kutta method within the ISIM package (Fang-column Appendix).

6.9.6 Results And Discussion

The parameters used in this column model simulations are either from the isotherm adsorption (q_m K_d) provided by BPS Ltd. or the results of pulse response experiment. The location of the 10% breakthrough point was matched by adjusting the dimensionless constant k_p which incorporates q_m, ϵ, ρ and C_o. Each parameter in k_p can influence the position of the breakthrough curve. q_m was chosen as the adjustable parameter, because it is most affected by operation conditions such as temperature. As shown in Fig.6.21, the higher q_m , the later the breakthrough occurs. If the unadjusted value of q_m (1360 g/kg) and using K_1 = 4.8 m3/kg/h, as estimated from Fig.5.12 (Chapter 5), the simulated curve can exactly predict the position of initial breakthrough

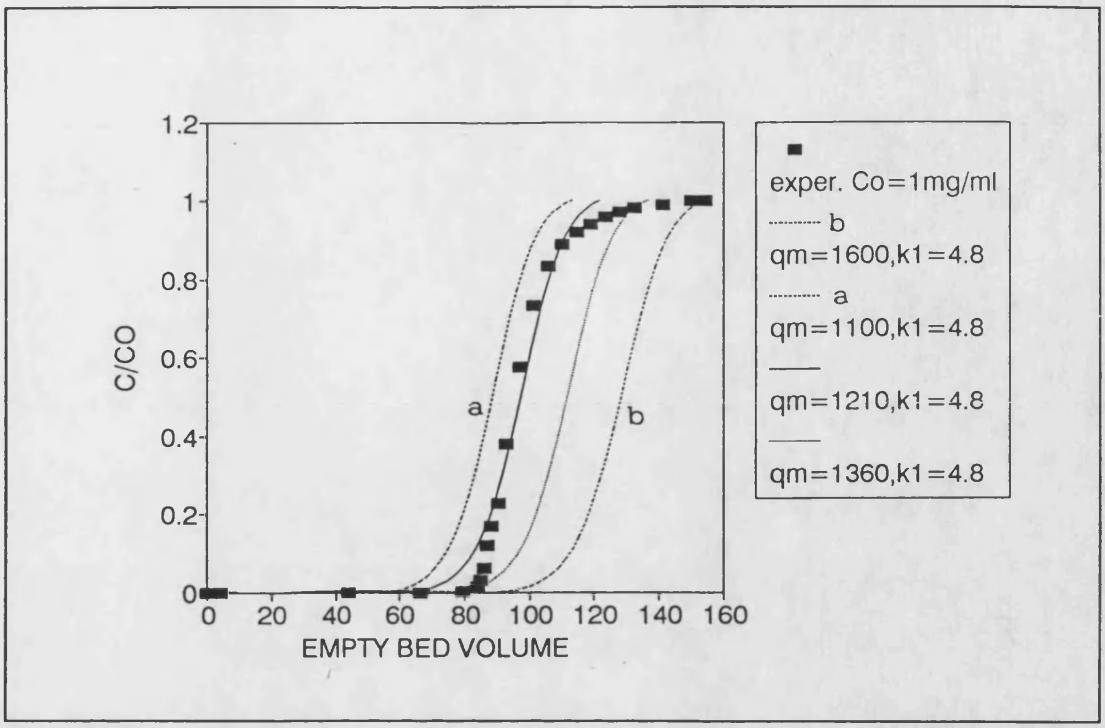

Fig.6.21 Effect of maximum capacity on the breakthrough curve simulation. Data for simulation: c0 = 1 kg/m^3, u = 7.69 m/h, kd=0.056 kg/m^3, K_1 = 4.8 m^3/kg/h.

curve in the experiment, in spite of the rest of the breakthrough curve not fitting well. q_m = 1210 g/kg gives the best average fit over the whole breakthrough curve.

The shape of the initial breakthrough curve is not strongly affected by q_m, but it is by K_1 which also affects the steepness of the breakthrough curve. It is shown in Fig.6.22, when K_1 increases from 2.5 to 7 m^3/kg/h, that the simulation curve becomes steeper and the initial stage of the simulation curve approaches the experimental one, although the tail of the simulation deviates from the experimental data. The K_1 used in the simulation was obtained from the differential bed experiment (Fig.5 12). One can see from Fig. 6.22 that K_1 = 7 m^3/kg/h gives

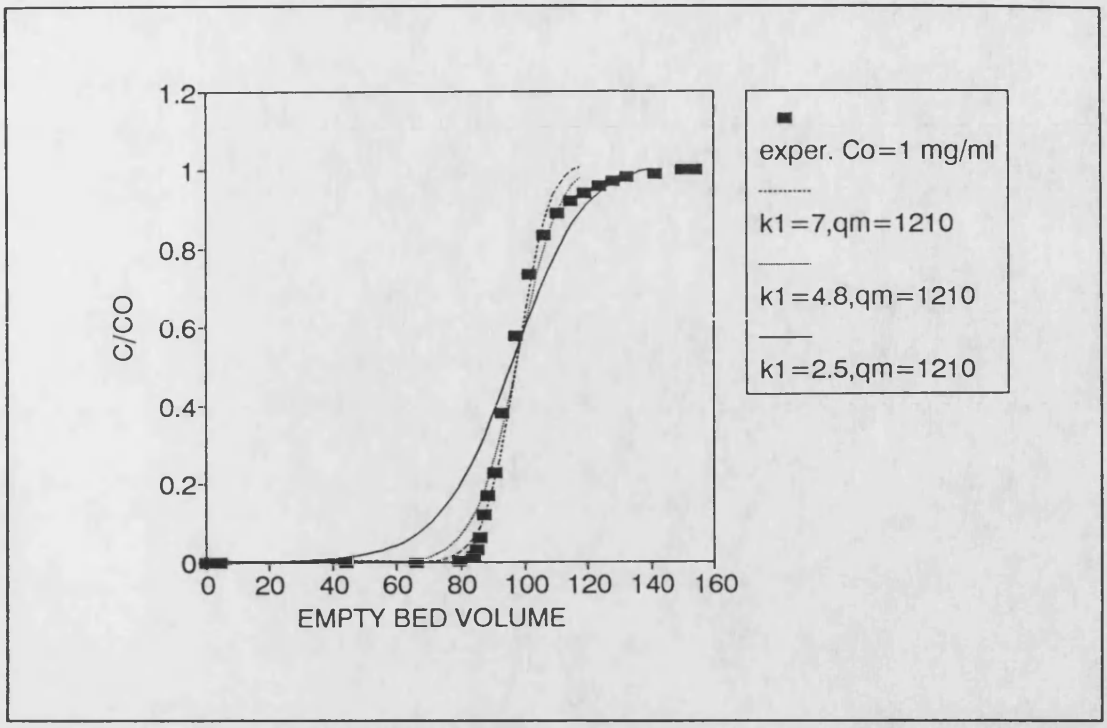

Fig.6.22 Effect of adsorption constant K_1 on the breakthrough curve simulation. Data of simulation: c0 = 1 kg/m^3, kd = 0.056 kg/m^3, q_m = 1210 g/kg, u = 7.69 m/h.

a better fit than either K_1 = 2.5 or 4.8 m^3/kg/h. More than 90% of the simulation curve agrees well with the experimental one deviation only at the curve tail. In practice, as mentioned in the beginning of this section, the column feed is usually stopped when 90% of the feed concentration appears at the outlet of the column. It is therefore important to predict the initial stage the breakthrough curve. Horstman (1988) was not successful in applying the forward rate constant k_1 obtained from stirred tank runs to the column model simulation. She stated that" from the stirred tank runs, it appeared that the forward rate constant was between 0.06 and 0.12 ml/mg/min, the value obtained for the column run was 0.033 ml/mg/min which was somewhat lower than the stirred tank values". She showed that the simulation curves excellently agreed with the experimental points when the K_1

chosen was obtained by pure curve fitting. The K_1 used in this study is in the range of results from both the recirculation differential column and the stirred tank, despite the K_1 value being higher than predicted (4.8 $m^3/kg/h$ at linear velocity 7.69 m/h in Fig. 5.12). This might be due to using a different batch of CM sponge.

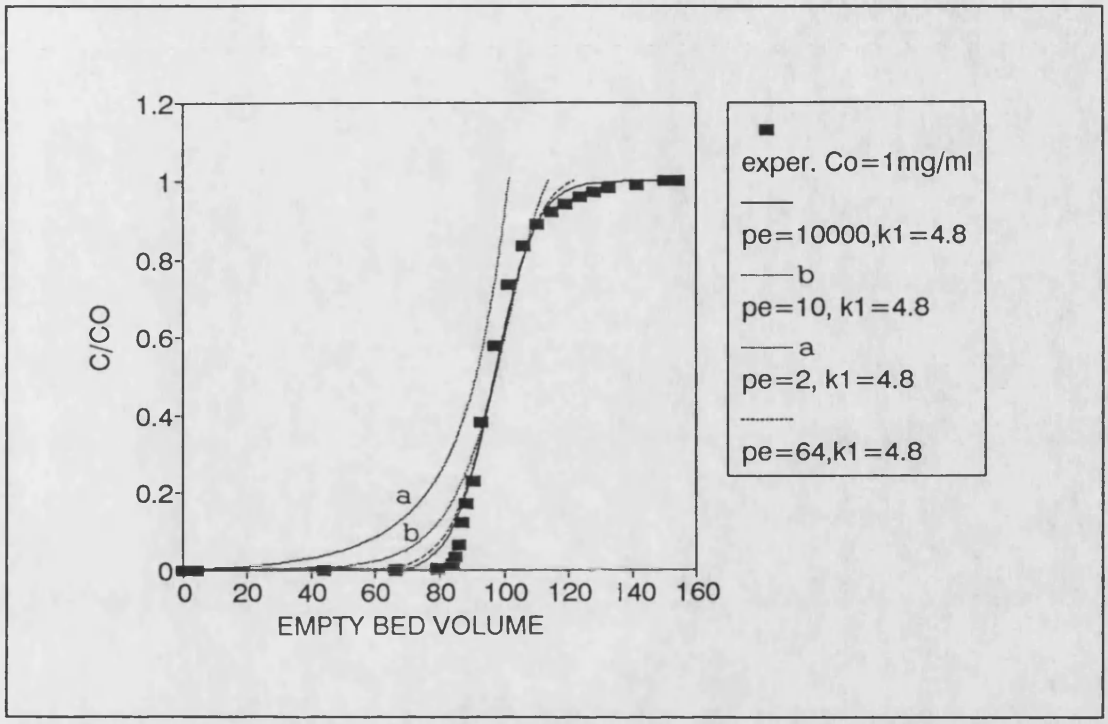

Fig.6.23 Effect of Peclet number on the breakthrough curve simulation. Data for simulation; c0 = 1 kg/m^3, u = 7.69 m/h, k_d = 0.056 kg/m^3, k_1 = 4.8 $m^3/kg/h$.

Fig.6.23 shows that the influence of the axial Peclet number on the breakthrough curve. It is evident that for an axial Peclet number of less than 10, the rising of the initial stage of the breakthrough curve tends to be flatter with a decrease the Peclet number, but if the Peclet number is greater than 10 the effect of this parameter tends to be minimal. This justifies that the use of the plug-flow assumption in a long column with small

diameter can also apply to a sponge ion-exchange column. The pulse response experiment gave Pe = 64, which indicated that the effect of axial dispersion would be negligible.

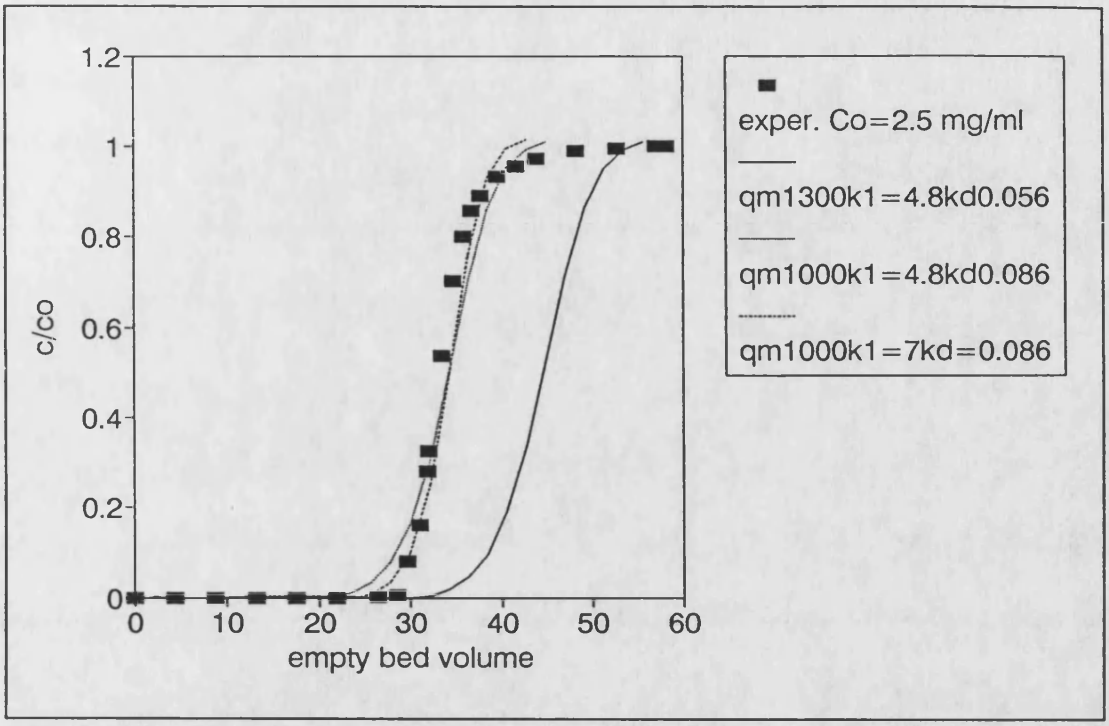

Fig.6.24 Effect of maximum capacity and K_1 on the breakthrough curve at the feed 2.5 kg/m^3. Data of simulation; c0 = 2.5 kg/m^3, k_d = 0.056 kg/m^3, u = 8.82 m/h.

Under the experimental conditions of various feed concentrations and linear velocities, Fig. 6.24 and Fig. 6.25 show that the simulation curves agree with the first half of the experimental data using K_1 = 7 m^3/kg/h and slightly adjusting the q_m. Otherwise the rest of parameters were obtained from the separate experiments. It is also evident from Fig.6.21 to Fig.24 that the appearance of breakthrough curve depends on the feed concentration.

6.10 Conclusion

Both the lumped K_{ff} model and the more sophisticated heterogeneous model which included external mass transfer and internal diffusion, described well the adsorption performance, but the latter model gave parameter values which can be related to fundamental properties.

The heterogeneous model demonstrated that the initial stage of adsorption was controlled by external mass transfer, whilst after the initial stage, the adsorption was governed by internal diffusion. The heterogeneous model can be used to gives a picture of the protein concentrations over the time in both phase inside the fibre cylinder. The effective diffusivity, D_e, estimated by the heterogeneous model was close to that obtained from the pulse response experiment. The external mass transfer K_f estimated from the heterogeneous model was probably more accurate than that obtained from correlations.

Solved by orthogonal collocation method, the heterogeneous model can rapidly predict the adsorption performance in both the recirculation batch reactor and stirred batch reactor under different protein loading, stirrer speeds and superficial velocities.

Applying the lumped K_{ff} model to the differential recirculation batch experiment, the values of K_{ff} as estimated were almost identical to those estimated using the heterogeneous

model (Table 6.7). This is because that the internal diffusion was not significant due to underloading (only 15% of total packed adsorbent protein capacity was used). In the case of stirred batch experiment, since the protein was overloaded, the internal diffusion was not negligible, the values of K_{ff} estimated were almost twice those estimated using the heterogeneous model and correlation (Geankoplis 1983). In this case the K_{ff} included significant internal diffusion effects. Also, the values of K_d estimated from stirred batch experiment by using the lump K_{ff} model were higher than those from the isotherm experiment (Table 6.7). It seems that the K_d is also a lumped parameter, which include the effect of internal diffusion, rather than being a pure disassociation constant.

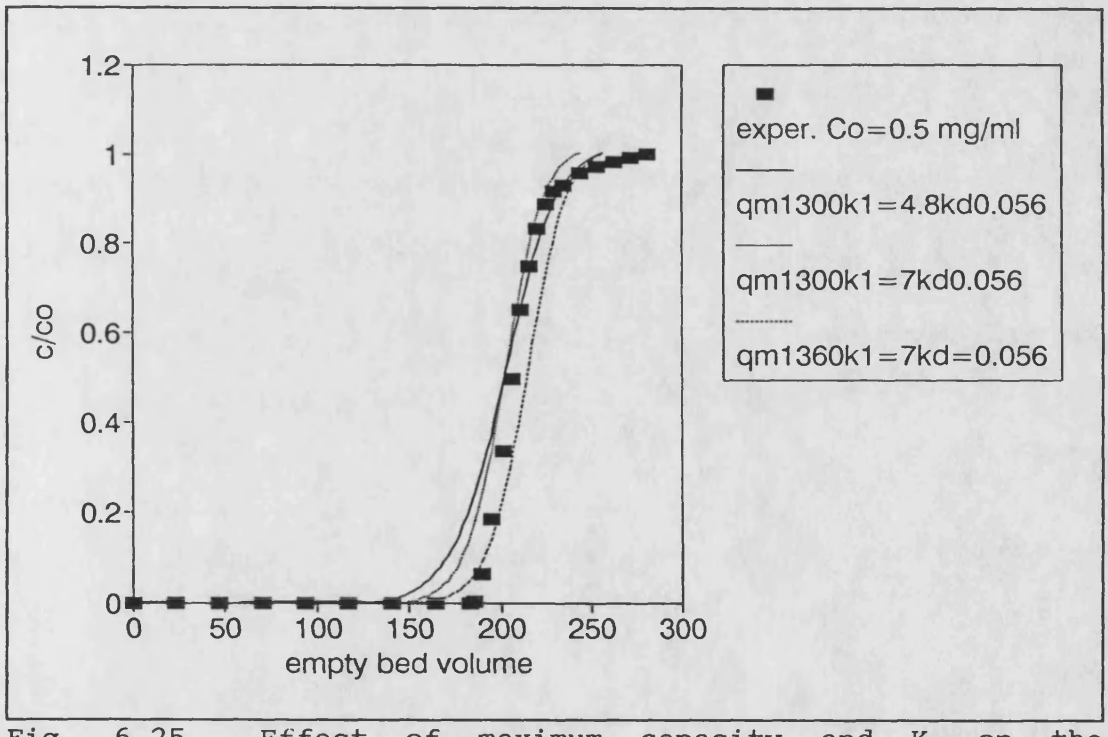

Fig. 6.25 Effect of maximum capacity and K_1 on the breakthrough curve at the feed 0.5 kg/m^3 . Data of simulation; c_0= 0.5 kg/m^3, K_d = 0.056 kg/m^3, u = 9.2 m/h.

The use of parameters determined from the differential bed and pulse response experiments, in predictions of CM sponge column performance, resulted in a reasonable agreement with the CM sponge column adsorption results. The column model showed that, even with the novel coherent sponge ion-exchanger, the axial dispersion was negligible as the Peclet number was larger than 10. In comparison with a differential bed, although the 250 mm length column was scaled-up 62 times, the K_1 determined by using differential bed column successfully described the adsorption preferences in the long column. Using K_1 = 7 $m^3/kg/h$, the column model, which did not differentiate the effects of film mass transfer and pore diffusion, predicted more than 90% the experimental breakthrough curve at various feed concentration and linear velocities. Same conclusions were similar to those drawn by Horstman and Chase (1989) and Horstman (1989), namely: (1) the value of q_m used in the simulation needed sometimes to be adjusted within its error range in order to get the best fits between simulation and experiment, (2) It was difficult to obtain a good fit to the early part of the breakthrough curve by using the lumped surface reaction model. In spite of the shape of the curve, it did not match particulary well for the complete curve, it might be adequate for a rough guide to scale-up and be easy to use for control due to having few parameters and needing little calculation time; (3) The initial part of the breakthrough curve might be controlled by a film mass transfer coefficient. Further development of the column model to include the film mass transfer and pore diffusion is suggested.

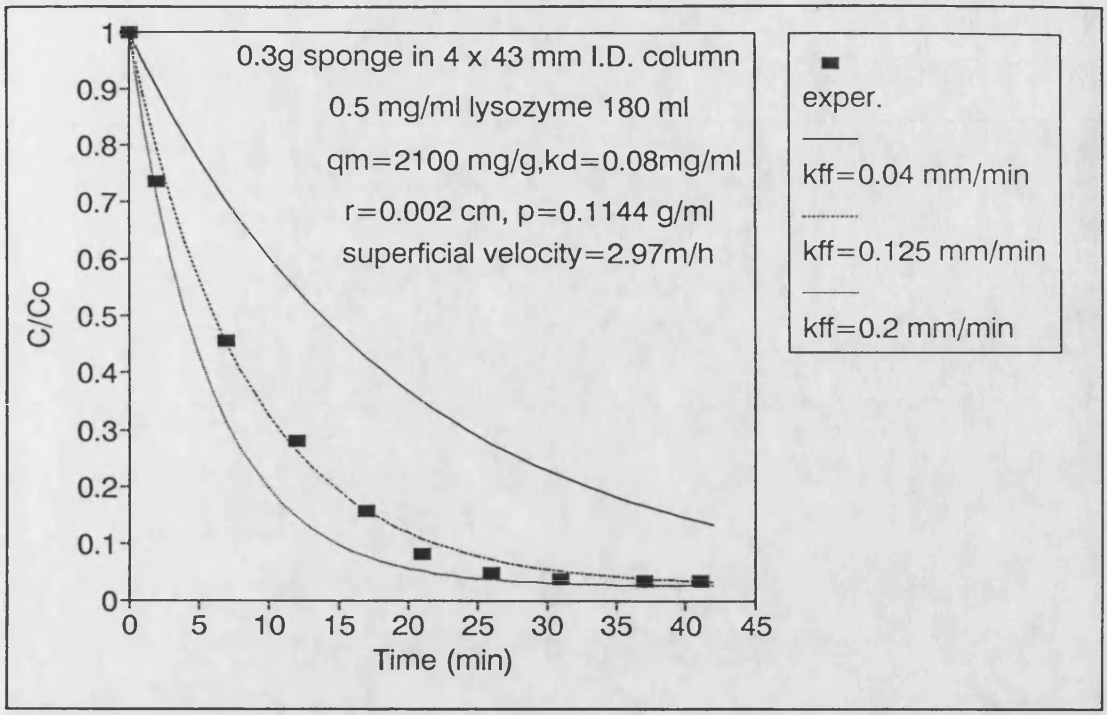

Fig. 6.6 Effect of lumped external mass transfer K_{ff} on the adsorption process at the superficial velocity 2.97 m/h

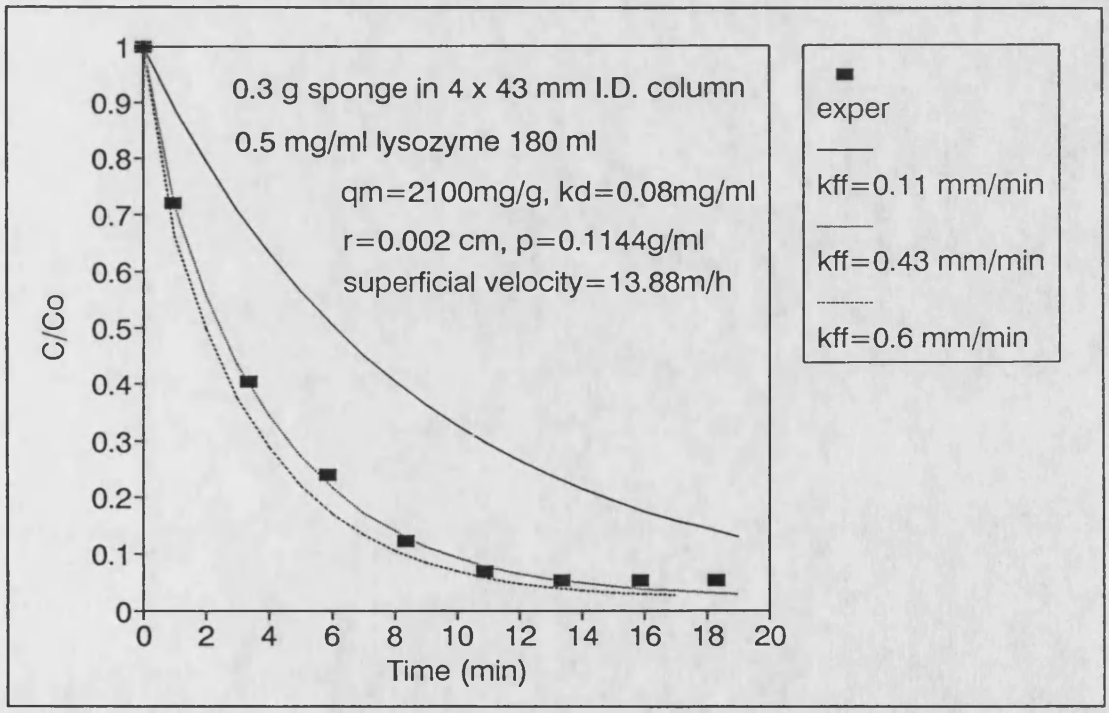

Fig. 6.7 Effect of lumped external mass transfer K_{ff} on the adsorption process at the superficial velocity 13.88 m/h

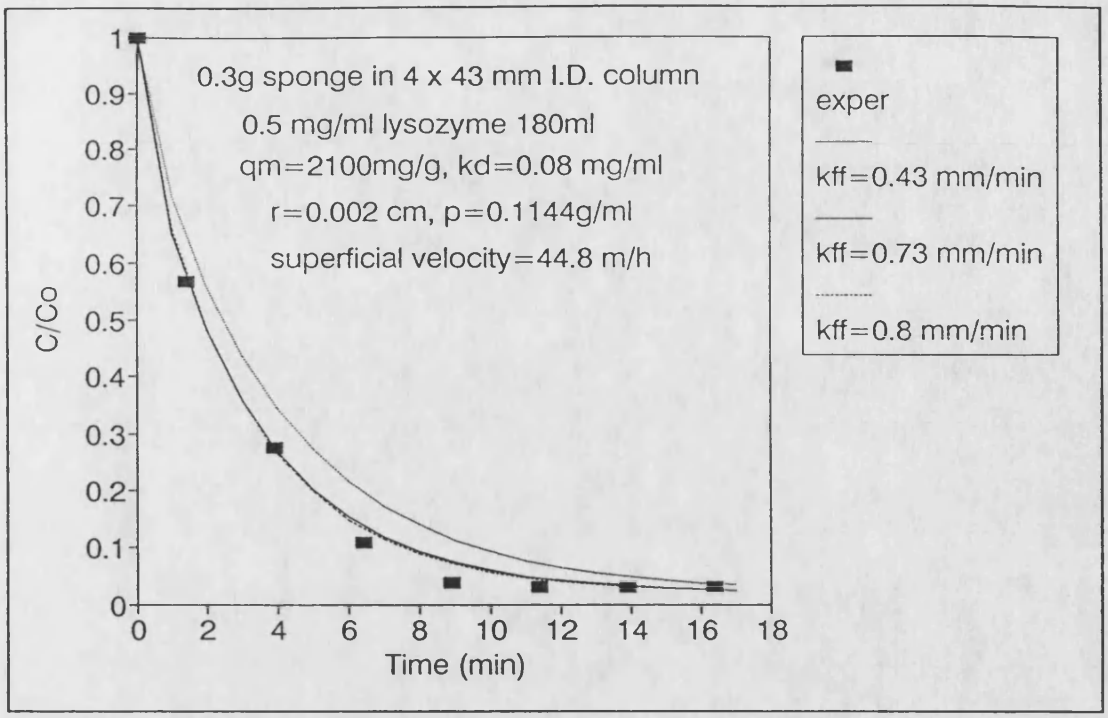

Fig.6.8 Effect of lumped external mass transfer K_{ff} on the adsorption process at the superficial velocity 44.4 m/h

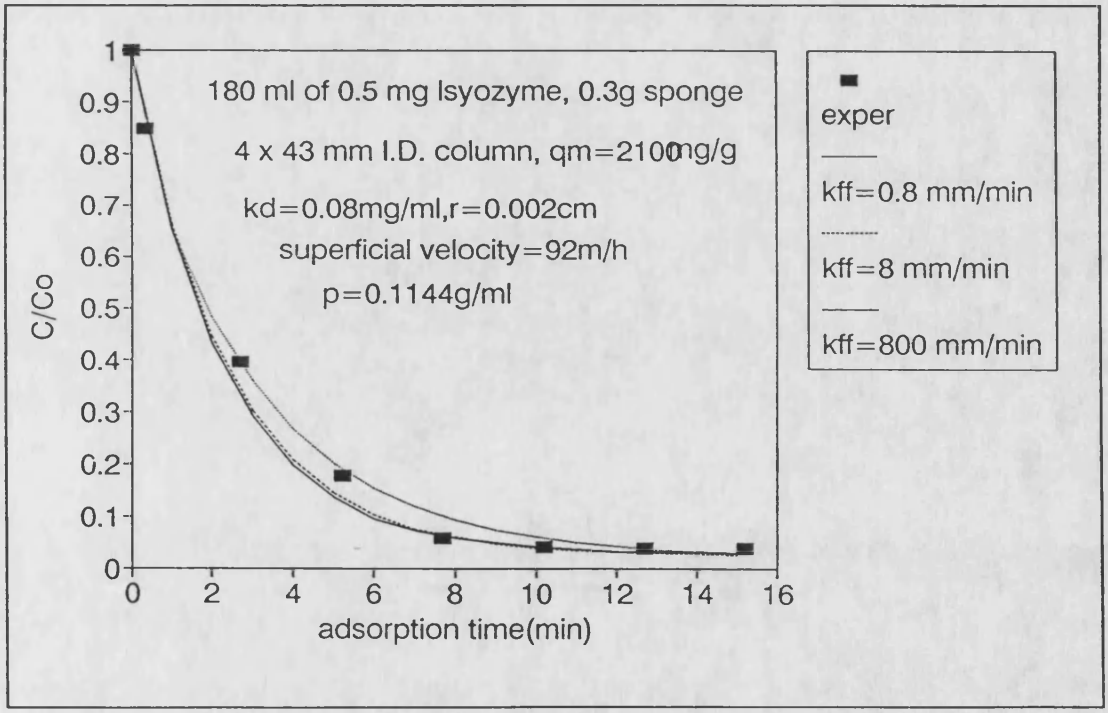

Fig. 6.9 Effect of lumped external mass transfer K_{ff} on the adsorption process at the superficial velocity 92.7 m/h

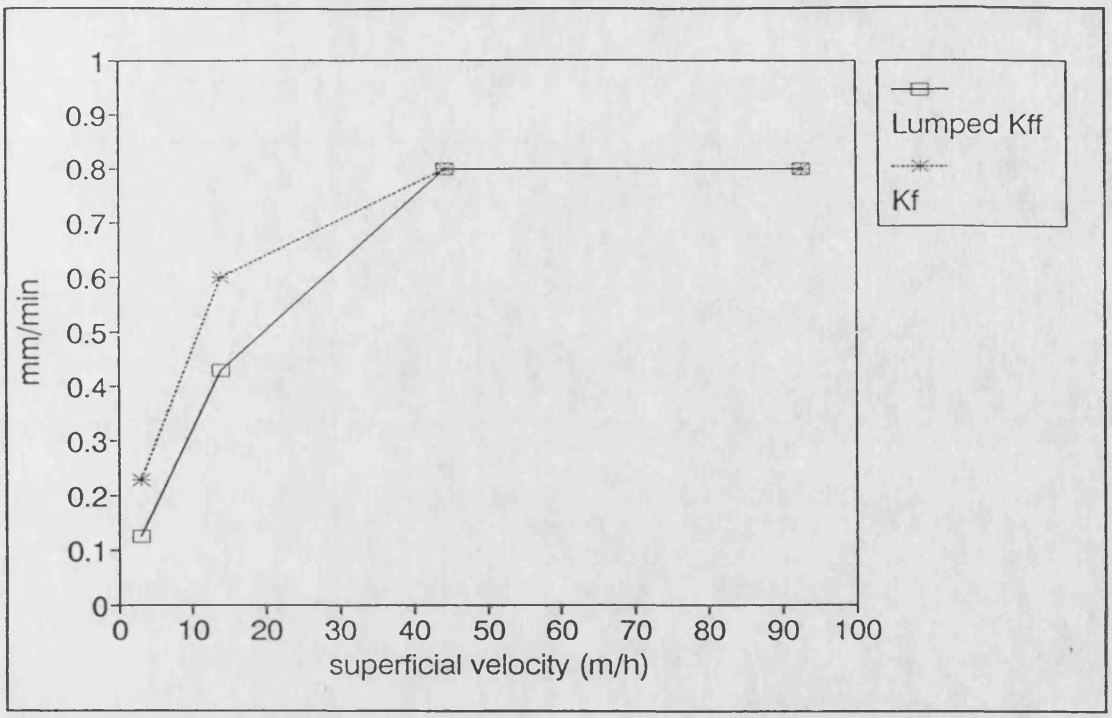

Fig. 6.10 Effect of superficial velocity on the lumped external mass transfer Kff and external mass transfer Kf

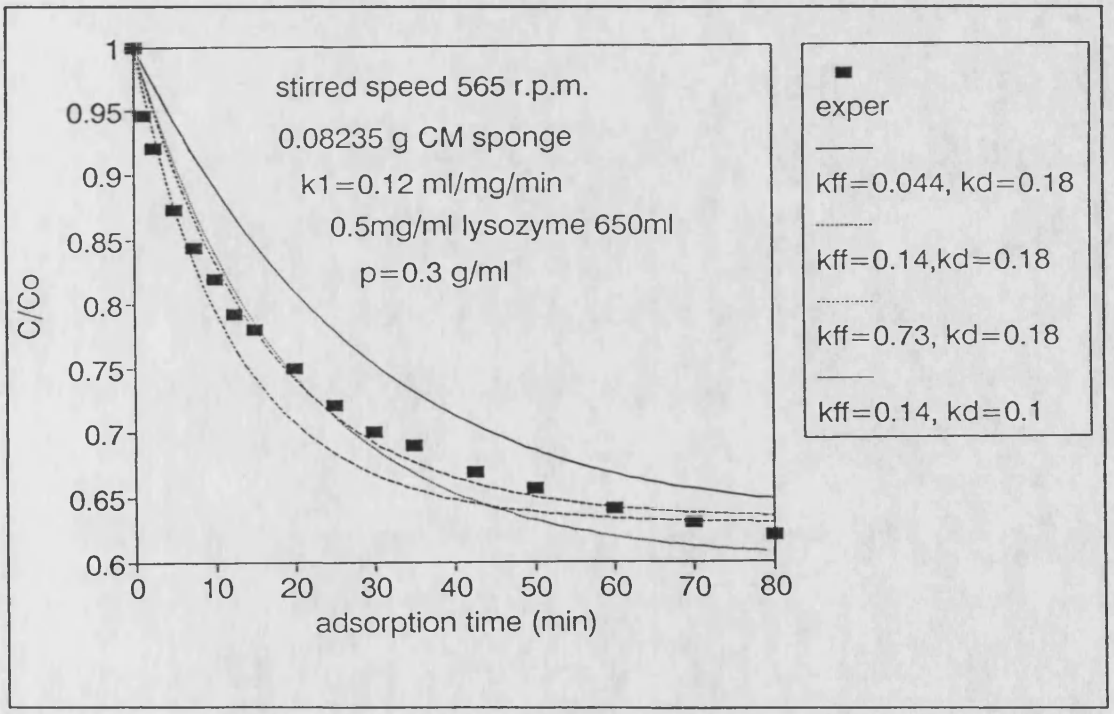

Fig. 6.11 Effect of Lumped external mass transfer K_{ff} and lumped K_d on the stirred vessel adsorption at 565 r.p.m

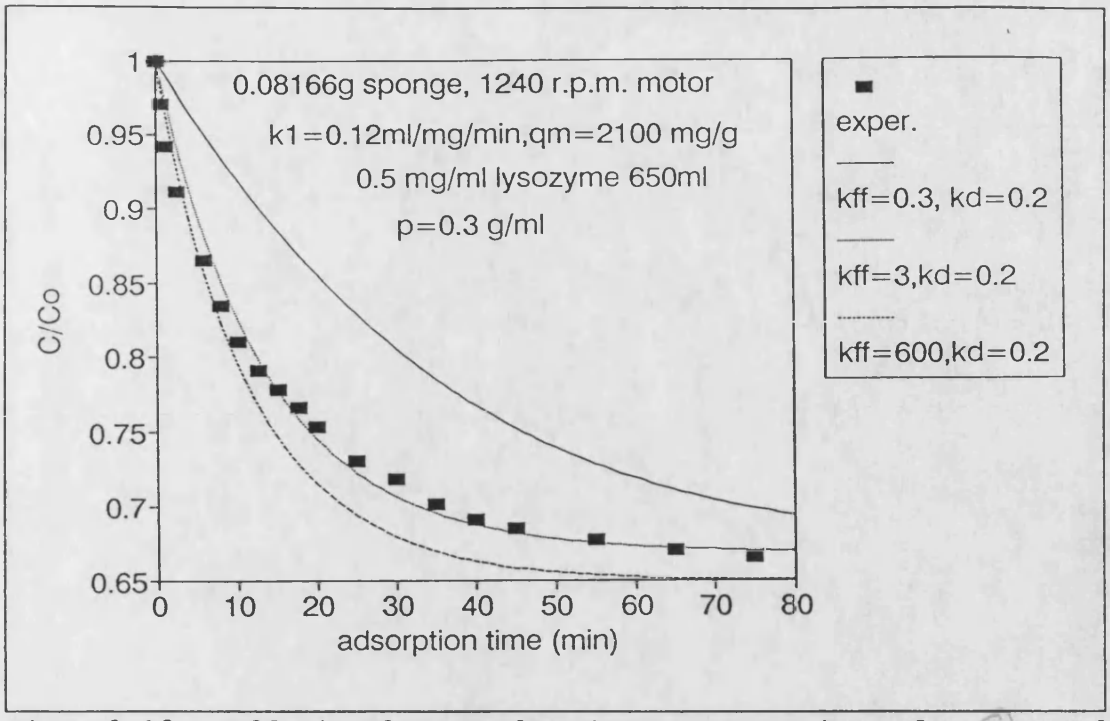

Fig. 6.12 Effect of lumped external mass transfer K_{ff} and lumped K_d on the stirred vessel adsorption at 1240 r.p.m

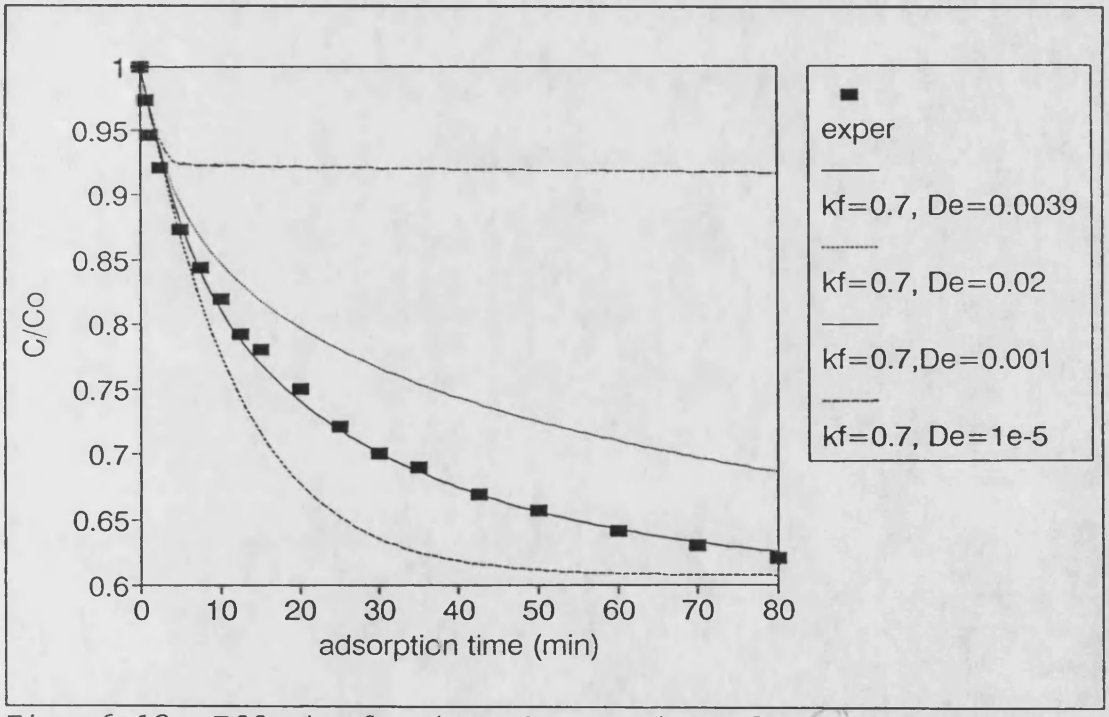

Fig. 6.13 Effect of external mass transfer K_f and effective diffusivity D_e on the stirred vessel adsorption at 565 r.p.m

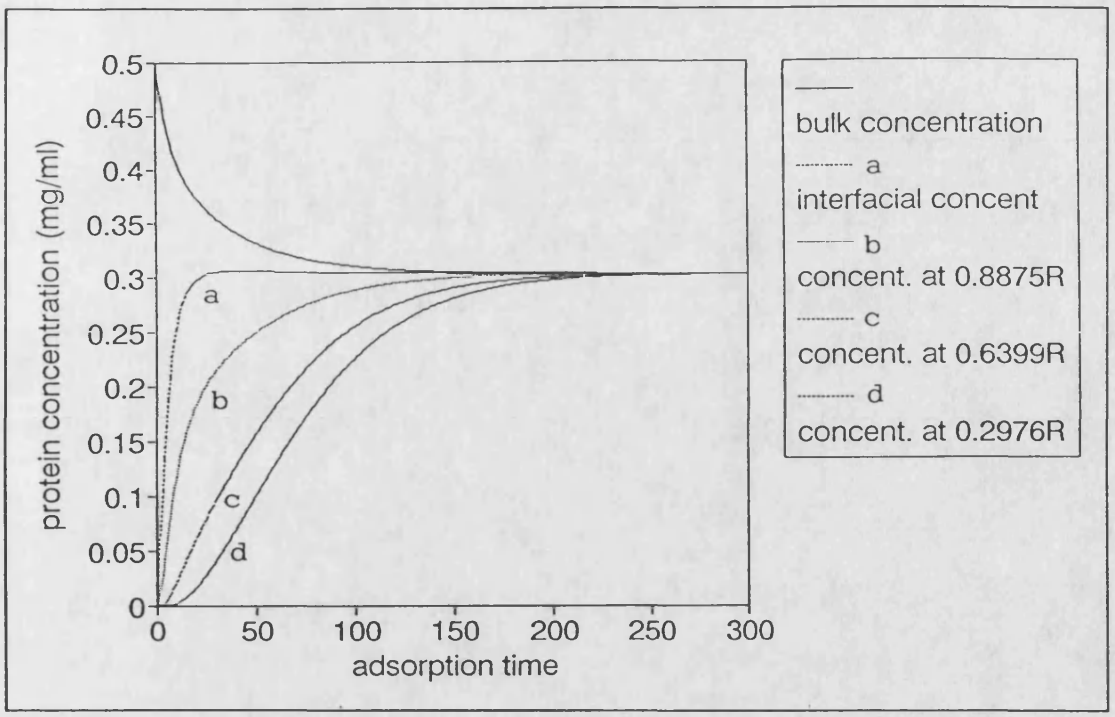

Fig. 6.14 lysozyme concentration various with time at the bulk liquid and liquid phase inside the sponge fibre cylinder

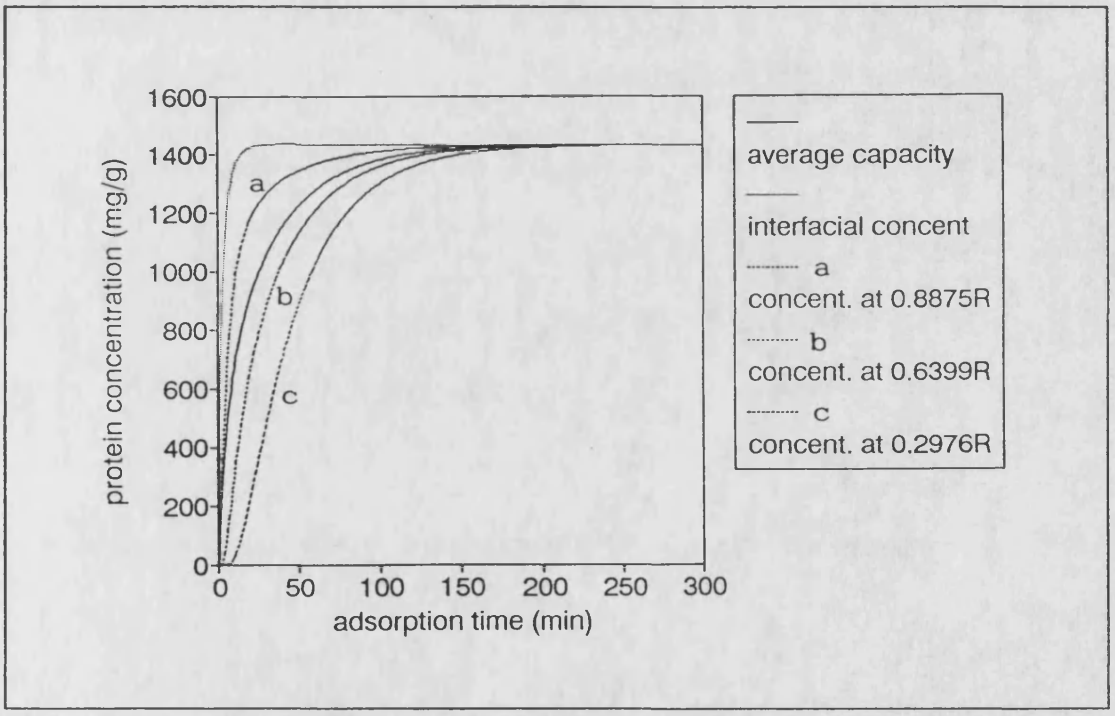

Fig. 6.15 Lysozyme concentration various with time in the solid phase

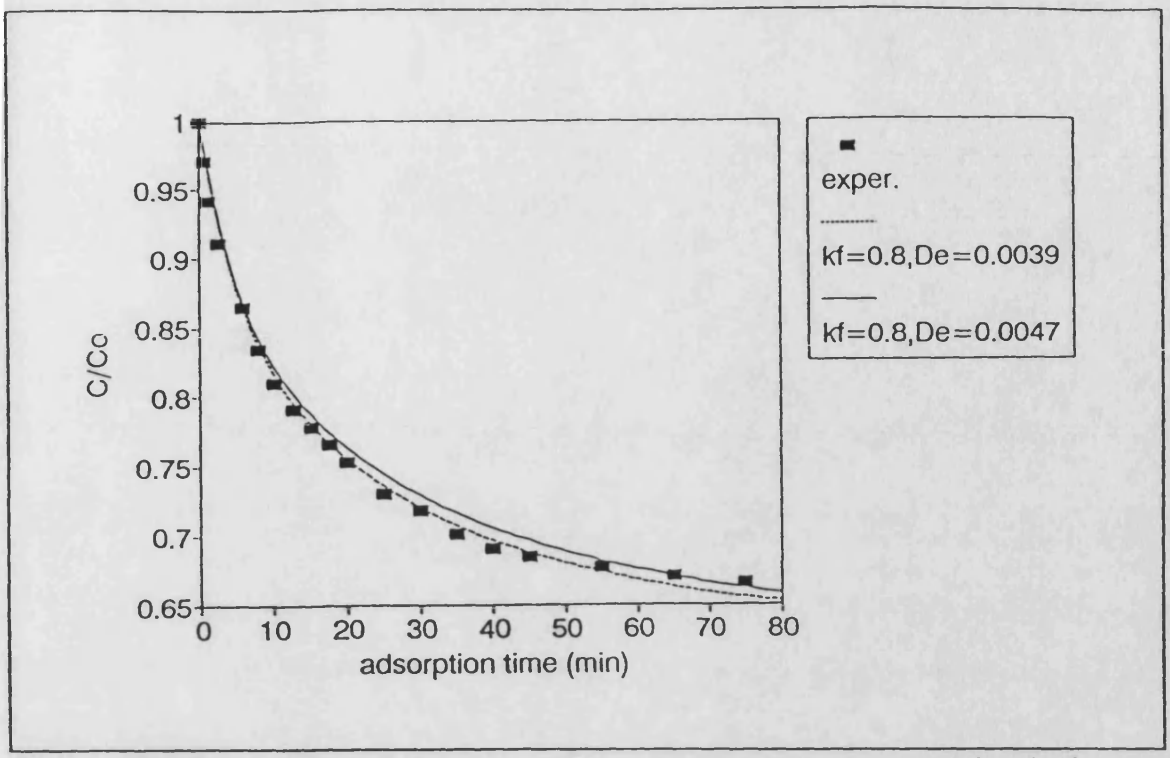

Fig. 6.16 Simulation adsorption curve estimated by heterogeneous model in comparison with experimental data at 1240 r.p.m stirrer speed

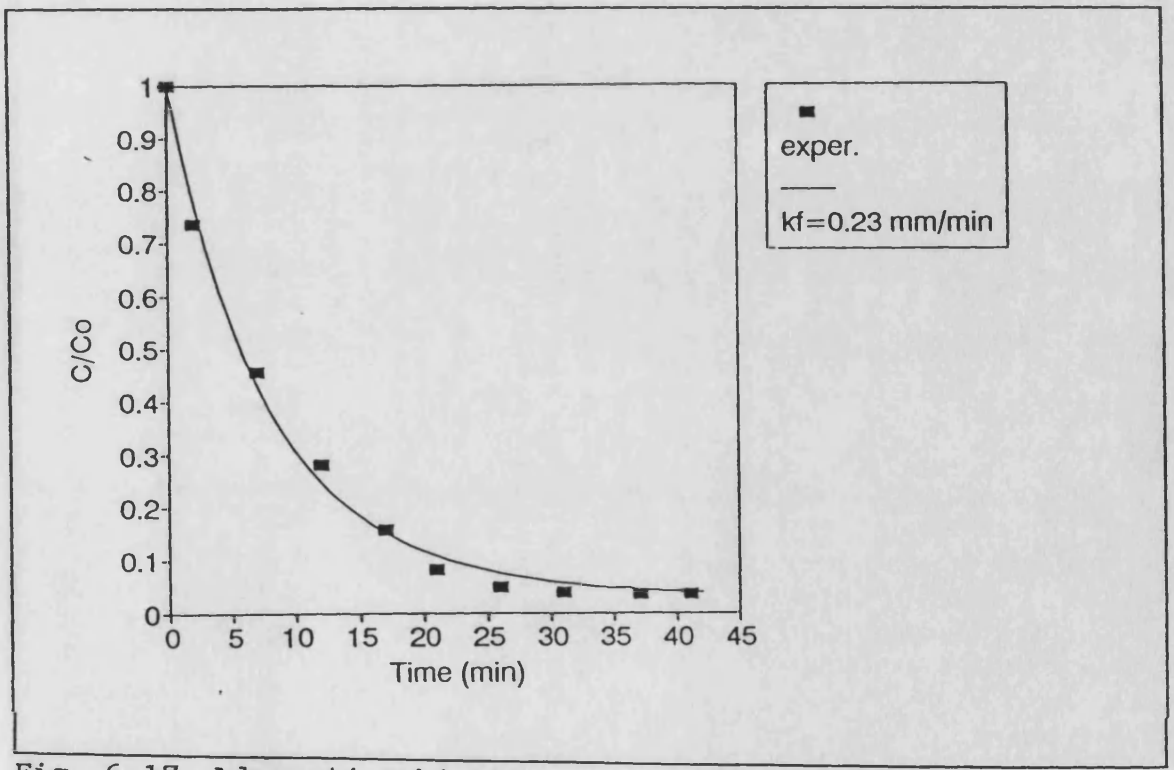

Fig. 6.17 Adsorption kinetics and prediction by $K_{f = 0.23\ mm/min}$ at the superficial velocity 2.97 m/h

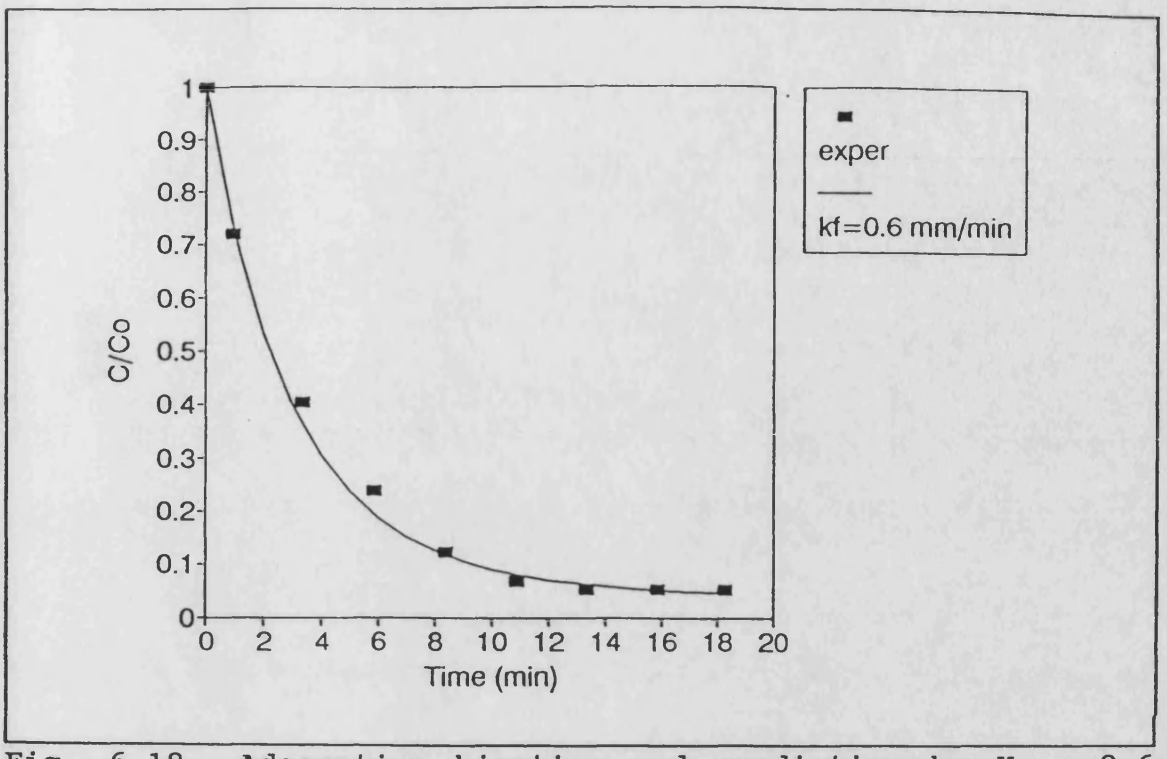

Fig. 6.18 Adsorption kinetics and prediction by K_f = 0.6 mm/min at the superficial velocity 13.88 m/h

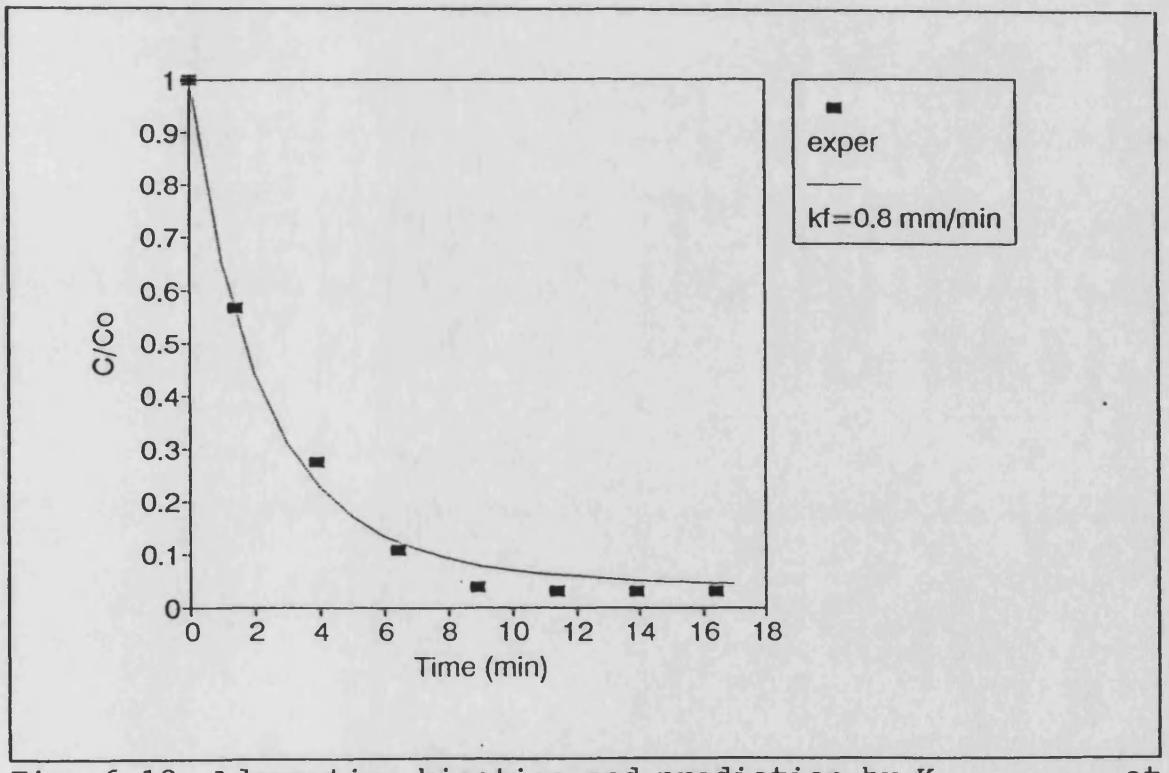

Fig. 6.19 Adsorption kinetics and prediction by $K_{f\ =\ 0.8\ mm/min}$ at superficial velocity 44.44 m/h

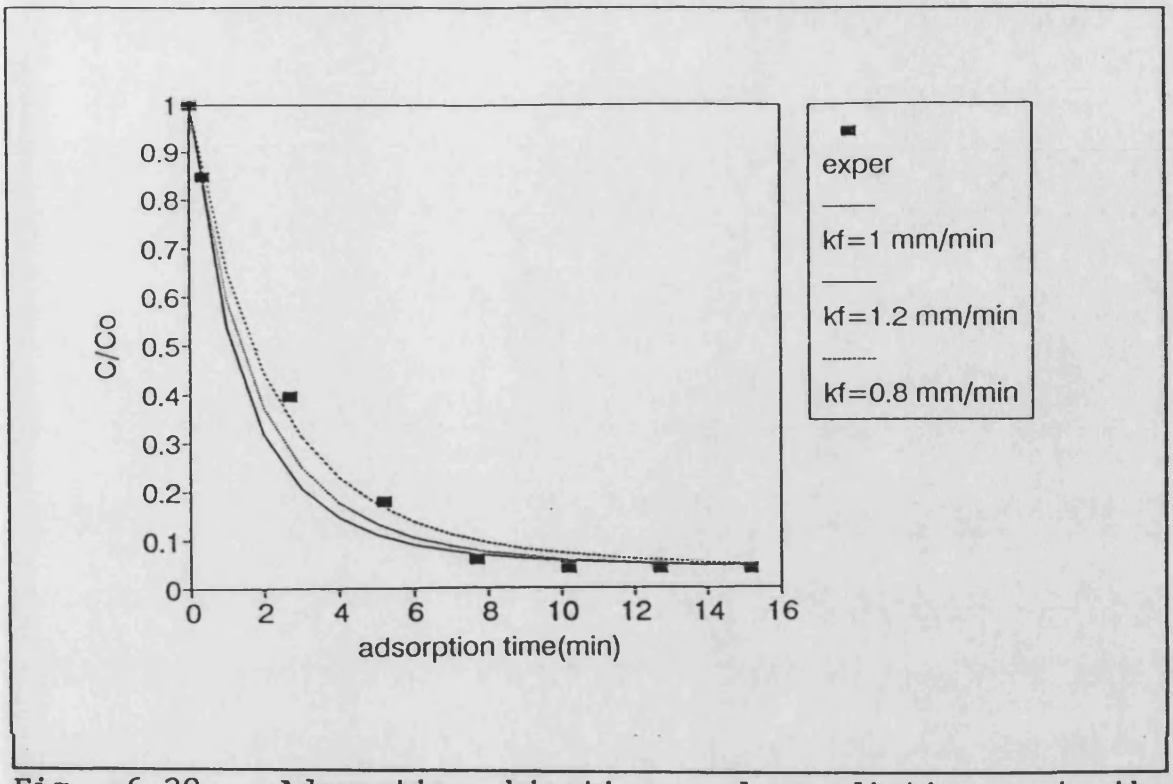

Fig. 6.20 Adsorption kinetics and predictions at the superficial velocity 92.7 m/h

CHAPTER 7

APPLICATION OF CM-HVFM ION-EXCHANGE COLUMN IN THE SEPARATION OF FRESH HEN EGG WHITE PROTEINS

CHAPTER 7

APPLICATION OF CM-HVFM ION-EXCHANGE COLUMN IN THE SEPARATION OF FRESH HEN EGG WHITE PROTEINS

7.1 Introduction

To concentrate or separate a substance of interest from a huge volume of raw solution, flow-rate and feed loading are important factors to be considered. High flow-rate can be beneficial in terms of high productivity, which is defined mass of the separated protein in per unit column volume and time. This design parameter is especially significant to engineers who must consider the process efficiency and cost.

In order to achieve the maximum productivity, control of the feed loading should be optimised. The maximum feed loading should be applied to the system so long as the eluted protein remains of acceptable purity (Regnier and Mazsaroff 1987). Increasing the feed loading can be simply done by increasing the feed volume or the concentration of feed. But this could lead to: (a) a lower specific capacity of the column due to an increase of ionic strength of the feed; (b) higher inlet pressure due to the increase of viscosity of the feed; (c) change of the shape and position of the elution peak due to the hydraulic overloading or concentration overloading (Knox and Pyper 1980); (d) unacceptable resolution due to an increase of the concentration of competitive impurities; (e) column fouling. To avoid these unfavourable possibilities, the ideal ion-exchanger should have

high selectivity, stability, good hydraulic properties, fast kinetics and be robust to cleaning and regenerating procedures. Very few ion-exchanger can meet all the above criteria. The available ion-exchangers either allow high flow-rate but have slow kinetics, or have fast kinetics but allow only slow flow-rate, and they usually swell or shrink when the pH value or ionic strength of the column solution is changed (Fang Ming and Howell 1990 and Janson and Hedman 1987).

The new CM sponge ion-exchanger, CM-HVFM, allows high flow-rates and shows fast kinetics, high protein capacity and is robust to cleaning. This chapter describes its use in a production chromatographic column to examine the effects of feed loading and high flow-rate on the performance of a 250 x 10 mm I.D. column in the separation of fresh hen egg-white protein.

Horn (1980) and Rhodes (1958) used ion-exchange chromatography to analyze egg-white and found that there are at least twelve protein components in hen egg white (Table 7.1). The pI's of eight of them is between 3.9-5.5, and the remainder is between 6.5-11. Among them there are three major proteins which are ovalbumin 65% conalbumin 12% and ovomucoids 13% respectively. Also, there is around 4% of the mixture of lysozyme and avidin.

Table 7.1 Composition of egg-white. (data from Rhodes[7] and Horn[6])

protein	pI	molecular weight	percentage composition
Ovomucoid 1	3.9-4.3	35000	11-13
Ovomucoid 2	3.9-4.3	28000	0.3

Ovalbumin A3	4.75		3.2
Ovalbumin A2	4.65	45000	10.8
Ovalbumin A3	4.58		50.5
Ovoglobulins	5.5-5.8	30-45000	1-1.5
Conalbumin	6.5-6.8	80000	12.4
Conalbumin	6.5-6.8		4.7
Avidin	9.5-10	53000	0.3
Lysozyme	10.7-11.3	14600	0.5-3.5
Globulins			2-3.6

Both anion and cation exchange can be used to separate the egg-white proteins. Levison et al.(1989 and 1990b) applied the anion exchange celluloses, DE 52 and QE 52 (Whatman Biochemical), to separate the major proteins of egg-white from fresh hen egg-white. In their work, fresh egg-white was pretreated by cell debris remover (CDR) first and then adsorbed by the DE 52 or QA 52 cellulose ion-exchanger. In a DE 52 analytical column two main peaks, the conalbumin fraction and the ovalbumin fraction, were separated in the elution curve. If the column loading was increased and also on a production size column, only one peak, crude ovalbumin fraction, was observed using the same elution conditions. The effluent was a mixture of lysozyme and conalbumin. This system processed a productivity, 6.4 $kg/m^3/h$ of total protein (crude ovalbumin and the unseparated lysozyme and conalbumin). Henry (1989) used a analytical column, a weak cation-exchange column of 250 mm x 4.6 mm I.D. packed with 5 micro BAKERBOND WP-CBX to separate the crude hen egg-white. Two main peaks, the conalbumin fraction and the lysozyme fraction, were separated using linear gradient elution.

7.2 Material and Methods

A 300 x 10 mm I.D. adjustable glass column (Amicon Ltd., Stonehouse, U.K.) packed with 1.775 g (dry weight) CM-HVFM (Batch B10) provided by BPS (Biotechnology Process Services, Mountjoy Research Centre, Durham University, U.K.) and adjusted to a length of 250 mm giving a packed volume of 19.625 ml. A fine nylon mash filter was set in the inlet of the column which had an inlet pressure of less than 0.9 bar. A simple device with two stirred vessels of equal cross-sectional area was used as a

gradient maker.

A peristaltic pump (Watson-Marlow Ltd., Falmouth Cornwall TR11 4 RU, U.K.) was used to pump the feed solution.

Individual protein standards were lysozyme (from hen egg white, 36368 u/mg) purchased from Fluka Chemika-Biochemika (Buchs, Switzerland), Conalbumin (from chicken egg white, electrophoretic purity 98%, Type IV) and ovalbumin (from chicken egg, electrophoretic purity, approx. 99% Grade V) purchased from Sigma Chemical Co. Ltd. (Sigma Chemical Co. Ltd., Poole, Doset, U.K.). In addition a high molecular weight standard mixture, a mixture of bovine albumin (MW 66000), eggalbumin (MW 45000). carbonic anhydrase (MW 29000), phosphorylase b (MW 974000), beta-galactosidase (MW 116000) and myosin (MW 205000) was purchased from Sigma Chem. Co. and used as a standard for gel electrophoresis.

Sodium dodecylsulfate-polyacrylamide gel electrophoresis (SDS-PAGE) was done according to the process described by Hames (1986) and proteins were stained with Coomassie brilliant blue.

An LKB Unicord II monitor (LKB-Produkter AB, Bromma, Sweden) was used on-line at 280 nm to detect the effluent protein concentration from the column.The pooled fractions obtained at various stages of the chromatography were assayed for protein concentration using A 280 nm in a Ultraviolet Spectrophotometer (Cecil Instruments Cop., Cambridge, U.K.) measured against a standard solution of ovalbumin (Levison et.al 1989 and 1990).

The whites of size 4 eggs (Thames Valley eggs, Lambourn Woodiands, Royal Berkshire, U.K.) were separated and diluted with pH 4.8 of 0.02 M sodium acetate buffer to give a 14% suspension of protein. The pH was adjusted to 4.8 . The suspension was settled at 4 C overnight and the supernatant liquid was collected by centrifuging (Koolspin centrifuge, Biotech Instruments Ltd., Luton, Beds, U.K.) at 4000 rpm for 5 min. or filtering with

Whatman 54 filter paper (Whatman Ltd., Maidstone, U.K.). The clear solution of egg-white was readjusted to pH 4.8 before being used. The protein concentration of this clear egg-white solution was about 20 g/l and the conductivity was around 3 ms/cm. 0.01 M sodium acetate buffer, pH 4.8 was used to dilute the egg white solution when necessary, and also for washing the column.

The column was washed and equilibrated with pH 4.8 of 0.01 M sodium acetate buffer before adsorption. The egg-white protein solution was pumped through the column, then the column was washed by 2 bed volumes of starting buffer and the adsorbed proteins were eluted by a gradient up to a 1:1 mixture of 0.6 M NaCl and 0.01 M sodium acetate buffer, pH 4.8. An 0.5 M NaOH solution was used to regenerate the column for 40 minutes.

The resolution for the gradient eluted lysozyme and conalbumin was calculated as follows:

$$R=\frac{(T_1-T_c)}{\frac{1}{2}(W_1+W_c)}$$

where T_1, W_1 and T_c, W_c are the lysozyme retention time, peak width at base, and conalbumin retention time, peak width at base respectively.

The productivity was calculated as the amount of recovered protein divided by the column volume, and the total time taken for feeding, washing and elution.

The number of theoretical plates was calculated by the graphical method of Barber and Carrr (1981) which was a practical technique for estimating the tailed chromatographic peaks. It was only used to indicate whether the column's kinetic performance was significantly degraded (Bidlingmeyer and Warren 1984) by loading and high flow-rate.

7.3 Results and Discussion

7.3.1 Effect of Feed Loading on The Resolution And Productivity

A fixed of superficial velocity of 6.12 m/h was used throughout this section. The inlet pressure of column was always less than 0.6 bar. Fig.7.1 shows the total capacity of column when progressively loaded with 20.31 g/l and 13.64 g/l egg-white solutions, respectively. It can be seen that the column dynamic capacity, i.e. the capacity under real working conditions, in both cases linearly increasing with the total feed load (Fig.7.1).

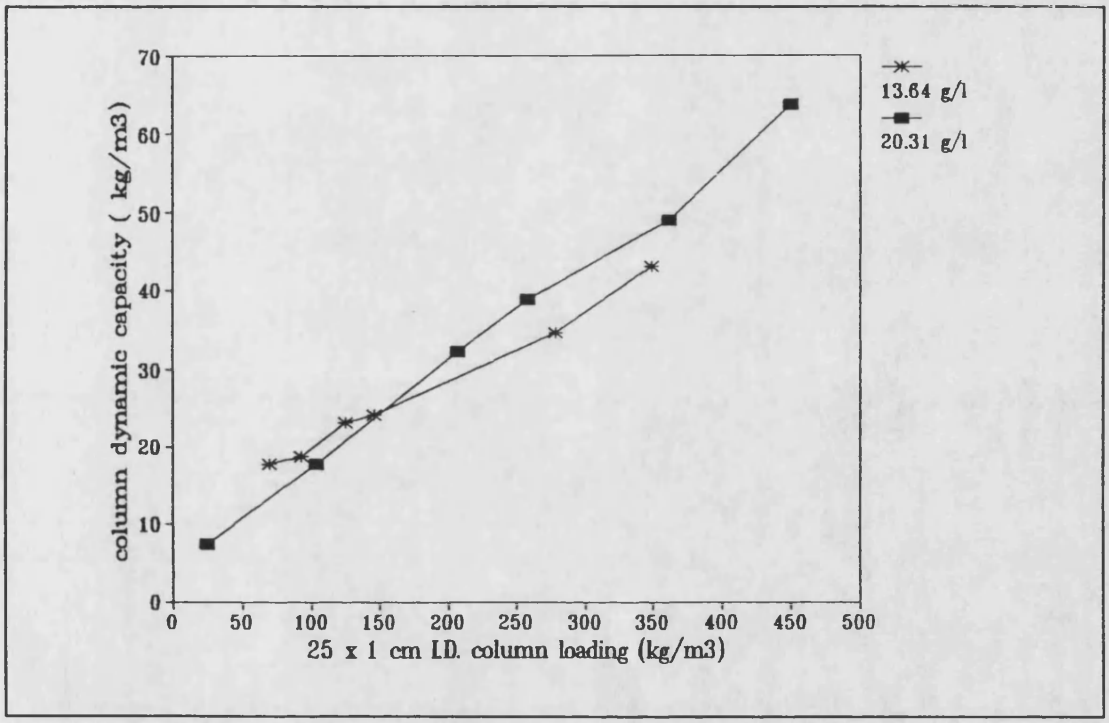

Fig. 7.1 Effect of concentration loading on the column dynamic capacity

There are some differences between these two cases due possibly to the ionic strength of the feed. Below a loading of 150 kg/m^3 protein on the column a high dynamic capacity and was reached with lower feed concentration (13.64 kg/m^3).This is possibly because it had a lower ionic concentration than the higher feed concentration (2.15 ms/cm vs 3.3 ms/cm). Above a loading of 150 kg/m^3 the higher feed concentration gave the higher dynamic capacity. The remaining results through Fig.7.1

to 7.4 were obtained for a feed concentration of 20.31 g/l.

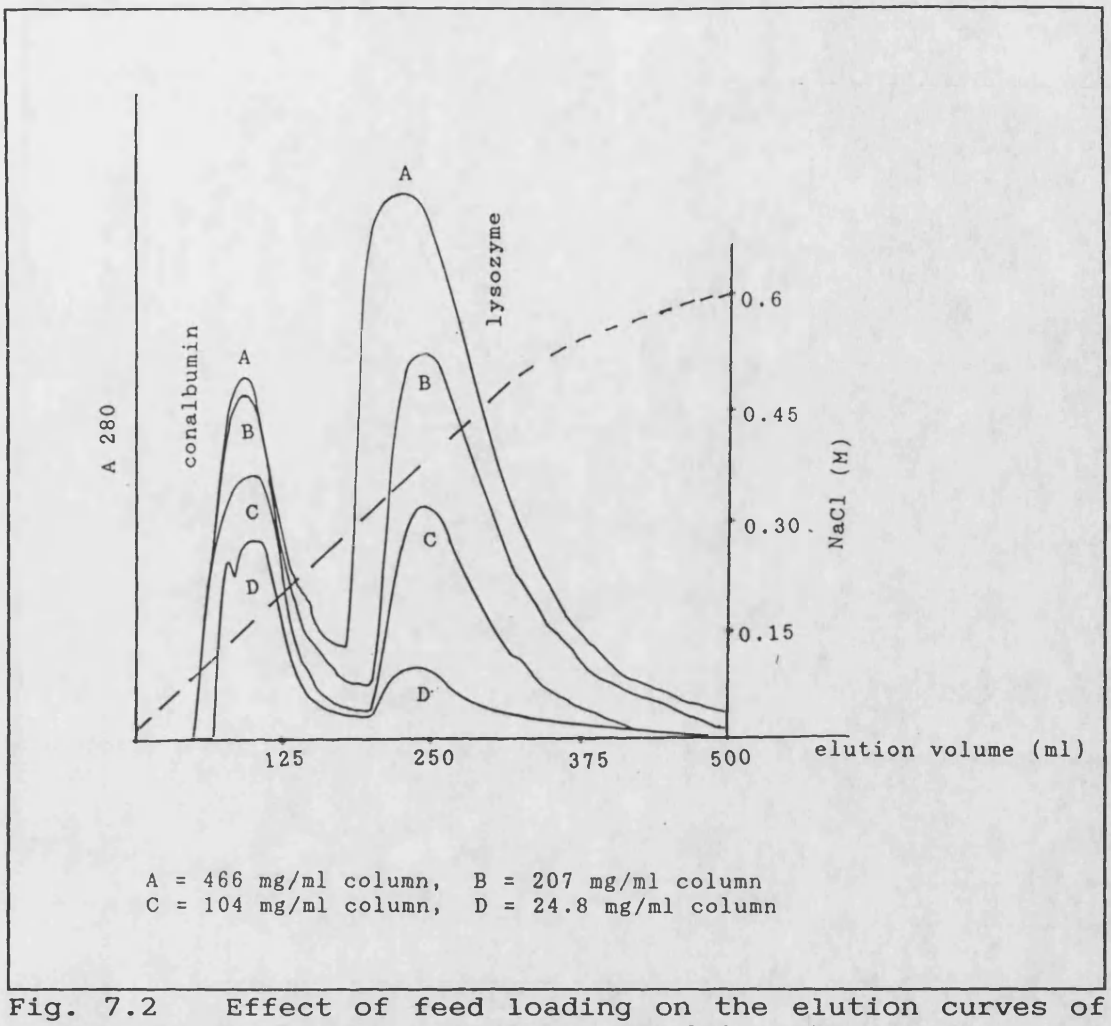

Fig. 7.2 Effect of feed loading on the elution curves of conalbumin and lysozyme fraction. The 250 x 100 mm I.D. column was fed by various volumes of 20.34 mg/ml egg-white solution.

Fig.7.2 indicates that for the elution curves of the conalbumin and lysozyme fraction the shape and position of the peaks are not affected by increasing the column loading. The CM-HVFM column was not blocked or channelled despite the high column loading and high flow-rate. The eluted lysozyme was directly proportional to the column loading, although the eluted conalbumin tended to a constant value. Even at these high column loadings and flow-rates, the peak resolution was only slightly degraded. As the relative amount of conalbumin eluted decreases the percentage of that protein in the non-adsorbed ovalbumin

fraction increases.

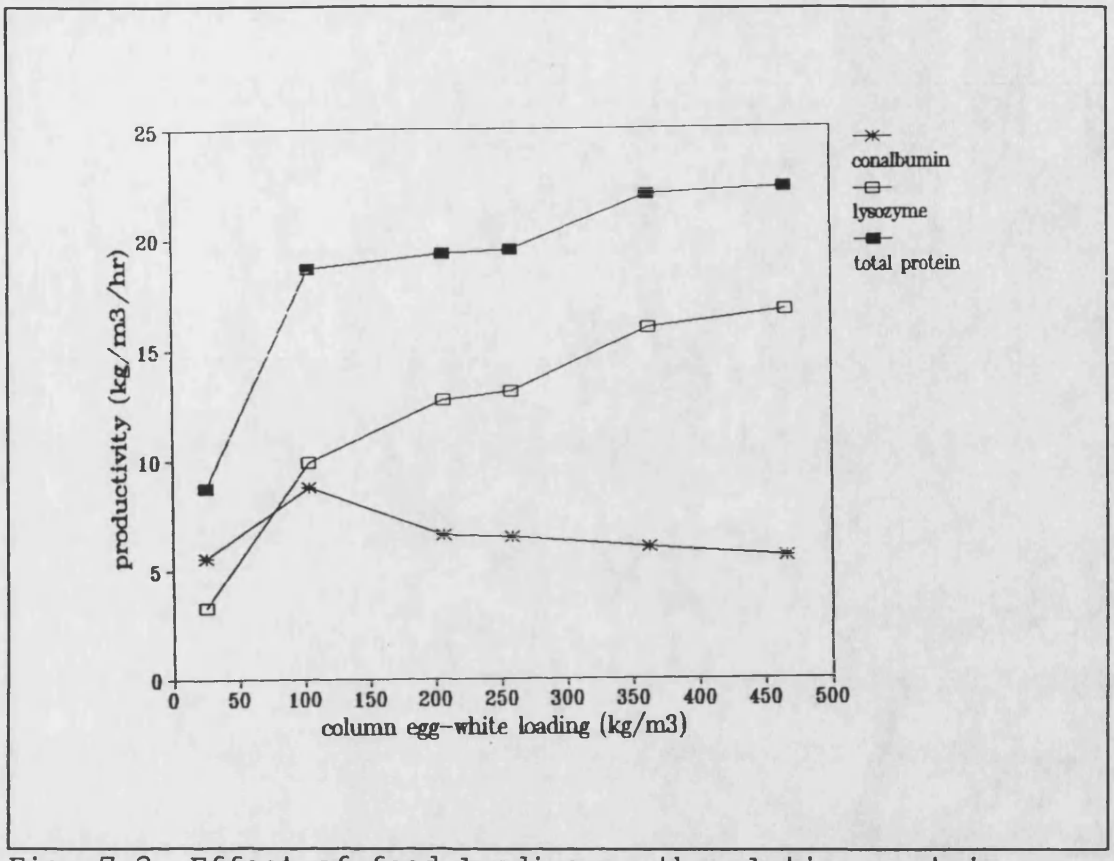

Fig. 7.3 Effect of feed loading on the elution protein productivity

The individual productivities of lysozyme and conalbumin are shown in the Fig. 7.3. The productivity of lysozyme increases with column loading up to 16.7 kg/m^3/h, whilst that of conalbumin increases to a maximum and then slightly decreases to 6 kg/m^3/h. As process time increases linearly with column loading, and the eluted conalbumin concentration, soon reaches a maximum value, the ratio of these quantities or productivity of conalbumin decrease once the maximum has been reached.

It is illustrated in Fig. 7.4 that the number of theoretical plates in the lysozyme and conalbumin fractions decreases with increasing column loading. The resolution between the conalbumin fraction and the lysozyme fraction is also decreased. The minimum number of theoretical plates required for resolution can only

be determined empirically by relating it to the purity of the separated protein.

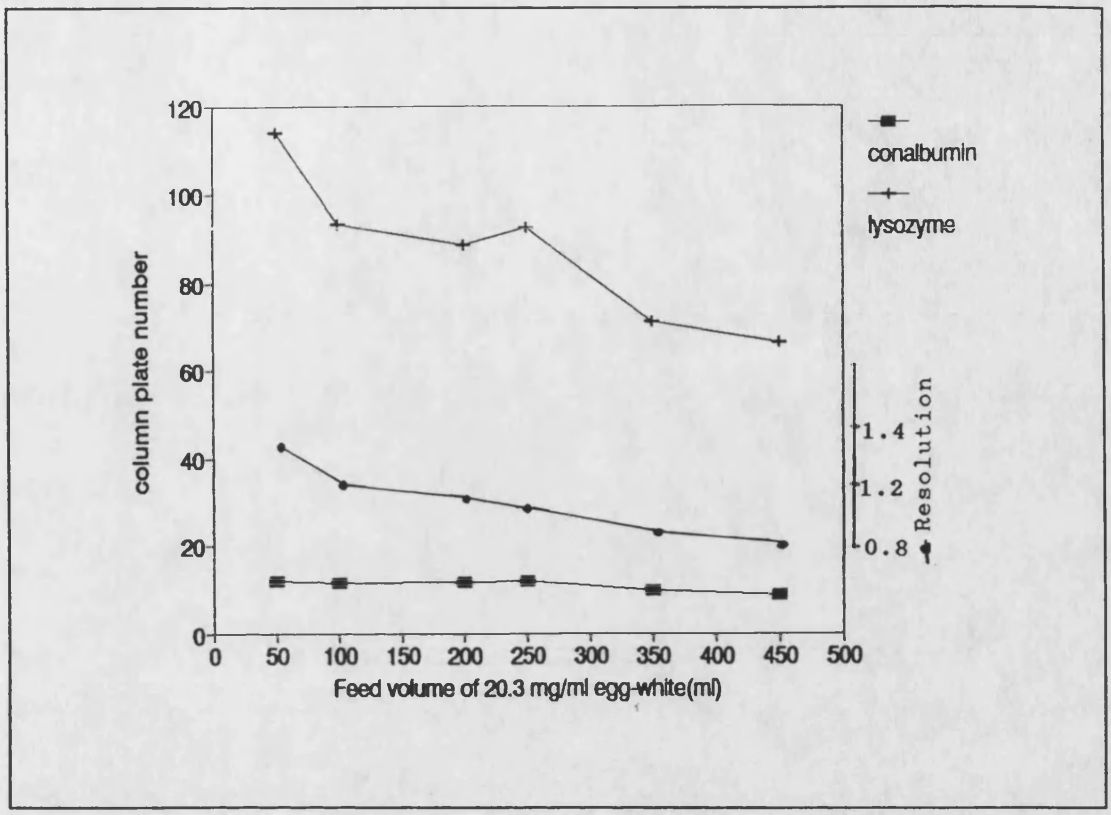

Fig. 7.4 Effect of feed loading on the resolution and column plate number

The three fraction obtained were subjected to 12.5% SDS-PAGE (Fig.7.5). Track 7 is that of the marker standard. Track 6 is the feed, egg-white solution. The first major band from the top is the conalbumin, the second major band the ovalbumin, and the major band at the bottom the lysozyme. Track 5 and 4 are the eluted conalbumin and lysozyme fractions respectively at the maximum column loading of 450 kg/m^3. These can be compared with tracks 3 and 2, Sigma's conalbumin and Fluka's lysozyme respectively. The eluted conalbumin fraction and lysozyme fraction have been separated from each other at a resolution of 0.8 (Fig. 7.4). There is no visible lysozyme band in the eluted conalbumin fraction although there is an indistinct conalbumin band in the eluted lysozyme. A resolution of 0.8 could be considered as the practical value to be used in the first step

of egg-white protein separation. Track 1 is the effluent, ovalbumin fraction, at a column loading of 80 kg/m^3. Conalbumin appears in the effluent and this increases when column loading is increased.

7.3.2 Effect of High Flow-Rate On The Kinetic Performance and Productivity

In order to compare the kinetic behaviour of adsorption at the different flow-rates, 180 ml of 13.64 mg/ml egg-white solution (column loading of 125 mg/ml), was cyclically pumped through the column at superficial velocities from 3.10 to 9.17 m/h for 1 hour. The results are shown in Fig. 7.6. The adsorption process increased with superficial velocity. The adsorption curves tend to rise slowly after having rapidly reached 55% of the total adsorbed protein. At a superficial velocity of 6.11 m/h, the adsorption process is much faster than that at 3.11 m/h. The adsorption process, however, is not dramatically faster by following further increase the superficial velocity to 9.17 m/h. It appears that the superficial velocity above 6.11 m/h, that is flow-rate of 8 ml/min, is no longer the main limiting factor for the adsorption process. It also can be seen from Fig. 7.6 that the pH value is smoothly decreased to around 4.65 during the adsorption processes.

The decreasing pH value (average) might be the cause of some protein such as ovalbumin 1 and 2 whose pI are around 4.7 (Table 7.1) being only gradually adsorbed. This may be the cause of the long tail in the adsorption process. At the pH 4.8 the adsorbable proteins are approximately 20% according to Table 7.1. This implies a column dynamic capacity of around 25 mg/ml at the column loading of 125 mg/ml, *i.e.* 78% of total adsorbed proteins being adsorbed at a superficial velocity of 9.17 m/h

The influence of flow-rate on the elution curve of the column is indicated in Fig. 7.7. The elution curves of the conalbumin and lysozyme fraction, the shape and position of the peaks, are not affected by increasing superficial velocities from

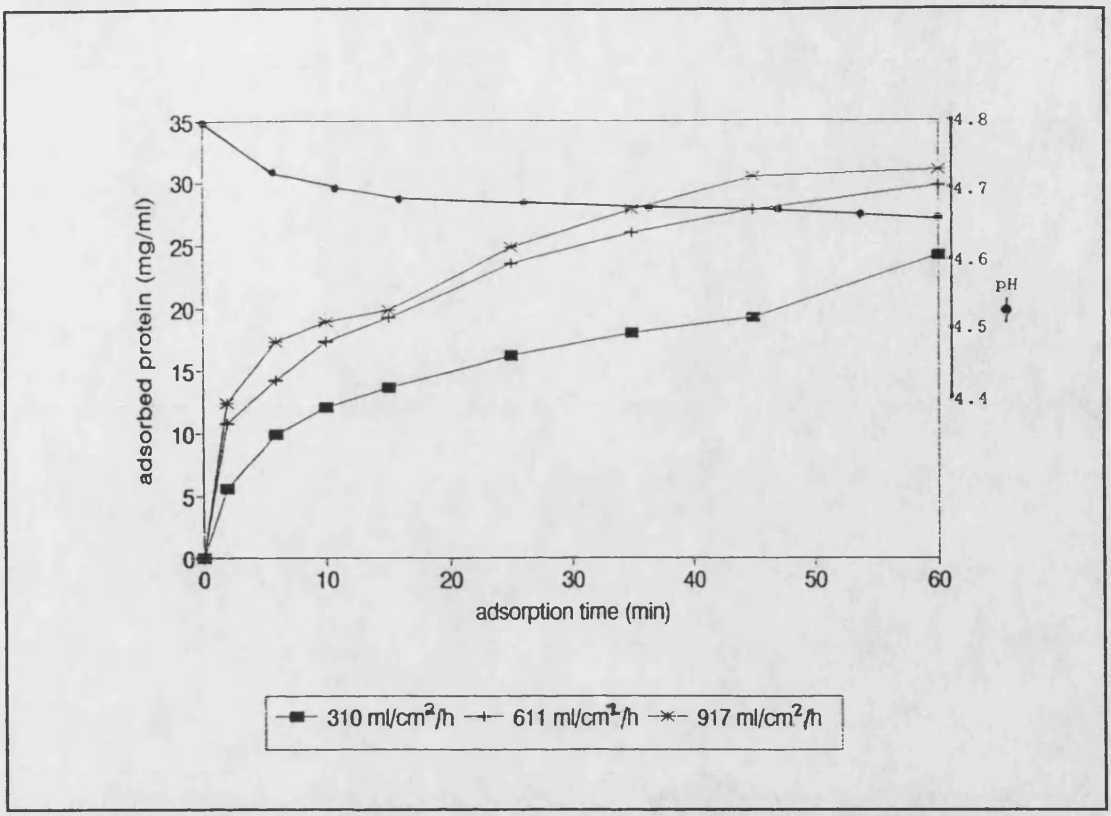

Fig. 7.6 Effect of superficial velocity on the adsorption kinetic process

3.11 to 9.17 m/h. The 250 x 10 mm I.D. CM-HVFM column was not blocked and channelled, nor was the column's kinetic performance degraded despite the high column loading and high flow-rate. There are two peaks in the conalbumin fraction (Fig. 7.7 and 7.10), which are considered to be identical in gel electrophoresis (track 11 and 12 in Fig.7.5) although the sample in the track 11 was overloaded. Rhodes (1958) mentioned that these unidentified conalbumins can give separate peaks depending upon the ionic strength and cationic composition of the buffer.

Fig. 7.8 illustrates that with increasing superficial velocity the number of theoretical plates in the lysozyme fraction is decreased to 88, whilst that in conalbumin fraction is enhanced. The resolution decreases to 1.1 with the increased flow-rate. There is no data on the criteria for resolution and number of theoretical plates to judge the performance of production ion-exchange chromatography, but these factors could

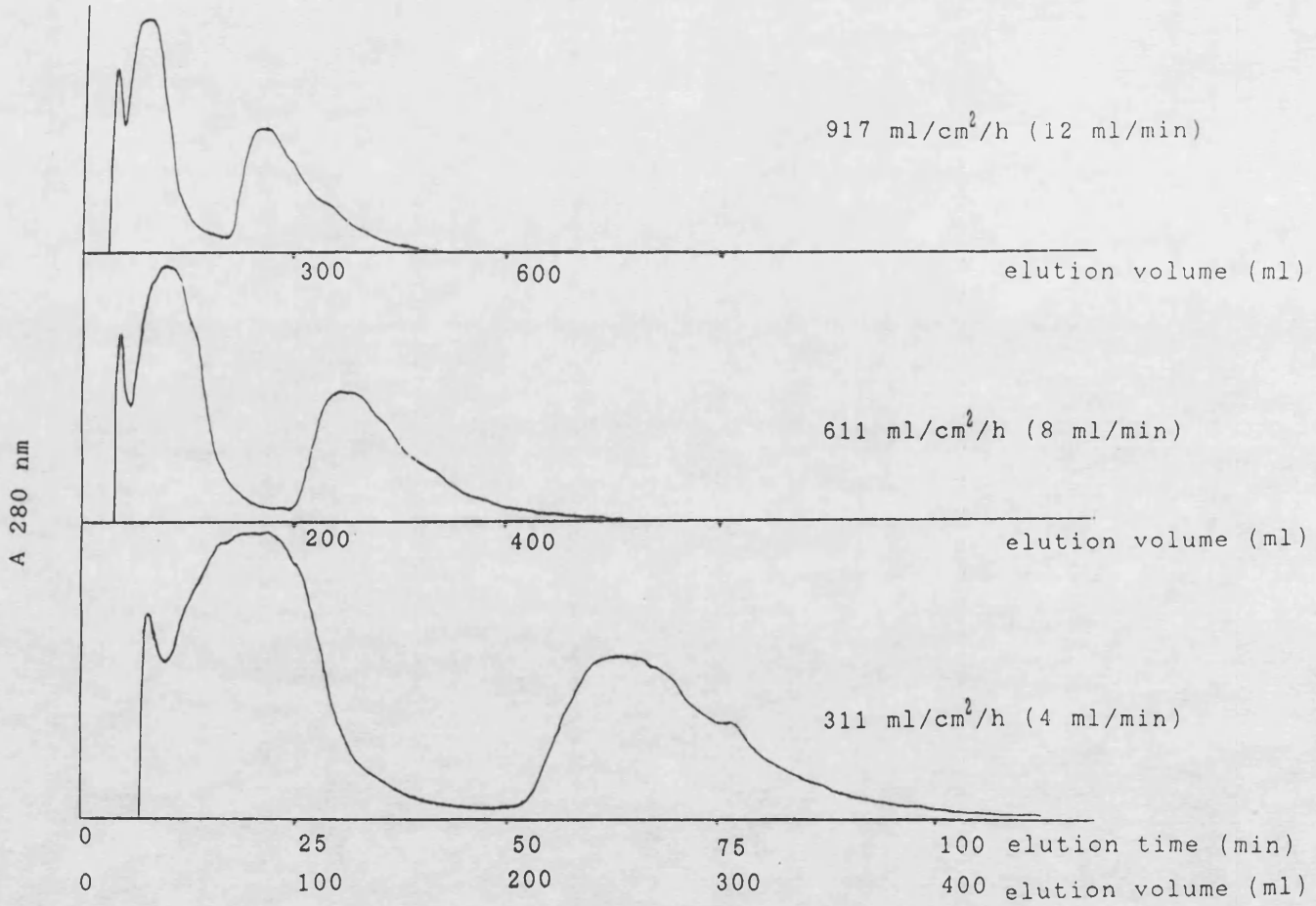

Fig.7.7 Effect of high flow-rate on the elution curves of conalbumin and lysozyme in a 250 x 10 mm I.D. CM-HVFM column. Gradient elution by 250 ml of 0.6 M NaCl and 250 ml of 0.01 M NaAc buffer, pH 4.8.

indicate a tendency. As long as the purity of the separated protein is acceptable, then that is minimum number of theoretical plates and the minimum resolution.

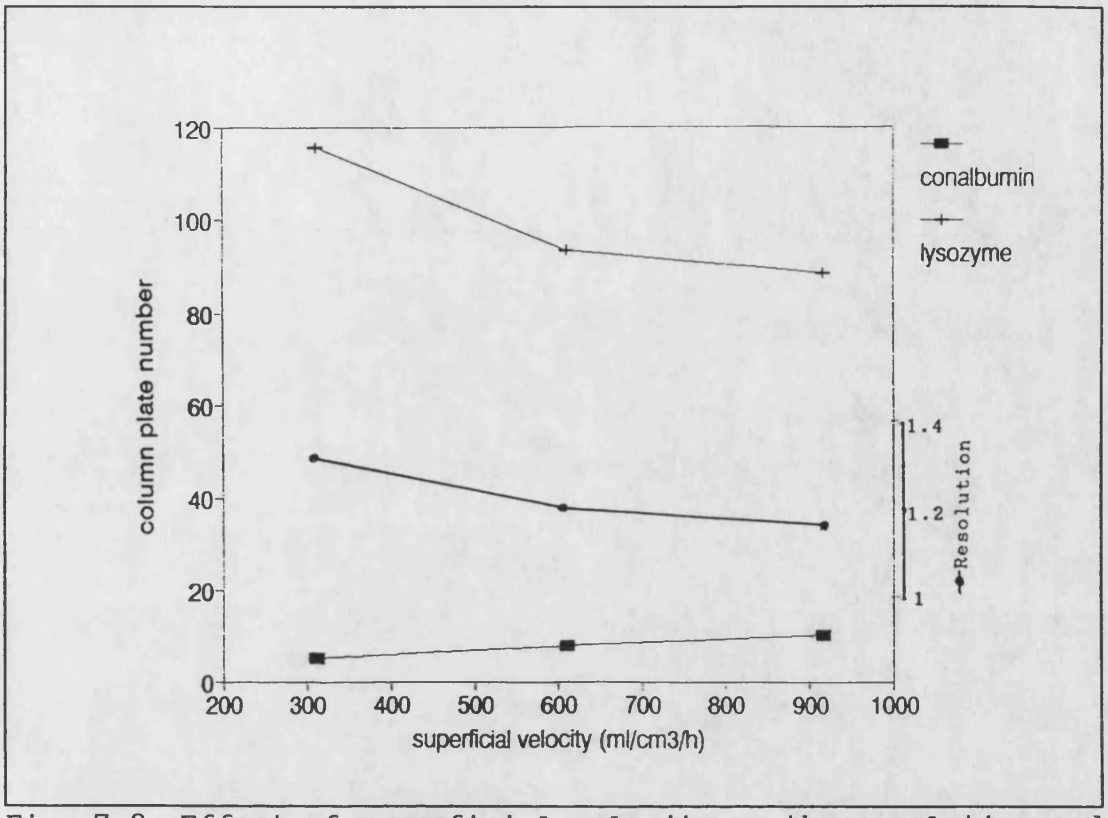

Fig. 7.8 Effect of superficial velocity on the resolution and column plate number

Nevertheless high flow-rate can be beneficial as it gives high productivity, although the protein recovery is slightly decreased, as shown in Fig. 7.9.

Taking the flow-rate, kinetic processes of adsorption and desorption, resolution and productivity into account, a sub-optimum separation process, whose protein recovery and productivity are 97% and 87.36 $kg/m^3/h$ respectively, has been developed and is shown in Fig. 7.10. The column was fed 130 ml of 14 mg/ml fresh egg-white solution (pH 4.8 and ionic concentration of 2.3 ms/cm) which was cycled through the column for 18 minutes. It was then washed with 0.01 M sodium acetate buffer (pH 4.8) for 3 minutes. A gradient elution using 250 ml

of 0.6 M NaoH and 250 ml of 0.01 M sodium acetate buffer, pH 4.8, was followed washing. A superficial velocity of 9.17 m/h (flow-rate of 12 ml/min) was applied throughout the whole process.

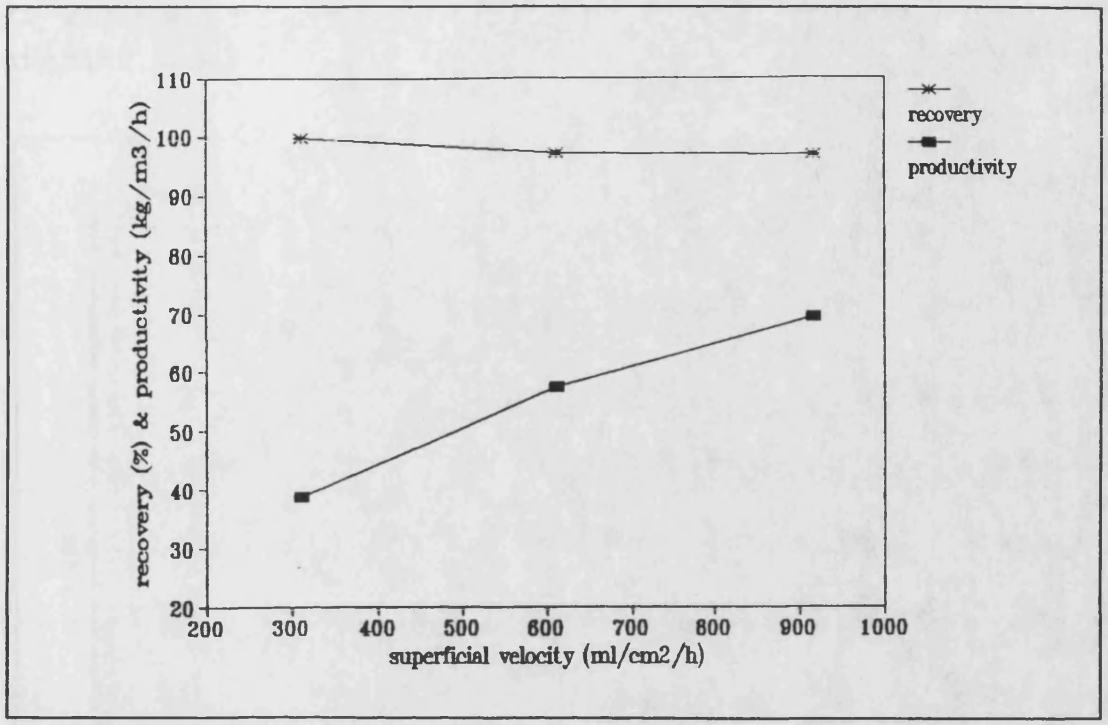

Fig. 7.9 Effect of superficial velocity on the protein recovery and productivity

The purities of lysozyme, conalbumin and ovalbumin are shown in Fig.7.5 (end of this chapter). Track 9 is for the column feed, in which the first major band from the top is conalbumin; the second major band is ovalbumin and the major band at the bottom is the lysozyme. Track 3, 8 and 2 are of the reference proteins, Sigma's conalbumin, Sigma's ovalbumin and Fluka's lysozyme respectively. The high molecular weight standards are in track 7 and 14. One can see that there is only an indistinct second band in the eluted lysozyme (track 13). The eluted conalbumin (track 11 and 12) identifies almost exactly with Sigma's conalbumin. There is however a conalbumin band in the effluent ovalbumin (track 10).

7.4 Conclusion

A production size CM-HVFM column can easily separate egg-

white into three crude fractions of mainly ovalbumin. lysozyme and conalbumin at a column loading of up to 450 kg/m^3. Process times overall are short enough to give high overall productivity. With all three fractions desired it is better to load at 13.64 g/l protein at up to 150 kg/m^3. When only lysozyme is of real a interest loading of 20.31 g/l protein at 450 kg/m^3 is preferred.

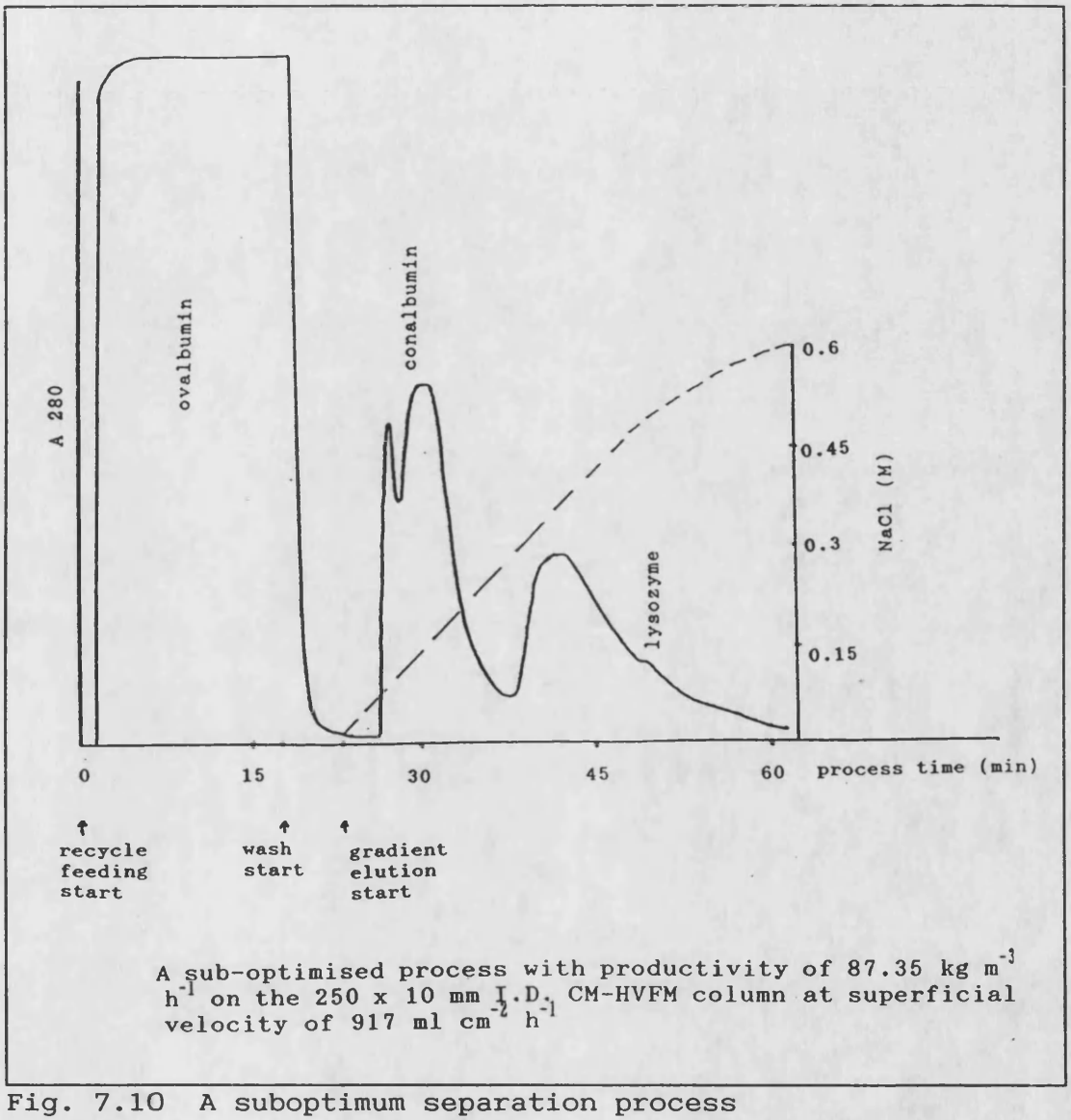

Fig. 7.10 A suboptimum separation process

The productivity of lysozyme is increased to 16.7 kg/m^3/h with an increase in the column loading, whilst the adsorption of conalbumin reaches a limit after which lysozyme is preferentially adsorbed.

The shape and position of the eluted conalbumin and lysozyme curves are not affected by increasing the column loading. The resolution and the number of theoretical plates are smoothly decreased with increased column loading. These results indicate that neither is the column's performance degraded, nor is the column blocked or channelled despite the high loading and high flow-rate.

No attempt was made to resolve the ovomucoid or the minor protein from the ovalbumin as neither adsorbs on the ion-exchange used under the operating conditions in force during these experiments.

The CM-HVFM production chromatographic column shows the characters of robustness, fast kinetic process in correspondence with high flow-rate. At superficial velocity of above 6.11 m/h, flow-rate of above 8 ml/min, the flow-rate is no longer the main limiting factor to affect the adsorption process. CM-HVFM column can deal with the egg-white solution without CDR pretreatment. Also, the column's kinetic performance is not degraded, nor is the column blocked and channelled despite high flow-rate and high column loading. High flow-rate can be beneficial in terms of high productivity.

A sub-optimum separation process has been suggested: 130 ml of 14 mg/ml egg-white solution is fed to a 250 x 10 mm I.D. column at a flow-rate of 12 ml/min and inlet pressure of 0.82 bar; The adsorbed proteins are then eluted by a gradient elution followed by the washing. This process can obtain a protein recovery of 97% and productivity of 87.63 $kg/m^3/h$. The purities of separated proteins which shows in gel electrophoresis are acceptable.

Fig. 7.5 Protein analysis in 12.5% SDS gel electrophoresis

CHAPTER 8

SUMMARY OF CONCLUSIONS AND RECOMMENDATIONS

CHAPTER 8

SUMMARY OF CONCLUSIONS AND RECOMMENDATIONS

A novel support matrix based on regenerated cellulose sponge were investigated for use in ion exchange separation. The following areas were considered:

(1) The technology and method for making sponge ion-exchanger with high flow-rate, protein capacity and robustness.
(2) Investigation of factors affecting the cross-linked and derivation of cellulose sponge.
(3) Estimation of isothermal adsorption parameters, adsorption and desorption kinetic parameters, transport parameters and hydrodynamic parameters of CM sponge column.
(4) Investigation of the chemical stability, physical stability and reproducibility of CM sponge.
(5) Investigation of the effect of flow-rate on the adsorption and desorption kinetic behaviour of CM sponge.
(6) Development of a simple lumped model for the stirred vessel reactor, differential recirculation bed column and long column.
(7) Development of a more sophisticated heterogeneous model for the stirred vessel reactor and differential recirculation bed column.
(8) Use of a rapid computational method in the model simulation and parameter estimation.
(9) Application of the CM sponge column in the separation of fresh hen egg-white proteins.
(10) Investigation of the effect of feed loading and flow-rate on the CM sponge column resolution, productivity and kinetic performance.

Summary of Conclusions

(1) Early work on making sponge ion-exchanger attempted: (A)

simultaneous cross-linking and derivation; (B) using too high or too low NaOH concentration, which led to the product with low flow rate, protein capacity and short life. It was found in this study that these procedures should carried out sequentially.

(2) If an NaOH concentration greater than 7% was applied at the cross-linking stages, the sponge structure would be damaged before the cross-linking reaction was complete. Using 4%(v/v) dichlorohydrin in 1 M NaOH at 100 °C from 10 to 60 minutes was successful.

(3) 20%(w/v) of sodium chloroacetate in 20%(w/v) of NaOH solution at 100 °C from 20 to 60 minutes is recommended for the derivative reaction, which ensures the highest protein capacity.

(4) In order to overcome the poor hydraulic and mechanical properties of the sponge ion-exchanger, the cross-linking reaction and derivative reaction were separated into two steps each using a different concentration of applied sodium hydroxide (refer to the points 2 and 3 above).

(5) The physical stability of CM sponge ion-exchanger was highly superior to that of Whatman CM52 and Phoenix CM resin. The CM sponge ion-exchanger was able to sustain superficial velocities of over 7 m/h in a 100 x 147 mm I.D. diameter column.

(6) The K_d and protein capacity of CM sponge were mainly affected by ionic strength. 2.1 g/g lysozyme capacity and 0.08 mg/ml Kd were obtained at the lowest ionic concentration. High protein capacity, for example 1.46 g/g, was still maintained even though the ionic concentration rose to 5.6 mS/cm.

(7) The adsorption kinetic was mainly affected by the flow-rate. When the superficial velocity was more than 40 m/h the adsorption process was no longer affected the flow-rate. An intrinsic adsorption rate thus was obtained at the superficial velocity 90 m/h.

(8) The desorption kinetic was hardly affected by the flow-rates, but was mainly controlled by the ionic concentration

at which was below 0.5 M NaCl. If the eluent ion concentration was higher than 0.5 M NaCl the desorption kinetic seemed to be independent of the ionic concentration of eluent.

(9) The adsorption rate K_1 and the desorption rate K_2 established by the differential recirculation column were identical with those obtained from the stirred vessel. This indicates that the differential recirculation column method is reliable and convenient for measuring K_1 and K_2.

(10) CM sponge column was not swollen or shrunk at varying pH, high NaCl and NaOH concentrations.

(11) The results of 340 cycles operation showed that the CM sponge ion-exchanger was very robust and withstood severe operation conditions.

(12) Both the lumped K_{ff} model and the more sophisticated heterogeneous model, which included external mass transfer and internal diffusion, described the adsorption performance well. The latter model gave the parameter values which can be related to the fundamental understanding.

(13) The external mass transfer coefficient K_f estimated from the heterogeneous model is probably more accurate than that obtained from correlations. Solved by the orthogonal collocation method, the heterogeneous model can rapidly predict the adsorption performance in both the recirculation batch reactor and stirred batch reactor under different protein loading, stirrer speeds and superficial velocities.

(14) The K_d in the lumped K_{ff} model seems to be a lumped parameter, which includes the effect of internal diffusion, rather than being a pure disassociation constant.

(15) The column model, which does not differentiate the effects of film mass transfer and pore diffusion, can predict more than 90% the experimental breakthrough curve at various feed concentrations and linear velocities.

(16) The column model showed that, even with the novel coherent sponge ion-exchanger, the axial dispersion was negligible,

as the Peclet number was larger than 10.

(17) The production size CM sponge column can separate egg-white into three crude fractions of mainly ovalbumin, lysozyme and conalbumin at a column loading of up to 450 kg/m^3 and high flow-rate. With all three fractions desired it was better to load 13.64 g/l protein at up to 150 kg/m^3, whilst only lysozyme was of real interest a loading of 20.31 g/l protein at 450 kg/m^3 was preferred.

(18) The productivity of lysozyme was increased to 16.7 kg.m^3/h with an increase in the column loading, whilst the adsorption of conalbumin reached a limit after which lysozyme was preferentially adsorbed.

(19) The production size CM sponge column can directly deal with the egg-white solution without CDR pretreatment. Also, the column's kinetics performance is not degraded, nor was the column blocked and channelled despite high flow-rate and high column loading. High flow-rate can be beneficial in terms of high productivity.

Recommendations for Further Work

(1) The derivative conditions for SP and DEAE ion-exchangers need to be optimized in order to get high protein capacity.

(2) A uniform sponge structure needs to be considered.

(3) The relationship of degree of cross-linked, protein capacity and hydraulic properties needs to be established.

(4) The effect of high ionic strength (such as from 0.2 to 1 M NaCl) on K_d and maximum protein capacity needs to be established, in order to provide these two parameters for the desorption model.

(5) A desorption model needs to be developed.

(6) A column model included liquid film mass transfer and intrapticle diffusion needs to be developed.

(7) The effect of a heterogeneous factor on the heterogeneous model needs to be investigated.

(8) An experimental method for measuring the pore diffusion coefficient and solid diffusion coefficient needs to be developed, so that they can be applied to the heterogeneous

model.

(9) A pilot plant for making sponge ion-exchanger could be developed.

(10) A pilot plant for the separation of egg-white protein could be developed.

REFERENCES

REFERENCES

Adams, B. A. and Holmes, E. L. (1935). "Adsorptive Properties of Synthetic Resins". J. Soc. Chem. Ind., 54, pp.1-6T.

Addo,M.A., (1988). "Developments In Ion Exchange Media For Protein Separation". Ph.D. Thesis, University of Bath, Bath, U.K..

Al-Duri, B. and McKay, G. (1990). "Comparison in Theory and Application of Several Mathematical Models to Predict Kinetics of Single Component Batch Adsorption Systems". Trans IChemE, Vol. 68, PartB, pp.254-268.

Alpert, A.J. and Regnier, F.E. (1979)." Preparation of A Porous Microparticulate Anion-Exchange Chromatography Support For Proteins". J. of Chromatography, 185, pp.375-392.

Atkinson, A. (1973). "Purification of Microbial Enzymes". Proc. Biochem., 8(8), 9, pp.28.

Ayers, J. S. (1980)." Hydroxyalkylated Cross-Linked Regenerated Cellulose and Method for Preparation Thereof". GB Patent 1573513.

Ayers, J.S., Peters, M.J. and Sheerin, B.E. (1984). "Cross-Linking Hydroxypropylated Cellulose Gel for Chromatography". J. of Chromatography, 294, pp.195-215.

Barber,W.E. and Carr, P.W. (1981)." Graphical Method for Obtaining Retention Time and Number of Theoretical Plates from Tailed Chromatographic Peaks". Anal. Chem. No. 53, pp.1939-1942.

Bernardi, G.(1971), in " Methods In Enzymology". (Jakoby, W. B., Ed.), Vol. 22, pp.325. New York: Academic Press.

Bite, M. G. Berezenko, S., and Reed, F, J. S. (1987). "Macrosorb Kieselygubr-Agarose Composite Adsorbents: New Tools for Downstream Process Design and Scale-up". in " Separations for Biote chnology". (Verrall,M. S.,and Hudson, M.J., Eds), Ch 13. London: Ellis Howood Ltd.

Bidlingmeyer,B.A. and F. Vincent Warren,Jr.(1984). " Column Efficiency Measurement". Analytical Chemistry, Vol. 56, No.4, pp.1583A-1596A.

Bio-Rad Laboratories, (1990). " New Macro-Prep™ 50Q,S, and CM

Ion Exchange Supports". Bio-Rad, Bulletin 1623, Bio-Rad Laboratories Ltd., Hemel Hempstead, U.K..

Bonnerjea, J., Hoare, S. Oh., and Dunnill, P. (1986). " Protein-Purification - The Right Step at The Right Time". Bio/Technology, No.4, pp.954-958.

Chang, S. H., Gooding, K. M., and Regnier, F.E. (1976). "Use of Oxirans in the Preparation of Bonded Phase Supports". J. Chromatography, 120, pp.321.

Cerro, R. L., and Smith, J. M. (1970). " Chromatography of Non Adsorbable Gases". AIChE. J., vol.16, No 6, pp.1034-1038.

Chase, H.A.(1984a)." Prediction of The performance of Preparative Affinity Chromatography". J. of Chromatography, 297, pp.179-202.

Cluff, J. R., and Hawkes, S. J. (1976). "Zone Dispersion in Packings of Impermeable Spheres". J. Chromatography Sci., 14, pp.248.

Chase, H.A. (1984a)." Prediction of the Performance of Affinity Chromatography". J. Chromatography, 297, pp.179-203.

Chase, H.A. (1984b)." Ion Exchange and Adsorbents Resins for the Purification of Proteins". in " Ion-Exchange Technology". (Naden, D. and Streat, M., Eds). Ellis Horwood Ltd. Chichester, U.K.

Chase, H. A. (1984d). "Affinity Separations Utilising Immobilised Monoclonal Antibodies-A New Tool for the Biochemical Engineer". Chem. Eng. Sci., 39, pp.1099.

Cohn, W. E. (1949). "The Separation of Purine and Pyrimidine Bases and of Nucleotides by Ion Exchange". Science, 109, pp.377.

Cowan, G.H., Gosling, I.S., Laws, J.F., and Sweetenham, W.P. (1986)." Physical and Mathematical Modelling to Aid Scale-up Of Liquid Chromatography ". J. Chromatography, 363, pp.37-56.

Crig, L.C., Carig, D. (1956) in " Technique of Organic Chemistry". (Weissberger, A., Ed.), Vol. 3, pp.149. New York Interscience.

Determann, H., and Wieland, Th(pharmacia) (1970). "Cellulose Based Ion-Exchangers". Ger. Offen. 2005408(Cl.c 08b, bo4b)

25pp.

Determann, H., and Wieland, Th(Pharmacia) (1976). "Ion Exchangers Based Cellulose". Swed Patent 382066 (Cl. C08B11/14) 6pp.

Dorfner, K. (1972). Ch.1 in " Ion Exchangers: Properties and Applications". (Coers, A. F., Ed). Ann Arbor Science Pub. Inc..

Dunnill, P. (1978), in "Enzyme Engineering". (Pye, E. K., and Weethall, H.H., Eds), Vol. 13, pp.207-215, Plenum, New York.

Eketorp, R. (1982). in " Affinity Chromatography and Related Techniques". (Gribnau, T.C. J., Visser, J., and Nivard, R. J. F., Ed.) pp.263, Elsevier, Amsterdam.

Fang Ming and Howell, J. (1987a). " Improved Technology for Making CM Sponge Ion-Exchange". Internal report, BioIsolates Ltd. and School of Chem. Eng., Bath University, U.K.

Fang Ming (1987b)." Dynamic modelling of Anaerobic Fixed Biofilm Digestion Processes And Simulation By the Orthogonal Collocation Method". Msc. Thesis, University of Bath, U.K..

Fang Ming and Howell, J.A. and Canovas-Diaz, M.(1989)." Mathematical Simulation of Anaerobic Stratified Biofilm processes". in "Computer Applications in Fermentation technology". (Fish, N.M., Fox, R. I. and Thomhill, N. F., Eds), pp.69-77, Elsvier Applied Science.

Fang Ming, Howell, J.A. and BioIslate Ltd. *et al.* (1990a)."Cellulosic Sponge Adsorbent Medium." European Patent, Application Number 9011378.8

Fang Ming and Howell J.A.(1991a). " Kinetic Behaviour of A Novel Matrix Ion-Exchanger, Carboxymethy-HVFM, Operated at High Flow-rate'. J. of Chromatography, 539, pp.255-265.

Fang Ming and Howell, J.A., and Canovas-Diaz, M.(1991b)." Stability of A Stratified Ecology: A Dynamic Model of An Anaerobic Fixed Biofilm Reactor". Biofulling, Special issue of biofulling on Biofilm Species Dynamics, in press.

Finlayson, B.A.,(1972). "The Method of Weighted Residuals and Variational Principles". Academic Press.

Fornsted , N., and Porath, J. (1989). " Sulphated Sepharose- A

Strong Cation Exchange". J. of Chromatography, 472, pp.261-264.

Foo, S.C., and Rice,R.G. (1975). "On the Prediction of Ultimate Separation in Parametric Pumps". AIChE J., 21, pp.1149.

Freundich, H. (1926)." Colloid and Capillary Chemistry". Methuen and Co. London.

Fritz, W., Merk, W. and Schlunder, E.U., (1981). " Competitative adsorption of Two Dissolved Organics onto Activated Carbon-11 ". Chem. Eng. Sci., 36 p731-741.

Furusawa, T. , Suzuki, M. and Smith, M. J. (1976). "Rate Parameters in Heterogeneous Catalysis by Pulse Techniques". Catal. Rev., 13, pp.43.

Freiling, E.C., (1955). " Ion Exchange as a Separation Method IX Gradient Elution Theory". J. Amer. Chem. Soc., 77, pp.2067.

Geankopolis, C.J. (1983)." Transport Processes and Unite Operations". 2nd Edition, Allyn and Bacon, Boston.

Giddlings, J. C. (1965)." Dynamics of Chromatography". Marcel Dekker, New York.

Glueckauf, E. (1955)."Theory of Chromatography IX. Theoretical Plate Concept in Column Separations. " Trans. Faraday Soc., 51, pp.34-44.

Glueckauf, E., Barker, K.H., and Kitt, G. P. (1949). Faraday Soc. Discussions, 7, pp.199.

Gosling, I.S.(1985)." Characterisation Of Ion Exchangers for Protein Recovery". PhD Thesis, University College Swansea, U.K.

Gosling, I.S., Cook, D., and Fry, M.D.M. (1989). "The Role of Adsorption Isotherms in the Design of Chromatographic Separation for Downstream processing. " Chem. Res. Des., Vol. 67, pp.232-282.

Goto,M.,Hayashi,N., and Goto, S. (1983). "Separation of Electrolyte and nonelectrolyte by an ion retardation Resin". Separation Sci. and Techno., 18(5), pp.475-484.

Goto, M., and Goto, S. (1990). " Kinetic Analysis of Ion-Exchange Chromatography by the Moment Method". Separation Sci. and Techno., 22(5), pp.1503-1514.

Graham, E. E. and Fook, C. F. (1982). " Rate of Protein Absorption and Desorption on Cellulose Ion Exchangers". AIChE Journal Vol. 28, No. 2, pp.245-250.

Grant, R.A. (1971)." Improvements in or relating to Ion-Exchange Materials". GB Patent 1226448.

Gregor, H. P. (1948). "General Thermodynamic Theory of Ion Exchange Processes". J. Amer. Chem. Soc., 70, pp.1293.

Hashimoto, N., and Smith, J. M. (1973). "Macropore Diffusion in Molecular Sieve Pellets by Chromatography". Chem. Eng. Sci., 26, pp.1555.

Hames,B.D. (1986), in "Gel Electrophoresis of Proteins; A practical Approach". (Hames,B.D. and Rickwood,D., Eds), pp.40, IRL Press, Oxford University Press, U.K.

Hefferich, F. (1959). "Ion Exchange". McGraw-Hill, New York.

Helfferin, F.,(1962). Ch. 4 in "Ion-Exchange". McGraw-Hill, N.Y..

Henry P.M.(1989). " Ion-exchange Chromatography of Proteins and Peptides". in " HPLC of Macromolecules A Practical Approach". (Oliver R.W.A., Ed), pp.91-125, IRL Press, Oxford University Press, U.K.

Hirs, C. H. W., Stein, W. H., and Moore, S. (1951). "Chromatograph of Proteins. Ribonuclease". J. Amer. Chem. Soc., 73, pp.1893.

Hjerten, S., and Mosbach, R. (1962)."Molecular-Sizeve" Chromatography of Proteins on Column of Cross-Linked Polyacrylaminde." Anal. Biochem., 3. pp.109-118

Hoffauir, C.L., and Guthris, J.D. (1950). " Charactistics of Chemical modified Cotton Fabrics". Textile Research J. 20, pp.617.

Horn J.D.(1980). Ch.3 in "Applied Protein Chemistry". (Grant R.A., Ed), Applied Science Publishers Ltd. Essex.

Horstmann, B. J., and Chase, H. A. (1989). " Modelling the Affinity Adsorption of Immunoglobulin G to Protein A Immobilised to Agarose Matrices". Chem. Eng. Res. Des.,

Vol. 67, pp.243-254.

Horstmann, B.J. (1989). "Affinity Adsorption on Agarose Materials". Ph.D. Thesis, Cambridge University.

Howell, J. A., Dove, R., and Kuwata, T. (1990). " Manufacture and Use of High Protein Whey Products" in Proceedings of 1990 Dairy Products Technical Conference. Centre for Dairy Research, pp.43. University of Wisconsin, Chicgo, Illinois, U.S.A..

Hubble, J. (1989)." A Simple Model for Predicting the Performance of Affinity Chromatography Column". Biotechnology Techniques, Vol.3, No.2, pp.113-118.

Janson, Jan-christer and Hedman, P. (1987). " On the Optimization of Process Chromatography of Proteins". Biotech. Progress, vol.3, No.1, pp.9-13.

Janson, J-C., and Hedman, P. (1982). "Large-Scale Chromatography of Proteins", in "Adv. Biochem. Eng.". (Fiechter, E., Ed), 25, pp.64-99, Springer-Verlag, N.Y..

Jones, D.T., Baynham, F., and Sponed Ltd. (1963). "Improvements in or Relating to Cellulosic Sponge Material". GB Patent 914421.

Kang, K., and McCoy, B.J. (1988). " Protein Separation by Ion Exchange Chromatography: A Model For Gradient Elution". Biotech. and Bioeng., Vol. 33, pp.786-790.

Kato, Y., Komiga, K., and Hashimoto, T. (1982). "Characterization of TSK-Gel DEAE-TOYOPEAL G50 Ion Exchanger". J. Chromatography, 245, pp.193.

Kato, Y., Nakamura, K., and Hashimoto, T. (1982). " Evaluation of Conventional and Medium-Performance Anion Exchangers for the Separation of Proteins". J. Chrom. 253, pp.219-225.

Knight, C.S., Riemer, A.C., Weaver, V.C., and W. & R. Balston Ltd. (1966). " Improvements in or Relating to Cellulose Derivatives". GB Patent 1026706.

Knight, T.C.S., (1967). " Some Fundamentals of Ion Exchange Cellulose Design and Usage in Biochemistry". Advances in Chromatography, 4, pp.61-110.

Knox, J.H. and Pyper, H.M. (1980). " Framework for Maximizing Throughput in Preparative Liquid Chromatography". J.

Chromatography, 303, pp.1-30

Kubin, M. (1965). "Beitrag Zur theorie Der Chromatographie". Collect. Czech. Chem. Commun., 30, pp.1104-1118 and pp.2900-2907.

Kubin, M. (1975). " A Model of the Mechanism of the Separation of Macromolecules in Gel Permeation Chromatography on Packing With Non-Homogeneous Pores". J. Chromatography, 108, pp.1.

Kucera, E. (1965). "Contribution to the Theory of Chromatography Linear Non-Equilibrium Elution Chromatography", J. Chromatography, 19, pp.237.

Langmuir, I.(1918). "The Adsorption of Gases On Plane Surfaces of Glass, Mica, and Platinum". J. Am. Chem. Soc. 60, pp.309.

Lapidus, L., and Amundson, N. R. (1952). J. Phy. Chem., 56, pp.984.

Leaver, G. (1984). " Large Scale Ion-Exchange Chromatography of Animal Blood Proteins". PhD Thesis, University College Swanssea, pp.162.

Leaver, G., Conder, J.R. and Howell, J.A. (1989). " A Method Development Study of the Production of Albumin From Animal Blood By Ion-Exchange Chromatography". in "Preparative-Scale Chromatography". (Grushka, E., Ed), pp.245-268, Marcel Dekker Inc. N.Y.

Levison, P.R., Toome, D.W., Badger, S.E., Brook, B.N. and Carcary D.(1989). " Influence of Mobile Phase Composition On The Adsorption of Hen Egg-White Proteins to Anion-Exchange Cellulose". Chromatography, Vol.28, No.3/4, pp.170-178.

Levison, P.R., Butts, E.T., Koslieluy, M.L., and Lane, L.(1990a). "High Flow Ion-Exchange Chromatography Cellulose-Based Media". in "Technologies De Purification Des Proteins". (Briund, Y., Doinel, C., and Fanre, A., Eds), Vol. 4, pp.137-142, G.R.B.P..

Levison, P.R., Toome, D.W., Carcary, D. and Butts, E.T. (1990b). "Studies on The Use of Anion-Exchange Cellulose at Process-Scale'. in " Advances in Separation Processes". The Institution of Chemical Engineers, Series No.118, pp.6.1-

6.11, Hemisphere Publishing Corporation, U.K.

Lewis, W.K., and Whitman, W.G. (1924). Ind. Eng. Chem.,16, pp.1215.

LKB-Produkter AB (1984)." A Practical Guide to Ion Exchange Chromatography". LKB-Produkter AB, Bromma, Sweden.

Maa, Y.-F., Antia, F. D., Rassi, Z.E., and Horvath, C. (1988)."Mixed-Bed Ion-Exchange Columns for Protein High-Performance Liquid Chromatography". J. of Chromatography, 452, pp.331-345.

Matson, R.S., Siebert, C.J.(1988). "Evaluation of a New N-Hydroxysuccinimide Activated Support For Fast Flow Immunoaffinity Chromatography". Preparative Chromatography, Vol. 1, pp.67-91.

Martin,A.J.P., Synge, R.L.M. (1941). "Volatile Aldehydes liberated by Periodic Acid from Protein Hydrolyzates". Biochem. J., 35, pp.1358.

Marrazzo, W. N., and Merson, R. L. (1975). " Enzyme Immobilized in a Packed-Bed Reactor: Kinetic Parameters and Mass Transfer Effects". Biotech and Bioeng., No. 1, XVII, pp.1515-1528.

Mayer, S.W., Tompkins, E.R. (1947). "Ion Exchange as a Separation Method. IV. A Theoretical Analysis of the Column Separations Process". J. Am. Chem. Soc., 69, pp.2866-2874.

Mathews, A.P., and Weber, JR. W.J., (1983). " Modeling and Parameter Evaluation for Adsorption in Slurry Reactors". Chem. Eng. Commun., Vol. 25, pp.155-171.

Mathew, A.P., and Weber, JR. W.J. (1977). "Effects of External Mass Transfer and Intraparticle Diffusion on Adsorption Rates in Slurry Reactor". AIChE Symposium Ser. 166, 73, pp.91-98.

McCoy, B. J. (1989). " Book Reviews". AIChe J., Vol. 35, No. 4, pp.700,

McKay, G., Allen, S.J., McConvey, I.F., and Walters,H.R.(1984). " External Mass Transfer and Homogeneous Solid-Phase Diffusion Effects During the Adsorption of Dyestuffs". Ind.Eng. Chem. Process Dev., 23, pp.221-226.

Moore, S., and Stein, W. H. (1951). "Chromatography of Amino

Acids on Sulfonated Pelystyrene Resines". J. Biol. Chem., 192, pp.663-681.

Morris, C. J., and Morris, P.(1976). " Separation Methods in Biochemistry". Pitman, London.

Morrison, R.H. and Boyd, R.N. (1973). Ch. 17 in " Organic Chemistry". (3rd Ed), pp.562-570, Allyn and Bacon Inc., Boston.

Nakanishi, K., Yamamoto, S., Matsuno, R., and Kamikubo, T.(1977)." Analysis of Dispersion Mechanism in Gel Chromatography". Agric. Biol. Chem., 41 (8), pp.1465-1473.

Motozato, y., and Hirayama, C. (1984). "Preparation and Proterties of Cellulose Spherical Particles and Their Ion Exchanger". J. of Chaomatography, 298, pp.499-507.

Onwuasoanya, D.I.(1987). " Development and Mathematical Modelling of Affinity System Based on Novel Matrix". PhD Thesis, University of Bath, U.K.

Peterson, E.A., (1970). " Cellulosic Ion Exchangers". North Holland/American Elsevier

Peterson, E. A., and Sober, H. A. (1956). " Chromatography of Proteins: (1) Cellulose Ion Exchange Adsorbents". J. Am. Chem. Soc., 78, pp.751-755.

Peska, J., Stamberg, J., Hradil, J., and Ilavsky, M. (1976)." Cellulose in Bead Form-Properties Related to Chromatographic uses". J. Chromatography., 125, pp.455-469.

Pharmacia LKB Biotechnolgy, " Gel Filtration Theory and Practice" Pharmacia LKB Biotechnology, S-75182, Uppsala, Sweden.

Pharmacia AB (1985), " FPLC Ion Exchange and Chromatofocusing, Principles and Methods", Pharmacia AB, Uppsala, Sweden.

Polson, A. (1950)."Some Aspects of Diffusion in Solution and a Definition of a Colloidal Paricle". J. Phys. Colloid Chem., 54, pp.649-652.

Porath, J., and Flodin, P.(1959). "Gel Filtration: A Method for Desalting and Group Separation". Nature, 183, pp.1657.

Porath, J., and Fornstedt, N. (1970). "Group Fractionation of Plasma Proteins on Dipolar Ion Exchangers". J. of Chromatography, 51, pp.479-489.

Porath, J., Janson, J. C., and Laas, T. (1971). " Agar

Derivatives for Chromatography Electrophoresis and Gel-Bound Enzyme I Desulphated and Reduced Cross-Linked Agar and Agarose in Spherical Bead Form". J. Chromatography, 60, pp.167.

Raghavan, N.S. and Ruthven, D.M., (1982). " Numerical Simulation of a Fixed-Bed Adsorption Column by the Method of Orthogonal Collocation", AIChE Journal, 29(6), pp.922-925.

Ramachandran, P.A. (1975). " Solution of Immobilized Enzyme Problems by Collocation Methods". Biotech. and Bioeng., Vol XVII, pp.211-226.

Regnier, F.E. and Mazsaroff, I. (1987). " A Theoretical Examination of Adsorption Processes in Preparative Liquid Chromatography of Proteins", Biotech. Progress, Vol.3, No.1, pp.22-26.

Rhodes M.B., Azari P.R., Feency R.E.(1958). " Analysis, Fractionation, and Purification of Egg White Proteins With Cellulose Cation Exchanger. J. Biol. Chem., 230, pp.399-408.

Roe, S. (1989). "Separation Based on Structure". in " Protein Purification Methods: A practical Approach". (Harris, E.L.V. and Angal, S., Eds), IRL Press, Oxford University Press. U.K..

Schneider, P., and Smith, J. M. (1968). " Adsorption Rate Constants from Chromatography". AIChE. J. vol.14, NO.5, pp.762-771.

Sirotti, D.A., and Emergy, A. (1983). "Mass Transfer Parameters in An Immobilized Glucoamy; ase Column by Pulse Response Analysis". Biotech. and Bioeng. XXV, pp.1773-1779.

Skidmore, G.L., and Chase, H.H. (1988). " A Study of Ion Exchangers for Protein Purification". in Ion-Exchanger for Industry. (Naden,D., Ed), Ellis Horwood Ltd., pp.520-532.

Skidmore, G.L., Horstmann, B.J., and Chase, H.A. (1990)." Modelling Single-Component Protein Adsorption to the Cation Exchange S Sepharose FF". J. of Chromatography, 498, pp.129-135.

Smith, M.A., and Gillespie, P.C. (1989). " Ionization of DEAE-Cellulose Dependence of pK on Ionic Strength", J. of

Chromatography, 469, pp.111-120.

Soffr,G.K. and Nystrom, L.-E. (Eds) (1989). " Process Chromatography: A Practical Guide". pp.55, Academic Press Ltd., London.

Stout, R.W., Sivakoff, S.I., Ricker, R.D., Palmer, H.C., Jackson, M.A., and Odiorne, T.J. (1986). " New Ion-Exchange Packing based On Zirconium Oxide Surface-Stabilized, Diol-Bonded, Silica Substrates". J. of Chromatography, 352, pp.381-397.

Thomas, H.C. (1944). "Heterogeneous Ion Exchange in A Flowing System". J. Amer. Chem. Soc. 66, pp.1664-1666.

Thomas, H.C. (1948). "Chromatography: A problem of Kinetics". Ann. N.Y. Acad. Sci. 49(1), pp.161-182.

Thompson, H. M.(1850). "On the absorbent power of soiles". J. Roy. Agric. Soc. Engl., 11, pp.68.

Thomson, A. R. (1984). " Recent Developments in Protein Recover and Purification". J. of Chem. Tech. and Biotech, 34B, pp.190-198.

Tayot, J. L., and Tardy, M. (1976). "Hydrophobic Ion-Exchange and Affinity Methods". in " Chromatogr. Synth. Biol. Polymer". (R, Epton, Ed.), 2, pp.95-110. Ellis Horwood CHichester.

Tsou, H., and Graham E.E. (1985). " Predication of Adsorption and Desorption of Protein on Dextran Based Ion Exchange Resins". AICHE Journal 31 (12), pp.1959-1966.

Tyn, M. T., and Gusek, T., (1990). " Prediction of Diffusion Coefficients of Proteins". Biotech. and Bioeng., 35, pp.327-338.

Unger, K.K., and Janzen, R.(1986). " Packing and Stationary Phases in Preparative Column Liquid Chromatography". J. Chromatography, 373. pp.227.

Van Deemter, J.J., Zuiderweg, F.J., Klinkenberg, A. (1956). "Longtudinal Diffusion and Resistance to Mass Transfer as Causes of Nonideality in Chromatography". Chem. Eng. Sci., 5, pp.271-289.

Villadsen, J,V.,(1970). " Selected Approximation Methods for Chemical Engineering Problems". Denmarks tekniske Hojskile, Lyngsby.

Villadsen, J.V., and Stewart, W.E. (1976). "Solution of Boundary-Value Problems by Orthogonal Collocation". Chem. Eng. Sci., 22, pp.1483-1501.

Way, J. T. (1850)."On the Power os Soiles to Absorb Manure". J.Roy. Agric. Soc. Engl., 11, 68, pp.313-380.

Whitley, R., Brown, J.M., Karajgikar, N.P. and Wang, N-H, L. (1989) " Determination of Ion-Exchange Equilibrium Parameters of Amino Acid and Protein Systems By An Impulse Response Technique". J. of Chromatography, 483, pp.263-287.

Wilson, J. N. (1966). "Liquid Mass Transfer at Very Low Reynolds Numbers in Packed Beds". Ind. Eng. Chem. Fund., 5, pp.9.

Wilson, J.N. (1940). "A Theory of Chromatography", J. Amer. Chem. Soc., 62, pp.1583-1591.

Yamamoto, S., Nakanishi, K., and Matsuno, R. (1988). " Ion-Exchange Chromatography of Proteins", Marcel Dekker, INc.,New York and Basel, pp.163.

Yamamoto, S., Nakanish, K., Matsuno, R. and Kamikubo, T., (1983a). " Ion Exchange Chromatography of Proteins - Prediction of Elution Curves and Operating Conditions I - Theoretical considerations". Biotech. and Bioeng., 25, pp.465-1483.

Yamamoto, S., Nakanishi,K., Matsun, R., and Kamikubo, T. (1983b). " Ion Exchange Chromatography of Proteins-- Prediction of Elution Curves and Operation Conditions. II Experimental verification". Biotech. and Bioeng., Vol. xxv, pp.1373-1391.

Yang, C-M. and Tsao, G.T. (1982). " Packed Bed Adsorption Theories and Their Application to Affinity Chromatography". In " Adv. Biochem. Eng., Vol. 25, (Fiechter, A., Ed.) Springer-Verlay, N.Y., pp.1-42.

Young, M. E., Carroed, P. A., and Ball, R. L., (1980). " Estimation of Diffusion Coefficients of Proteins". Biotech. and Bioeng., 22, pp.947-955.

NOMENCLATURE

NOMENCLATURE

A_1	constant in equation 5.8a (mg/ml)
a_i	arbitrary coefficient in equation 6.21
AI	ion exchanger
A_{ji}, A'_{ji}	symmetric and nonsymmetric matrices
A_f	Freundlich equation constant (ml/g)
a_v	particle surface volume ratio (mm)
b	Freundlich equation constant
B_1	constant in equation 5.8a
B_{ji}, B'_{ji}	symmetric and nonsymmetric matrices
C	protein concentration in bulk liquid (mg/ml)
C_e	equilibrium protein concentration in bulk liquid (mg/ml)
C_i	protein concentration of liquid phase inside the adsorbent (mg/ml)
c_i, c_j	protein concentration in liquid phase at the collocation points (mg/ml)
C_f	equilibrium correcting factor
C_o	initial protein concentration (mg/ml)
c_s	protein concentration on the surface of adsorbent (mg/ml)
d_1	heterogeneity factor
D_e	effective intraparticle diffusivity (mm^2/min)
D_L	axial dispersion (mm^2/min)
D_m	molecular diffusion coefficient in free liquid (mm^2/min)
d_p	particle diameter (m)
F	flow rate (ml/min)
g	q/q_m dimensionless parameter
g_o	gravity (9.80665 m/s^2)
I	counter ions
I.D.	internal diameter
J	number of collocation points
K_a	(C_o 1 K1/u) dimensionless parameter
K_1	adsorption constant (ml/mg/min)

K_2	desorption constant (1/min)
Kb	(K_1 K_d l/u) dimensionless parameter
K_d	dissociation constant (mg/ml)
K_f	mass transfer coefficient (mm/min)
K_{ff}	lumped mass transfer coefficient (mm^2/min)
K_p	(ρ $q_m/\epsilon/C_o$)dimensionless parameter
l, L	length of column (m)
M	protein molecular weight
meq	milliequivalent
N	number of collocation point
N_{NaoH}	normality of NaOH (M)
P	protein
Pe	Peclet number
$P_{i-1}(x^2)$	orthogonal polynomial in equation 6.21
Pro	protein ions
q	protein concentration in adsorbent (mg/g)
q_e	equilibrium protein concentration in adsorbent (mg/g)
qi, q_j	protein concentration on solid phase inside the adsorbent (mg/g)
q_m	maximum protein capacity (mg/g)
q_o	initial protein concentration of adsorbent (mg/g)
q_s	interfacial protein concentration of adsorbent (mg/g)
R	adsorbent particle radius (mm)
R_e	particle Reynolds number
R_m	rate of interface mass transfer
R_h	hydraulic radius of the particle (m)
R_v	reaction uptake rate
r	space coordinate for adsorbent particle (mm)
S	x/l dimensionless parameter
S_c	Schmidt number
T	ut/l dimensionless parameter
t	time
T_1	retention time for lysozyme (min)
T_c	retention time for conalbumin (min)
t_1	time at the beginning of the elution peak (min)
t_2	time at the end of the elution peak (min)
u	linear mobile phase velocity (m/h)

u_o superficial velocity (m/h)
V feed volume (ml)
V_{NaOH} consuming alkali volume (ml) in titration
V_o void volume (ml)
V_s volume of stationary phase (ml)
V_t total column volume (ml)
v_i volume of ion-exchanger (ml)
W weight of ion-exchanger (g)
W_l eluted peak width for lysozyme (mm)
W_c eluted peak width for conalbumin (mm)
x space coordinate for column (cm)
y C/Co dimensionless parameter
Z space coordinate (cm)

GREEK LETTERS

γ labyrinth factor
k_D the item of $[\epsilon_i^2 R^2(1-\epsilon)]/(15 D_e)$ (second)
k_f the item of $[\epsilon_i^2 R (1-\epsilon)]/(3K_f)$ (second)
ϵ_i column voidage
ϵ intrparticle porosity
λ correction factor for eddy diffusion
μ solution viscosity (kg/ms)
μ_1 first moment (min)
μ_2 second moment (min)
μ_n nth statistical moment (min)
ν nondimensional reduced velocity
$\Delta\rho$ density difference between adsorbent and liquid (kg/m^3)
ρ density of ion-exchanger (g/ml)
τ tortuosity

APPENDIX

```
:Fang-ads
:CM sponge adsorb lysozyme in a stirred vessel or a differential
:bed column
:kd=k2/k1,  kd(mg/ml), k1(ml/mg/min),  k2(1/min), qm(mg/g)
:co= intinal lysozyme concentration (mg/ml)
:k1 = adsroption constant
:V = lysozyme solution (feed) volumn (ml)
:M = mass of CM sponge (g dry weight)
:$
constant co=0.5
constant qm=2100
constant kd=0.08
constant k1=0.04
constant M=0.08235
constant V=600
initial
t=0;c=co;q=0
dynamic
q'=k1*(co-(M*q/V))*(qm-q)-kd*k1*q
c=co-(M*q)/V
a=c/co
plot t,a,0,65,0.6,1
print t,a
$ VAL TFIN     =    65.000
$ VAL KD       =  0.30000
$ VAL K1       =  0.11000
$ VAL V        =    650.00
$ VAL M        =  0.81505E-01
```

```
:Fang-des
:CM sponge desorb lysozyme in a stirred vessel or differential
:bed column
:at t=0, q=qo, c=0.   when t>0, c=M(qo-q)/V
:k1=k2/kd, kd=0.08 mg/ml
:qo= initial lysozyme concentration in the sponge solid
:k2=desorption constant (ml/mg/min)
:kd= dissocation constant (mg/ml)
:qm=maximum sponge lysozyme capacity (mg/g)
:c= lysozyme concentration (mg/ml)
:k1=adsorption constant (ml/mg/min)
:v= the volumn of eluent (ml)
:M = mass of CM sponge (g dry weight)
:$
constant qm=2100
constant qo=1700
constant k2=0.7
constant kd=16
constant M=0.081505
constant V=300
initial
t=0;c=0;q=qo
dynamic
q'=(k2/kd)*((qo-q)*M/V)*(qm-q)-k2*q
c=(qo-q)*M/V
a=1-(q/qo)
plot t,a,0,25,0,1
print t,a
$ VAL M        =  0.30000
$ VAL V        =   180.00
$ VAL TFIN     =   22.000
$ VAL QM       =   180
$ VAL K2       =  0.90000
$ VAL QO       =   300.00
$ VAL KD       =   2.5
```

```
:film-ad7
:Fang-film-ad7
:film-ad7 assumes that the mass transfer to the surface of sponge
:ion-exchanger fibre is governed by the lumped mass transfer
:coefficient Kff. The mass transfer rate is equal to the surface
:reaction rate.
:film-ad4 base on film-ad1
:film-ad1  = film diffusion control model base on fang-ads
:lysozyme diffused from bulk liquid to surface of sponge
:the adsorption reaction only occures on the surfacr
:without considering the diffusion into the inside particle.
:CM sponge adsorb lysozyme in a stirred vessel or a differential
:bed column
:kd=k2/k1,  kd(mg/ml), k1(ml/mg/min),  k2(1/min), qm(mg/g)
:co= intinal lysozyme concentration (mg/ml)
:k1 = adsroption constant
:V = lysozyme solution (feed) volumn (ml)
:w=mass os cm sponge(g dry), p=density of sponge(g/ml)
:r=radius of sponge particle (mm)
:Kff=lumped film mass transfer coefficient (mm/min)
:cb=protein concentration in bulk liquid
:c6= protein concentration on the surface of particle
constant co=0.5
constant qm=2100
constant kd=0.08
constant k1=0.12
constant kff=0.07, w=0.3
constant p=0.1144
constant r=0.02
constant v=180
initial
t=0;cb=co;q=0
dynamic
cb'=-((2*w*kff)/(r*v*p))*(cb-c6)
q'=k1*c6*(qm-q)-kd*k1*q
b1=k1*kd*q+2*kff*cb/(r*p)
b2=k1*(qm-q)+2*kff/(r*p)
c6=b1/b2
a=cb/co
plot t,a,0,19,0,1
print t,a
$ VAL V       =   180.00
$ VAL K1      =  0.12000
$ VAL P       =  0.11440
$ VAL QM      =   2100.0
$ VAL TFIN    =   19.000
$ VAL W       =  0.30000
$ VAL KFF     =  0.40000
$ VAL R       =  0.20000E-01
```

```
:Fang-C.2
:fi-corr2
:fi-corr2 is the heterogeneous model solved by orthogonal
collocation
:method with three collocation points.
:CM sponge adsorbs lysozyme in either a stirred vessel or a
differential
:recicuration bed column.
:liquid film mass transfer, intraparticle diffusion in the solid
:and liquid phases are included in this model.
:kd=k2/k1,  kd(mg/ml), k1(ml/mg/min),  k2(1/min), qm(mg/g)
:co=initial lysozyme concentration (mg/ml)
:k1 = adsroption constant
:V = lysozyme solution (feed) volumn (ml)
:w=mass of cm sponge (g dry), p=density of sponge(g/ml)
:r=radius of sponge fibre (mm)
:cb=protein concentration in bulk liquid
:c6= protein concentration on the surface of particle
:cb(mg/ml),c6(mg/ml)
:d=diffusion coefficient of liquid phase (mm2/min)
:d1=diffusion coefficient of solid phase (mm2/min)
:x= collocation point value
:aji, bji= orthogonal collocation matrix
:cf= equilibrium correction factor
:e=prosity of CM sponge fibre for lysozyme
:kf=liquid film mass transfer coefficient (mm/min)
constant co=0.5
constant qm=2030
constant kd=0.1
constant k1=0.12
constant kf=0.1
constant w=0.08
constant e=0.95
constant p=0.303
constant r=0.02
constant d=0.0036
constant d1=0.0036
constant v=600
constant b11=-15.8814, b12=19.6364, b13=-5.281186
constant b14=1.5262,b21=11.1519,b22=-34.4974,b23=29.2357
constant b24=-5.89016,b31=-3.5406,b32=34.51211,b33=-99.6213
constant b34=68.6496,b41=-33.8699,b42=136.2497,b43=-252.379
constant b44=150, a41=-1.2267,a42=5.4011,a43=-19.1744
constant a44=15, x1=0.29763,x2=0.6399,x3=0.8875,x4=1
initial
t=0;cb=co;q=0
dynamic
s1=x1*x1
s2=x2*(x2-x1)
s3=x3*(x3-x2)
s4=x4*(x4-x3)
cb'=-2*kf*w*(cb-cs)/(r*p*v)
q=(co-cb)*v/w
tp=p*(1-e)/e
f1=k1*c1*(qm-q1)-k1*kd*q1
f2=k1*c2*(qm-q2)-k1*kd*q2
f3=k1*c3*(qm-q3)-k1*kd*q3
cs=k1*kd*qs/(k1*(qm-qs))
c1'=d*(b11*c1+b12*c2+b13*c3+b14*cs)-tp*f1
```

```
c2'=d*(b21*c1+b22*c2+b23*c3+b24*cs)-tp*f2
c3'=d*(b31*c1+b32*c2+b33*c3+b34*cs)-tp*f3
cf=0.5/(s1+s2+s3+s4)
qs=((q/(2*cf))-(q1*s1+q2*s2+q3*s3))/s4
q1'=d1*(b11*q1+b12*q2+b13*q3+b14*qs)+f1
q2'=d1*(b21*q1+b22*q2+b23*q3+b24*qs)+f2
q3'=d1*(b31*q1+b32*q2+b33*q3+b34*qs)+f3
a=cb/co
plot t,a,0,80,0.6,1
print t,a
$ VAL TFIN     =   80.000
$ VAL KF       =  0.70000
$ VAL W        =  0.82350E-01
```

```
      PROGRAM FANG MOMENT
C=======================================================================
C  Calculating First and Second Moment using Spline Interporation for
C  Tablefunction
C  and then using Adaptive Gauss-Kronrod quadrature with extrapolation for
C  integration
C=======================================================================
      IMPLICIT DOUBLE PRECISION(A-H,O-Z,K)
      PARAMETER(OMEGA=.628318531718D1,err1=1.d-40,
     1  err2=1.d-8,DMU=1.D-3,RO=1.D3,RADIUS=.0125D0,TWOFOUR=24.D0,
     2  NTABLE=14,LW=50000,LIW=LW/8+LW/4+2,N=NTABLE,LCK=N+4
     3  ,LWRK=6*N+16,DELTNEW=.0005D0)
      DIMENSION W(LW),IW(LIW),X(NTABLE),Z(NTABLE)
      DIMENSION C(LCK),K(LCK),WRK(LWRK)
      COMMON K,C
      COMMON /mu/dmu1
      EXTERNAL TLU,TTLU,T2TLU
C----------Z=PRESSURE( AT POINT X)-----------------------------------
      do 100 i=1,NTABLE
      READ(1,*)X(i),Z(i)
100   continue
C-------E01BAF FROM NAG LIBRARY
C     FOR CALCULATING SPLINE COEFFIENT,STORING IN COMMON-------
      CALL E01BAF(N,X,Z,K,C,LCK,WRK,LWRK,IFAIL)
      IFAIL=0
      a=x(1)
      b=x(n)
C-------D01AJF FROM NAG LIBRARY
C     FOR SPLINE VALUES FOR THE MOMENTS-----------------------
      CALL D01AJF(TLU,A,B,err1,err2,RESULT0,ABSERR,W
     1  ,LW,IW,LIW,IFAIL)
      CALL D01AJF(TTLU,A,B,err1,err2,RESULT1,ABSERR,W
     1  ,LW,IW,LIW,IFAIL)
      dmu1=RESULT1/RESULT0
      CALL D01AJF(T2TLU,A,B,err1,err2,RESULT2,ABSERR,W
     1  ,LW,IW,LIW,IFAIL)
      dmu2=RESULT2/RESULT0
      WRITE(2,999)Result0,result1,result2,dmu1,dmu2
999   FORMAT(1X,'RESULT0=',F12.4,2X,'RESULT1=',F12.4,2X,
     1 'RESULT2=',F12.4,/,1X,'MU1=',F12.4,2X,'MU2=',2x,F12.4,//)
      END
      FUNCTION TTLU(T)
      IMPLICIT DOUBLEPRECISION(A-H,O-Z,K)
      TTLU=T*TLU(T)
      END
      FUNCTION T2TLU(T)
      IMPLICIT DOUBLEPRECISION(A-H,O-Z,K)
      COMMON /mu/dmu1
      T2TLU=(T-dmu1)*(T-dmu1)*TLU(T)
      END
      FUNCTION TLU(XINTER)
C-------------SPLINE INTERPOLATION-----------------------------
C N: THE NUMBER OF THE BASE POINTS
C X(N):INDEPENTENT INPUT
C Y(N):DEPENDENT INPUT
C XINTER:NEM INDEPENDENT POINT TO BE INTERPOLATED
      PARAMETER(N=15,LCK=N+4)
      IMPLICIT DOUBLEPRECISION(A-H,O-Z,K)
      DIMENSION C(LCK),K(LCK)
      COMMON K,C
      CALL E02BBF(LCK,K,C,XINTER,YINTER,IFAIL)
      TLU=YINTER
      RETURN
      END
```

AS AN EXAMPLE FOR THIS PROGRAM, THE VALUES

66.759	0.0
71.918	0.00246
74.042	0.01489
78.897	0.03472
81.932	0.05196
84.966	0.06156
89.2143	0.06353
91.64	0.06156
101.959	0.03447
111.669	0.0144
121.38	0.00985
133.518	0.00569
151.725	0.0031
178.429	0.00118
230.622	0.0

PRODUCE THE FOLOWING MOMENTS:

MU1=	98.7087	MU2=	338.3672
MU3=	7679.9995	MU4=	197685.9772

```
:fang-column
:CM-HVFM ion-exchanger column model
:250 x 100 mm I.D. column packed with 1.766g CMB10
:This column model includes the porosity of the adsorbent,
:flow convecton and axial dispersion within the column and
:surface reaction rate as the kinetic equation. The external
:film mass transfer and intrparticle diffusion are not included
:, but these factors might be included in the lumped kinetic
:parameters.
:$
:e = column voidage, t = dimensionless time
:ka = dimensionless forward constant
:kb = dimensionless backward constant
:tr, kp = dimensionless parameter
:The dimensionless concentration y (liquid phase) has been
:replaced by the dimensionless concentration, c.
:The dimensionless concentration g (adsorbent) has been
:replaced by the dimensionless concentration, Q.
:c1,c2,c3,c4,c5,c6,c7 are the dimensionless concentration
:at the collocation point and boundary point(liquid phase)
:Q1,Q2,Q3,Q4,Q5,Q6,Q7 are the dimensionless concentration
:at the collocation point and boundary point (adsobent)
:u (linear velocity) = f/(ax*e) (m/h)
:f = flow rate (m3/h)
:ax = column cross area (m2)
:DL = axial disperson coefficient (m2/h)
:Pe = Pelect number (u lc/DL)
:lc = length of column
:qm = maximum protein capacity (kg/kg)
:kl = adsorption constant (m3/kg/h)
:edv = empty bed volume
:kd = dissociation constant (kg/m3)
:c0 = initial feed concentration (kg/m3)
: pp = density of column packed (kg/m3)
:A(7,7), B(7,7) = nonsymmetrical collocation matrices
constant c0=1
constant e=0.8547
constant kl=4.8
constant ax=0.0000785
constant pp=0.086
constant pe=64
constant kd=0.08
constant lc=0.25,u=7
DIMENSION A(7,7),B(7,7)
constant A=-31.0,-13.09609,3.73216,-1.875
constant 1.11962,-0.64458,1.0,34.69972,10.13408
constant -7.62512,3.36805,-1.94084,1.10353
constant -1.70788,-5.03152,3.87973,1.51671
constant -4.04306,1.85712,-0.98752,1.50942
constant 2.1333,-1.44628,3.41215,0.0
constant -3.412125,1.44628,-2.1333,-1.50942
constant 0.98752,-1.85712,4.04306,-1.51671
constant -3.87973,5.03152,1.70788,-1.10353
constant 1.94084,-3.36805,7.62512,-10.13408
constant -34.69972,-1.0,0.64458,-1.11962
constant 1.8750,-3.73216,13.09609,31.0
constant B=480.0,292.91504,-21.02473,7.5
constant -6.30728,14.41697,60.0,-671.96836
```

```
constant -390.42093,59.8168,-14.86704,11.26125
constant -24.80217,-102.3049,268.3469,120.83914
constant -66.91239,30.03371,-12.53116,22.74946
constant 89.65971,-123.73334,-35.6975,35.6975
constant -45.333,35.69749,-35.69749,-123.7333,89.65971
constant 22.74946,-12.53116,30.03371,-66.9124
constant 120.83915,268.34691,-102.3045,-24.80217
constant 11.26125,-14.86704,59.81681,-390.42094
constant -671.9680,60.0,14.41697,-6.30728
constant 7.5,-21.02472,292.91503,480.0
INITIAL
C1=0;C2=0;C3=0;C4=0;C5=0;C6=0;C7=0
Q1=0;Q2=0;Q3=0;Q4=0;Q5=0;Q6=0;Q7=0
DYNAMIC
:compute the dimensionless kinetic parameters
kp=pp*qm/(c0*e)
tr=t*lc/u
ka=k1*c0*lc/u
ebv=(u*ax*e*tr)/(ax*lc)
kb=k1*kd*lc/u
M1=1/PE;PJ=A(7,7)*PE
PIE=((A(1,1)-PE)*A(7,7))-(A(1,7)*A(7,1))
PI=1/PIE;B1=A(7,1)/A(7,7)
D2=(M1*B(2,1))-(A(2,1))
D3=(M1*B(3,1))-(A(3,1))
D4=(M1*B(4,1))-(A(4,1))
D5=(M1*B(5,1))-(A(5,1))
D6=(M1*B(6,1))-(A(6,1))
:$
E2=(M1*B(2,7))-(A(2,7))
E3=(M1*B(3,7))-(A(3,7))
E4=(M1*B(4,7))-(A(4,7))
E5=(M1*B(5,7))-(A(5,7))
E6=(M1*B(6,7))-(A(6,7))
:COMPUTR THE POINT 1 CONSTANTS
A2=(A(1,2)*A(7,7))-(A(7,2)*A(1,7))
A3=(A(1,3)*A(7,7))-(A(7,3)*A(1,7))
A4=(A(1,4)*A(7,7))-(A(7,4)*A(1,7))
A5=(A(1,5)*A(7,7))-(A(7,5)*A(1,7))
A6=(A(1,6)*A(7,7))-(A(7,5)*A(1,7))
:COMPUTE THE C7 CONSTANTS
B2=A(7,2)/A(7,7);B3=A(7,3)/A(7,7)
B4=A(7,4)/A(7,7);B5=A(7,5)/A(7,7)
B6=A(7,6)/A(7,7)
S2=(M1*B(2,2))-(A(2,2))
S3=(M1*B(2,3))-(A(2,3))
S4=(M1*B(2,4))-(A(2,4))
S5=(M1*B(2,5))-(A(2,5))
S6=(M1*B(2,6))-(A(2,6))
:COMPUTE POINT 3 CONSTANTS
P2=(M1*B(3,2))-(A(3,2))
P3=(M1*B(3,3))-(A(3,3))
P4=(M1*B(3,4))-(A(3,4))
P5=(M1*B(3,5))-(A(3,5))
P6=(M1*B(3,6))-(A(3,6))
:COMPUTE POINT 4 CONSTANTS
M2=(M1*B(4,2))-(A(4,2))
M3=(M1*B(4,3))-(A(4,3))
```

```
M4=(M1*B(4,4))-(A(4,4))
M5=(M1*B(4,5))-(A(4,5))
M6=(M1*B(4,6))-(A(4,6))
:COMPUTE POINT 5 CONSTANTS
N2=(M1*B(5,2))-(A(5,2))
N3=(M1*B(5,3))-(A(5,3))
N4=(M1*B(5,4))-(A(5,4))
N5=(M1*B(5,5))-(A(5,5))
N6=(M1*B(5,6))-(A(5,6))
:COMPUTE POINT 6 CONSTANTS
T2=(M1*B(6,2))-(A(6,2))
T3=(M1*B(6,3))-(A(6,3))
T4=(M1*B(6,4))-(A(6,4))
T5=(M1*B(6,5))-(A(6,5))
T6=(M1*B(6,6))-(A(6,6))
C1=PI*(-PJ-(C2*A2+C3*A3+C4*A4+C5*A5+C6*A6))
X2=C2*S2+C3*S3+C4*S4+C5*S5+C6*S6+D2*C1+E2*C7
c2'=x2-kp*q2'
Q2'=(KA*C2*(1-Q2))-(KB*Q2)
X3=C2*P2+C3*P3+C4*P4+C5*P5+C6*P6+D3*C1+E3*C7
c3'=x3-kp*q3'
Q3'=(KA*C3*(1-Q3))-(KB*Q3)
X4=C2*M2+C3*M3+C4*M4+C5*M5+C6*M6+C1*D4+C7*E4
c4'=x4-kp*q4'
Q4'=(KA*C4*(1-Q4))-(KB*Q4)
X5=C2*N2+C3*N3+C4*N4+C5*N5+C6*N6+D5*C1+E5*C7
c5'=x5-kp*q5'
Q5'=(KA*C5*(1-Q5))-(KB*Q5)
X6=C2*T2+C3*T3+C4*T4+C5*T5+C6*T6+D6*C1+C7*E6
c6'=x6-kp*q6'
Q6'=(KA*C6*(1-Q6))-(KB*Q6)
C7=-(C1*B1+C2*B2+C3*B3+C4*B4+C5*B5+C6*B6)
terminate c7.gt.1
plot ebv,c7,0,250,0,1
print ebv,c7
$ VAL C0      =   1.0000
$ VAL TFIN    =   200.00
$ VAL NOCI    =   5.0000
$ VAL CINT    =  0.50000
$ VAL K1      =   4.8000
$ VAL QM      =   1210.0
$ VAL PP      =  0.86000E-01
$ VAL U       =   7.6900
$ VAL LC      =  0.25000
```